

SAFETY ANALYSIS REPORT

FOR

TN 6-4 PACKAGE

MAY 1992

POWER REACTOR AND NUCLEAR FUEL DEVELOPMENT CORPORATION

9601260203 951107
PDR ADOCK 071*****
C PDR

Safety Analysis Report for TN6-4

Package (Design Changes)

Prepared by: Kazushige Doumoto*, Saburo Takahashi**,
Eiichi Kawashima***, Yoshikazu Kamino***

Abstract

The TN6-4 package is to be used for transporting such substances as irradiated fast-breeder-reactor nuclear fuel between post-irradiation test facilities for subjection to post-irradiation testing.

Although the design of the package was authorized in 1981, and approval for the last design change was granted in 1986 [per approval No. J/85/B(U) F(Rev. 4)], this design-change application has been filed for the reasons given below:

(1) Addition of contents specifications

The need has arisen to transport fuel materials that have been irradiated in the fast breeder reactors (FFTFs) in U.S.A. or the like for subjection to post-irradiation testing. Since such fuel materials fail to meet existing conditions for authorization, it has become necessary to revise existing specifications covering Contents III such as those that apply to the fluence and the number of cooling days. At this time, Contents VIII must also be added to the existing contents.

(2) Review of the contents of the existing pertinent documents in light of the amendment of the pertinent domestic laws, rules, and regulations

Following the amendment of "The rule for transporting nuclear fuel material and the like outside of a factory or business site," etc., which was implemented as a result of the incorporation of the IAEA Regulations for the Safe Transport of Radioactive Material 1985 Edition into the pertinent domestic laws, rules, and regulations, items such as terms, units, analysis conditions, and evaluation criteria have been revised. As a result, it has become necessary to review the contents of the existing pertinent documents.

This report is the product of work conducted by Atom Transport Service Ltd. under contract from the Power Reactor and Nuclear Fuel Development Corporation.
Contract No. 03C1337

Responsible PNC staff member and section: Shinichi Uruwashi, Fuel Monitoring
Section, Fuels and Materials Division

* : Technical Engineering Dept., Atom Transport Service Ltd.

** : Design and Development Sect., Tokai Office, Atom Transport Service Ltd.

*** : Engineering Dept., Nuclear Head Quarters, Kimura Chemical Plants Co., Ltd.

(3) Changes to safety analysis techniques

To ensure that safety analyses can be performed based on revisions governing analysis work and the latest knowledge, it has become necessary to change the analysis codes used in shield analysis and criticality analysis.

Although the safety-analysis changes made in accordance with the above revisions apply to the whole range of analysis and evaluation, i.e., structural evaluation, thermal analysis, containment analysis, shield analysis, and criticality analysis, the results of the safety analysis performed proved to satisfy all engineering criteria.

This application was submitted to the Science and Technology Agency on May 20, 1992 [Official document No. 039 of the nuclear material control division of PNC, 1992] as a package design change application for approval. The package was approved by the Science and Technology Agency as a package capable of satisfying all pertinent engineering criteria established for application to type B(U) (fissile) package, and the certificate of approval of package design for nuclear fuel material [Official document No. 363 of the nuclear material regulation section of the nuclear safety bureau of STA, 1992] was issued by the Director-General of the Agency on August 7, 1992. [Design approval No. J/85/B(U)F-85]

SAFETY ANALYSIS REPORT

FOR

TN 6-4 PACKAGE

MAY 1992

POWER REACTOR AND NUCLEAR FUEL DEVELOPMENT CORPORATION

CONTENTS

CONTENTS

CHAPTER I EXPLANATION OF THE PACKAGE

A. Objectives and Conditions	(I)-1
B. Package Type	(I)-2
C. Packaging	(I)-4
D. Contents of the Packaging	(I)-61

CHAPTER II SAFETY ANALYSIS OF A PACKAGE FOR NUCLEAR MATERIAL

A. Structural Evaluation	(II)-A-1
A.1 Structural Design	(II)-A-1
A.1.1 Outline	(II)-A-1
A.1.2 Design Criteria	(II)-A-2
A.2 Weight and Center of Gravity	(II)-A-18
A.3 Mechanical Properties of Materials	(II)-A-20
A.4 Package Requirements	(II)-A-25
A.4.1 Chemical and Galvanic Reactions	(II)-A-25
A.4.2 Low-Temperature Strength	(II)-A-26
A.4.3 Containment System	(II)-A-28
A.4.4 Lifting Device	(II)-A-29
A.4.5 Tie-Down Device	(II)-A-55
A.4.6 Pressure	(II)-A-78
A.4.7 Vibration	(II)-A-79
A.5 Normal Test Conditions	(II)-A-81
A.5.1 Thermal Test	(II)-A-81
A.5.1.1 Summary of the Temperature and Pressure	(II)-A-81
A.5.1.2 Thermal Expansion	(II)-A-82
A.5.1.3 Stress Calculation	(II)-A-87
A.5.1.4 Comparison with Allowable Stress	(II)-A-87
A.5.2 Water Spray	(II)-A-90
A.5.3 Free Drop	(II)-A-90
A.5.4 Stacking Test	(II)-A-93
A.5.5 Penetration	(II)-A-99
A.5.6 Free Drop onto a Corner or onto Each of the Quarters of Each Rim	(II)-A-100
A.5.7 Summary and Evaluation of Results	(II)-A-101
A.6 Accident Test Conditions	(II)-A-103
A.6.1 Mechanical Test - Drop Test I (with a 9-m Drop)	(II)-A-103
A.6.1.1 Vertical Drop	(II)-A-107
A.6.1.2 Horizontal Drop	(II)-A-143
A.6.1.3 Corner Drop	(II)-A-156
A.6.1.4 Oblique Drop	(II)-A-164
A.6.1.5 Summary and Examination of Results	(II)-A-168
A.6.2 Mechanical Test and Drop Test II (1-m Drop)	(II)-A-168
A.6.2.1 Summary of Results	(II)-A-181
A.6.3 Thermal Test	(II)-A-182
A.6.3.1 Summary of Temperatures and Pressures	(II)-A-182
A.6.3.2 Thermal Expansion	(II)-A-184
A.6.3.3 Comparison with the Allowable Stress	(II)-A-199

A.6.4	Water Immersion	(II)-A-203
A.6.5	Summary and Evaluation of Results	(II)-A-206
A.7	Special-Form Nuclear Fuel Materials	(II)-A-207
A.7.1	Outline	(II)-A-207
A.7.2	Impact	(II)-A-207
A.7.3	Percussion	(II)-A-207
A.7.4	Heating	(II)-A-207
A.7.5	Bending	(II)-A-207
A.7.6	Water Immersion	(II)-A-207
A.7.7	Summary and Evaluation of Results	(II)-A-207
A.8	Radioactive Contents	(II)-A-208
A.9	Fissile Package	(II)-A-209
A.9.1	Normal Test Conditions	(II)-A-209
A.9.2	Accident Test Conditions	(II)-A-211
A.10	Appendix	(II)-A.App-1
B.	Thermal Analysis	(II)-B-1
B.1	Outline	(II)-B-1
B.2	Thermal Properties of the Materials	(II)-B-27
B.3	Specifications of the Components	(II)-B-35
B.4	Normal Test Conditions	(II)-B-36
B.4.1	Thermal Analysis Model	(II)-B-36
B.4.1.1	Analysis Model	(II)-B-36
B.4.1.2	Test Model	(II)-B-40
B.4.2	Maximum Temperature	(II)-B-41
B.4.3	Minimum Temperature	(II)-B-56
B.4.4	Maximum Internal Pressure	(II)-B-57
B.4.5	Maximum Thermal Stress	(II)-B-63
B.4.6	Summary and Evaluation of Results	(II)-B-63
B.5	Accident Test Conditions	(II)-B-64
B.5.1	Thermal Analysis Model	(II)-B-64
B.5.1.1	Analysis Model	(II)-B-64
B.5.1.2	Test Model	(II)-B-67
B.5.2	Evaluation Conditions of the Package	(II)-B-68
B.5.3	Temperature of the Package	(II)-B-70
B.5.4	Maximum Internal Pressure	(II)-B-78
B.5.5	Maximum Thermal Stress	(II)-B-81
B.5.6	Summary and Evaluation of Results	(II)-B-81
B.6	Appendix	(II)-B.App-1
C.	Containment Analysis	(II)-C-1
C.1	Outline	(II)-C-1
C.2	Containment System	(II)-C-1
C.2.1	Containment System	(II)-C-1
C.2.2	Penetration Sections of the Containment System	(II)-C-5
C.2.3	Containment System Gaskets and Welded Joints	(II)-C-6
C.2.4	Lids	(II)-C-7
C.3	Normal Test Conditions	(II)-C-7
C.3.1	Leakage of Radioactive Material	(II)-C-8
C.3.2	Pressurization of Containment System	(II)-C-14
C.3.3	Contamination of Coolant	(II)-C-14

C.3.4	Loss of Cooling Water	(II)-C-15
C.4	Accident Test Conditions	(II)-C-15
C.4.1	Fission Product Gases	(II)-C-16
C.4.2	Leakage of Radioactive Materials	(II)-C-18
C.5	Summary and Evaluation of Results	(II)-C-20
D.	Shield Analysis	(II)-D-1
D.1	Outline	(II)-D-1
D.2	Specifications of Radiation Sources	(II)-D-8
D.2.1	Sources of Gamma Rays	(II)-D-8
D.2.2	Neutron Sources	(II)-D-9
D.3	Specifications of Models	(II)-D-21
D.3.1	Analysis Models	(II)-D-21
D.3.2	Number Density of Atom in Each Individual Analysis-Model Region	(II)-D-37
D.4	Shield Evaluations	(II)-D-39
D.5	Summary and Evaluation of Results	(II)-D-46
E.	Criticality Analysis	(II)-E-1
E.1	Outline	(II)-E-1
E.2	Items Subject to Analysis	(II)-E-3
E.2.1	Contents	(II)-E-3
E.2.2	Packaging	(II)-E-3
E.2.3	Neutron Absorber	(II)-E-3
E.3	Specifications of Models	(II)-E-6
E.3.1	Analysis Model	(II)-E-6
E.3.2	Number Density of Atom in Each Individual Region of the Criticality-Analysis Models	(II)-E-12
E.4	Subcriticality Evaluation	(II)-E-13
E.4.1	Calculation Conditions	(II)-E-13
E.4.2	Entry of Water into the Package	(II)-E-13
E.4.3	Calculation Methods	(II)-E-13
E.4.4	Calculation Results	(II)-E-14
E.5	Summary and Evaluation of Results	(II)-E-14
E.6	Appendix	(II)-E.App-1
F.	Evaluations of Compliance to Ordinance of the Prime Minister's Office and Notification of the Science and Technology Agency	(II)-F-1

CHAPTER III MANUFACTURE OF PACKAGING

A.	Packaging Manufacturing Method	(III)-2
A.1	Outline	(III)-2
A.1.1	Manufacture Components	(III)-2
A.1.2	Assembling of Components	(III)-6
A.2	Description of Materials	(III)-32
A.2.1	Sheet Materials	(III)-32
A.2.2	Tubing	(III)-32
A.2.3	Forging, Nuts and Bolts	(III)-32
A.2.4	Welding Electrodes, Bars and Lines	(III)-32
A.2.5	Special Materials	(III)-32
A.2.6	Certified Material Test Report	(III)-37

A.2.7	Repair of Defects in the Materials	(III)-38
A.2.8	Cutting of Materials	(III)-38
A.2.9	Forming of Materials	(III)-38
A.3	Welding	(III)-39
A.3.1	Welding Method and Materials	(III)-39
A.3.2	Welding Machine Management and Welder Qualification	(III)-39
A.3.3	Description of the Main Welding Items	(III)-41
A.3.4	Repair of Weld Defects	(III)-46
A.3.5	Heat Treatment after Welding	(III)-46
A.3.6	Special Welding	(III)-46
A.3.7	Weld Quality Assurance Plan, etc.	(III)-46
A.4	Shield Manufacturing Method	(III)-48
A.4.1	Casting of Lead Shield Material	(III)-48
A.4.2	Uranium Shield Material Manufacturing Method	(III)-51
A.4.3	Other Shield Materials Manufacturing Method	(III)-51
A.5	Manufacturing Method for Valves and Other Attachments	(III)-52
A.6	Assembly and Manufacturing Method for Other Components	(III)-52
B.	Test and Inspection Methods	(III)-53
B.1	Material Inspection	(III)-53
B.2	Dimension Inspection	(III)-53
B.3	Welding Inspection	(III)-54
B.4	Visual Inspection	(III)-55
B.5	Pressure Inspection	(III)-55
B.6	Leakage Test	(III)-55
B.7	Inspection for Shielding Integrity	(III)-56
B.8	Shielding Dimensional Inspection	(III)-56
B.9	Heat Transfer Inspection	(III)-57
B.10	Lifting Load Inspection	(III)-59
B.11	Weight Inspection	(III)-59
B.12	Subcriticality Inspection	(III)-59
B.13	Operational and Functional Test	(III)-59
B.14	Handling Inspection	(III)-59
C.	Packaging Manufacturing Schedule	(III)-65
D.	Quality Control	(III)-67
D.1	Organization	(III)-67
D.1.1	Operational Scope of PNC (Power Reactor and Nuclear Fuel Development Corporation)	(III)-68
D.1.2	Manufacturer's Quality Assurance System	(III)-68
D.2	Quality Assurance Program	(III)-69
D.3	Design Control	(III)-72
D.4	Instructions and Procedures	(III)-72
D.5	Management of Documentation	(III)-72
D.6	Provision of Materials, Machinery and Services	(III)-72
D.7	Administration of the Identification of Materials, Equipment, and Components	(III)-72
D.8	Control of Special Progresses	(III)-73
D.9	Control of the Testing	(III)-73
D.10	Control of Measuring Instruments and Test Equipment	(III)-74

D.11 Handling and Storage	(III)-74
D.12 Control of Inspection and Manufacturing Progress	(III)-74
D.13 Control of Corrections	(III)-74
D.14 Quality Control Record	(III)-76
D.15 Quality Assurance Audit	(III)-76

CHAPTER IV OPERATION PROCEDURES AND MAINTENANCE CONDITIONS OF THE PACKAGE FOR NUCLEAR MATERIAL

A. Operation Procedures for the Package	(IV)-1
A.1 Procedures for Loading the Package	(IV)-1
A.2 Inspections before Shipping the Package	(IV)-6
A.3 Unloading Method	(IV)-9
A.4 Preparing the Empty Packaging	(IV)-12
B. Maintenance Conditions	(IV)-20
B.1 Visual and Pressure Inspections	(IV)-20
B.2 Leakage Test	(IV)-20
B.3 Maintenance of the Auxiliary System	(IV)-20
B.4 Maintenance of the Valves and Gaskets	(IV)-20
B.5 Shielding Dimension Test	(IV)-23
B.6 Subcriticality Inspection	(IV)-23
B.7 Thermal Test	(IV)-23
B.8 Others	(IV)-23

CHAPTER V SPECIAL NOTES ON SAFETY DESIGN AND SAFETY TRANSPORTATION (V)-1

EXPLANATION OF DRAWING

CHAPTER I

Fig. (I)-1	Cutout View of Package	(I)-22
Fig. (I)-2	General Drawing of Packaging	(I)-23
Fig. (I)-3	Schematic Drawing of Packaging Equipped with the Skid for Transportation	(I)-24
Fig. (I)-4	Drawing of Vertical Lifting Condition	(I)-25
Fig. (I)-5	Drawing of Horizontal Lifting Condition	(I)-26
Fig. (I)-6	Detailed Drawings of Front Lid and Rear Lid Units	(I)-27
Fig. (I)-7	Assembling Drawing of Rear Lid Unit	(I)-28
Fig. (I)-8	Assembling Drawing of Front Lid Unit	(I)-29
Fig. (I)-9	Inner Container	(I)-30
Fig. (I)-10	Loading Procedures of Contents (1)	(I)-31
	Loading Procedures of Contents (2)	(I)-32
Fig. (I)-11	Drawing of Status of Contents I, IV and V Loaded in Inner Container	(I)-33
Fig. (I)-12	Drawing of Status of Contents VI and VIII Loaded in Inner Container	(I)-34
Fig. (I)-13	Drawing of Status of Contents VII	(I)-35
Fig. (I)-14	Drawing of Status of Contents II (Minority Pins) Loaded in Inner Container	(I)-36
Fig. (I)-15	Detailed Drawing of Fuel Supporting Can I	(I)-37
Fig. (I)-16	Supporting Can	(I)-38
Fig. (I)-17	Detailed Drawing of Fuel Supporting Can II	(I)-39
Fig. (I)-18	Receiving Tube I	(I)-40
Fig. (I)-19	Receiving Tube II	(I)-41
Fig. (I)-20	Rack	(I)-42
Fig. (I)-21	Schematic Drawing of Rack	(I)-43
Fig. (I)-22	Drawing of Containment Boundary	(I)-44
Fig. (I)-23	Front and Rear Shock Absorbers	(I)-45
Fig. (I)-24	Outer Container	(I)-46
Fig. (I)-25	Lifting Trunnion and Pivoting Trunnion	(I)-47
Fig. (I)-26	Lifting Lug for Horizontal Operation	(I)-48
Fig. (I)-27	Front and Rear Base Plates	(I)-49
Fig. (I)-28	Transport Skid	(I)-50
Fig. (I)-29	Penetration Hole Lid for Rear Sampling Valve	(I)-51
Fig. (I)-30	Penetration Hole Lid for Front Sampling Valve	(I)-52
Fig. (I)-31	Penetration Hole Lid for Rotating Plug	(I)-53
Fig. (I)-32	Shielding Plug	(I)-54
Fig. (I)-33	Shielding Plug Lid	(I)-55
Fig. (I)-34	Rear Lid	(I)-56
Fig. (I)-35	Rotating Plug	(I)-57
Fig. (I)-36	Rotating Plug Lid	(I)-58
Fig. (I)-37	Rotating Plug Lid Cover	(I)-59
Fig. (I)-38	Front Lid	(I)-60
Fig. (I)-39	Contents I (An Example of Fuel Elements)	(I)-69
Fig. (I)-40	Contents II (An Example of Fuel Elements)	(I)-70

CHAPTER II

Fig. (II)-A.1	Position of the Center of Gravity of the Package	(II)-A-18
Fig. (II)-A.2	Tensile Stress and Yield Stress of Stainless Steel	(II)-A-22
Fig. (II)-A.3	Crushing Curve of Balsa Wood	(II)-A-24
Fig. (II)-A.4	Horizontal Lifting	(II)-A-31
Fig. (II)-A.5	Lifting Lug for Horizontal Operation	(II)-A-32
Fig. (II)-A.6	Analysis of the Outer Shell during Horizontal Lifting	(II)-A-37
Fig. (II)-A.7	Analysis Model of the Lifting Trunnion	(II)-A-42
Fig. (II)-A.8	Strength Analysis Model of the Outer Shell during Vertical Lifting	(II)-A-46
Fig. (II)-A.9	Relation of the Bending Moment and the Torsional Moment	(II)-A-47
Fig. (II)-A.10	End Plate Analysis Model	(II)-A-54
Fig. (II)-A.11	Package Equipped with the Skid in Transport	(II)-A-56
Fig. (II)-A.12	Analysis Model of the Tie-Down Device	(II)-A-58
Fig. (II)-A.13	Welded Section of the Rear Base Plate	(II)-A-62
Fig. (II)-A.14	Analysis Model of the Pivoting Trunnion	(II)-A-69
Fig. (II)-A.15	Outer Shell (Trunnion-Mounting Part)	(II)-A-73
Fig. (II)-A.16	Stress Analysis Model	(II)-A-82
Fig. (II)-A.17	Dimensions of the Contents under a Normal Temperature	(II)-A-86
Fig. (II)-A.18	Free Drop (1/2)	(II)-A-91
	Free Drop (2/2)	(II)-A-92
Fig. (II)-A.19	Stacking Test	(II)-A-94
Fig. (II)-A.20	Analysis Diagram of the Stacking Test	(II)-A-95
Fig. (II)-A.21	Penetration Test for the Outer Shell	(II)-A-100
Fig. (II)-A.22	Vertical Drop	(II)-A-108
Fig. (II)-A.23	Outer Shell of the Outer Container	(II)-A-109
Fig. (II)-A.24	Analysis Model of the Inner Shell	(II)-A-111
Fig. (II)-A.25	Rear Lid Unit (Rear-End-First Vertical Drop)	(II)-A-113
Fig. (II)-A.26	(1/2) Loading Model of the Rear Lid Unit	(II)-A-114
	(2/2) Analysis Model of the Rear Lid Unit	(II)-A-115
Fig. (II)-A.27	Sampling Valve Lid Fastening Bolt	(II)-A-120
Fig. (II)-A.28	Fuel Supporting Can I (Vertical Drop)	(II)-A-125
Fig. (II)-A.29	Rack	(II)-A-127
Fig. (II)-A.30	Front Lid Unit (Front-End-First Vertical Drop)	(II)-A-132
Fig. (II)-A.31	Loading Model of the Front Lid Unit	(II)-A-133
Fig. (II)-A.32	Analysis Model of the Front Lid Unit	(II)-A-134
Fig. (II)-A.33	Locking Plate	(II)-A-139
Fig. (II)-A.34	Inner Container Screw	(II)-A-140
Fig. (II)-A.35	Inner Container	(II)-A-142
Fig. (II)-A.36	Horizontal Drop	(II)-A-144
Fig. (II)-A.37	Horizontal Drop Model	(II)-A-145
Fig. (II)-A.38	Horizontal Drop of the Supporting Can	(II)-A-149
Fig. (II)-A.39	Horizontal Drop of Receiving Tube I	(II)-A-151
Fig. (II)-A.40	Sampling Valve Lid and Penetration Hole Lid (during a Horizontal Drop)	(II)-A-154
Fig. (II)-A.41	Corner Drop	(II)-A-157
Fig. (II)-A.42	Shielding Plug Lid Fastening Bolt	(II)-A-159
Fig. (II)-A.43	Fastening Bolt for the Rotating Plug Lid	(II)-A-162
Fig. (II)-A.44	Oblique Drop Model	(II)-A-165
Fig. (II)-A.45	Deformation during Oblique Drop	(II)-A-167

Fig. (II)-A.46	Drop Test II on the Center of the Outer Shell	(II)-A-171
Fig. (II)-A.47	Horizontal Drop on the Shock Absorber	(II)-A-173
Fig. (II)-A.48	Vertical Drop on the Shock Absorber	(II)-A-175
Fig. (II)-A.49	Corner Drop onto the Mild Steel Bar	(II)-A-180
Fig. (II)-A.50	Packaging (Thermal Test)	(II)-A-183
Fig. (II)-A.51	Stress - Strain Curve	(II)-A-185
Fig. (II)-A.52	Analysis Model of the Thermal Stress	(II)-A-186
Fig. (II)-A.53	Thermal Stress Evaluation Results	(II)-A-188
Fig. (II)-A.54	Analysis Model of the Inner Shell	(II)-A-190
Fig. (II)-A.55	Rear Lid Unit (Thermal Test)	(II)-A-191
Fig. (II)-A.56	Front Lid Unit (Thermal Test)	(II)-A-193
Fig. (II)-A.57	Analysis Model of Penetration Hole Lid	(II)-A-195
Fig. (II)-A.58	Fuel Supporting Can	(II)-A-197
Fig. (II)-A.59	Receiving Tube II	(II)-A-198
Fig. (II)-A.60	Water Immersion Test	(II)-A-205
Fig. (II)-A.61	Free Drop onto a Corner or onto Each of the Quarters of Each Rim	(II)-A-218
Fig. (II)-A.62	Thermal Analysis Model under Accident Test Conditions (Contents I/eccentric)	(II)-A-220
Fig. (II)-A-App.1	Shock Absorber Side Plate	(II)-A.App-3
Fig. (II)-A-App.2	Analysis Model of Rear Lid Unit	(II)-A.App-6
Fig. (II)-A-App.3	Analysis Model of Front Lid Unit	(II)-A.App-7
Fig. (II)-A-App.4	Analysis Model of Penetration Hole Lid	(II)-A.App-8
Fig. (II)-A-App.5	Model for Thermal Stress Analysis	(II)-A.App-9
Fig. (II)-A-App.6	1/2 Scale Model Container	(II)-A.App-17
Fig. (II)-A-App.7	Contents of the Test	(II)-A.App-22
Fig. (II)-A-App.8	Drop Test Stand	(II)-A.App-24
Fig. (II)-A-App.9	Block Diagram of Deceleration and Strain Measurements	(II)-A.App-25
Fig. (II)-A-App.10	Installation Positions of the Acceleration Converter and Strain Gauge	(II)-A.App-26
Fig. (II)-A-App.11	Phenomenal Wave of Deceleration	(II)-A.App-27
Fig. (II)-A-App.12	Output Waveform of the Acceleration Converter Following a Hammer Stroke	(II)-A.App-27
Fig. (II)-A-App.13(a)	Phenomenal Waveforms Reproduced on a Synchroscope	(II)-A.App-42
Fig. (II)-A-App.13(b)	Phenomenal Waveforms Reproduced on a Synchroscope	(II)-A.App-43
Fig. (II)-A-App.13(c)	Phenomenal Waveforms Reproduced on a Synchroscope	(II)-A.App-44
Fig. (II)-A-App.13(d)	Phenomenal Waveforms Reproduced on a Synchroscope	(II)-A.App-45
Fig. (II)-A-App.13(e)	Phenomenal Waveforms Reproduced on a Synchroscope	(II)-A.App-46
Fig. (II)-A-App.13(f)	Phenomenal Waveforms Reproduced on a Synchroscope	(II)-A.App-47
Fig. (II)-A-App.13(g)	Phenomenal Waveforms Reproduced on a Synchroscope	(II)-A.App-48
Fig. (II)-A-App.13(h)	Phenomenal Waveforms Reproduced on a Synchroscope	(II)-A.App-49
Fig. (II)-A-App.13(i)	Phenomenal Waveforms Reproduced on a Synchroscope	(II)-A.App-50
Fig. (II)-A-App.13(j)	Phenomenal Waveforms Reproduced on a Synchroscope	(II)-A.App-51
Fig. (II)-A-App.13(k)	Phenomenal Waveforms Reproduced on a Synchroscope	(II)-A.App-52
Fig. (II)-A-App.13(l)	Phenomenal Waveforms Reproduced on a Synchroscope	(II)-A.App-53
Fig. (II)-A-App.13(m)	Phenomenal Waveforms Reproduced on a Synchroscope	(II)-A.App-54
Fig. (II)-A-App.14(a)	Before a Drop Test	(II)-A.App-55
Fig. (II)-A-App.14(b)	Horizontal Drop	(II)-A.App-56
Fig. (II)-A-App.14(c)	Drop Test II on the Shell	(II)-A.App-56
Fig. (II)-A-App.14(d)	Drop Test II on Circumference of the Shock Absorber	(II)-A.App-56

Fig. (II)-A-App.14(e)	Horizontal Drop	(II)-A.App-57
Fig. (II)-A-App.14(f)	Drop Test II on the Shell	(II)-A.App-57
Fig. (II)-A-App.14(g)	Drop Test II on Circumference of the Shock Absorber	(II)-A.App-57
Fig. (II)-A-App.14(h)	Vertical Drop	(II)-A.App-58
Fig. (II)-A-App.14(i)	Drop Test II on the Center of the Shock Absorber	(II)-A.App-58
Fig. (II)-A-App.14(j)	Drop Test II on the End Surface of the Shock Absorber	(II)-A.App-58
Fig. (II)-A-App.14(k)	Corner Drop	(II)-A.App-59
Fig. (II)-A-App.14(l)	Drop Test II on the Shock Absorber	(II)-A.App-59
Fig. (II)-A-App.14(m)	Oblique Drop	(II)-A.App-59
Fig. (II)-A-App.14(n)	Drop Test II on the Shock Absorber	(II)-A.App-60
Fig. (II)-B.1	Thermal Analysis Model under Normal Test Conditions (Contents I/eccentric) (1/2)	(II)-B-4
	Thermal Analysis Model under Normal Test Conditions (Contents I/eccentric) (2/2)	(II)-B-5
Fig. (II)-B.2	Thermal Analysis Model under Normal Test Conditions (Contents I/center)	(II)-B-6
Fig. (II)-B.3	Thermal Analysis Model under Normal Test Conditions (Contents II)	(II)-B-7
Fig. (II)-B.4	Thermal Analysis Model under Accident Test Conditions (Contents I/eccentric, Vertical Drop) (1/2)	(II)-B-8
	Thermal Analysis Model under Accident Test Conditions (Contents I/eccentric, Vertical Drop) (2/2)	(II)-B-9
Fig. (II)-B.5	Thermal Analysis Model under Accident Test Conditions (Contents I/center, Vertical Drop)	(II)-B-10
Fig. (II)-B.6	Thermal Analysis Model under Accident Test Conditions (Contents II/Vertical Drop)	(II)-B-11
Fig. (II)-B.7	Thermal Analysis Model under Accident Test Conditions (Contents I/eccentric, Horizontal Drop) (1/2)	(II)-B-12
	Thermal Analysis Model under Accident Test Conditions (Contents I/eccentric, Horizontal Drop) (2/2)	(II)-B-13
Fig. (II)-B.8	Change in Temperature under Accident Test Conditions (Contents I/eccentric, Vertical Drop)	(II)-B-22
Fig. (II)-B.9	Change in Temperature under Accident Test Conditions (Contents I/center, Vertical Drop)	(II)-B-23
Fig. (II)-B.10	Change in Temperature under Accident Test Conditions (Contents II, Vertical Drop)	(II)-B-24
Fig. (II)-B.11	Change in Temperature under Accident Test Conditions (Contents I/eccentric, Horizontal Drop)	(II)-B-25
Fig. (II)-B.12	Homogeneous Model of Contents I	(II)-B-37
Fig. (II)-B.13	Homogeneous Model of Contents II	(II)-B-39
Fig. (II)-B.14	Temperature of Package under Normal Test Conditions (Contents I/eccentric) (1/2)	(II)-B-42
	Temperature of Package under Normal Test Conditions (Contents I/eccentric) (2/2)	(II)-B-43
Fig. (II)-B.15	Temperature of Package under Normal Test Conditions (Contents I/center) (1/2)	(II)-B-44
	Temperature of Package under Normal Test Conditions (Contents I/center) (2/2)	(II)-B-45
Fig. (II)-B.16	Heat Transfer Model in Fuel Supporting Can I	(II)-B-46

Fig. (II)-B.17	Temperature of Package under Normal Test Conditions (Contents II) (1/2)	(II)-B-49
	Temperature of Package under Normal Test Conditions (Contents II) (2/2)	(II)-B-50
Fig. (II)-B.18	Heat Transfer Model of Inner Container Holding Receiving Tube I	(II)-B-51
Fig. (II)-B.19	Heat Transfer Model of Receiving Tube I	(II)-B-52
Fig. (II)-B.20	Temperature Distribution in Inner Container Holding Receiving Tube I	(II)-B-52
Fig. (II)-B.21	Remaining Thickness of Shock Absorber after Drop Tests I and II	(II)-B-69
Fig. (II)-B.22	Heat Transfer Model in Fuel Supporting Can I	(II)-B-72
Fig. (II)-B.23	Heat Transfer Model of Inner Container Holding Receiving Tube I	(II)-B-75
Fig. (II)-B.24	Heat Transfer Model of Receiving Tube I	(II)-B-76
Fig. (II)-B.25	Temperature Distribution in Inner Container Holding Receiving Tube I	(II)-B-76
Fig. (II)-B-App.1	Heat Transfer Model of the Cement Layer and Heat Dispersion Fins	(II)-B.App-2
Fig. (II)-B-App.2	Shape of the Shock Absorber Damaged during Drop Test II	(II)-B.App-10
Fig. (II)-B-App.3	Form Factor Model	(II)-B.App-11
Fig. (II)-B-App.4	Cross-Sectional View of the Inner Container Holding Contents II	(II)-B.App-15
Fig. (II)-B-App.5	Correlation Between Receiving Tube I and Supporting Rod	(II)-B.App-17
Fig. (II)-B-App.6	Heat Transfer Model of Heat Dispersion Fin	(II)-B.App-20
Fig. (II)-B-App.7	Change in Temperature under Accident Test Conditions (Heat Dispersion Fin)	(II)-B.App-21
Fig. (II)-B-App.8	Thermal Test Analysis Model	(II)-B.App-23
Fig. (II)-B-App.9	Combustion Area	(II)-B.App-27
Fig. (II)-B-App.10	Furnace Test	(II)-B.App-27
Fig. (II)-B-App.11	Maximum Temperature and Time When It Was Reached by the Measurement Position	(II)-B.App-30
Fig. (II)-B-App.12	Annealing Furnace	(II)-B.App-32
Fig. (II)-B-App.13	Test Model A	(II)-B.App-33
Fig. (II)-B-App.14	Test Model B	(II)-B.App-34
Fig. (II)-B-App.15	Change in Temperature of Test Model A (Treated Side)	(II)-B.App-36
Fig. (II)-B-App.16	Change in Temperature of Test Model A (Non-Treated Side)	(II)-B.App-37
Fig. (II)-B-App.17	Carbonization of Balsa Wood	(II)-B.App-38
Fig. (II)-B-App.18	Change in Temperature of Test Model B	(II)-B.App-39
Fig. (II)-B-App.19	Carbonization of Resin (Sectional View)	(II)-B.App-40
Fig. (II)-C.1	Containment System and Boundary of Containment	(II)-C-2
Fig. (II)-C.2	Fuel Supporting Can, Receiving Tubes I and II	(II)-C-3
Fig. (II)-C.3	Leakage Analysis Flow	(II)-C-11

Fig. (II)-D.1	Structure of the Packaging	(II)-D-3
Fig. (II)-D.2	Shielding Structure of the Packaging (No. 1) (Adjacent Rear Lid Unit)	(II)-D-4
Fig. (II)-D.3	Shielding Structure of the Packaging (No. 2) (Adjacent Front Lid Unit)	(II)-D-5
Fig. (II)-D.4	Surface of the Package and the Position 1 m from the Surface for Shield Analysis	(II)-D-6
Fig. (II)-D.5	Shock Absorber Model under Normal Test Conditions	(II)-D-22
Fig. (II)-D.6	Surface of the Package for Shield Analysis	(II)-D-23
Fig. (II)-D.7	Shield Analysis Model of the Packaging Side Section under Normal Test Conditions	(II)-D-25
Fig. (II)-D.8	Shield Analysis Model of the Packaging Side Section under Accident Test Conditions	(II)-D-26
Fig. (II)-D.9	Rear Lid Unit	(II)-D-27
Fig. (II)-D.10	Shield Analysis Model of the Packaging Rear Section under Normal Test Conditions	(II)-D-28
Fig. (II)-D.11	Front Lid Unit	(II)-D-29
Fig. (II)-D.12	Shield Analysis Model of the Packaging Front Section under Normal Test Conditions	(II)-D-30
Fig. (II)-D.13	Contents I Loading Conditions	(II)-D-31
Fig. (II)-D.14	Model of Contents I Loading Conditions	(II)-D-31
Fig. (II)-D.15	Positions of the Radiation Source of Contents I	(II)-D-32
Fig. (II)-D.16	Contents II Loading Conditions	(II)-D-33
Fig. (II)-D.17	Model of Contents II Loading Conditions	(II)-D-33
Fig. (II)-D.18	Positions of the Radiation Source of Contents II	(II)-D-34
Fig. (II)-D.19	Positions of the Radiation Source of Contents III	(II)-D-36
Fig. (II)-D.20	Distribution of the Dose Equivalent Rates on and around the Package Holding Contents I	(II)-D-48
Fig. (II)-D.21	Distribution of the Dose Equivalent Rates on and around the Package Holding Contents II	(II)-D-49
Fig. (II)-D.22	Distribution of the Dose Equivalent Rates on and around the Package Holding Contents III	(II)-D-50
Fig. (II)-E.1	Analysis Model of the Package in Isolation	(II)-E-8
Fig. (II)-E.2	The Arrangement of Contents	(II)-E-9
Fig. (II)-E.3	Model of Contents-Storage Region	(II)-E-10
Fig. (II)-E.4	Analysis Model of Array of Packages	(II)-E-11
Fig. (II)-E-App.1	Analysis Model for Optimum Hydrogenous Density	(II)-E.App-2
Fig. (II)-E-App.2	Hydrogenous Density and Infinite Multiplication Factor	(II)-E.App-3

CHAPTER III

Fig. (III)-1	Manufacturing Procedure for Packaging (1)	(III)-7
Fig. (III)-2	Manufacturing Procedure for Packaging (2)	(III)-8
Fig. (III)-3	Manufacturing Procedure for Packaging (3)	(III)-9
Fig. (III)-4	Package Assembly Drawing	(III)-10
Fig. (III)-5	Outer Container	(III)-11
Fig. (III)-6	Rear Base Plate	(III)-12

Fig. (III)-7	Front Base Plate	(III)-13
Fig. (III)-8	Lifting Lug for Horizontal Operation	(III)-14
Fig. (III)-9	Lifting Trunnion, Pivoting Trunnion	(III)-15
Fig. (III)-10	Rotating Plug Lid	(III)-16
Fig. (III)-11	Rotating Plug Lid Cover	(III)-17
Fig. (III)-12	Rotating Plug	(III)-18
Fig. (III)-13	Shielding Plug Lid	(III)-19
Fig. (III)-14	Shielding Plug	(III)-20
Fig. (III)-15	Front and Rear Sampling Valve and Penetration Hole Lid . . .	(III)-21
Fig. (III)-16	Rear Lid	(III)-22
Fig. (III)-17	Front Lid	(III)-23
Fig. (III)-18	Front and Rear Shock Absorbers	(III)-24
Fig. (III)-19	Inner Container	(III)-25
Fig. (III)-20	Fuel Supporting Can I	(III)-26
Fig. (III)-21	Fuel Supporting Can II	(III)-27
Fig. (III)-22	Supporting can	(III)-28
Fig. (III)-23	Rack	(III)-29
Fig. (III)-24	Receiving Tube I	(III)-30
Fig. (III)-25	Receiving Tube II	(III)-31
Fig. (III)-26	Arrangement of Weld Lines	(III)-45
Fig. (III)-27	Lead Casting Manual	(III)-49
Fig. (III)-28	Heat Transfer Test	(III)-58
Fig. (III)-29	Packaging Quality Assurance Organization Chart (A Sample)	(III)-67
Fig. (III)-30	Correction Control Flow	(III)-75

CHAPTER IV

Fig. (IV)-1	Schematic Drawing of Packaging Equipped with the Skid for Transportation	(IV)-13
Fig. (IV)-2	General Drawing of Packaging	(IV)-14
Fig. (IV)-3	Drawing of Vertical Operation	(IV)-15
Fig. (IV)-4	Opening and Closing Procedures of Rotating Plug	(IV)-16
Fig. (IV)-5	Drawing of Horizontal Operation	(IV)-17
Fig. (IV)-6	Loading Procedures for Contents (1)	(IV)-18
Fig. (IV)-7	Loading Procedures for Contents (2)	(IV)-19

EXPLANATION OF TABLE

CHAPTER I

Table (I)-1	Specifications of Radioactive Materials to be Accommodated	(I)-3
Table (I)-2	Table of Components of the Packaging	(I)-18
Table (I)-3	Weight, Dimensions and Materials of the Constituent Components of the Packaging	(I)-19
Table (I)-4	Lifting Devices of the Constituent Components of the Packaging	(I)-21
Table (I)-5	Specifications of Nuclear-Fuel Contents	(I)-65
Table (I)-6	Specifications of Contents III	(I)-67
Table (I)-7	Prime Nuclides and their Radioactivity (Bq)	(I)-68

CHAPTER II

Table (II)-A.1	Structural Design Conditions and Analysis Methods (Normal Transport Conditions)	(II)-A-5
Table (II)-A.2	Structural Design Conditions and Analysis Methods (Normal Test Conditions)	(II)-A-9
Table (II)-A.3	Structural Design Conditions and Analysis Method (Accident Test Conditions)	(II)-A-11
Table (II)-A.4	Package Weight List	(II)-A-19
Table (II)-A.5	Design Weight of Package under Structural Evaluation	(II)-A-19
Table (II)-A.6	Mechanical Properties of the Packaging's Principal Materials (under a Normal Temperature)	(II)-A-21
Table (II)-A.7	Tensile Stress and Yield Stress of Stainless Steel under Each Temperature	(II)-A-22
Table (II)-A.8	Longitudinal Elasticity Modulus of Stainless Steel at High Temperature	(II)-A-23
Table (II)-A.9	Materials of a Different Kinds Making Contact with Each Other	(II)-A-25
Table (II)-A.10	Allowable Service Temperature (Minimum)	(II)-A-27
Table (II)-A.11	Stress Generated in the Outer Shell (during Vertical Lifting)	(II)-A-50
Table (II)-A.12	Reaction Force List	(II)-A-60
Table (II)-A.13	Stress Generated in the Outer Shell (Horizontal Lifting)	(II)-A-77
Table (II)-A.14	Summary of the Pressure and Temperature under Normal Test Conditions	(II)-A-81
Table (II)-A.15	Physical Properties and Temperature of the Outer Container Materials	(II)-A-83
Table (II)-A.16	Comparison with the Allowable Stress (I)	(II)-A-88
Table (II)-A.17	Free Drop (0.6 m) Calculation Results	(II)-A-91
Table (II)-A.18	Drop Attitude of a 9-m Drop Test	(II)-A-104
Table (II)-A.19	Material Property Value of the Rear Lid Unit (80°C)	(II)-A-117
Table (II)-A.20	Calculation Results of the Rear Lid Unit	(II)-A-118
Table (II)-A.21	Physical Property Value the Front Lid Unit	(II)-A-136
Table (II)-A.22	Calculation Results of the Front Lid Unit	(II)-A-137

Table (II)-A.23	Impact Force and Deformation during an Oblique Drop	(II)-A-167
Table (II)-A.24	Shock Absorber Deformation in Drop Test I	(II)-A-168
Table (II)-A.25	Acceleration during Drop Test I and II in a 1/2-Scale Model, and the Corresponding Maximum Stress Generated in the Outer Shell of Outer Container	(II)-A-169
Table (II)-A.26	Deformation of the Balsa Wood Shock Absorber during Drop Tests I and II	(II)-A-181
Table (II)-A.27	Maximum Temperatures and Pressures under Thermal Test Conditions	(II)-A-182
Table (II)-A.28	Physical Property Value of the Inner and Outer Shells at High Temperatures	(II)-A-185
Table (II)-A.29	Calculation Results for the Thermal Stress	(II)-A-187
Table (II)-A.30	Physical Property Value of the Rear Lid Unit (Temperature: 200°C)	(II)-A-190
Table (II)-A.31	Calculation Results for Main Parts of the Rear Lid Unit	(II)-A-190
Table (II)-A.32	Calculation Results for Main Parts of the Front Lid Unit	(II)-A-192
Table (II)-A.33	Physical Property Value of the Penetration Hole Lid Unit (Temperature: 200°C)	(II)-A-194
Table (II)-A.34	Calculation Results for the Main Parts of the Penetration Hole Lid	(II)-A-194
Table (II)-A.35	Comparison with the Allowable Stress (2)	(II)-A-200
Table (II)-A.36	Comparison of the Radioactive Contents with the Design Criterion Values	(II)-A-208
Table (II)-A.37	Calculation Results of a Free Drop (0.3 m + 0.6 m)	(II)-A-209
Table (II)-A.38	Calculation Results of a Free Drop (0.3 m + 0.6 m + 9.0 m)	(II)-A-213
Table (II)-A.39	Comparison with the Allowable Stress	(II)-A-214
Table (II)-A.40	Maximum Temperature under Accident Test Conditions (Contents I)	(II)-A-219
Table (II)-A-App.1	Shielding Plug Lid Bolt and Hole Portion	(II)-A.App-10
Table (II)-A-App.2	Rotating Plug Lid Bolt and Hole Portion	(II)-A.App-13
Table (II)-A-App.3	Penetration Hole Lid Bolt and Hole Portion	(II)-A.App-15
Table (II)-A-App.4	Portions Omitted from the 1/2-Scale Model	(II)-A.App-18
Table (II)-A-App.5	Test Sequence	(II)-A.App-21
Table (II)-A-App.6	Test Conditions and Measurement Results	(II)-A.App-29
Table (II)-A-App.7	Comparison of Results Between the 1/2-Scale Model Test and Evaluation	(II)-A.App.62
Table (II)-A-App.8	Comparison of the 1/2-Scale Model Test, 1/2-Scale Model Evaluation, and Actual Packaging Evaluation Results	(II)-A.App.63
Table (II)-B.1	Maximum Decay Heat of the Contents	(II)-B-2
Table (II)-B.2	Thermal Analyses Conditions	(II)-B-15
Table (II)-B.3	Thermal Analyses Method	(II)-B-16
Table (II)-B.4	Package Temperature under Normal Test Conditions (Contents I)	(II)-B-18
Table (II)-B.5	Package Temperature under Normal Test Conditions (Contents II)	(II)-B-19
Table (II)-B.6	Maximum Temperature under Accident Test Conditions (Contents I)	(II)-B-20

Table (II)-B.7	Maximum Temperature under Accident Test Conditions (Contents II)	(II)-B-21
Table (II)-B.8	Maximum Internal Pressure under Normal Test Conditions	(II)-B-26
Table (II)-B.9	Maximum Internal Pressure under Accident Test Conditions	(II)-B-26
Table (II)-B.10	Thermal Properties of the Stainless Steel	(II)-B-29
Table (II)-B.11	Thermal Properties of the Lead	(II)-B-29
Table (II)-B.12	Thermal Properties of the Copper	(II)-B-30
Table (II)-B.13	Thermal Properties of the Fuel	(II)-B-30
Table (II)-B.14	Thermal Properties of the Balsa Wood (Flame Resistance Treated)	(II)-B-31
Table (II)-B.15	Thermal Properties of the Cement	(II)-B-31
Table (II)-B.16	Thermal Properties of Air	(II)-B-32
Table (II)-B.17	Thermal Properties of the Fir-Plywood	(II)-B-32
Table (II)-B.18	Thermal Properties of the Resin	(II)-B-33
Table (II)-B.19	Thermal Properties of the Tungsten	(II)-B-33
Table (II)-B.20	Thermal Properties of the Helium	(II)-B-34
Table (II)-B.21	Thermal Specifications of the Fluoro Rubber	(II)-B-35
Table (II)-B.22	Thermal Specifications of the Fusible Plug	(II)-B-35
Table (II)-B.23	Volume of the Homogenized Fuel Area and Weight of the Component Materials	(II)-B-38
Table (II)-B.24	Physical Properties of the Homogenous Fuel	(II)-B-38
Table (II)-B.25	Thermal Conditions under Normal Test Conditions	(II)-B-40
Table (II)-B.26	Heat Transfer Value of the Solar Heat Radiation	(II)-B-40
Table (II)-B.27	Maximum Temperature under Normal Test Conditions (Contents I)	(II)-B-55
Table (II)-B.28	Maximum Temperature under Normal Test Conditions (Contents II)	(II)-B-56
Table (II)-B.29	FP Gas Generation of Contents I	(II)-B-58
Table (II)-B.30	FP Gas Generation of Contents II	(II)-B-60
Table (II)-B.31	Maximum Internal Pressure under Normal Test Conditions	(II)-B-62
Table (II)-B.32	Deformation of the Shock Absorber (Balsa Wood) during Drop Tests I and II	(II)-B-65
Table (II)-B.33	Thermal Conditions under Accident Test Conditions	(II)-B-67
Table (II)-B.34	Maximum Temperature under Accident Test Conditions (Contents I)	(II)-B-70
Table (II)-B.35	Maximum Temperature under Accident Test Conditions (Contents II)	(II)-B-71
Table (II)-B.36	Maximum Internal Pressure under Accident Test Conditions	(II)-B-79
Table (II)-B-App.1	Heat Transfer Coefficient Between the Outer Shell and the Surrounding Environment	(II)-B.App-5
Table (II)-B-App.2	Total Form Factor Between the Outer Shell and the Surrounding Environment	(II)-B.App-6
Table (II)-B-App.3	Heat Transfer Coefficient Between the Shock Absorber's Vertical Plane and the Surrounding Environment	(II)-B.App-7
Table (II)-B-App.4	Heat Transfer Coefficient Between the Shock Absorber's Horizontal Plane and the Surrounding Environment	(II)-B.App-9
Table (II)-B-App.5	Total Form Factor between the Damaged Part Surface and the Surrounding Environment	(II)-B.App-13
Table (II)-B-App.6	Total Form Factor of the Inner Container	(II)-B.App-18
Table (II)-B-App.7	Thermal Conditions Used for the Calculation	(II)-B.App-24

Table (II)-B-App.8	Ambient Temperature	(II)-B.App-24
Table (II)-B-App.9	Thermal Properties of Carbon Steel	(II)-B.App-25
Table (II)-C.1	Constituent Materials of Containment System	(II)-C-4
Table (II)-C.2	Containment System's Maximum Pressure and O-Ring Sections' Maximum Temperature	(II)-C-4
Table (II)-C.3	Maximum Pressure and Temperature Registered in the Worst Case by Fuel Supporting Can I and Receiving Tube I	(II)-C-5
Table (II)-C.4	O-Ring Specifications for Lids	(II)-C-6
Table (II)-C.5	Specified Tightening Torque of Bolts for the Lids	(II)-C-7
Table (II)-C.6	Leak of Radioactive Gases under Normal Test Conditions (Contents VIII)	(II)-C-10
Table (II)-C.7	Leak of Radioactive Solids under Normal Test Conditions (Contents VIII)	(II)-C-14
Table (II)-C.8	Radioactivity of Fission Product Gases	(II)-C-17
Table (II)-C.9	Leak of Radioactive Gases under Accident Test Conditions (Contents VIII)	(II)-C-19
Table (II)-C.10	Leak of Radioactive Solids under Accident Test Conditions (Contents VIII)	(II)-C-20
Table (II)-D.1	Summary Listing of Maximum Dose Equivalent Rates	(II)-D-7
Table (II)-D.2	Burn-up Conditions for Radiation-Source Intensity Calculations	(II)-D-10
Table (II)-D.3	Burn-up Conditions for Radiation-Source Intensity Calculations	(II)-D-11
Table (II)-D.4	Contents-I Radiation-Source Intensity Calculation Results	(II)-D-12
Table (II)-D.5	Contents-IV Radiation-Source Intensity Calculation Results	(II)-D-13
Table (II)-D.6	Contents-V Radiation-Source Intensity Calculation Results	(II)-D-14
Table (II)-D.7	Contents-VI Radiation-Source Intensity Calculation Results	(II)-D-15
Table (II)-D.8	Contents-VII Radiation-Source Intensity Calculation Results	(II)-D-16
Table (II)-D.9	Contents-VIII Radiation-Source Intensity Calculation Results	(II)-D-17
Table (II)-D.10	Gamma Ray Source Specification (For Shield Analysis)	(II)-D-18
Table (II)-D.11	Contents-II Radiation-Source Intensity Calculation Results	(II)-D-19
Table (II)-D.12	Contents-III Radiation-Source Intensity Calculation Results	(II)-D-20
Table (II)-D.13	Specifications of Neutron Sources (For Shield Analysis)	(II)-D-20
Table (II)-D.14	Number Density of Atom in Each Region of the Shield Analysis Model	(II)-D-38
Table (II)-D.15	Gamma Ray Energy Group Structure and Gamma Ray Radiation-Source Spectrum (Contents I)	(II)-D-40
Table (II)-D.16	Gamma Ray Energy Group Structure and Gamma Ray Radiation-Source Spectrum (Contents II)	(II)-D-41
Table (II)-D.17	Gamma Ray Energy Group Structure and Gamma Ray Radiation-Source Spectrum (Contents III)	(II)-D-42
Table (II)-D.18	DLC23 Neutron Group Structure, Nuclear Fission Spectrum, and Dose Equivalent Rate Conversion Factor	(II)-D-44
Table (II)-D.19	The Maximum Dose Equivalent Rates under Different Conditions	(II)-D-47
Table (II)-E.1	Specifications of Contents	(II)-E-4
Table (II)-E.2	Moderating Power and Ratio of Water and Resin	(II)-E-7

Table (II)-E.3	Number Density of Atom of Package-in-Isolation and Array-of-Package Analysis Models	(II)-E-12
Table (II)-E.4	Calculation Results	(II)-E-14
Table (II)-F.1	Evaluations of Compliance to the Ordinance of the Prime Minister's Office and Notification of the Science and Technology Agency	(II)-F-2

CHAPTER III

Table (III)-1	Applicable Specifications for Main Materials	(III)-33
Table (III)-2	Welding Materials	(III)-34
Table (III)-3	Special Materials	(III)-35
Table (III)-4	Characteristics of Main Materials	(III)-36
Table (III)-5	List of Method of Welding Procedures	(III)-40
Table (III)-6	Weld Groove	(III)-41
Table (III)-7	Instructions for Inspection during Manufacture and upon Completion of the Packagings	(III)-60
Table (III)-8	Packaging Manufacturing Schedule	(III)-66

CHAPTER IV

Table (IV)-1	Manual for Inspections before Shipping the Package	(IV)-7
Table (IV)-2	List of Periodic Inspections	(IV)-21
Table (IV)-3	Maintenance Plan for Replacement Parts	(IV)-22

CHAPTER I EXPLANATION OF THE PACKAGE

(I)-A Objectives and Conditions

1. Usage Objectives

The packaging is used to transport irradiated uranium/plutonium mixed oxide fuel as well as test pieces of structural materials from nuclear reactors, both at home and abroad, to facilities operated by the Power Reactor and Nuclear Fuel Development Corporation (e.g., the Oarai Engineering Center).

2. Packaging model : TN6-4
3. Package type : Type B(U) package (fissile)
4. Allowable number of packages : No restriction
5. Transport index : 6.6
6. Package weight : Max. 11,000 kg
7. Outer dimensions of packaging : Length: approx. 3,270 mm
Width: approx. 1,400 mm
Height: approx. 1,400 mm
8. Packaging weight : Approx. 10,900 max. kg
9. Main packaging materials : Outer shell, inner shell, intermediate shell, lids/covers:
Stainless steel (SUS304)

Shielding materials : Lead (as per JIS H2105), resin (approx. 52% resin,
approx. 14% aluminum hydroxide, approx. 24%
polypropylene) and a tungsten alloy (containing 95%
tungsten)

Heat dispersion fins : Copper (C1020P)
Heat insulator : Alumina cement (approx. 70% alumina cement and
30% water)

Shock-absorption materials : Balsa wood, fir-plywood

Inner container, fuel supporting cans, supporting cans, racks, receiving tubes: Stainless
steel (SUS304)
10. Specifications of radioactive material accommodated by the packaging: As per Table (I)-1
11. Transportation method
Transportation by road shall be conducted by truck, whereas transportation by sea shall be
conducted by freighter.
12. Cooling system
Natural-air cooling

(I)-B Package Type

Type B(U) package for fissile material

Table (I)-1 Specifications of radioactive materials to be accommodated

	Contents I	Contents II	Contents III	Contents IV	Contents V	Contents VI	Contents VII	Contents VIII
Classification	Uranium/plutonium mixed oxide fuel	Uranium/plutonium mixed oxide fuel	Radioactive stainless steel	Uranium/plutonium mixed oxide fuel	Uranium/plutonium mixed oxide fuel	Uranium/plutonium mixed oxide fuel	Uranium/plutonium mixed oxide fuel	Uranium/plutonium mixed oxide fuel
Weight	2,160 g or less	432 g or less	not applicable	1,960 g or less	1,960 g or less	1,590 g or less	7,140 g or less	1,710 g or less
Oxide mixtures (Fissile substances)	990 g or less	324 g or less	not applicable	2,632 or less	2,632 g or less	740 g or less	150 g or less	1,535 g or less
Uranium oxides (Fertile substances)	428 g or less	57 g or less	not applicable	388 g or less	233 g or less	337 g or less	171 g or less	423 g or less
Pu-fissile	1,197 g or less	273 g or less	not applicable	1,113 g or less	327 g or less	881 g or less	47 g or less	1,032 g or less
U-235	2,650 g or less	594 g or less	5,000 g or less	2,385 g or less	2,385 g or less	1,470 g or less	1,800 g or less	1,705 g or less
Test pieces from structural or cladding materials								
Level of radioactivity	2.03×10^{15} Bq or less	4.96×10^{14} Bq or less	1.63×10^{14} Bq or less	1.99×10^{15} Bq or less	3.85×10^{14} Bq or less	1.97×10^{15} Bq or less	3.74×10^{13} Bq or less	1.27×10^{15} Bq or less
State	Solid (Sintered metal)	Solid (Sintered metal)	Solid (Metal)	Solid (Sintered metal)	Solid (Sintered metal)	Solid (Sintered metal)	Solid (Sintered metal)	Solid (Sintered metal)
Plutonium enhancement and uranium enrichment								
Plutonium enhancement	31% PuO ₂ or less	21% PuO ₂ or less	not applicable	31% PuO ₂ or less	18% PuO ₂ or less	31% PuO ₂ or less	3.2% PuO ₂ or less	31% PuO ₂ or less
Uranium enrichment	90% or less	90% or less	not applicable	90% or less	23% or less	90% or less	0.72% or less	97% or less
Burnup	90,000 MWD/MTM or less	150,000 MWD/MTM or less	not applicable	90,000 WMD/MTM or less	5,200 MWD/MTM or less	110,000 MWD/MTM or less	11,000 MWD/MTM or less	200,000 MWD/MTM or less
Fluence	17×10^{22} nvt or less	17×10^{22} nvt or less	50×10^{22} nvt or less	17×10^{22} nvt or less	7.5×10^{22} nvt or less	17×10^{22} nvt or less	1×10^{21} nvt or less	50×10^{22} nvt or less
Total decay heat	260 W or less	64 W or less	30 W or less	250 W or less	63 W or less	260 W or less	3 W or less	170 W or less
Cooling time	180 days or more	180 days or more	300 days or more	180 days or more	93 days or more	300 days or more	3600 days or more	360 days or more

(I)-C Packaging

C.1 Outline of Packaging

This is a dry-type packaging. As shown in Fig. (I)-1, it consists primarily of an outer container, front and rear shock absorbers, and a transport skid which serves as an attachment. The packaging body is cylindrical, with an outer diameter of approx. 0.8 m and length of approx. 2.6 m. Attached to its ends are the front and rear shock absorbers, each measuring approx. 1.4 m in outer diameter and approx. 0.8 m in length. The packaging measures approx. 3.3 m in overall length and has a total weight of approx. 11 tons.

As shown in Fig. (I)-2, the outer container body consists of outer and inner shells, which is a double-cylindrical structure, and the front and rear lid units that are connected to the ends of the outer container. Going from the outermost layer to the inner layer, the space between the outer and inner shells of the outer container is filled with resin to shield against neutrons, then with cement to secure an adequate degree of heat insulation under accident test conditions, and then with lead to shield against gamma rays. In the resin layer, several columns of heat dispersion fins made of copper welded on the inner surface of the outer shell in the longitudinal direction are inserted in order to dissipate heat that has been generated within the package during transport under normal conditions. Furthermore, to allow gases that develop within the cement layer to escape under accident test conditions, thereby preventing a buildup of excessive pressure in the outer container, a total of eight small bore holes are furnished, which penetrate the resin layer and the fin and reach the surface of the outer shell. Each hole is blocked by a fusible plug (made of bismuth).

As shown in Fig. (I)-3, the lifting trunnions, the pivoting trunnions, the four lifting lugs for horizontal operation, and the four fastening lugs in vertical position are furnished on the outer surface of the outer shell. The lifting trunnions are used to vertically hang the package as shown in Fig. (I)-4, while the pivoting trunnions serve as a rotation axis when the package is raised from a horizontal position to an upright position (or vice versa) on the transport skid. The pivoting trunnions are also used in conjunction with the rear base plate to tie the package onto the transport skid, as shown in Fig. (I)-3.

The rear and front base plates are used when the package is placed horizontally on a floor other than the transport skid. The lifting lugs for horizontal operation are used to hang the package in a horizontal position as shown in Fig. (I)-5, while the fastening lugs in vertical position are used to tie down the outer container in a vertical position when the contents are put in or taken out of the container. Bolts are inserted into the holes of the fastening lugs in vertical position and sealed to prevent the lugs from being used when hanging the package in a horizontal position or for a purpose other than that originally intended.

In the vicinity of both ends of the outer container, penetration holes are provided for operating the front/rear sampling valves as shown in Fig. (I)-2 from the outside, (hereafter called the "penetration hole for sampling valve") and another penetration hole is provided in the vicinity of the front end to permit the insertion of a handle when actuating the rotating plug (hereafter called the "penetration hole for the rotating plug") which will be explained later. These penetration hole parts are built such that gas-tight sealing is achieved by means of front and rear sampling valve lids and the penetration hole lid, all of which feature double O-ring sealing. Each of these lids has a leakage test hole which is used when a leakage test (halogen leakage test) is conducted on the package prior to shipment. Each of these leakage test holes is hermetically sealed with an O-ring-equipped plug. The sampling valves are used to extract

small amounts of air from the interior. These samples are then measured for radioactive contamination. The sampling valves are fixed to the seat located inside the inner shell of the outer container.

The locking plug is inserted through the penetration hole for the rotating plug into a hexagonal hole pierced through the inner shell of the outer container to the extreme end of the rotating plug in order to fix the rotating plug in place during transport. Furthermore, the locking plug is fastened to the inner shell by being screwed down with an O-ring-equipped orifice plug.

Structurally, the rear end of the outer shell is sealed by the shielding plug and then the rear lid, whereas the front end of the outer shell is sealed by the rotating plug lid and the front lid. (Fig. (I)-6) In conjunction with the front and rear sampling valve lids, the penetration hole lid, and the inner shell, these lids equipped with O-rings form the boundary of containment. As with the front and rear sampling valve lids and the penetration hole lid, the front and rear lids are equipped with double-O-ring sealing and leakage test holes for use when performing a leakage test prior to shipment.

The rear lid unit consists of the shielding plug, the shielding plug lid, and the rear lid, as shown in Fig. (I)-6.

The shielding plug is designed to retain the shielding plug (which, as discussed later on, is installed at the end of rear side to enhance the shielding effect in the longitudinal direction of the package) together with the locking plate, and is bolted on the end plate of the rear side of the shell of the outer container. Just like the shielding plug, the shielding plug lid is made of lead and a tungsten alloy in order to enhance the shielding effect. As shown in Fig. (I)-7, the rear lid is fixed to the plug lid with bolts. The inner container is removed from the outer container by using the following procedure. First, the rear lid is removed. Then the threaded portion of a connector of the lifting apparatus (when vertical lifting work is required) or a horizontal-operation bar (when horizontal work is required) is connected to the threaded portion of the shielding plug. Then the shielding plug lid is separated from the shielding plug by unlocking the locking plate to remove the inner container connected to the shielding plug. At this time, the removed inner container with its shielding plug can be introduced directly into a cell.

As shown in Fig. (I)-6, the front lid consists of the rotating plug, the rotating plug lid, the rotating plug lid cover, and the front lid. The rotating plug lid is combined with the rotating plug lid cover into a single piece to accommodate the rotating plug inside, then bolted to the end plate of the shell of the outer container. As shown in Fig. (I)-8, the rotating plug is a thick disk with a shaft. A cylindrical penetration hole whose diameter is the same as the inner diameter of the inner shell is bored perpendicular to the shaft.

The rotating plug is integrated into the rotating plug lid and the rotating plug lid cover in such a manner that the axis of the shaft coincides with that of the outer container's penetration hole for the rotating plug. The tips of the shaft are supported with bearings provided inside the front lid unit. A hexagonal socket is provided at the tip of this shaft. The rotating plug can be opened/closed by inserting a handle which fits into this hexagonal socket through the penetration hole for rotating plug and by rotating this handle 90 degrees from the outside of the container. Since the rotating plug must be held in the closed position during transport as mentioned earlier, the locking plug is inserted into the hexagonal socket of the rotating plug shaft. Furthermore, the O-ring-equipped orifice plug is inserted on top of the locking plug to anchor the rotating plug

to the inner shell. The rotating plug is made of lead and a tungsten alloy to enhance the shielding effect in the axial direction during transport. The front lid is fixed on the rotating plug lid with bolts.

Shock absorption equipment consists of front and rear shock absorbers. As shown in Fig. (I)-2, the shock absorbers are bolted to the end plates of the outer container to lessen the impact of a possible drop. Each of these shock absorbers consists of a shock absorption section made up of balsa wood and fir-plywood, the stainless steel of plating sheath covering the shock absorber part, and a thermal insulation part filled with alumina cement. The role of the balsa wood in the shock absorber part is to lessen mechanical impact in the event that the packaging is dropped. Furthermore, a depression is provided at the bottom-end of the front/rear shock absorber in order to reduce the area of the bottom, thereby reducing the impact deceleration in the event of a vertical drop. To fill the depression, fir-plywood which is harder than balsa wood is used to prevent the package from being penetrated with a mild steel bar during Drop Test II under accident test conditions. Stainless steel is used as the cover plating of the shock absorbers. The cover plating at the depression is thicker than at any other place so that a mild steel bar will not penetrate the cover plating during Drop Test II. Balsa wood that has been treated for flame resistance is used so that its combustion rate may be kept to a minimum when subjected to a thermal test and its combustion will halt spontaneously upon removal of the heat, even if/when cracks and/or penetration openings would have developed in the balsa wood under the preceding Drop Tests I and II.

The front and rear shock absorbers cover all of the outer container's opening sections (the front and rear lid units, the front and rear sampling valve lids, and the penetration hole lid), and thereby protect those sections from direct collision during Drop Test II. Furthermore, the insides of the shock absorbers that come into contact with the outer container are filled with alumina cement which serves as a thermal insulator. In conjunction with the balsa wood and fir-plywood, the alumina cement prevents the influx of heat from the outside under accident test conditions (in the event of a fire), and thereby ensures the soundness of the O-rings used in the individual lids located in the opening sections.

The inner container is cylindrical and made of stainless steel. As shown in Fig. (I)-9, the inner container consists of the inner container tube, and the front and rear caps. Both the front and rear caps are equipped with O-rings, and are screwed into both ends of the inner container tube until they are tightly secured.

The shielding plug is tightened to the rear cap by means of the inner container screw. The inner container is removed with the shielding plug as mentioned earlier so that it can be placed into a cell as it is (See Fig. (I)-10). As will be discussed later, materials to be placed into this packaging include irradiated fuel elements (Contents I, II, IV, V, VI, VII, and VIII) and the test pieces of irradiated structural materials (Contents III). These are placed into the inner container in accordance with their type as follows:

Irradiated fuel elements (Contents I, II, IV, V, VI, VII, and VIII) are put into stainless-steel fuel supporting cans as shown in Figs. (I)-11, (I)-12, and (I)-13 (for Contents I, IV, V, VI, VII, VIII) or the stainless-steel receiving tube I as shown in Fig. (I)-14 on a one-on-one basis, and then fastened to the rack and placed into the inner container (Contents II). The activated test pieces of structural materials (stainless steel: Contents III) are placed directly into the inner container. The fuel supporting can I for holding Contents I, IV, and V, the supporting can for holding Contents VI, and the fuel supporting can II for holding Contents VII are of dual-cylinder construction as shown in Figs. (I)-15, (I)-16, and (I)-17. The annular space enclosed by the

annular space enclosed by the inner and the outer cylinders is divided into 5, 9, and 6 compartments, respectively, for the above three types of cans. The fuel supporting can I, the supporting can, and the fuel supporting can II are able to accommodate up to 15, 9, and 6 fuel elements, respectively. The lids of the fuel supporting cans I and II are welded down after fuel elements have been housed. Then the air inside is replaced with helium through the penetration hole in the grip portion which is attached to the lid. After completion of this replacement operation, the penetration hole is sealed by welding.

The lid of the supporting can is screwed in after fuel elements have been placed inside.

Fuel elements are put into the supporting can after they have been hermetically contained by welding in the receiving tube II which is identical in construction to the receiving tube I discussed later (See Fig. (I)-19.).

The receiving tube I, as shown in Fig. (I)-18, is made up of a tube section with a bottom plate and an O-ring-equipped plug section. Fuel elements are placed into the tube section, then the plug is screwed in. Next, the plug and the tube are welded together. Up to six units of this receiving tube I can be placed on a rack (Figs. (I)-20 and (I)-21).

The transport skid which is an attachment to the packaging is made of rolled steel used for general structures. The skid is provided with front and rear fixing devices.

The rear fixing device is designed to fasten the rear base plate of the outer container to the transport skid, while the front fixing device is designed to tie down the outer container to the transport skid by supporting the outer container's pivoting trunnions with the bearing supports and by fastening the retaining pieces to the supports.

The main components of the packaging are shown in Table (I)-2. The weight of each individual component, principal dimensions, and major materials in use are listed in Table (I)-3.

C.1.1 Boundary of Containment

The boundary of containment of the packaging is shown in Fig. (I)-22. The boundary of containment consists of inner surfaces of the inner shell of the outer container body and the following individual opening-closing lids: the front and rear sampling valve lids, the penetration hole lid, the shielding plug lid and the rear lid that combine to form the rear lid unit, and the rotating plug lid and the front lid that combine to form the front lid unit.

The lids of the individual openings employ O-ring-sealed construction to maintain gas-tight conditions. The sampling valves located inside the boundary of containment and the orifice plug used to tie down the rotating plug to the inner shell, include also of O-ring-equipped gas-tight construction. In addition, the fuel supporting can and the receiving tubes, both of which are used to accommodate uranium/plutonium mixed oxide fuel and the like, include also secondary containment systems although they are not categorized as containment systems on the basis of containment design criteria.

The lid units at the ends of the packaging body are covered with front and rear shock absorbers so that a mild steel bar will not directly hit either of the lid units during the Drop Test II under accident conditions.

C.1.2 Lifting Device and Fastening Device

The packaging comprises an outer container, and front and rear shock absorbers. The structure, configuration and objective of the individual constituent units are discussed below.

The lifting trunnions are used to vertically hang the package as shown in Fig. (I)-4 by using a special lifting yoke, while the pivoting trunnions serve as a rotation axis when the package is raised from a horizontal position to an upright position, and vice versa, on the transport skid. Furthermore, the pivoting trunnions are also used in conjunction with the rear base plate to tie the package down to the transport skid as shown in Fig. (I)-3. The lugs for horizontal operation are used to hang the package in a horizontal position as shown in Fig. (I)-5, using eyebolts and a four-point-hanging wire rope. The fastening lugs in vertical position are used to tie down the packaging in a vertical position by using wire ropes when the contents are removed or placed inside. Bolts are inserted into the holes in the fastening lugs in vertical position and sealed to prevent the lugs from being used by mistake when hanging the package in a horizontal position. The front and rear base plates are designed for use when the package is placed in a horizontal position on a surface other than the transport skid.

The front and rear shock absorbers shown in Fig. (I)-23 are each equipped with a shock-absorber sealing lug which is to be connected to the sealing lugs of the outer container to form a wire-type seal so that the outer container's lidded sections cannot be opened unintentionally. The front and rear shock absorbers are outfitted with two shock-absorber lifting lugs each on their sides. These lugs are used when shock absorbers are to be disconnected and lifted (by connecting wire ropes to the lifting rings for two-point slinging). The lifting rings and the lifting lugs are interconnected for sealing during transport to prevent them from accidentally being used to horizontally lift the package. The constituent components of the packaging's lifting devices are listed in Table (I)-4.

C.2 Structure

The packaging consists of an outer container and front and rear shock absorbers. The structure, configuration and objective of the individual constituent units are discussed hereafter.

C.2.1 Outer Container

As shown in Fig. (I)-24, the outer container consists largely of a dual-cylinder shell body, which is made up of outer and inner shells and front and rear lid units (See Fig. (I)-6) that are connected to the ends of the above shell body.

C.2.1.1 Shell of the Outer Container

(1) Outer and Inner Shells, Lifting Units and Base plates

The shell of the package is of double-shell construction consisting of an outer shell and an inner shell, both of which are made of stainless steel (SUS304). The space between the outer shell (measuring 800 mm in outer diameter, 2,532 mm in length, and 16 mm in thickness) and the inner shell is filled, going from the outermost layer to the inner layer, with a resin (thickness $t = 82$ mm: a mixture of resin, flame retardant, polypropylene, and glass fiber) to shield neutrons, then with cement (thickness $t = 10$ mm: a mixture of alumina cement and water) to prevent heat from entering under accident test conditions, and then with lead (thickness $t = 202$ mm) to shield gamma rays. In the resin layer, L-shaped heat dispersion fins [measuring 84 mm in width, 1,000 mm in length, and 2 mm in thickness, made of copper sheet metal (C1020P)], are welded in the longitudinal direction on the inner surface of the outer shell in order to dissipate heat generated within the contents during transport under normal conditions. Furthermore, in order to let gases that develop within the cement layer escape under accident test conditions, and thereby prevent the buildup of excessive pressure in the outer container, a total of eight small bore holes are drilled through the resin layer and the fin to reach the surface of the outer shell. Each individual hole is blocked by a fusible plug (made of bismuth, measuring 8 mm in maximum diameter, and 15 mm in length). These fusible plugs are designed to melt at temperatures above 271°C (the melting point of bismuth) to prevent the internal pressure from building up excessively. For manufacturing convenience, both ends of the packaging body partially employ triple-cylindrical construction. In other words, an intermediate shell [made of stainless steel (SUS304), measuring 600 mm in inner diameter and 6 mm in thickness] is provided in these portions, which is sandwiched between the resin layer and the cement layer.

As shown in Fig. (I)-2, lifting trunnions and pivoting trunnions are provided on the outer surface of the outer shell along with four lifting lugs for horizontal operation and four fastening lugs in vertical position. After the shock absorbers have been dismantled, the stainless steel (SUS304) lifting trunnions [as shown in Fig. (I)-25, measuring 100 mm in outer diameter and 65 mm in length], are used to raise the packaging from a horizontal position on the transport skid, to lay down the packaging from an upright position, or to move the packaging from one place to another while it is suspended in an upright position. The pivoting trunnions [as shown in Fig. (I)-25, measuring 100 mm in outer diameter, 65 mm in length, and made of stainless steel (SUS304)] are used as a rotation axis in conjunction with the lifting trunnions when the packaging is raised from a horizontal position to an upright position and vice versa. The pivoting trunnions are also used in conjunction with the rear base plate for transport to tie the packaging onto the transport

skid. The four lifting lugs for horizontal operation [Fig. (I)-26, measuring 180 mm in maximum width, approx. 230 mm in height, 30 mm in thickness, and made of stainless steel (SUS304)] are used to lift the package or the packaging in a horizontal position. The four fastening lugs in vertical position [measuring 200 mm in width, 100 mm in height, 20 mm in thickness, made of stainless steel (SUS304)] are used to fasten the packaging in the vertical position when contents are placed inside or removed from the container. The holes in the fastening lugs in vertical position are inserted with bolts to prevent these lugs from accidentally being used for horizontal lifting work or for some other purpose.

Furthermore, the rear base plate [as shown in Fig. (I)-27 measuring 280 mm in width, 650 mm in length, approx. 200 mm in height, and made of stainless steel (SUS304)] and the front base plate [as shown in Fig. (I)-27 measuring 270 mm in length, 650 mm in length, approx. 200 mm in height, and made of stainless steel (SUS304)] are welded to the surface of the outer container. The front and the rear base plates are used mainly when the packaging is placed in a horizontal position. The rear base plate is also used in conjunction with the pivoting trunnions to tie the package onto the transport skid as shown in Fig. (I)-28. One sealing lug [measuring 30 mm in width, 65 mm in height, 12 mm in plate thickness, and made of stainless steel (SUS304)] is welded to each end section of the outer shell of the outer container. These lugs are intended to be connected with the sealing lugs of the front and rear shock absorbers and sealed so that the shock absorbers covering the opening sections of the outer container will not be removed unintentionally during transport.

(2) Penetration Hole Parts of the Outer Container

In the vicinity of both extremities, penetration holes for sampling valves that permit the manipulation of these sampling valves [quick couplers made of stainless steel (SUS304)] from the outside are provided as shown in Fig. (I)-23, as well as the penetration hole for the rotating plug through which the handle that operates the rotating plug, discussed later, will be inserted. Structurally, each of these penetration holes is covered by a lid equipped with two O-rings [measuring 72 mm and 96 mm in diameter, respectively, 5.7 mm in width, and made of fluoro rubber], which are fastened to the shell of the outer container for gas-tight sealing by means of four hexagonal socket bolts [M12 \times 25, made of precipitation-hardening stainless steel (SUS630)]. A leakage test hole is provided between each pair of O-rings for use in leakage testing to be performed prior to shipment. These leakage test holes are sealed with O-ring-equipped plugs. The sampling valve lids (see Figs. (I)-29 and -30) and the penetration hole lid (see Fig. (I)-31) both contain lead in their stainless-steel cylindrical-shaped shells measuring 48.6 mm and 41.2 mm in outer and inner diameter, respectively, to shield gamma rays. Each lid has a stainless-steel disk flange (150 mm in diameter) at one end for fastening by bolts. Each sampling valve is mounted on a valve seat which is located in the inner shell of the outer container, and is used, as explained earlier, to sample the gas contained inside and to check the collected gas for radioactive contamination. The penetration hole for the rotating plug is used, as explained earlier, to insert the handle to actuate the rotating plug. The tip of the rotating plug's shaft is projecting at the bottom of the penetration hole. To prevent the rotating plug from turning during transport, a locking plug [made of precipitation-hardening stainless steel (SUS630)] is placed into the rotating plug shaft hole. In addition, the O-ring-equipped orifice plug [M52 \times 24, made of precipitation-hardening stainless steel (SUS630)] is screwed in for fastening the locking plug into inside the inner shell of the outer container.

C.2.1.2 Front and Rear Lid Units

The front and rear lid units are designed to cover the front and rear opening sections of the shell of the outer container. The rear lid unit, as shown in Fig. (I)-6, comprises the shielding plug, the shielding plug lid, and the rear lid, whereas the front lid unit is, as shown in Fig. (I)-4, made up of the rotating plug, the rotating plug lid, the rotating plug lid cover, and the front lid.

(1) Rear Lid Unit

The shielding plug [measuring 136 mm in maximum diameter, 210 mm in height, and made of stainless steel (SUS304), lead, and a tungsten alloy as shown in Fig. (I)-32] acts as a shield which is effective in the longitudinal direction of the packaging. Structurally, the interior of its stainless-steel cover plating is filled with lead and a tungsten alloy for use as shielding materials. The shielding plug can be attached to the inner container using the inner container screw [made of precipitation-hardening stainless steel (SUS630)], and insertion/removal of the inner container is to be performed with the shielding plug connected. Furthermore, the shielding plug is fastened to the shielding plug lid [measuring 365 mm in maximum diameter, 222.5 mm in height, and made of stainless steel (SUS304), lead and a tungsten alloy] as shown in Fig. (I)-33 through the locking plate [made of stainless steel (SUS304)], with the result that the inner container is also tied down. To remove or insert the inner container, the screw (threaded) portion of a connector of lifting apparatus (when lifting work is required) or a horizontal-operation bar (when horizontal work is required) is connected to the threaded portion of the shielding plug. Then, the locking plate is unlocked to undo the coupling between the shielding plug and the shielding plug lid. The shielding plug lid is tightened to the end plate of the shell of the outer container by means of 16 hexagonal socket head bolts [M20 × 45, made of precipitation-hardening stainless steel (SUS630)]. As with the shielding plug, shielding materials (lead and an alloy of tungsten) are used in the shielding plug lid in order to enhance the shielding effect in the longitudinal direction of the packaging. The shielding plug is hermetically tightened using an O-ring (measuring 280 mm in diameter and 8.4 mm in width, made of fluoro rubber), and constitutes an integral part of the boundary of containment.

The rear lid [measuring 220 mm in outer diameter, 24.5 mm in plate thickness, and made of stainless steel (SUS304) as shown in Fig. (I)-34] is hermetically anchored to the shielding plug lid using two O-rings (measuring 130 mm and 165 mm in diameter, 5.7 mm in width, and made of fluoro rubber) with 12 hexagonal socket head bolts [M12 × 25, made of precipitation-hardening stainless steel (SUS630)]. A leakage test hole is provided between these O-rings for use in leakage testing to be performed prior to shipment. Furthermore, a mechanism to lock the coupling between the locking plate and the shielding plug by preventing the movement of the shielding-plug locking plate (Fig. (I)-32) mentioned earlier is housed on the inner surface of this lid. By virtue of this construction, the position of the shielding plug will remain fixed unless this lid is removed.

(2) Front Lid Unit

As shown in Fig. (I)-6, the front lid unit consists of a rotating plug, rotating plug lid, rotating plug lid cover, and a front lid. The rotating plug lid is combined with the rotating plug lid cover to form a single piece to house the rotating plug and is fastened with bolts to the end plate of the shell of the outer container. Structurally, the front lid is further anchored to the rotating plug lid with bolts.

The rotating plug [measuring 284 mm in outer diameter, 333 mm in height, and made with stainless steel (SUS304), lead, and a tungsten alloy] is a thick disk having a center axial rod (shaft) as shown in Fig. (I)-35. It has a cylindrical penetration hole which is bored perpendicular to the axis of the shaft and whose diameter is the same as the inner diameter (inner diameter $\phi = 142$ mm) of the inner shell.

The rotating plug is integrated into the rotating plug lid and the rotating plug lid cover in such a manner that the axis of the shaft coincides with that of the outer container's penetration hole for the rotating plug, and the tip of the shaft is supported with bearings provided inside the rotating plug lid unit. A hexagonal socket is provided at the tip of this shaft, and the rotating plug can be opened/closed by inserting a handle which fits into this hexagonal socket through the penetration hole for rotating plug, and by rotating this handle 90 degrees from the outside of the container.

In the rotating plug, lead and a tungsten alloy are used to enhance its shielding effect in the longitudinal direction during transport. Since the rotating plug must be held in its closed position during transport as mentioned earlier, the locking plug is inserted into the hexagonal socket provided in the shaft end of the rotating plug through the penetration hole for the rotating plug in order to fix it to the inner shell. Furthermore, the O-ring-equipped orifice plug is inserted to keep the locking plug in place and hermetically seal the unit.

The rotating plug lid [measuring 520 mm in maximum diameter, 345.5 mm in height, and made of stainless steel (SUS304), lead, and bronze (BC2) as shown in Fig. (I)-36] pairs with the rotating plug lid cover [measuring 304 mm in width, 348 mm in length, 101 mm in thickness, and made of stainless steel (SUS304), lead, and bronze (BC2) as shown in Fig. (I)-37] to house the rotating plug as mentioned above. Since the rotating plug lid is used to support the rotation of the rotating plug, it is equipped with a bearing (BC2).

The combined rotating plug lid and the rotating plug lid cover are fastened to the end plate of the outer container with 20 hexagonal socket head bolts [M20 \times 45, made of precipitation-hardening stainless steel (SUS630)] to form a hermetically sealed structure together with the front lid to be discussed below.

The front lid [measuring 272 mm in outer diameter, 46.5 mm in maximum thickness, and made of stainless steel (SUS304) as shown in Fig. (I)-38] is secured to the rotating plug lid using two O-rings [one measures 165 mm and the other measures 195 mm in outer diameter, both measure 5.7 mm in width, and are made of fluoro rubber] with 12 hexagonal socket head bolts [M12 \times 25, made of precipitation-hardening stainless steel (SUS630)] to form a hermetically sealed structure. A leakage test hole is provided between these O-rings for use in leakage testing to be performed prior to shipment.

Pins are attached to the inside of the front lid. Structurally, these pins mate with the corresponding holes in the rotating plug to lock the rotating plug in the closed position, thereby preventing the rotating plug from turning during transport.

C.2.2 Front and Rear Shock Absorbers

Shock-absorption equipment consists of front and rear shock absorbers. They are fastened to the end plates of the shell of the outer container, each with 12 hexagonal socket head bolts [M24 × 65, made of precipitation-hardening stainless steel (SUS630)] to help lessen the impact caused by a possible drop.

These shock absorbers cover the penetration hole parts, namely the front and rear lid units, the front and rear sampling valve lids, and the outer surfaces of the penetration hole lid, in order to protect those sections from direct collision in the course of Drop Test II, which is performed under accident test conditions.

Furthermore, a depression is provided at the bottom-end of the front/rear shock absorber, in order to reduce the area of the bottom, and thereby to reduce the impact deceleration in the event of a vertical drop.

The front and rear shock absorbers are identical in outer shape and dimensions, and each is made up of stainless-steel cover plating, the shock-absorption section consisting of balsa wood and fir-plywood, and the thermal-insulation section which is the alumina cement layer. The front and rear shock absorbers (each measuring 1400 mm in outer diameter and 750 mm in height) are sheathed with stainless steel (SUS304). Ten fusible plugs [measuring 8 mm in maximum diameter, 15 mm in length, and made of bismuth] are mounted on the cover plating of each shock absorber in order to allow gases that develop within the cement layer as well as in the balsa wood and fir-plywood escape under accident test conditions (in the event of a fire), thereby preventing the buildup of excessive pressure in the shock absorber.

Two shock-absorber lifting lugs are welded on the periphery of each shock absorber. During transport, these lugs are sealed to prevent them from accidentally being used for hanging the package in a horizontal position. The shock absorber parts are mainly filled with flame-resistance-treated balsa wood in order to lessen the impact on the package resulting from a possible drop from any attitude. As shown in Fig. (I)-23, balsa wood prepared in block form is packed into the shock absorbers in such a manner that the grain of the individual blocks is oriented to produce the best possible shock-absorption effect. Since the balsa wood in use has been treated for flame resistance, it does not burn easily and its combustion may come to a halt swiftly in the course of a thermal test upon the completion of heat application, even if/when the stainless-steel surface cover plating would have been pierced and perforated during the preceding Drop Tests I and II conducted under accident test conditions.

The fir-plywood charged into the depressions in the midsections of the shock absorbers is harder than balsa wood, and its major role is to prevent penetration by a protruding object in Drop Test II, etc. Furthermore, the portion of the stainless-steel surface cover plating covering the fir-plywood is rendered thicker than the portion covering the balsa wood-filled section so as to prevent the possibility of penetration during Drop Test II.

Since these shock absorbers fully cover the opening sections of the outer container, they structurally provide heat insulation under accident test conditions (in the event of a fire) and thereby prevent the O-rings that are used in each individual lid from heating up, thereby ensuring the soundness of these O-rings.

C.2.3 Inner Container and Receiving Containers

Contents that are to be accommodated into the packaging are, as discussed later, irradiated mixed fuel elements (Contents I, II, IV, V, VI, VII, and VIII) and test pieces of radioactivated structural materials (Contents III).

Receiving containers for accommodating Contents I, IV, and V are fuel supporting cans I (there are, however, cases where they are used to hold Contents III: test pieces of radioactivated structural materials), whereas receiving containers for holding Contents VII are fuel supporting cans II. The receiving containers for accommodating Contents VI and VIII are supporting cans and receiving tubes II, whereas the containers for accommodating Contents II are receiving tubes I and racks.

Structurally, these receiving containers are put into the inner container prior to consolidated accommodation into the packaging.

The inner container and receiving containers are explained hereafter.

(1) Inner Container (Fig. (I)-9)

The inner container [measuring 139 mm in maximum diameter, 2,030.8 mm in length, and made of stainless steel (SUS304)] is a cylindrical-shaped container designed to accommodate receiving containers (fuel supporting cans I and II as shown in Figs. (I)-15 and -17), which are discussed below, or receiving tubes I and II (Figs. (I)-18 and -19) and racks (Figs. (I)-20 and -21), or directly hold radioactivated structural materials. Both top and bottom sections feature a construction in which a cap equipped with an O-ring [measuring in 99.5 mm in inner diameter, 3.5 mm in width, and made of fluoro rubber] is screwed in, making it possible to put in/take out contents through the top or bottom section.

Furthermore, the caps have a provision to prevent loosening due to extraneous impact and vibration. A spacer is welded on the outer surface so that proper on-center alignment with the inner shell can be achieved during transport.

(2) Receiving Containers

Receiving containers are classified according to their structure as follows: fuel supporting cans I and II as well as supporting cans are referred to as fuel supporting cans, whereas receiving tubes I and II are categorized as receiving tubes.

(2)-1 Fuel Supporting Cans

Fuel supporting cans consist of fuel supporting can I (as shown in Fig. (I)-15), fuel supporting can II (as shown in Fig. (I)-17) and the supporting can (as shown in Fig. (I)-16). Although they feature a dual-cylinder construction made up of an outer cylinder and an inner cylinder, they differ from one another in terms of the maximum number of fuel pins that can be held, and the type of atmosphere inside the fuel-pin-holding cavity.

The fuel supporting can I [measuring 89.1 mm in outer diameter, 1,944.5 mm or less in length, and made of stainless steel (SUS304)] is used largely for accommodating Contents I (low-burnup pins). It is designed to be hermetically sealed by welding and features a dual-cylinder construction made up of an outer cylinder [measuring 89.1 mm in outer

diameter, 83.1 mm in inner diameter, 1,906 mm or less in length, and made of stainless steel (SUS304)] and an inner cylinder [measuring 60.5 mm in outer diameter, 57.2 mm in inner diameter, 1,890 mm or less in length, and made of stainless steel (SUS304)].

Irradiated fuel pins are accommodated in the annular space enclosed by the inner and outer cylinders. This annulus-shaped space is divided into five compartments. Each compartment is designed to hold up to three fuel pins. In this way, fuel pins can be accommodated so as to prevent uneven distribution during transport. After fuel pins have been placed inside, the rear lid is welded and the air inside is replaced with helium through the penetration hole in the grip portion which is attached to the rear lid. On completion of this replacement operation, this penetration hole is welded to ensure gas-tight sealing. The helium gas has a double function of improving heat transfer and serving as a tracer gas in leakage test of fuel supporting can I. Since fuel supporting can I is hermetically sealed by welding as explained above, it is referred to as a "secondary containment system."

The fuel supporting can II [measuring 89.1 mm in outer diameter, 1,944.5 mm or less in length, and made of stainless steel (SUS304)] is used largely for accommodating Contents VII (low-burnup pins). It is designed to be hermetically sealed by welding and features a dual-cylinder construction made up of an outer cylinder [measuring 89.1 mm in outer diameter, 83.1 mm in inner diameter, 1,906 mm or less in length, and made of stainless steel (SUS304)] and an inner cylinder [measuring 42.7 mm in outer diameter, 39.4 mm in inner diameter, 1,809 mm or less in length, and made of stainless steel (SUS304)].

Irradiated fuel pins are accommodated in the annular space enclosed by the inner and outer cylinders. This annular-shaped space is divided into six compartments, so that fuel pins can be accommodated separately in order to prevent uneven distribution during transport. After fuel pins have been placed inside, the rear lid is welded and the air inside is replaced with helium through the penetration hole in the grip portion attached to the rear lid. On completion of this replacement operation, this penetration hole is welded to provide gas-tight sealing. The helium gas has the double function of improving heat transfer and serving as a tracer gas in leakage test of fuel supporting can II. Since fuel supporting can II is hermetically sealed by welding as discussed above, it is referred to as a "secondary containment system."

The supporting can [measuring 89.1 mm in outer diameter, 1,944.5 mm or less in length, and made of stainless steel (SUS304)] is mainly used to hold Contents VI (low-burnup pins). It features a dual-cylinder construction made up of an outer cylinder [measuring 89.1 mm in outer diameter, 83.1 mm in inner diameter, 1,906 mm or less in length, and made of stainless steel (SUS304)] and an inner cylinder [measuring 32.7 mm or more in outer diameter, 1.65 mm or more in wall thickness, 1,890 mm or less in length, and made of stainless steel (SUS304)].

Irradiated fuel pins are accommodated in the annular space enclosed by the inner and outer cylinders. This annulus-shaped space is divided into nine compartments. Each compartment holds one fuel pin loaded in receiving tube II discussed below to keep fuel pins separated from each other and thereby preventing uneven distribution in transport. After fuel pins have been loaded inside, the rear lid is screwed in.

(2)-2 Receiving Tubes and Rack (Figs. (I)-18 ~ -21)

Receiving tubes consist of receiving tube I (Fig. (I)-18) and receiving tube II (Fig. (I)-19).

Receiving tube I [measuring 13.8 mm in outer diameter, 10.5 mm in inner diameter, 1,035 mm or less in length, and made of stainless steel (SUS304)] is designed to accommodate Contents II (a high-burnup pin). After a single high-burnup fuel pin has been placed inside, a plug equipped with an O-ring (measuring 7.8 mm in diameter, 1.9 mm in width, and made of fluoro rubber) is screwed in, after which the receiving tube is hermetically sealed by welding.

Receiving tube II [measuring 22 mm or less in outer diameter, 1.5 mm or more in wall thickness, 1,880 mm or less in length, and made of stainless steel (SUS304)] is designed to accommodate Contents VI (a low-burnup pin). After a single low-burnup fuel pin has been placed inside, a plug equipped with an O-ring (measuring 12.8 mm in inner diameter, 2.4 mm in width, and made of fluoro rubber) is screwed in, after which the receiving tube is hermetically sealed by welding.

The rack [measuring 92 mm in maximum diameter, 1,944.5 mm or less in length, made of stainless steel (SUS304)] is capable of accommodating up to six pieces of receiving tube I discussed above in groups in order to prevent uneven distribution. To facilitate rack withdrawal in relatively narrow cells, it employs a three-part split construction.

Receiving tube I is hermetically sealed by welding as mentioned above, and is referred to as a "secondary containment system."

C.2.4 Transport Skid (Fig. (I)-28)

The transport skid [measuring approx. 1,500 mm in width, approx. 2,700 mm in length, approx. 965 mm in height, and made of rolled steel used for general structures (SS41)] is used to transport the packaging in a horizontal position. It is constructed chiefly with shaped steel and features a construction in which the weight of the packaging is borne by the supports, which support the pivoting trunnions of the packaging, and the base carrier which retains the rear base plate.

The fixing equipment consists of the rear fixing device and the front fixing device. The rear fixing device is designed to secure the rear base plate of the packaging to the base carrier of the transport skid with six hexagonal socket head bolts [M24, made of chromium-molybdenum steel (SCM4345)]. With this construction, it is capable of withstanding acceleration which takes place during transport in conjunction with the front fixing device.

The front fixing device is designed to support the packaging's pivoting trunnions by means of bearing-type supports, and to fasten the retaining pieces to the supports with four stud bolts [M20, made of chromium-molybdenum steel (SCM435)]. By virtue of this construction, and in conjunction with the rear fixing device, it is capable of withstanding acceleration which is produced during transport.

Table (I)-2 Table of Components of the Packaging

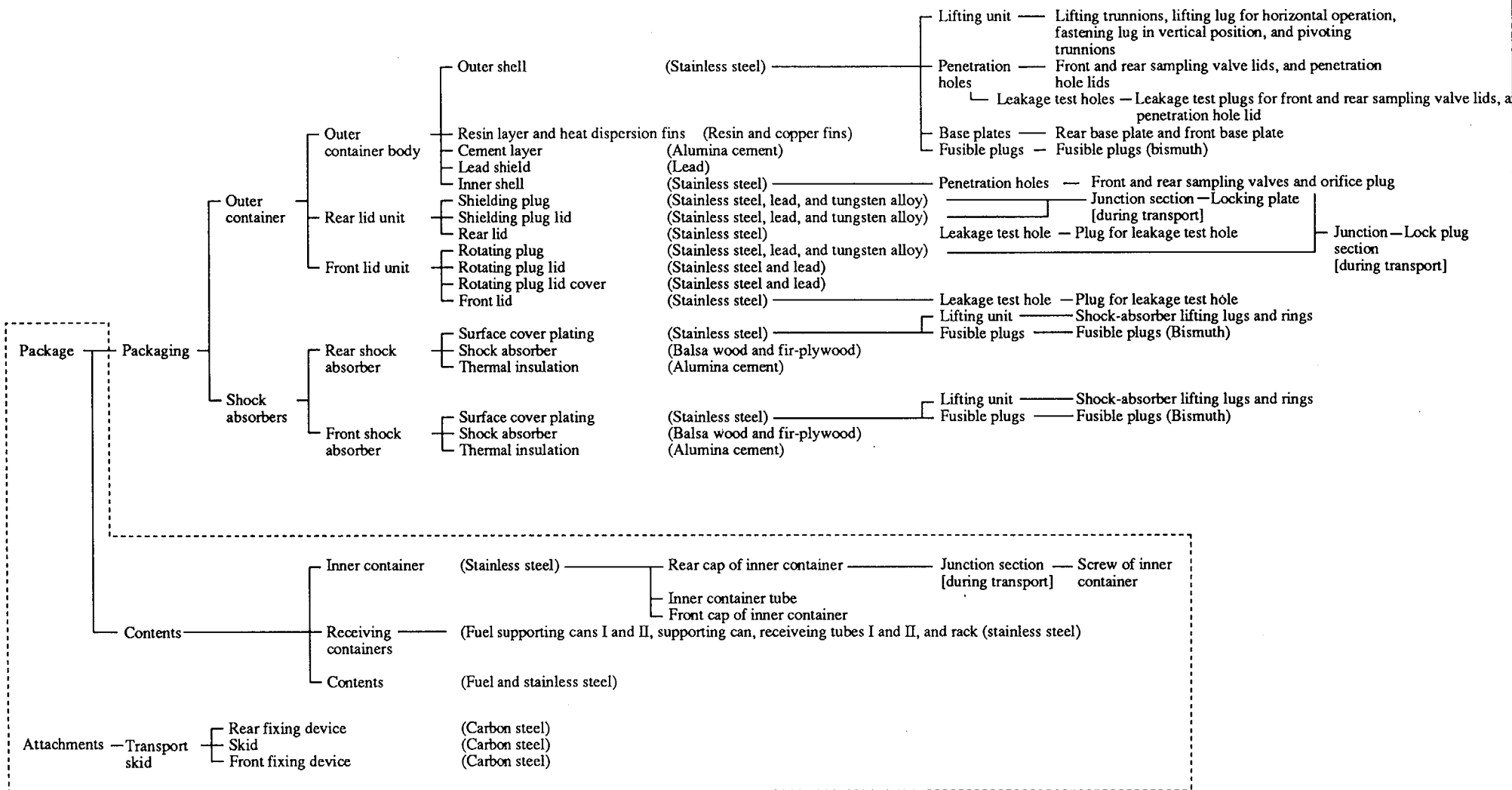


Table (I)-3 Weight, dimensions, and materials of the constituent components of the packaging (1/2)

Constituent component	Major materials in use	Design weight	Outside dimensions
1. Outer container body	Stainless steel (SUS304 or SUS304 equivalent) Lead, resin, and balsa wood, copper (C1020P), and alumina cement	(approx.) (kg) 8,750	Outer dia. $\phi = 800 \times$ Length $\ell = 2,564$ (mm)
2. Shielding plug lid	Stainless steel (SUS304), lead, fluoro rubber (O-ring), and tungsten alloy	120	Max. dia. $\phi = 365 \times$ Height $H = 222.5$
3. Shielding plug	Stainless steel (SUS304), lead, and tungsten alloy	30	Max. dia. $\phi = 136 \times$ Height $H = 210$
4. Rotating plug lid	Stainless steel (SUS304), lead, gunmetal (BC2), and fluoro rubber (O-rings)	220	Max. dia. $\phi = 520 \times$ Height $H = 345.5$
5. Rotating plug lid cover	Stainless steel (SUS304) and lead	75	Width $W = 304 \times$ Length $\ell = 348 \times$ Thickness $t = 101$
6. Rotating plug	Stainless steel (SUS304), lead, and tungsten alloy	125	Outer dia. $\phi = 284 \times$ Height $H = 333$
7. Rear sampling valve lid	Stainless steel (SUS304), lead, and fluoro rub- ber (O-rings)	6	Max. dia. $\phi = 150 \times$ Height $H = 161$
8. Front sampling valve lid	Stainless steel (SUS304), lead, and fluoro rub- ber (O-rings)	5	Max. dia. $\phi = 150 \times$ Height $H = 91$
9. Penetration hole lid	Stainless steel (SUS304), lead, and fluoro rub- ber (O-rings)	6	Max. dia. $\phi = 150 \times$ Height $H = 148$
10. Rear lid	Stainless steel (SUS304) and fluoro rubber (O-rings)	7	Outer dia. $\phi = 220 \times$ Plate thickness $t = 24.5$
11. Front lid	Stainless steel (SUS304) and fluoro rubber (O-rings)	15	Outer dia. $\phi = 272 \times$ Max. thickness $t = 46.5$

Table (I)-3 Weight, dimensions, and materials of the constituent components of the packaging (2/2)

Constituent component	Major materials in use	Design weight	Outside dimensions
12. Rear shock absorber	Stainless steel (SUS304), balsa wood, fir-plywood, and alumina cement	(approx.) (kg) 750	(mm) Outer dia. $\phi = 1,400 \times$ Height $H = 750$
13. Front shock absorber	Stainless steel (SUS304), balsa wood, fir-plywood, and alumina cement	750	Outer dia. $\phi = 1,400 \times$ Height $H = 750$
14. Inner container	Stainless steel (SUS304) and fluoro rubber (O-rings)	35	Max. dia. $\phi = 139 \times$ Length $\ell = 2,030.8$
15. Fuel supporting can I	Stainless steel (SUS304)	25	Outer dia. $\phi = 89.1 \times$ Length $\ell = 1,944.5$ or less
16. Fuel supporting can II	Stainless steel (SUS304)	20	Outer dia. $\phi = 89.1 \times$ Length $\ell = 1,944.5$ or less
17. Supporting can	Stainless steel (SUS304)	20	Outer dia. $\phi = 89.1 \times$ Length $\ell = 1,944.5$ or less
18. Rack	Stainless steel (SUS304)	20	Max. dia. $\phi = 92 \times$ Length $\ell = 1,944.5$ or less
19. Receiving tube I	Stainless steel (SUS304)	1	Outer dia. $\phi = 13.8 \times$ Inner dia. $\phi = 10.5 \times$ Length $\ell = 1,035$ or less
20. Receiving tube II	Stainless steel (SUS304)	1	Outer dia. $\phi = 22$ or less \times Wall thickness = 1.5 or less \times Length $\ell = 1,880$ or less
21. Transport skid	Rolled steel for general structure (SS41)	1,000	Width $W =$ approx. 1,500 \times Length $\ell =$ approx. 2,700 \times Height $H =$ approx. 965

Table (I)-4 Lifting devices of the constituent components of the packaging

Item subject to lifting	Type of lifting metal piece	Material in use	Applicable lifting equipment
1. Packaging body (w/o shock absorbers)	Trunnions and lugs	Stainless steel (SUS304)	Yoke-type lifting equipment, 4-point hoisting wire rope or the like
2. Rear lid	Two tapped holes (M10)	Stainless steel (SUS304)	Eyebolts (M10) and wire rope or the like
3. Front lid	Two tapped holes (M10)	Stainless steel (SUS304)	Eyebolts (M10) and wire rope or the like
4. Rear shock absorber	Lifting rings	Stainless steel (SUS304)	2-point lifting wire rope or the like
5. Front shock absorber	Lifting rings	Stainless steel (SUS304)	2-point lifting wire rope or the like
6. Inner container	Boss	Stainless steel (SUS304)	—
7. Fuel supporting can I	Grip lug	Stainless steel (SUS304)	Special lifting gripper
8. Fuel supporting can II	Grip lug	Stainless steel (SUS304)	Special lifting gripper
9. Supporting can	Grip lug	Stainless steel (SUS304)	Special lifting gripper
10. Rack	Grip lug	Stainless steel (SUS304)	Special lifting gripper
11. Transport skid	Lugs	Rolled steel used for general structures (SS41)	4-point lifting wire rope or the like
12. Packaging (w/shock absorbers) + Transport skid	Lugs	Stainless steel (SUS304)	4-point lifting wire rope or the like

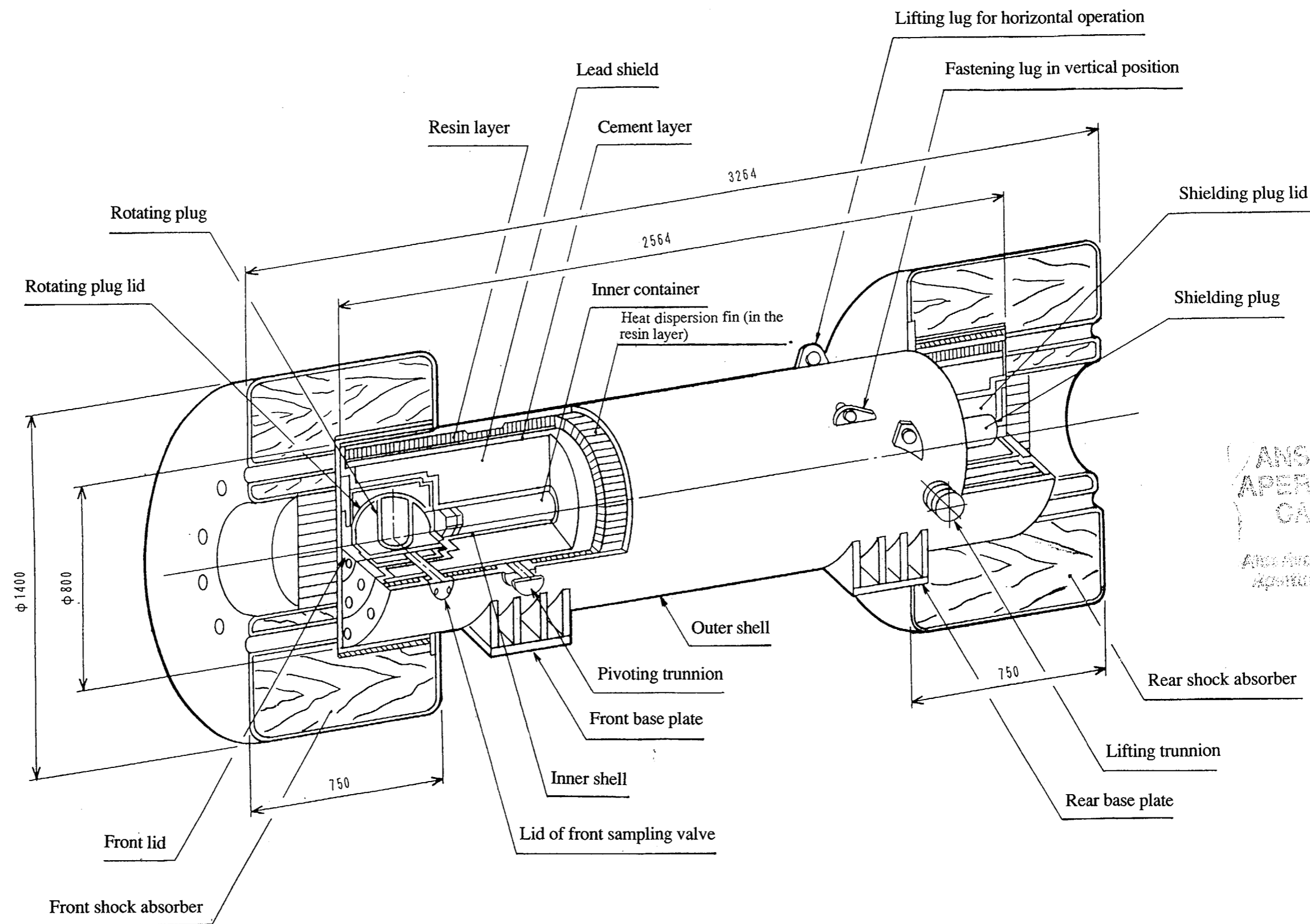
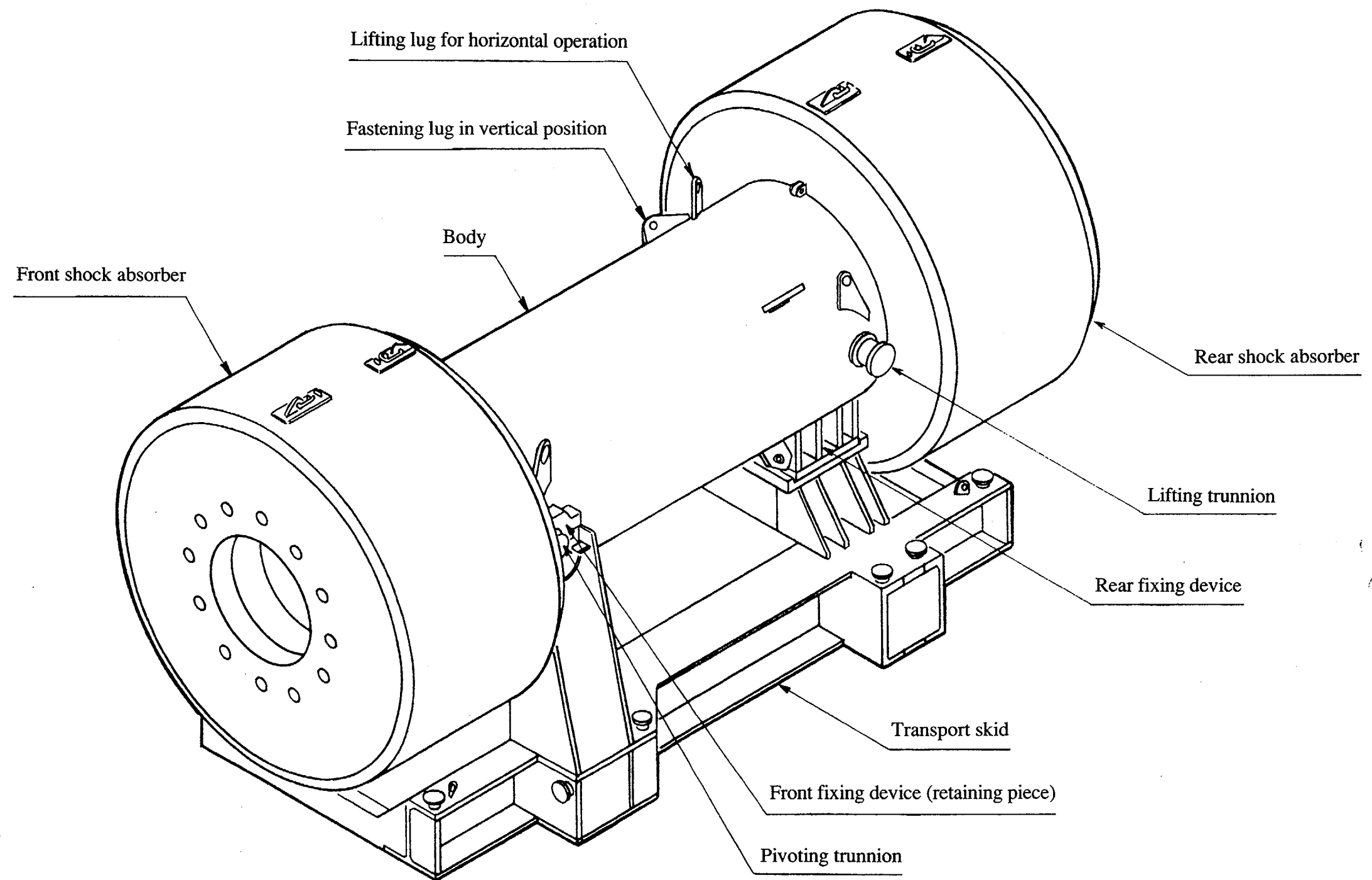


Fig. (I)-1 Cutout view of package (Dimensions in mm)

9601260203-01



ANSTEC
APERTURE
CARD

Also Available on
Aperture Card

Fig. (I)-3 Schematic Drawing of Packaging (6-4) Equipped with the Skid for Transportation

9601260203-03

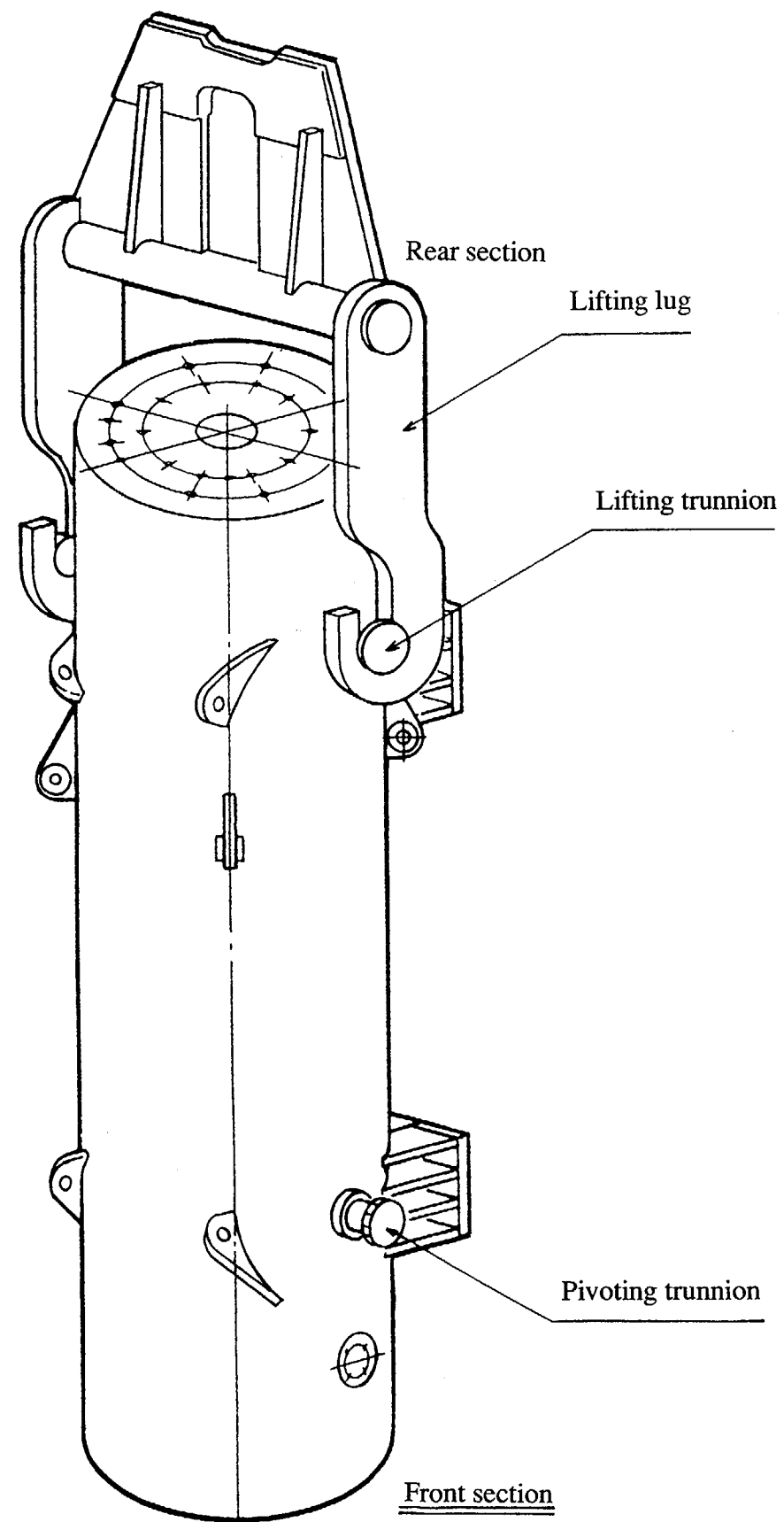


Fig. (I)-4 Drawing of Vertical Lifting Condition

ANSTEC
APERTURE
CARD

Also Available on
Aperture Card

9601260203 -04

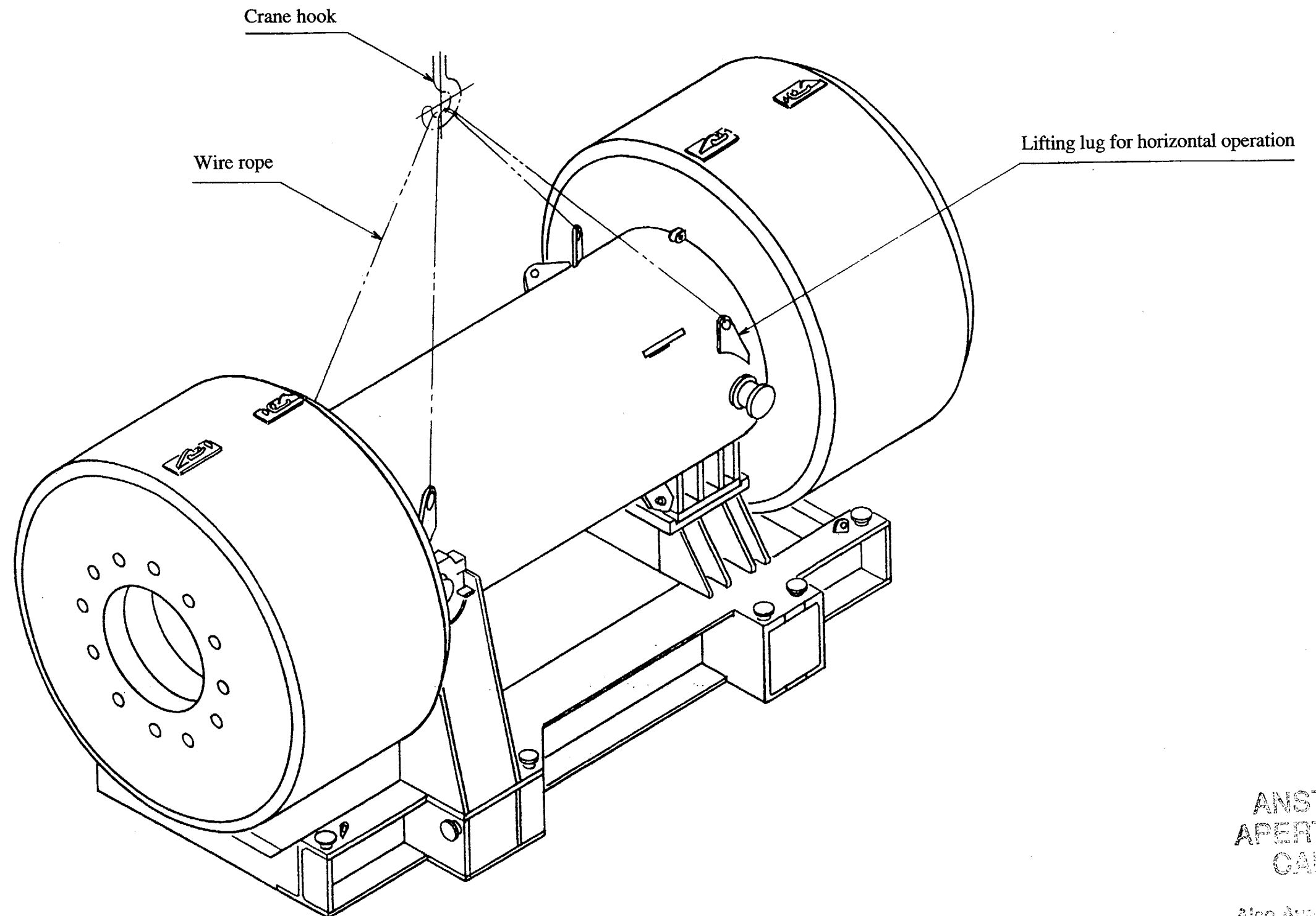
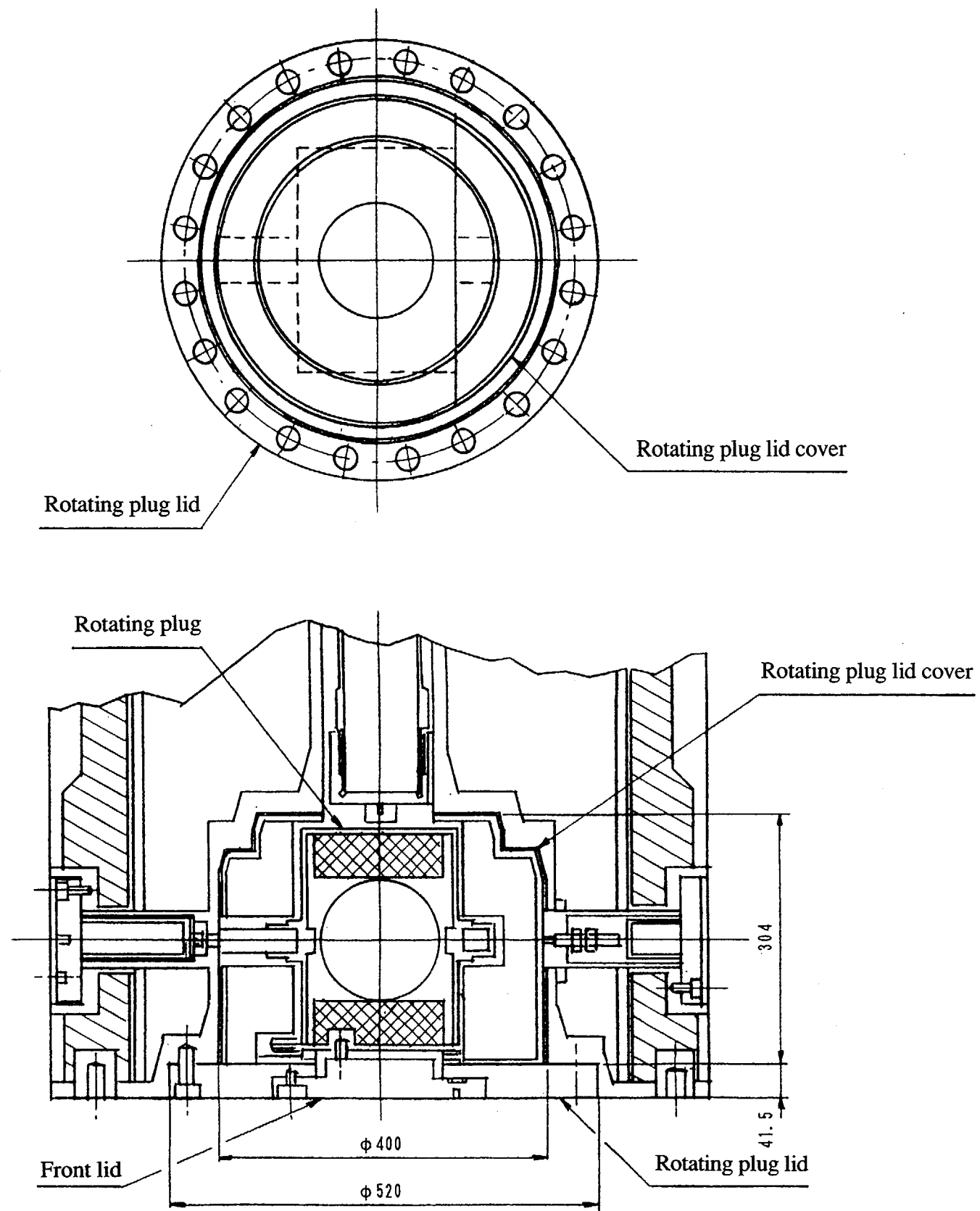


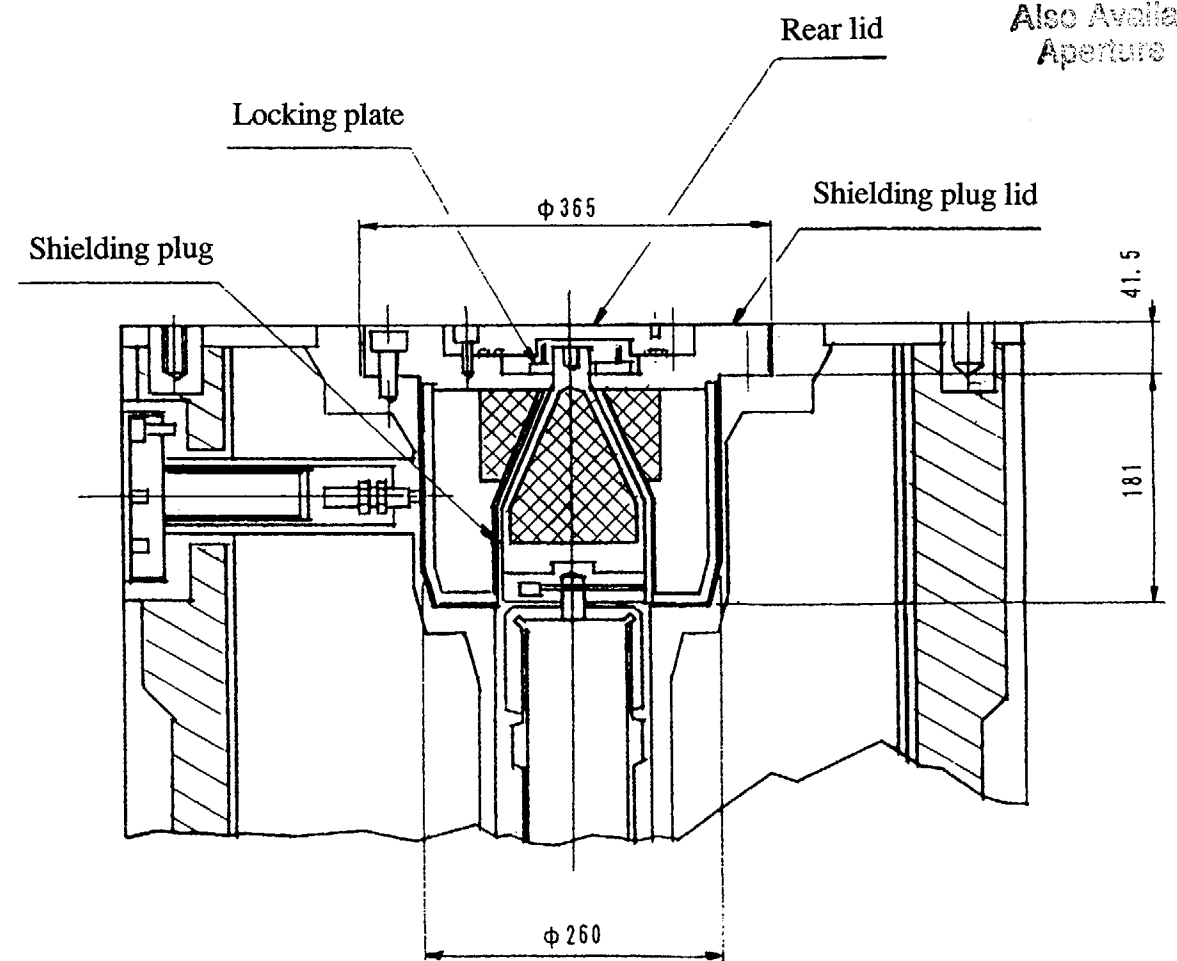
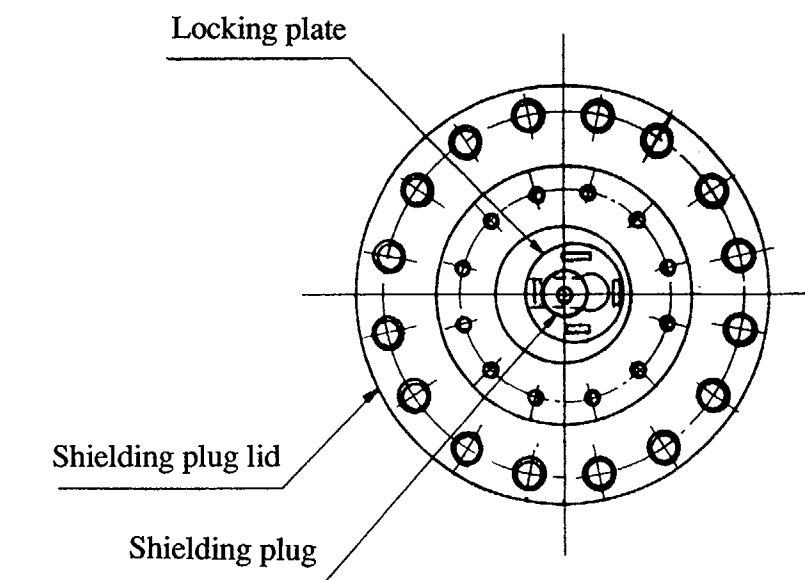
Fig. (I)-5 Drawing of Horizontal Lifting Condition

ANSTEC
APERTURE
CARD

Also Available on
Aperture Card



(A) Front Lid Unit



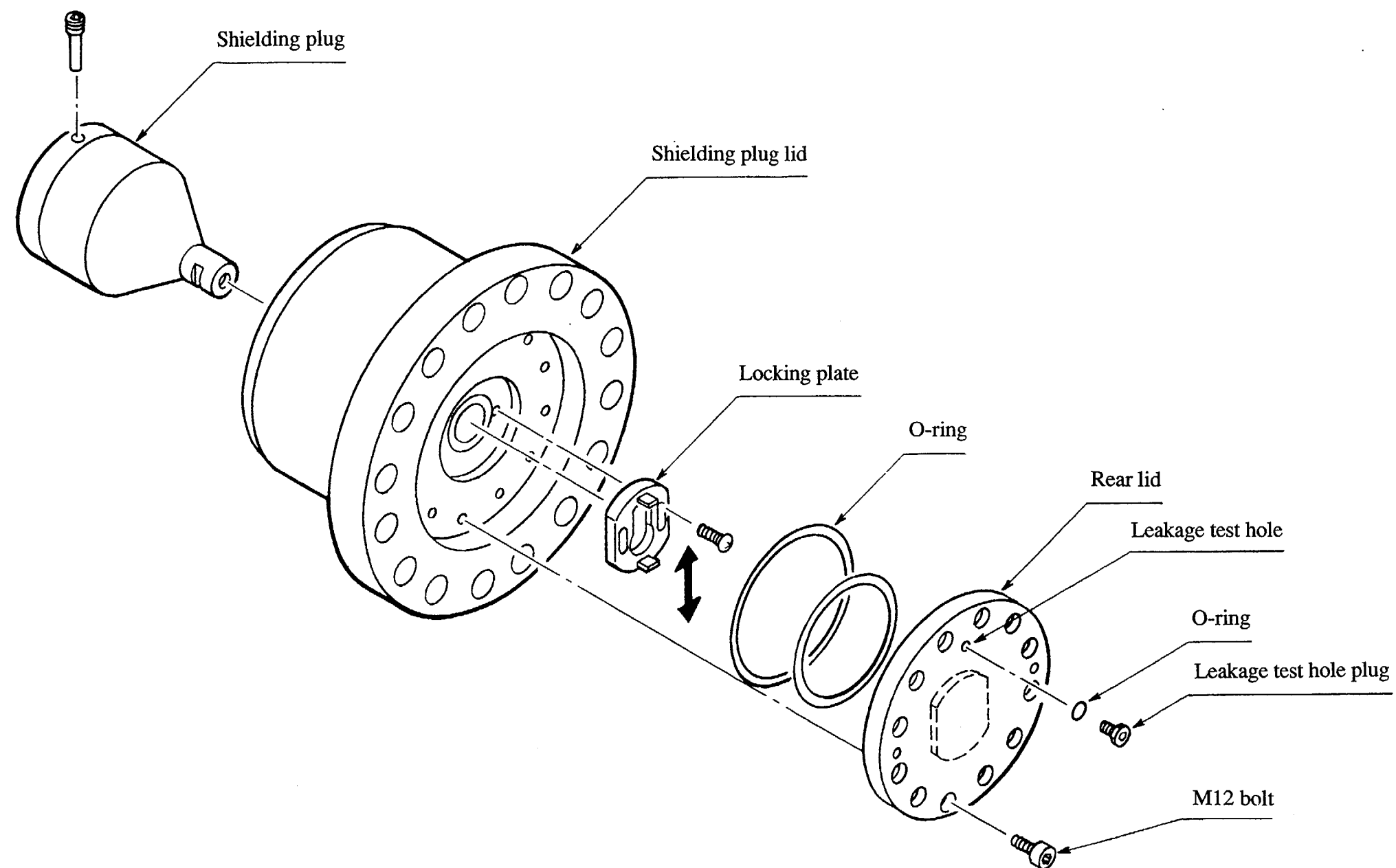
(B) Rear Lid Unit

Fig. (I)-6 Detailed Drawings of Front Lid and Rear Lid Units (in mm)

ANSTEC
APERTURE
CARD

Also Available on
Aperture Card

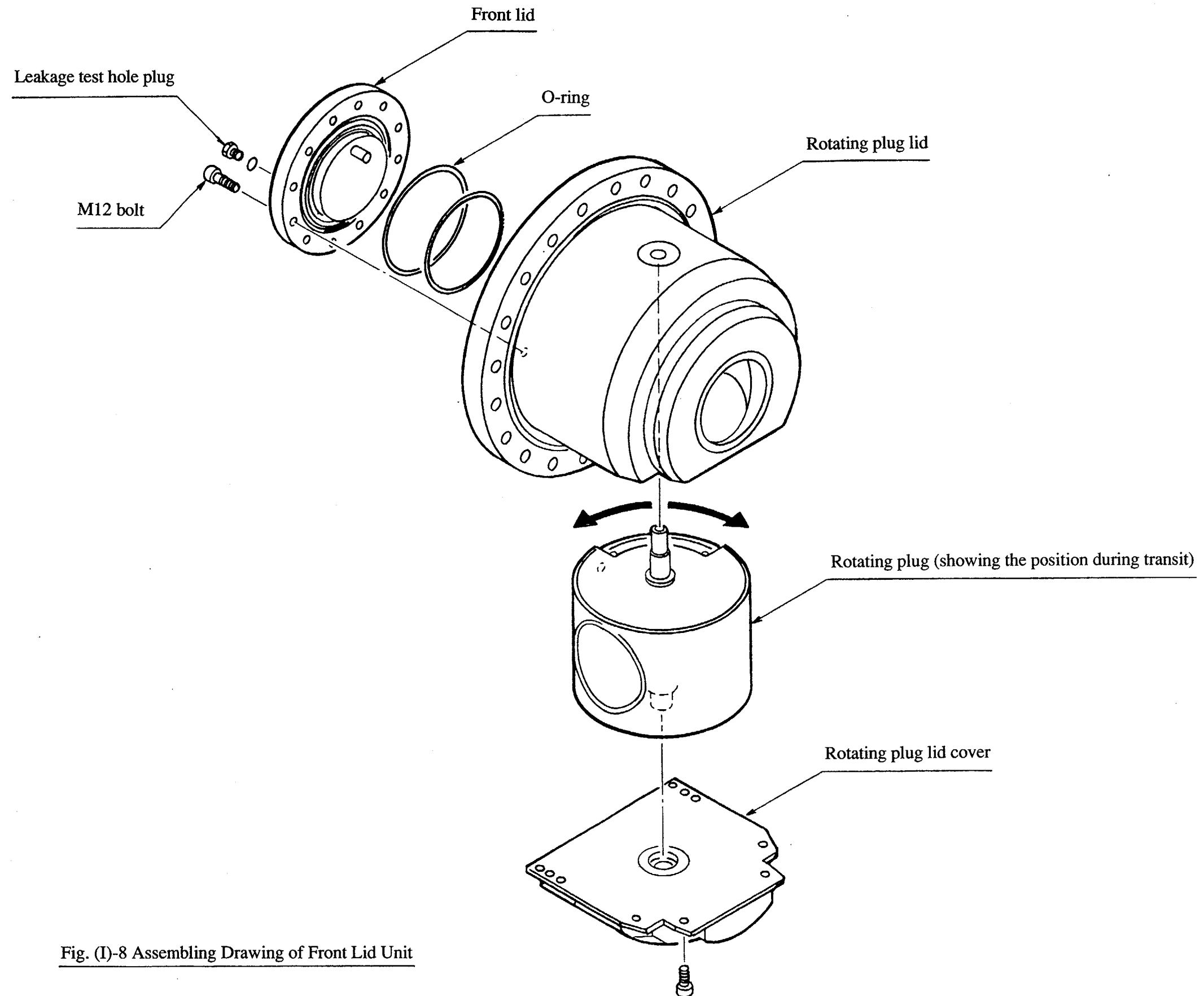
9601260203-06



**ANSTEC
APERTURE
CARD**

Also Available on
Aperture Card

Fig. (I)-7 Assembling Drawing of Rear Lid Unit



ANSTEC
APERTURE
CARD

Also Available on
Aperture Card

Fig. (I)-8 Assembling Drawing of Front Lid Unit

9601260203-08

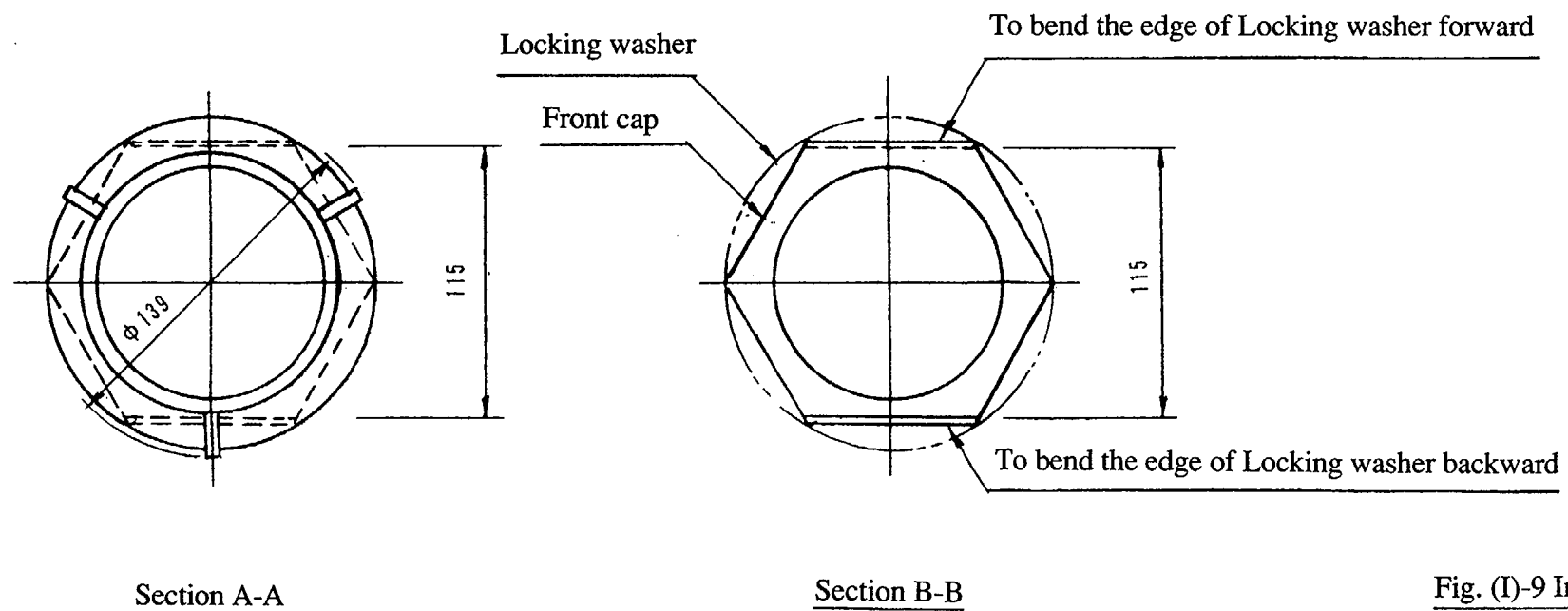
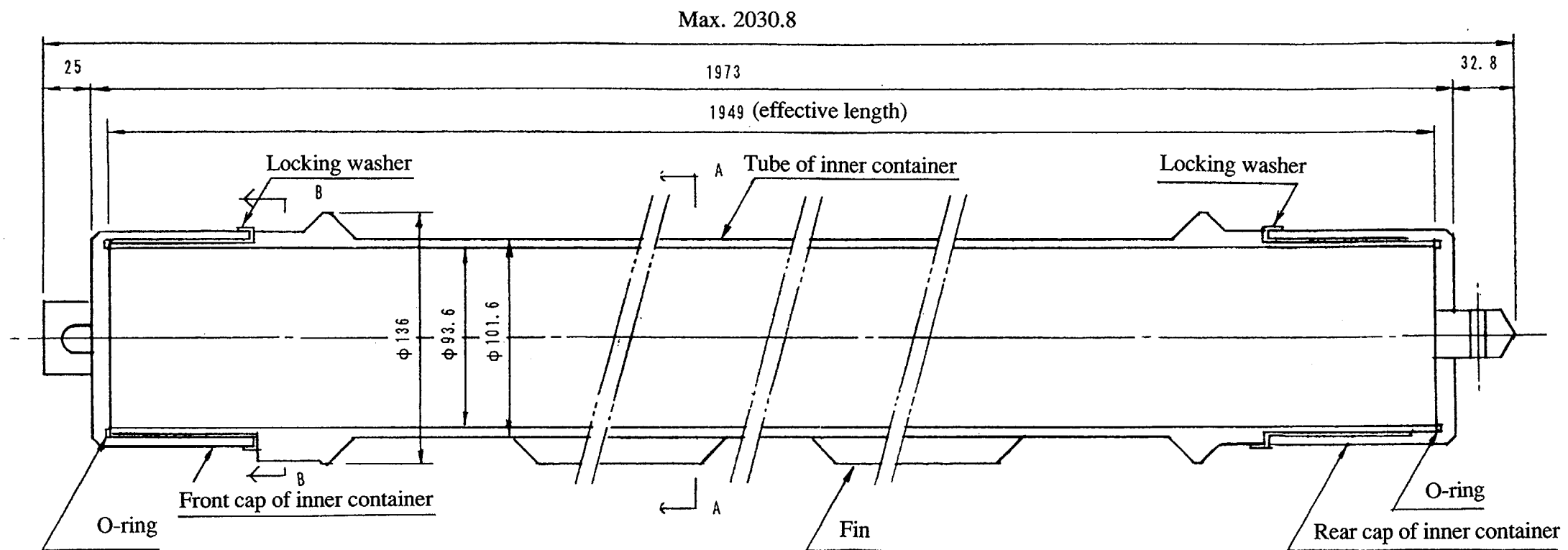


Fig. (I)-9 Inner Container (in mm)

ANSTEC
APERTURE
CARD

Also Available on
Aperture Card

9601260203-09

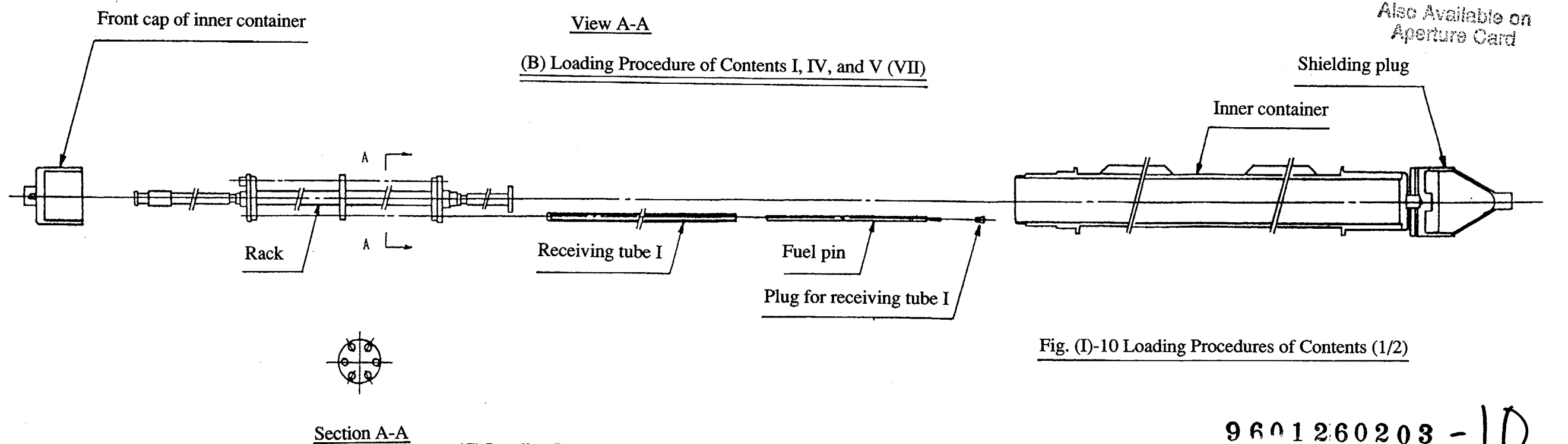
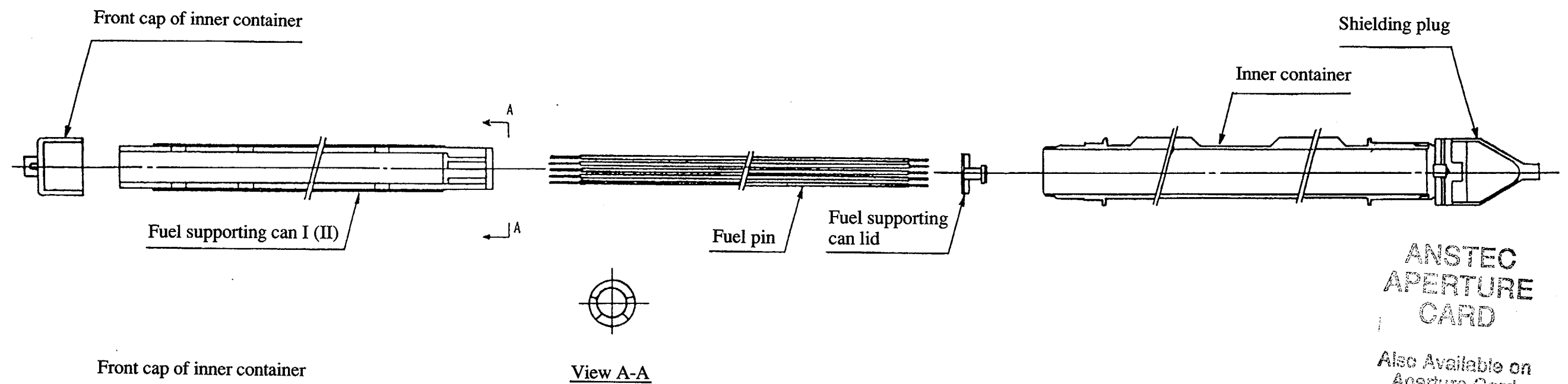
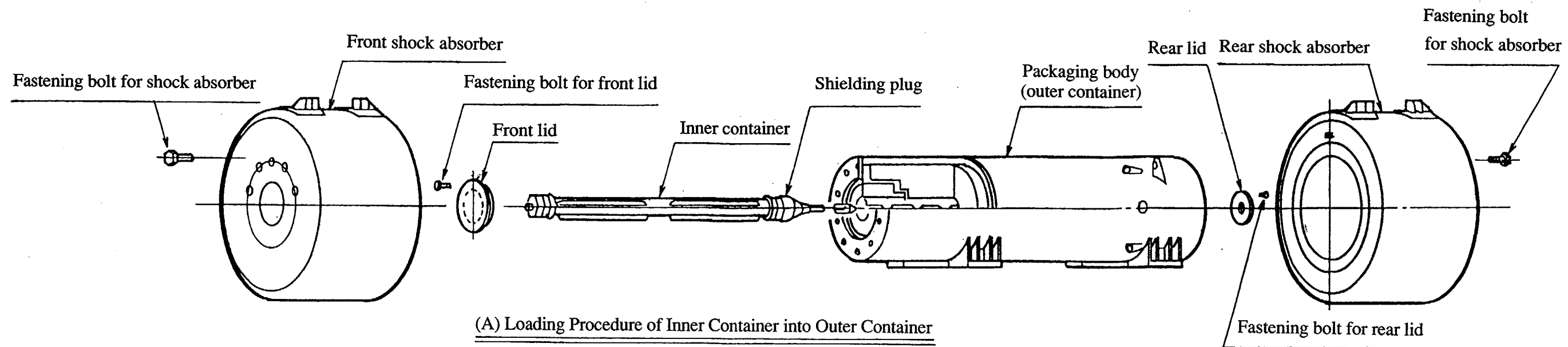
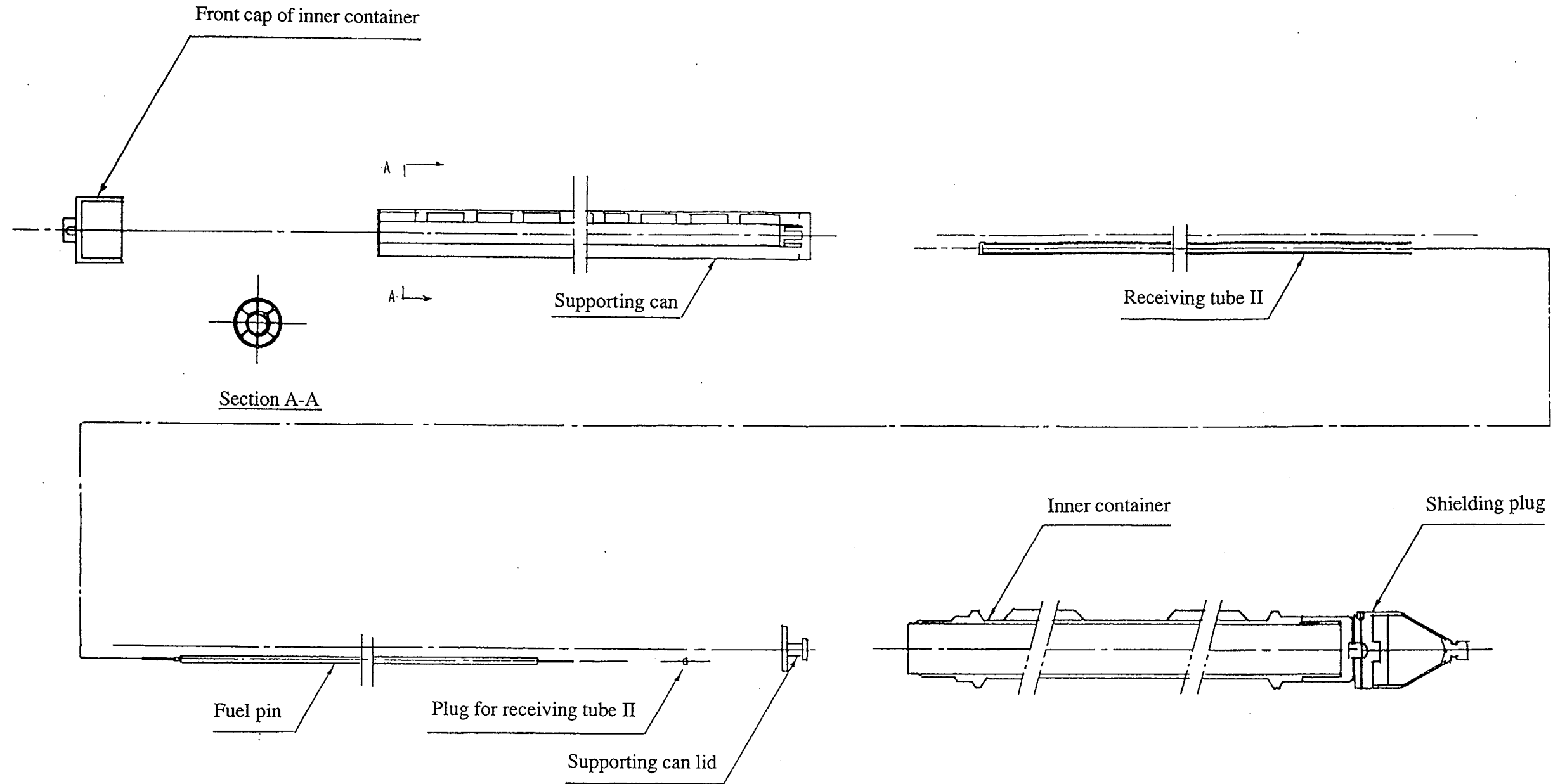


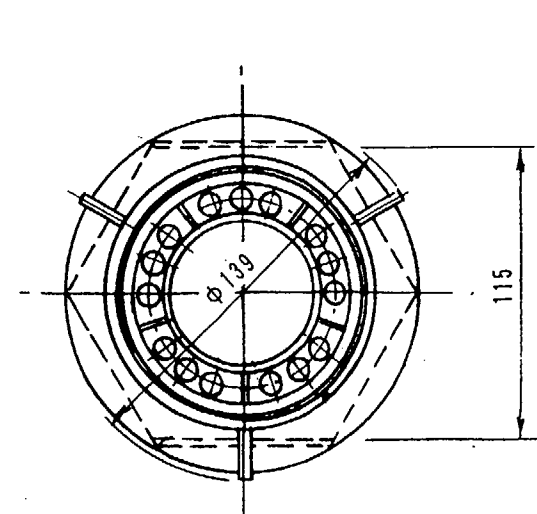
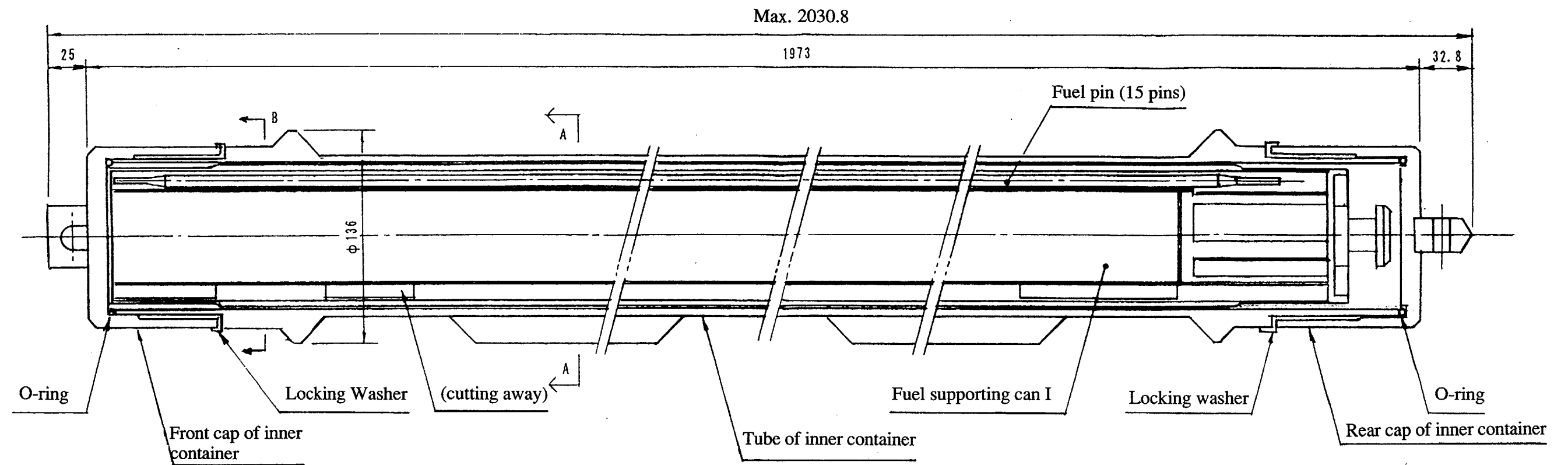
Fig. (I)-10 Loading Procedures of Contents (1/2)



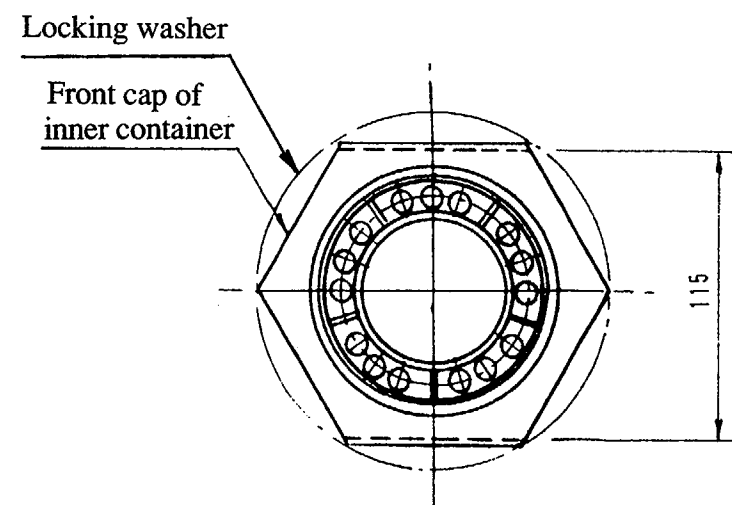
(D) Loading Procedure of Contents VI and VIII

ANSTEC
APERTURE
CARD

Also Available on
Aperture Card



Section A-A



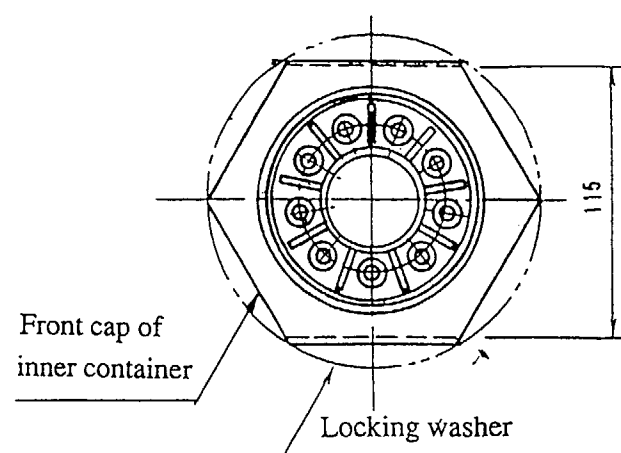
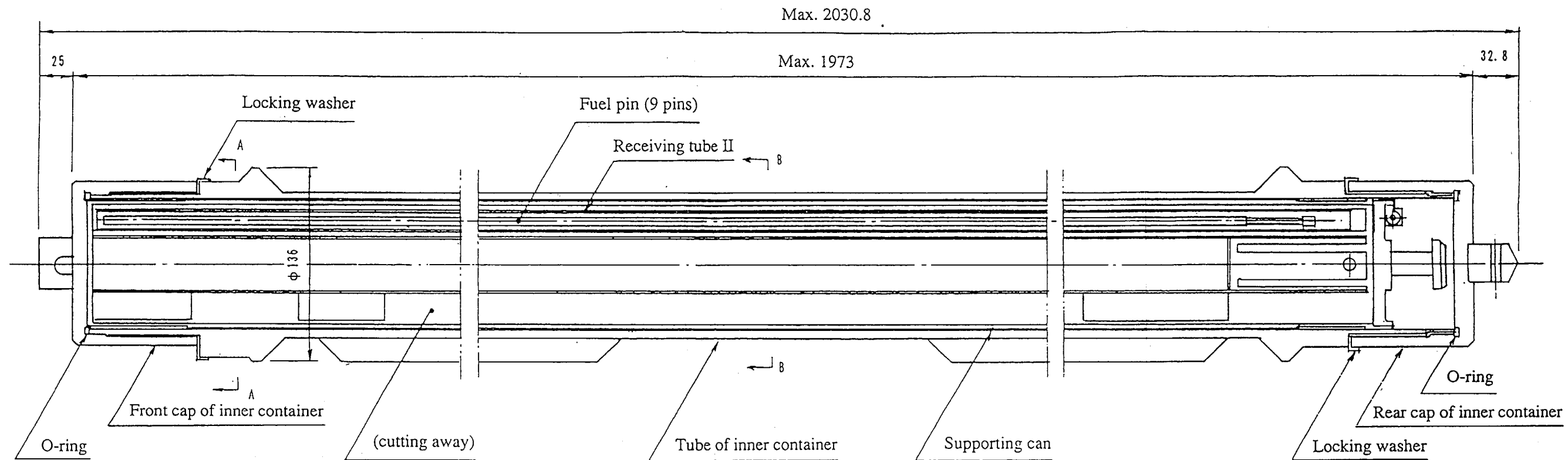
Section B-B

ANSTEC
APERTURE
CARD

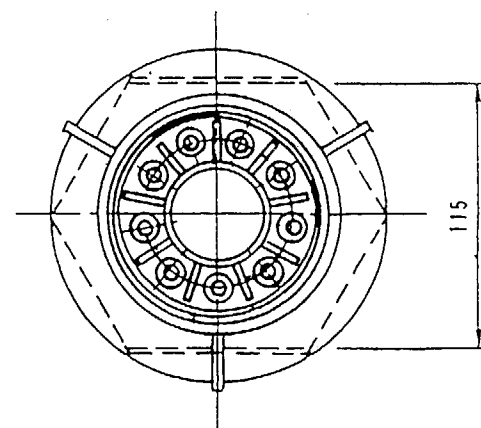
Also Available on
Aperture Card

Fig. (I)-11 Drawing of Status of Contents I, IV and V Loaded in Inner Container (in mm)

9601260203-12



Section A-A



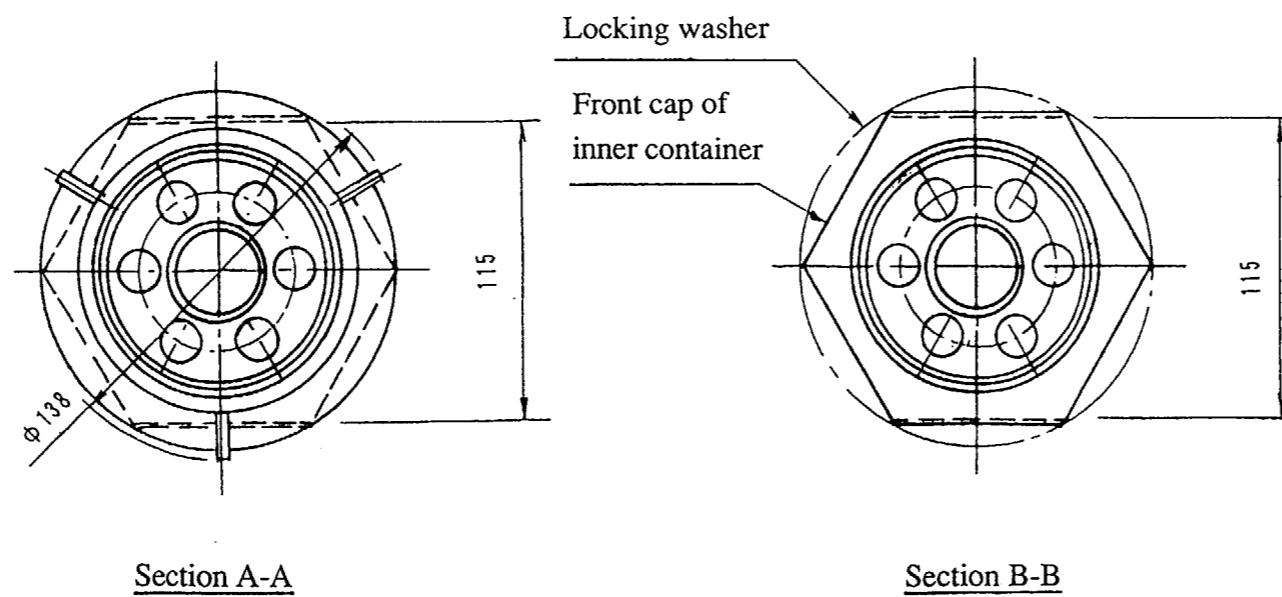
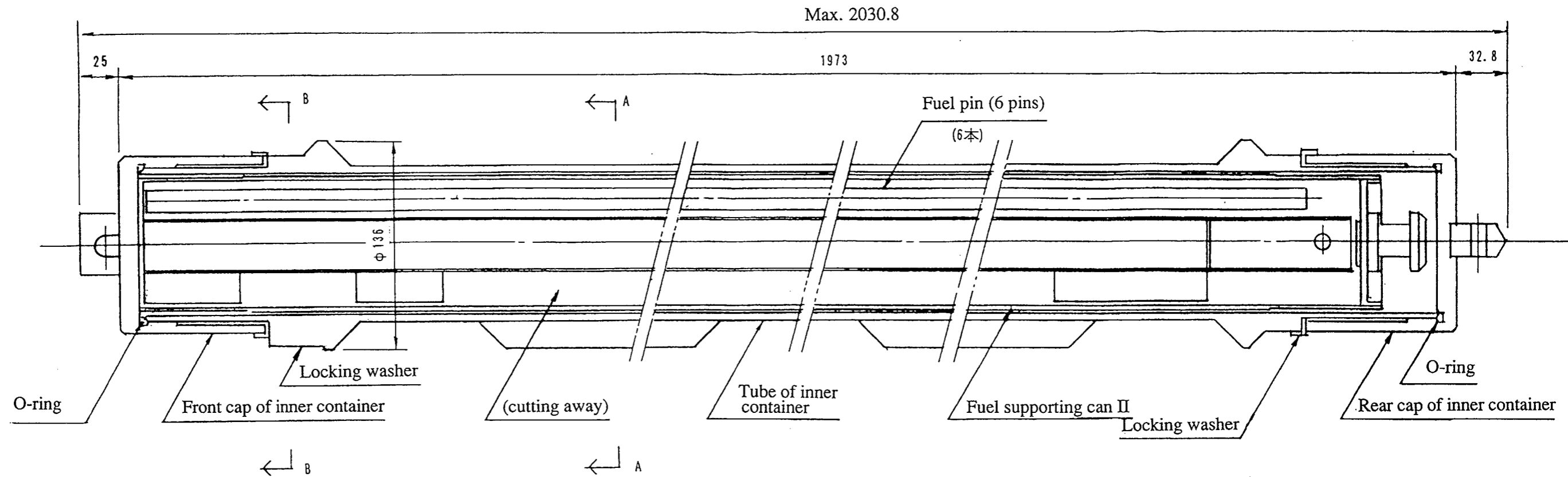
Section B-B

ANSTEC
APERTURE
CARD

Also Available on
Aperture Card

Fig. (I)-12 Drawing of Status of Contents VI and VIII Loaded in Inner Container (in mm)

9601260203-13



ANSTEC
APERTURE
CARD

Also Available on
Aperture Card

Fig. (I)-13 Drawing of Status of Contents VII (in mm)

9601260203-14

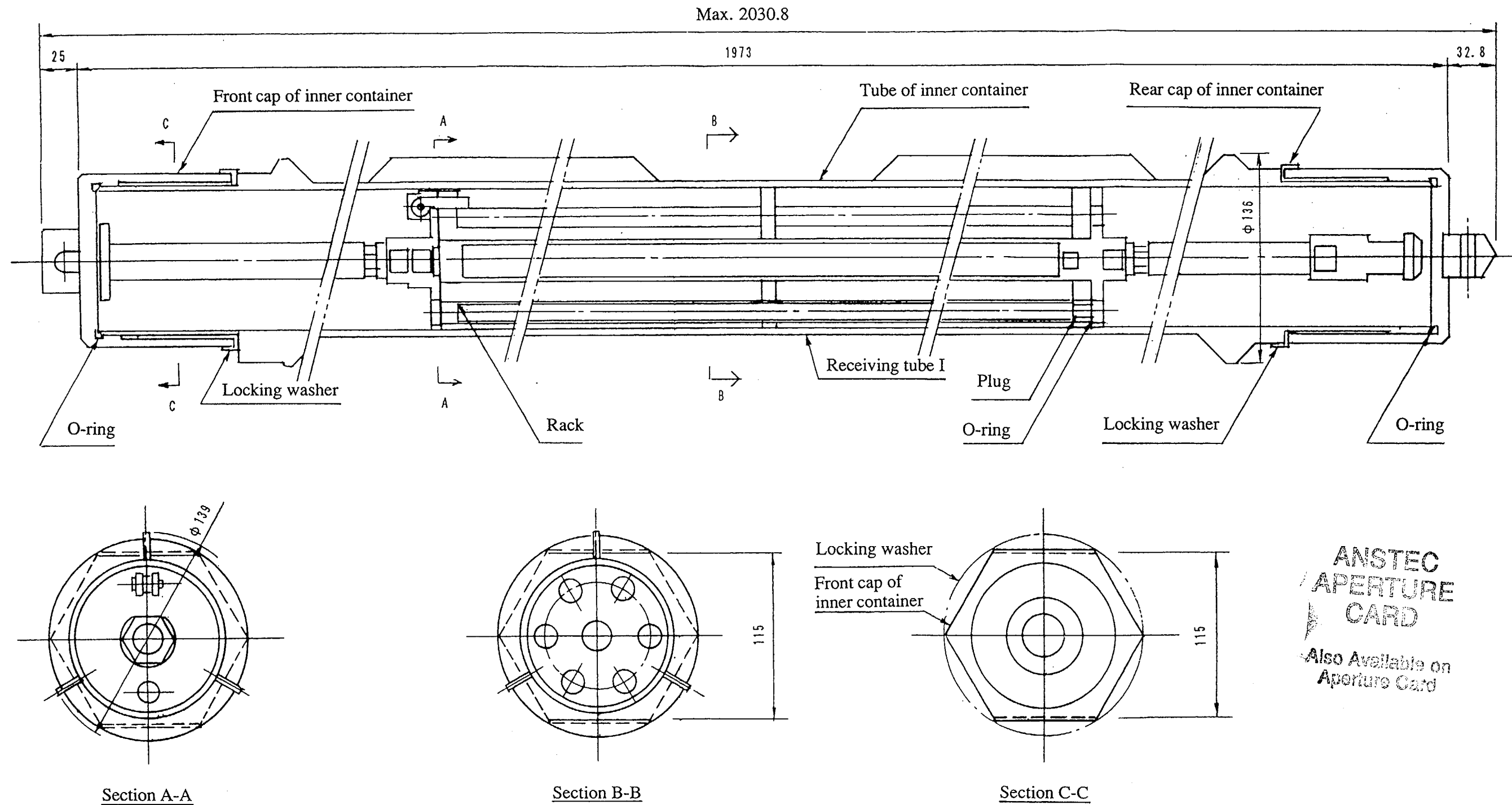


Fig. (I)-14 Drawing of Status of Contents II (minority pins) Loaded in Inner Container (in mm)

9601260203-15

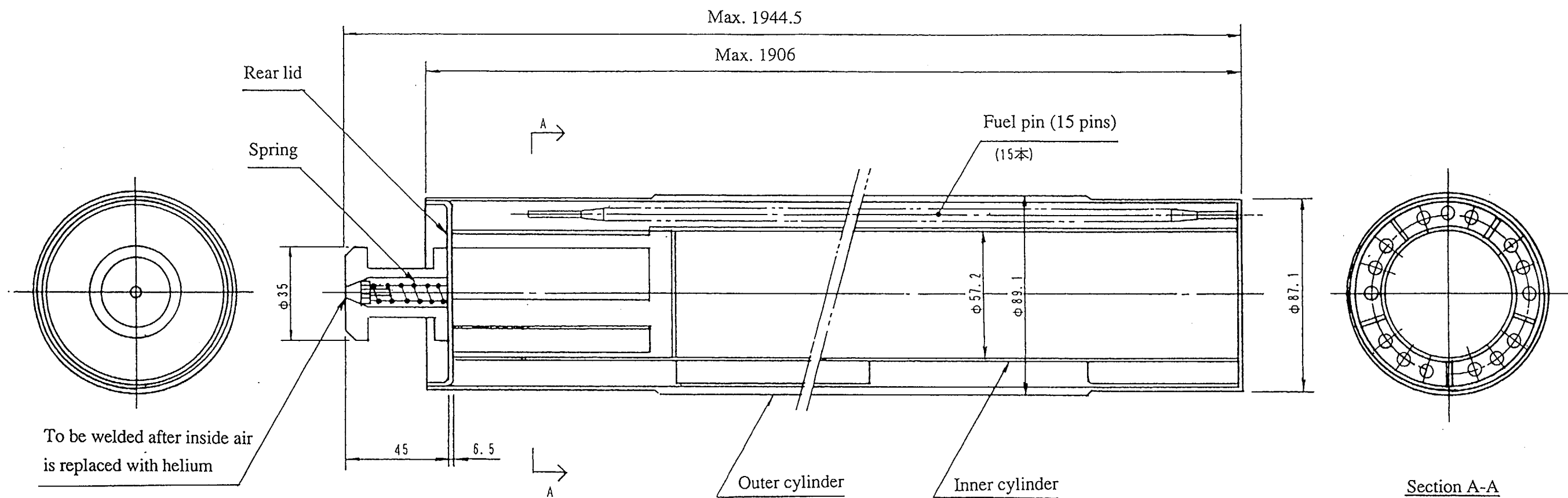


Fig. (I)-15 Detailed Drawing of Fuel Supporting Can I (in mm)

ANSTEC
APERTURE
CARD

Also Available on
Aperture Card

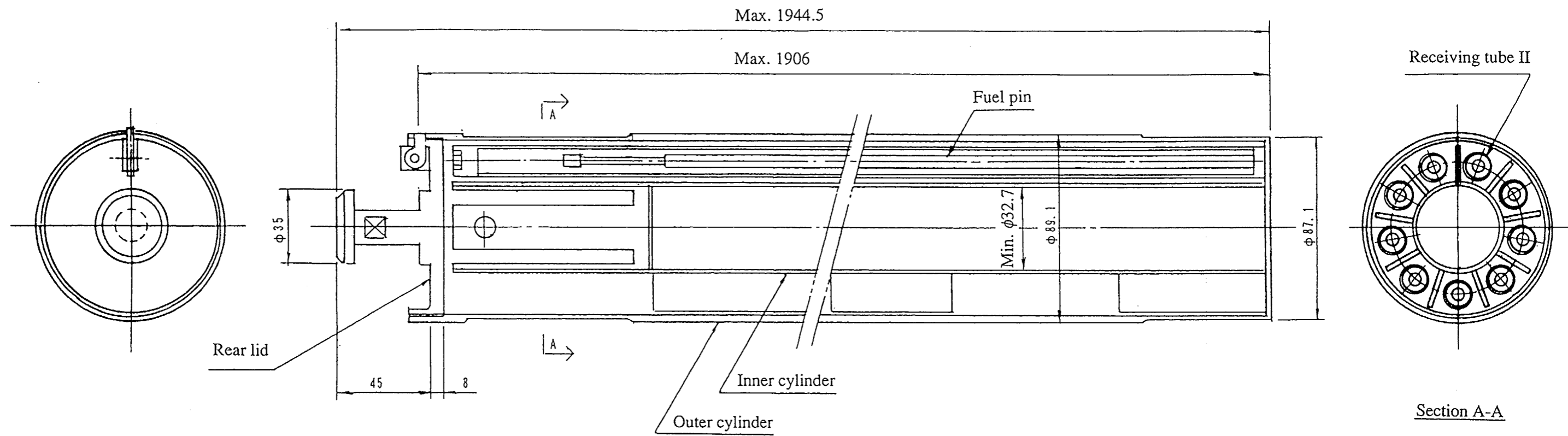


Fig. (I)-16 Supporting Can (in mm)

ANSTEC
APERTURE
CARD

Also Available on
Aperture Card

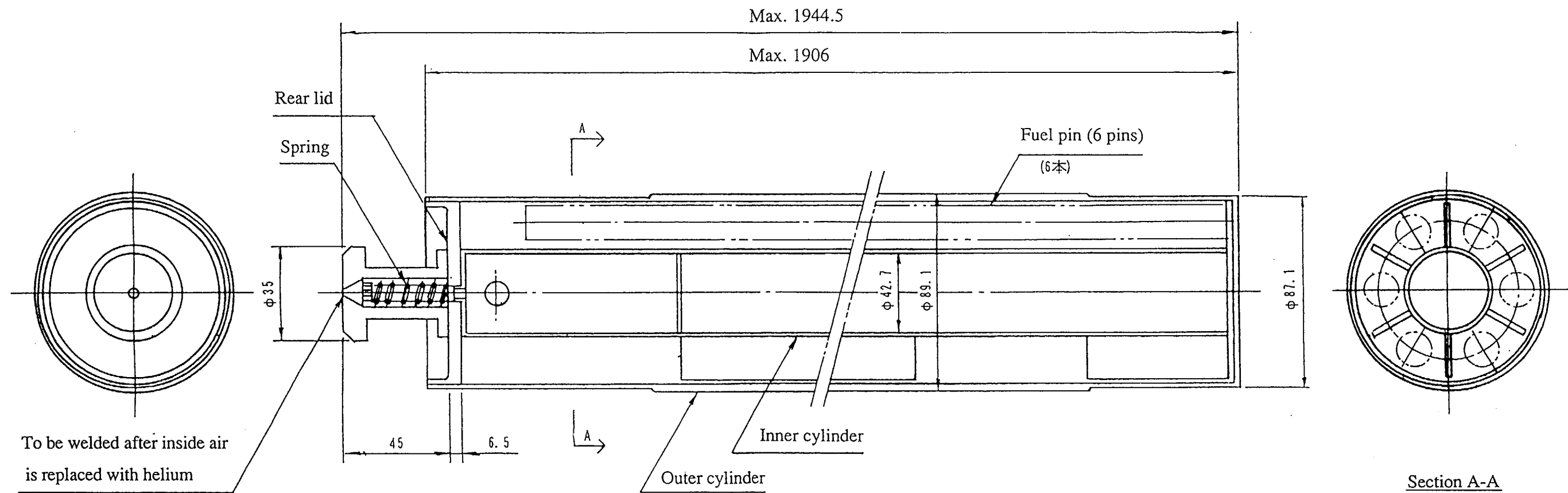


Fig. (I)-17 Detailed drawing of Fuel Supporting can II (in mm)

ANSTEC
APERTURE
CARD
Also Available on
Aperture Card

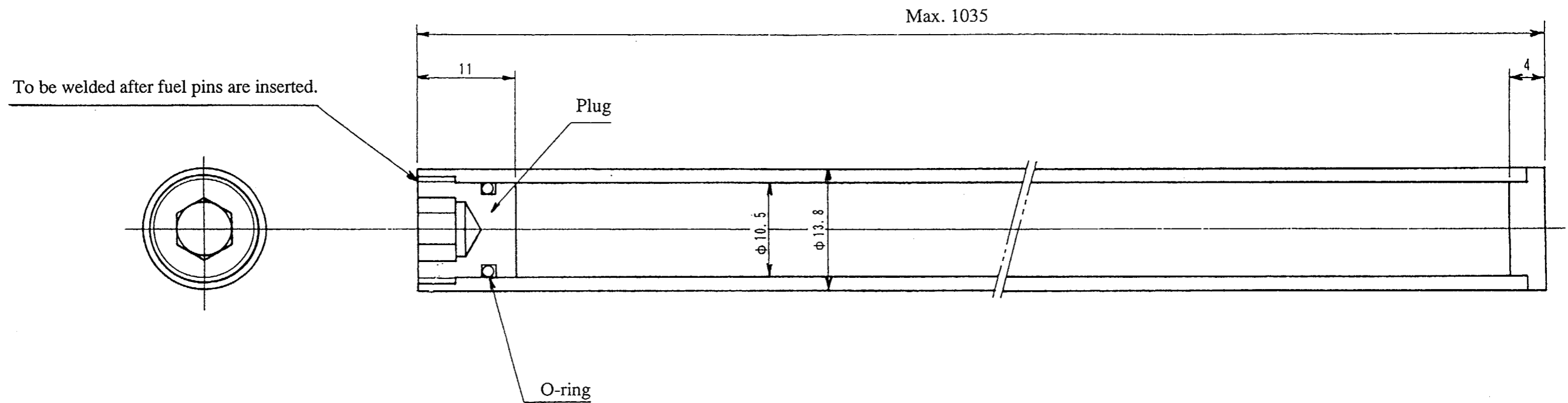


Fig. (I)-18 Receiving tube I (in mm)

ANSTEC
APERTURE
CARD

Also Available on
Aperture Card

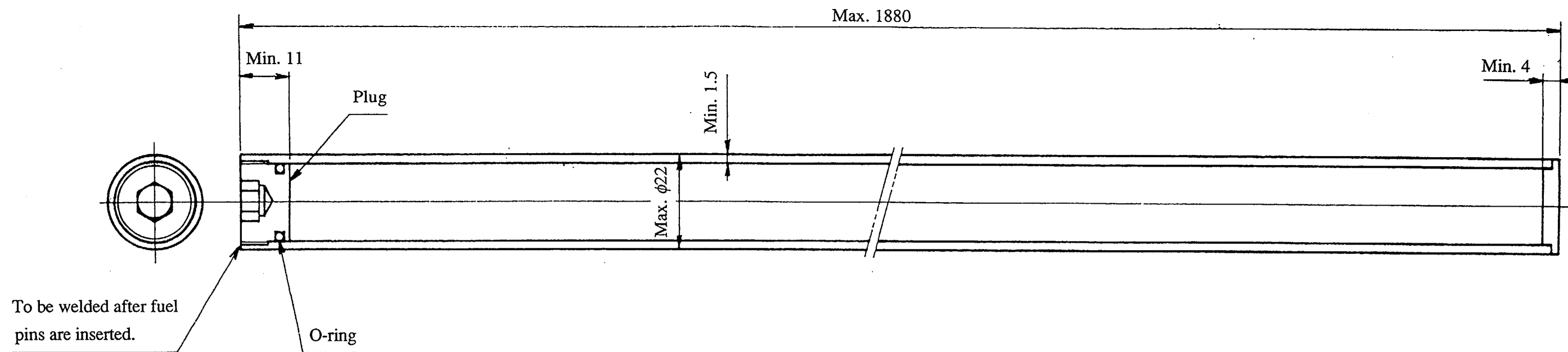
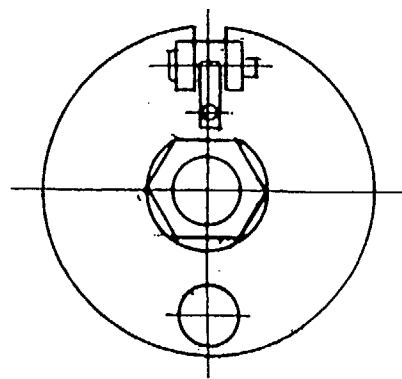
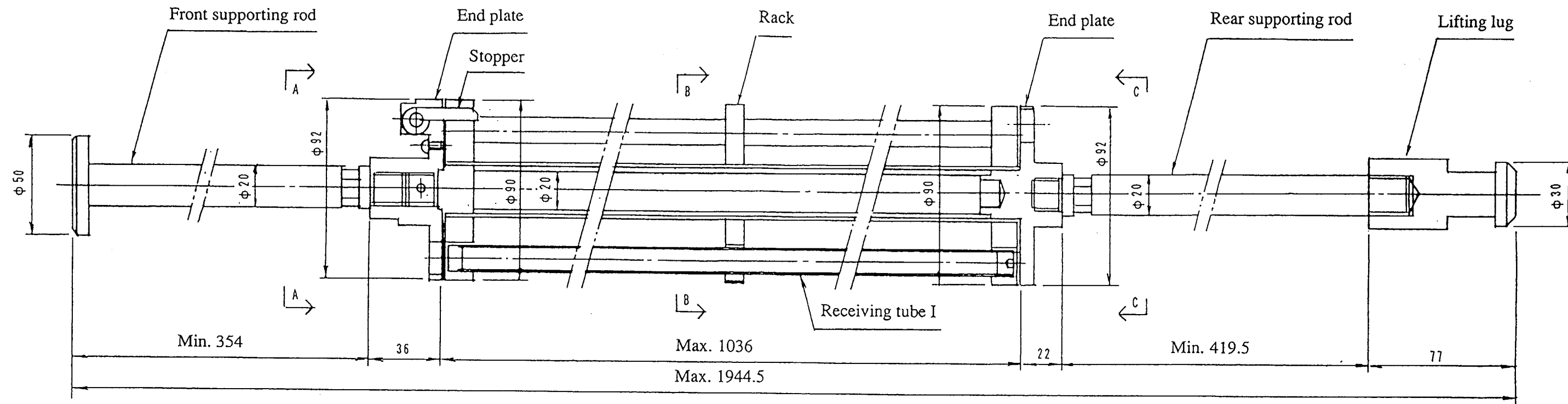


Fig. (I)-19 Receiving tube II (in mm)

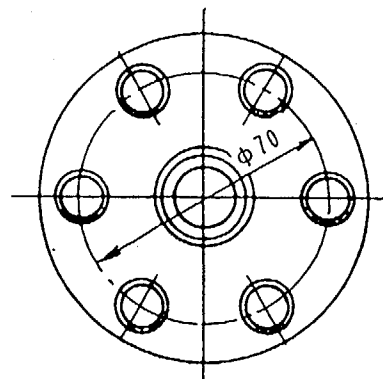
ANSTEC
APERTURE
CARD

Also Available on
Aperture Card

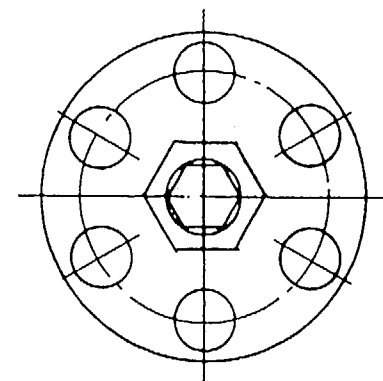
9601260203 - 20



View A-A



Section B-B



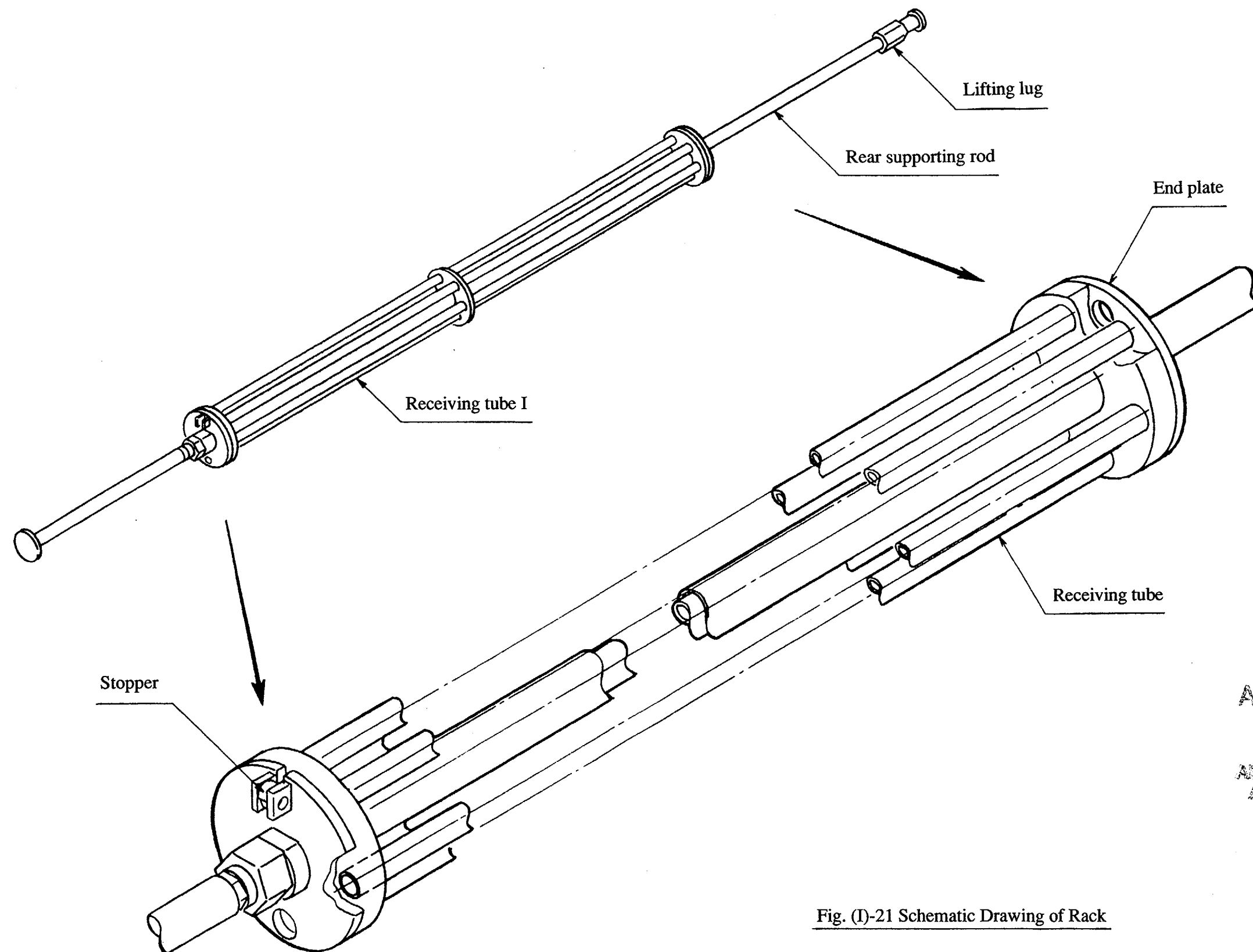
View C-C

ANSTEC
APERTURE
CARD

Also Available on
Aperture Card

Fig. (I)-20 Rack (in mm)

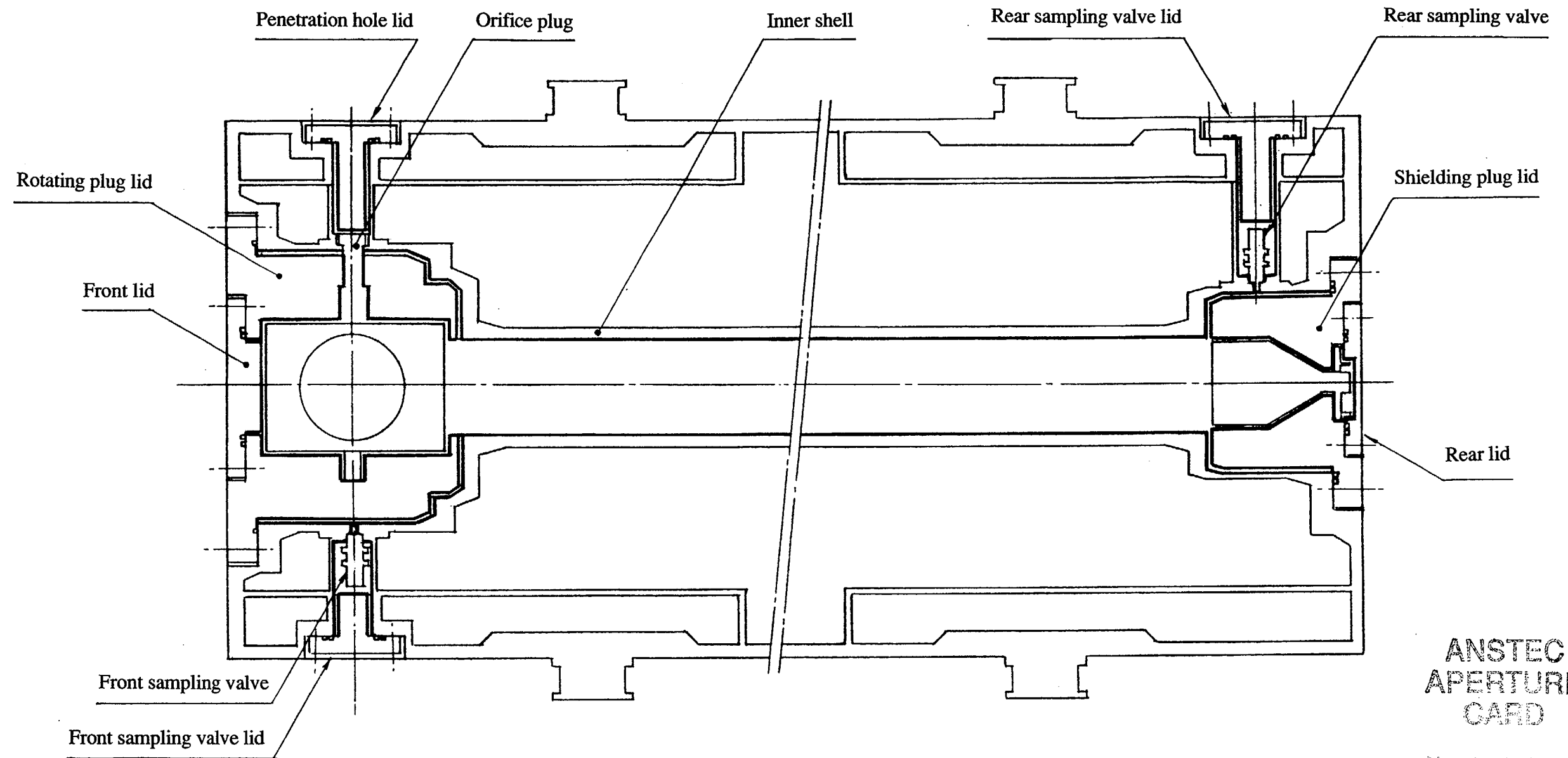
9601260203 - 21



ANSTEC
APERTURE
CARD

Also Available on
Aperture Card

Fig. (I)-21 Schematic Drawing of Rack



**ANSTEC
APERTURE
CARD**

*Also Available on
Aperture Card*

— This line shows the boundary of containment.

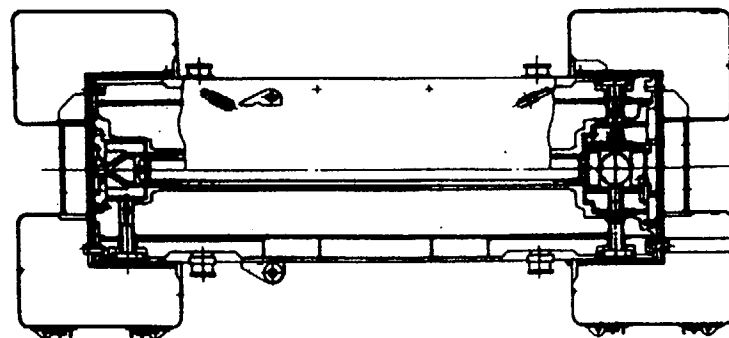


Fig. (I)-22 Drawing of Containment Boundary

9601260203 - 23

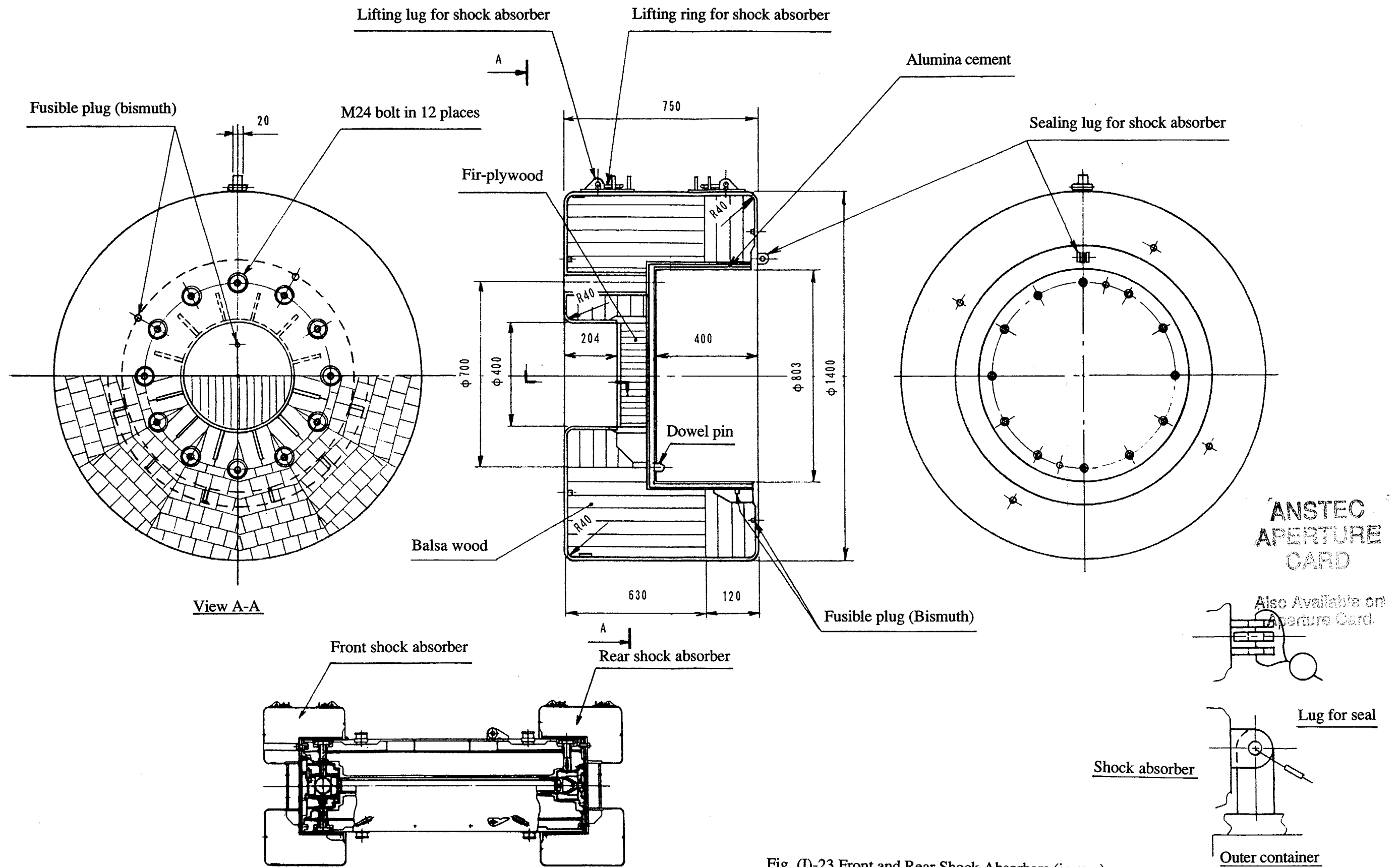


Fig. (I)-23 Front and Rear Shock Absorbers (in mm)

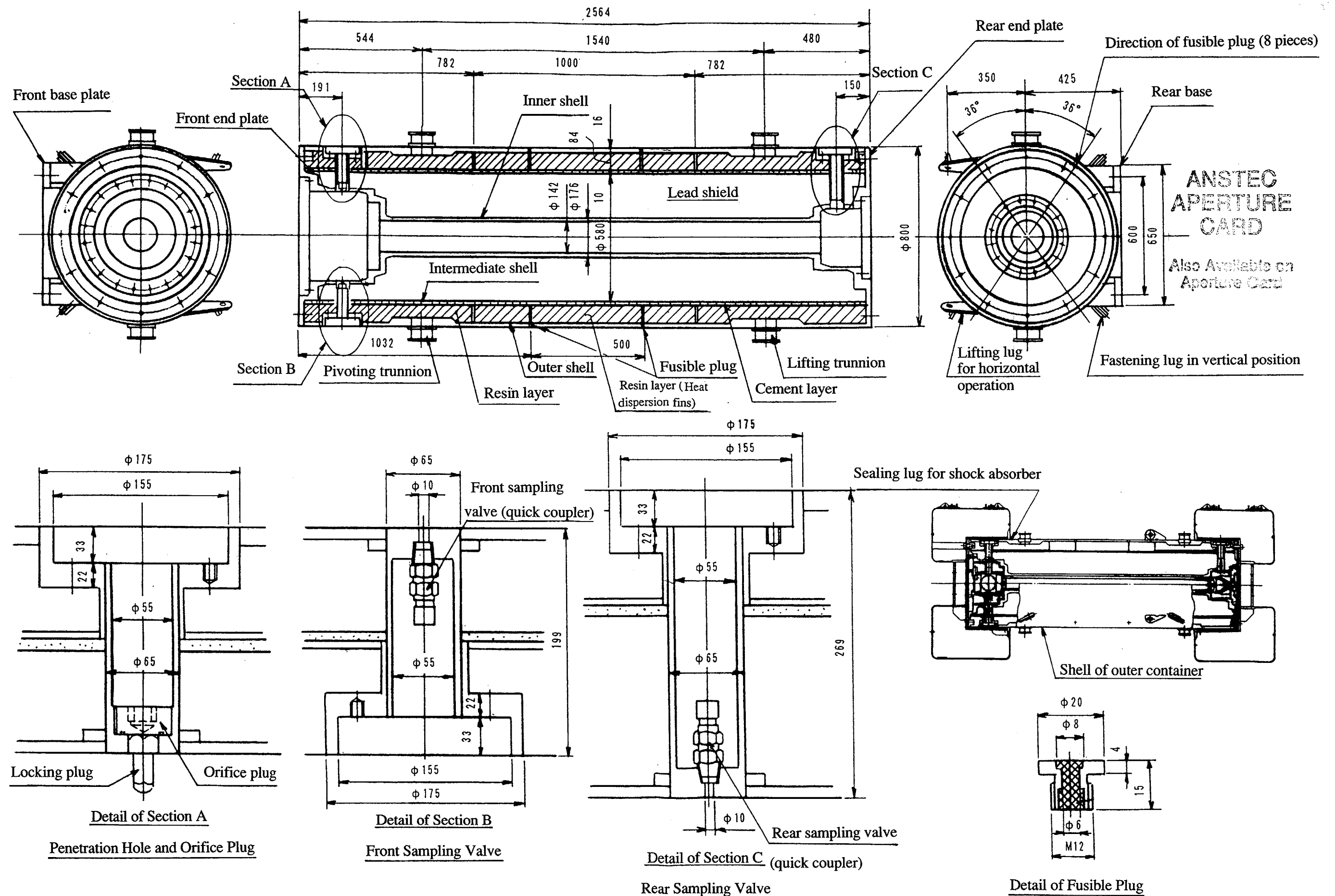


Fig. (I)-24 Outer Container (in mm)

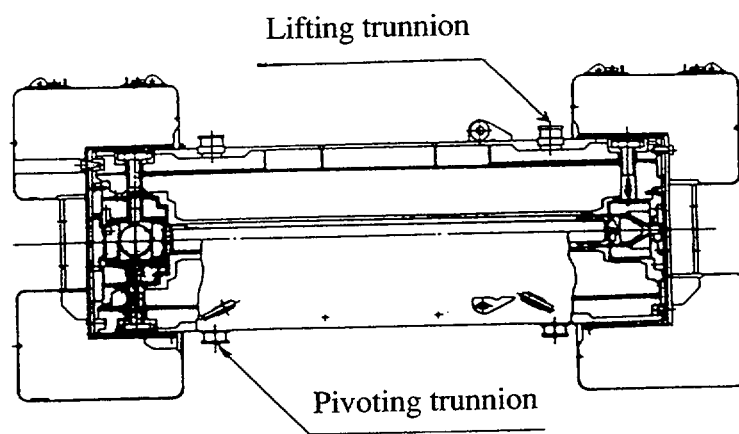
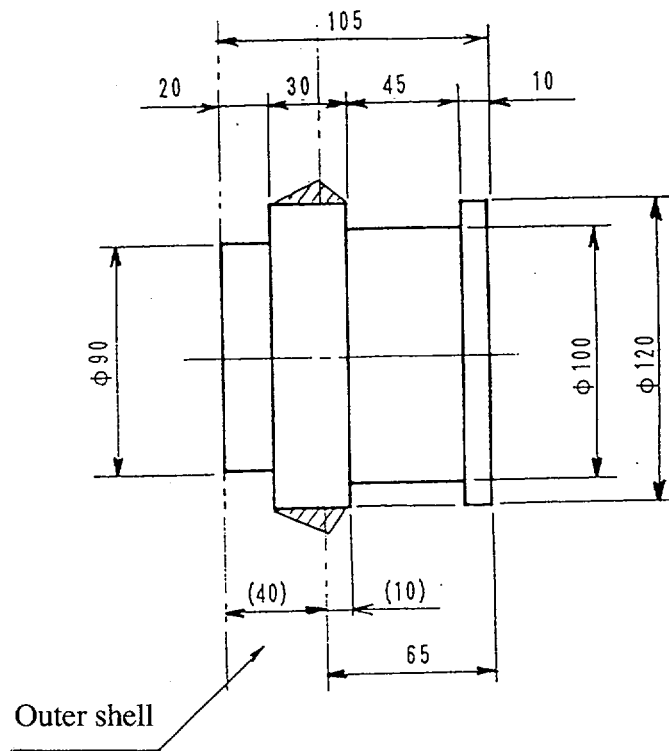


Fig. (I)-25 Lifting Trunnion and Pivoting Trunnion (in mm)

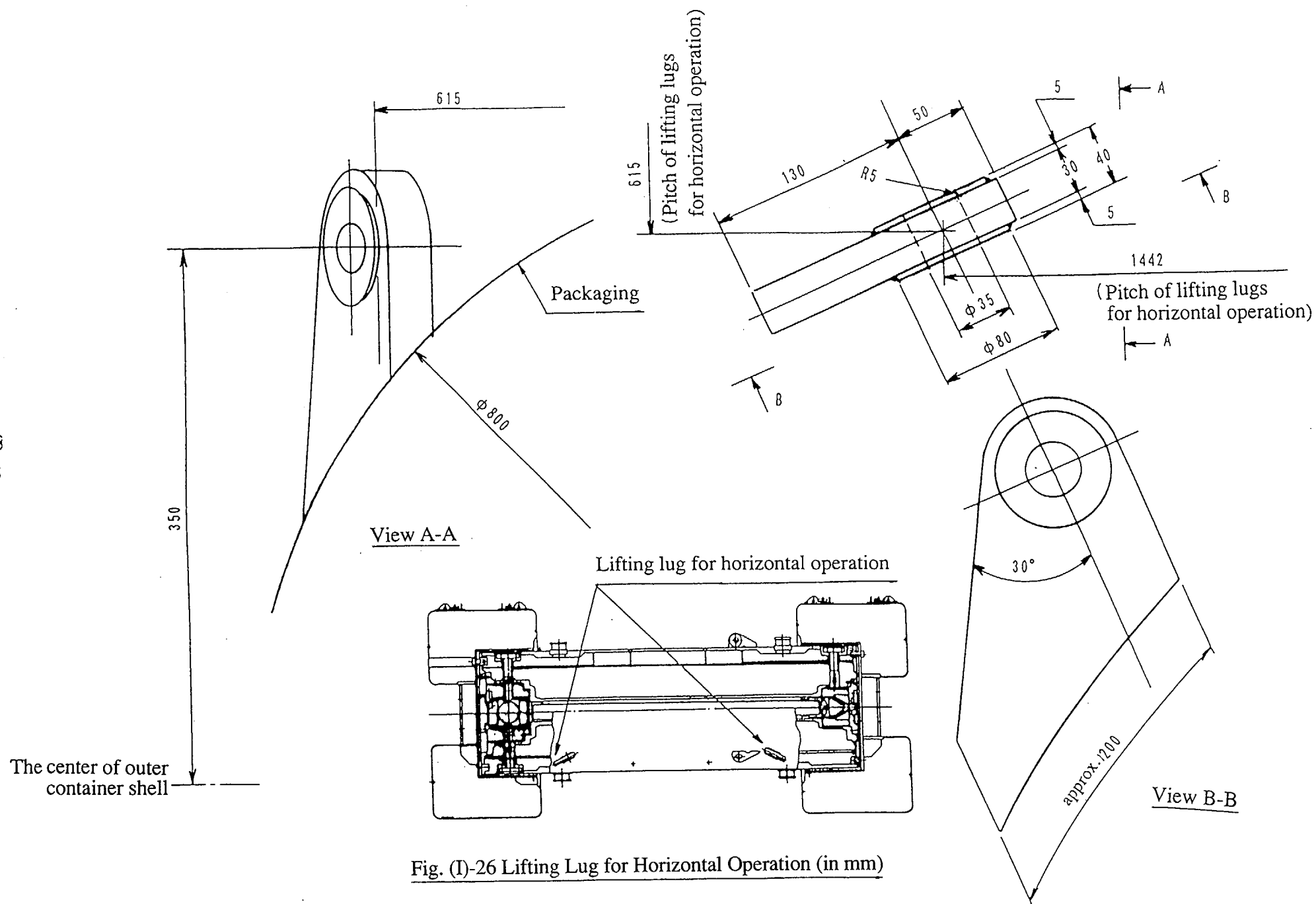
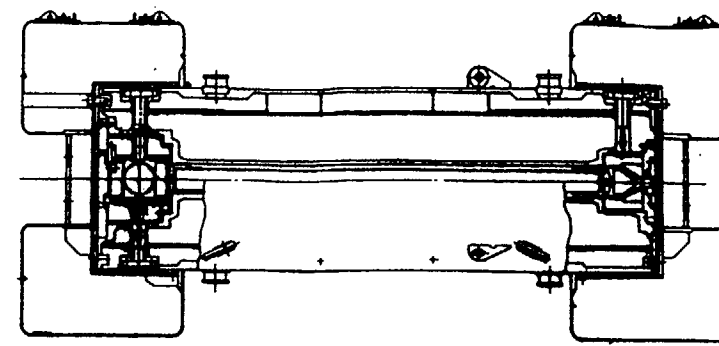


Fig. (I)-26 Lifting Lug for Horizontal Operation (in mm)



Front base plate

Rear base plate

ANSTEC
APERTURE
CARD

Also Available on
Aperture Card

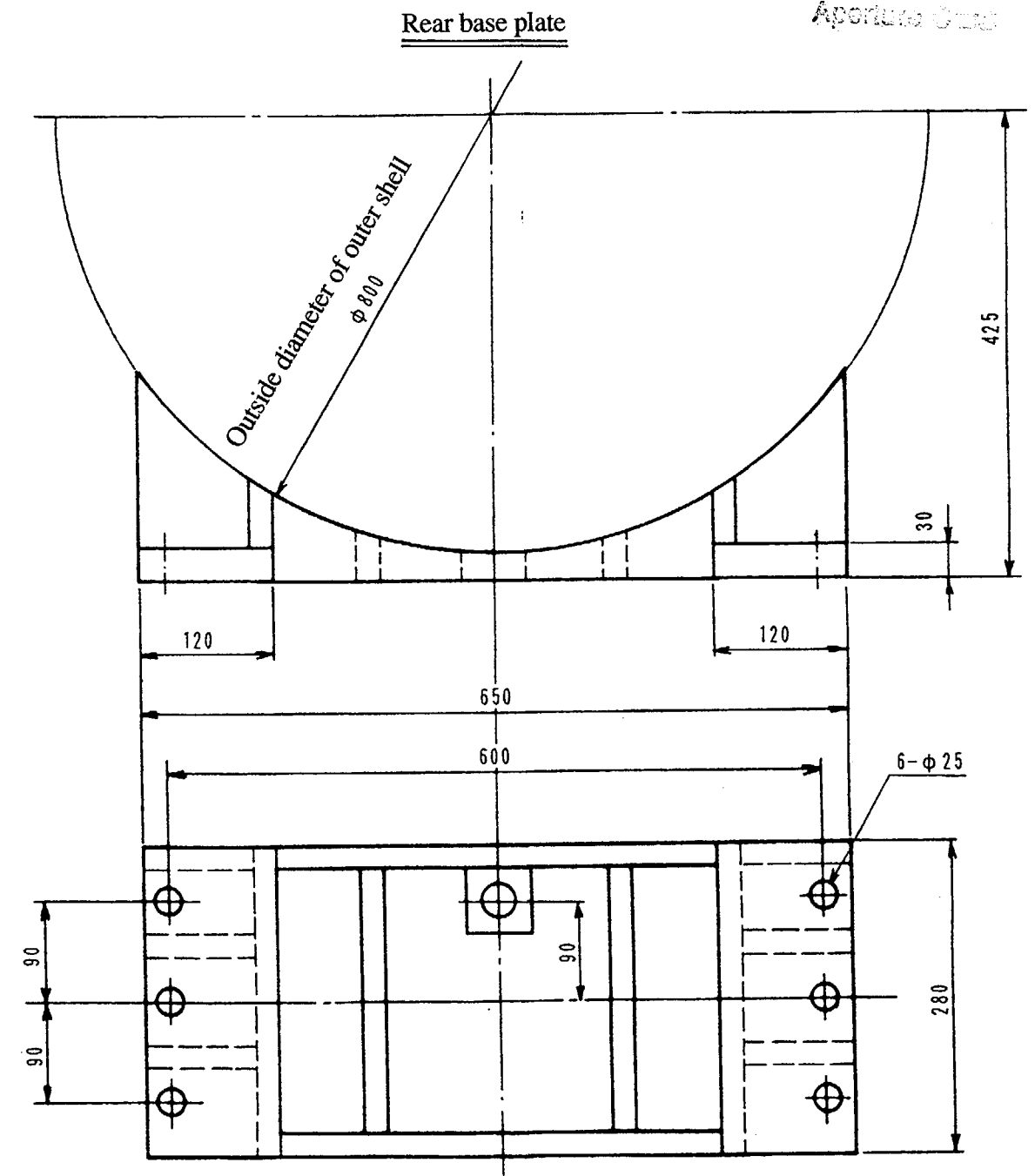
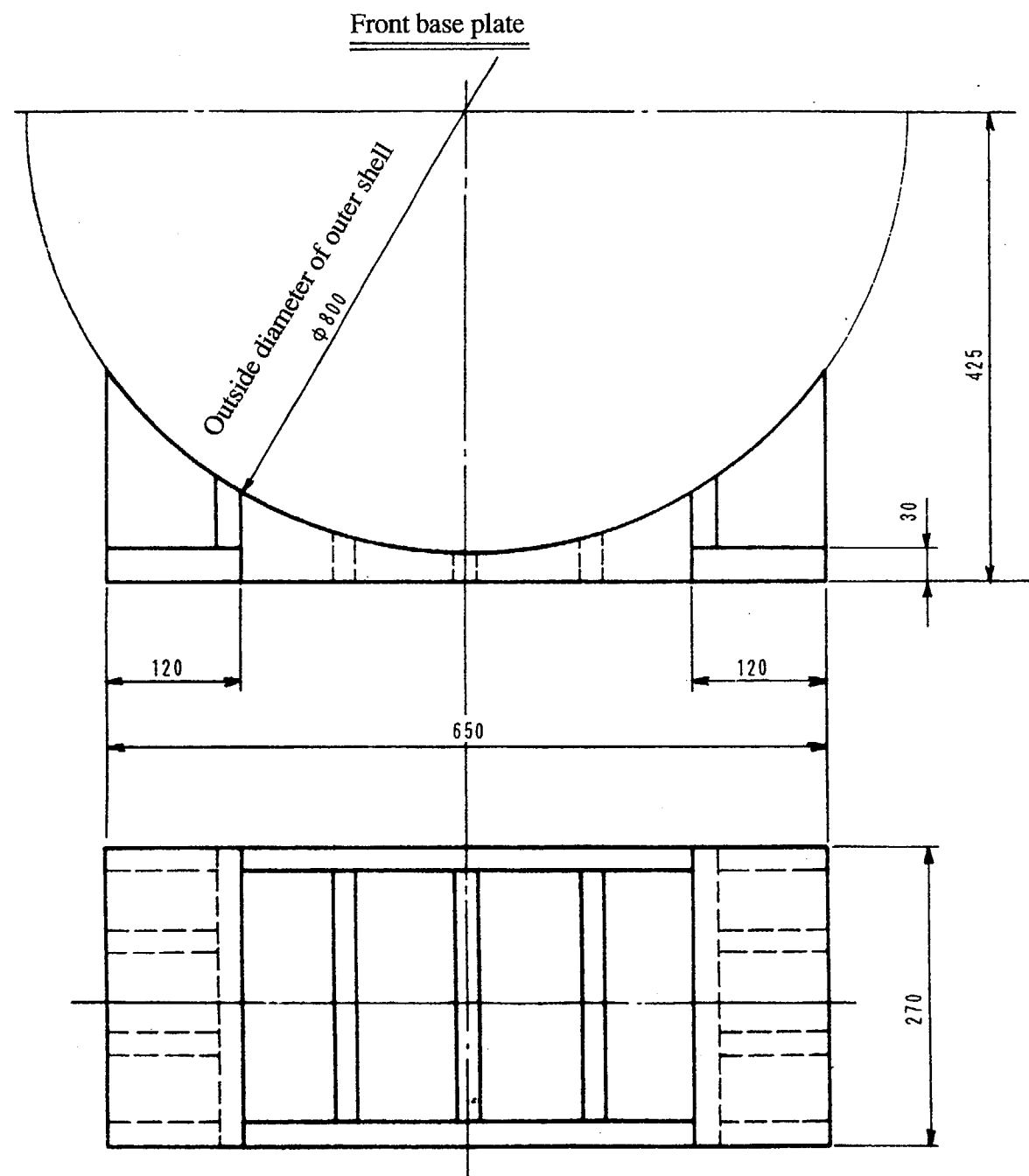


Fig. (I)-27 Front and Rear Base Plates (in mm)

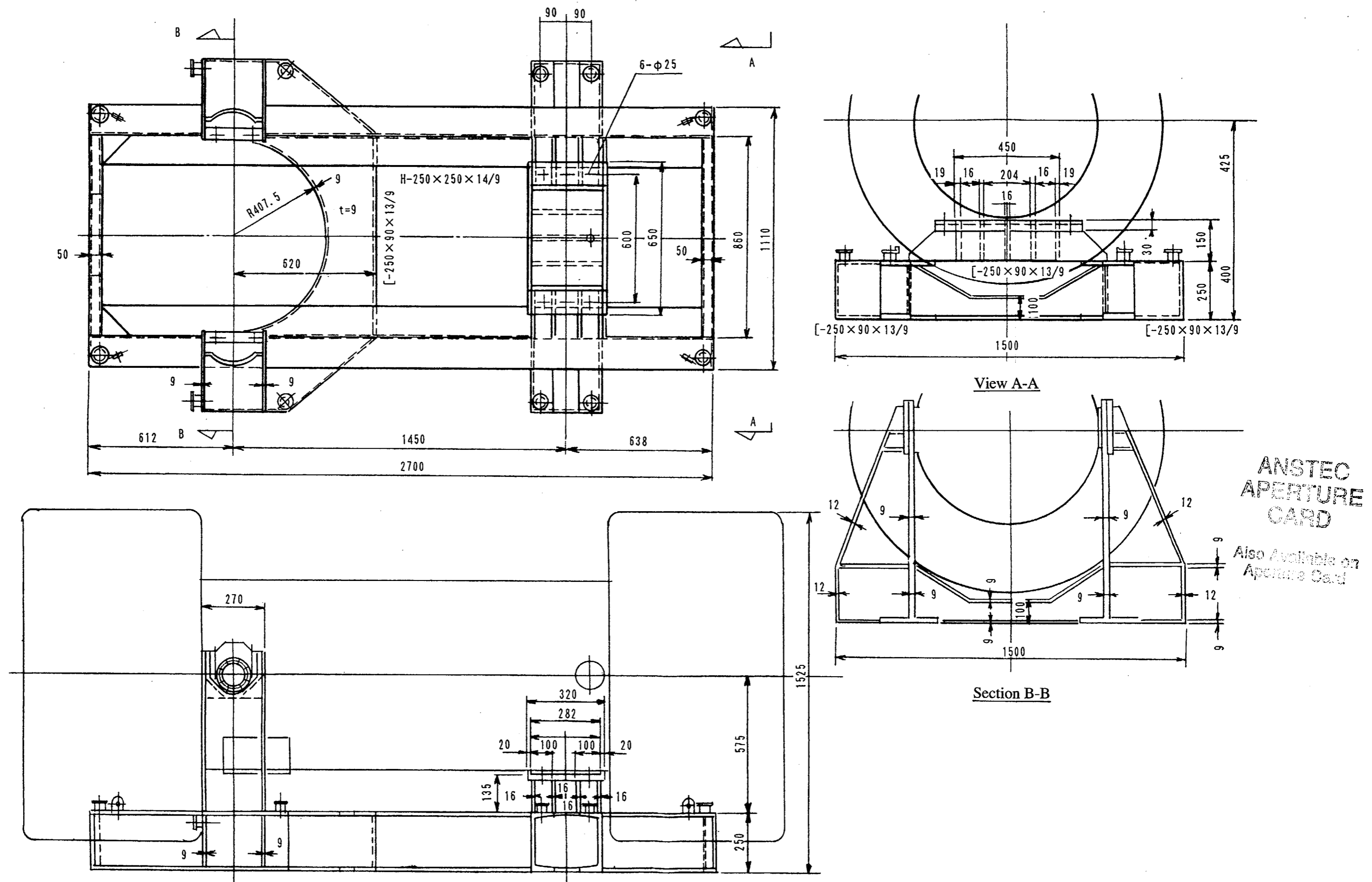


Fig. (I)-28 Transport Skid (in mm)

9601260203 - 27

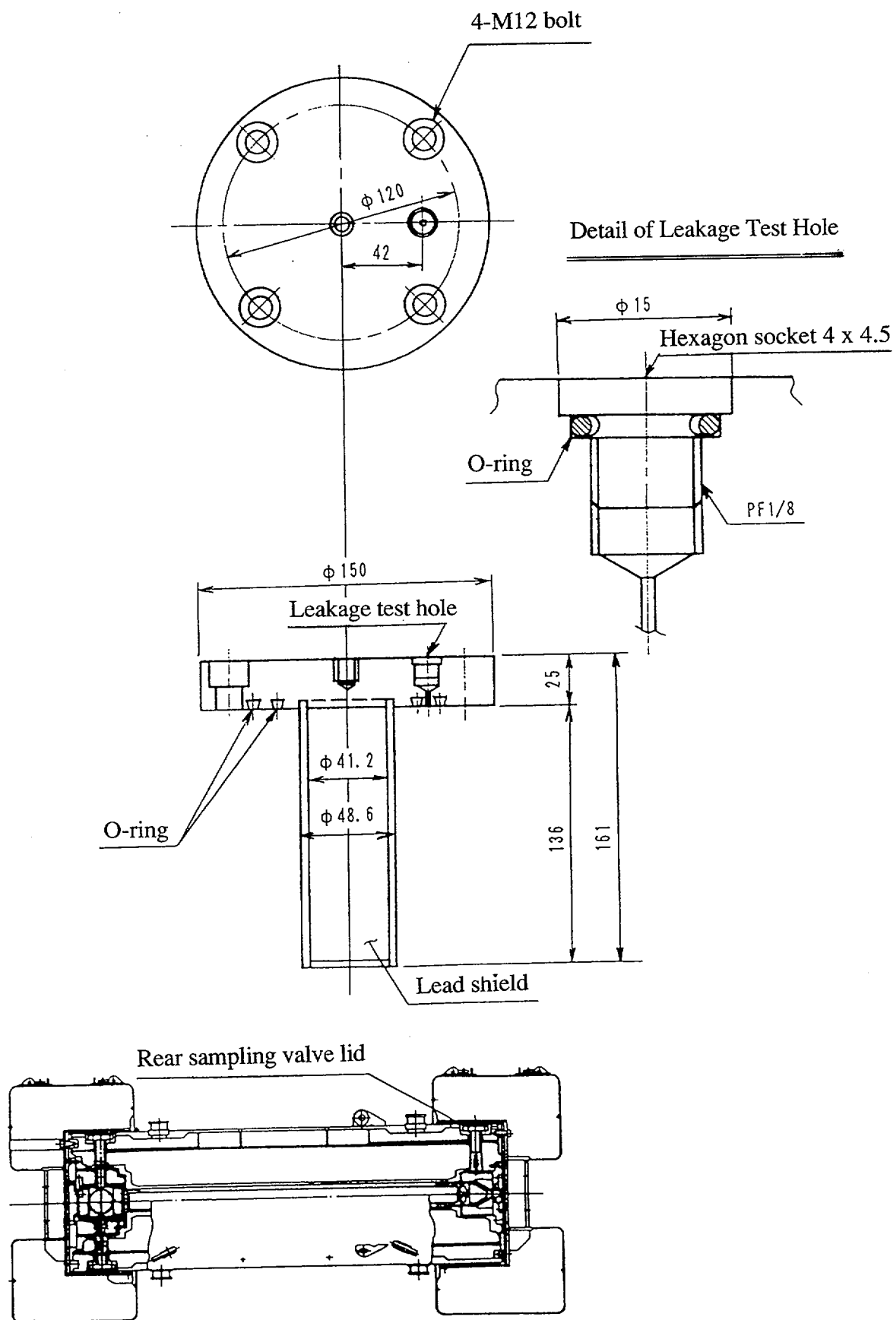


Fig. (I)-29 Penetration Hole Lid for Rear Sampling Valve (in mm)

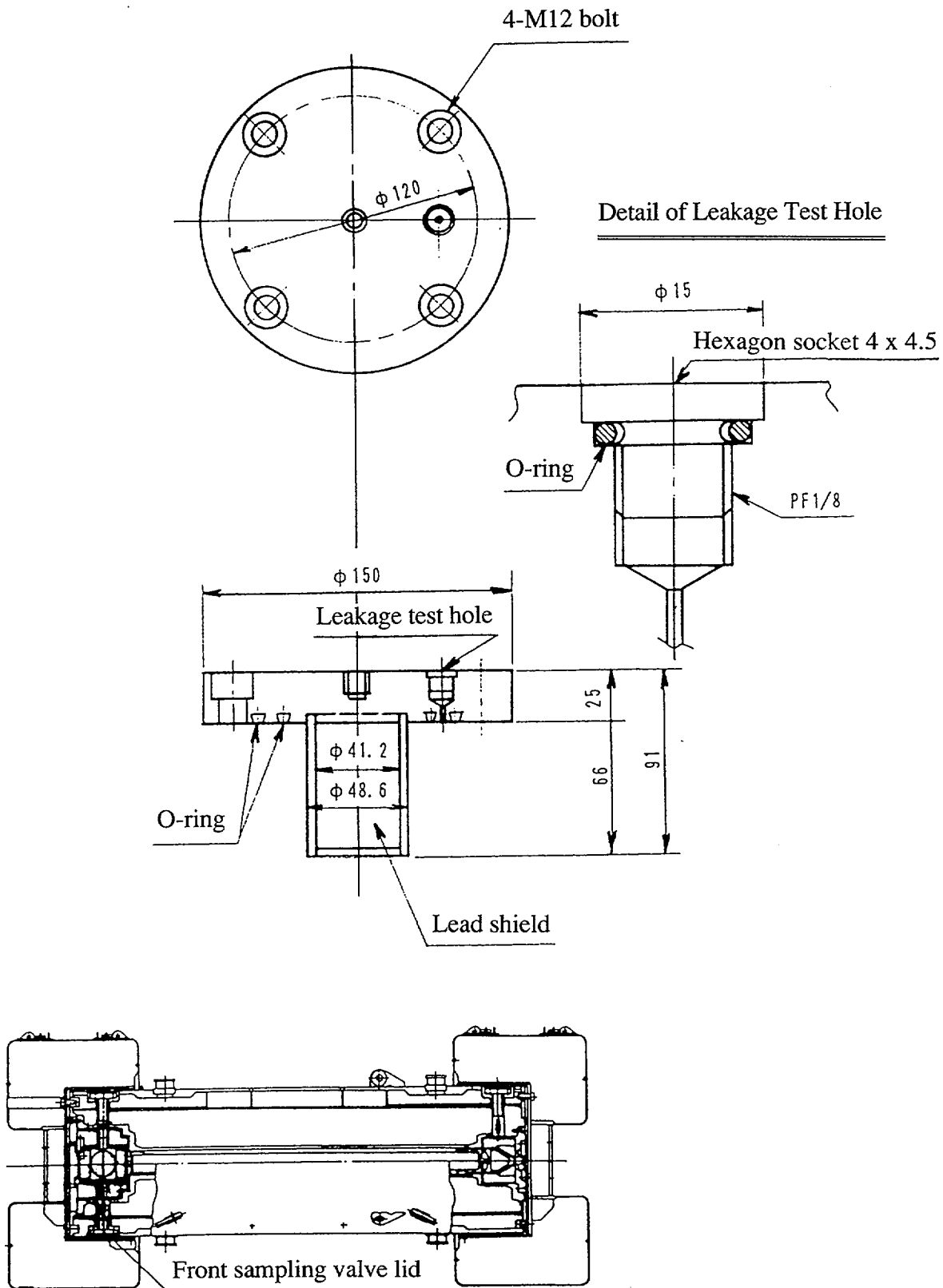


Fig. (I)-30 Penetration Hole Lid for Front Sampling Valve (in mm)

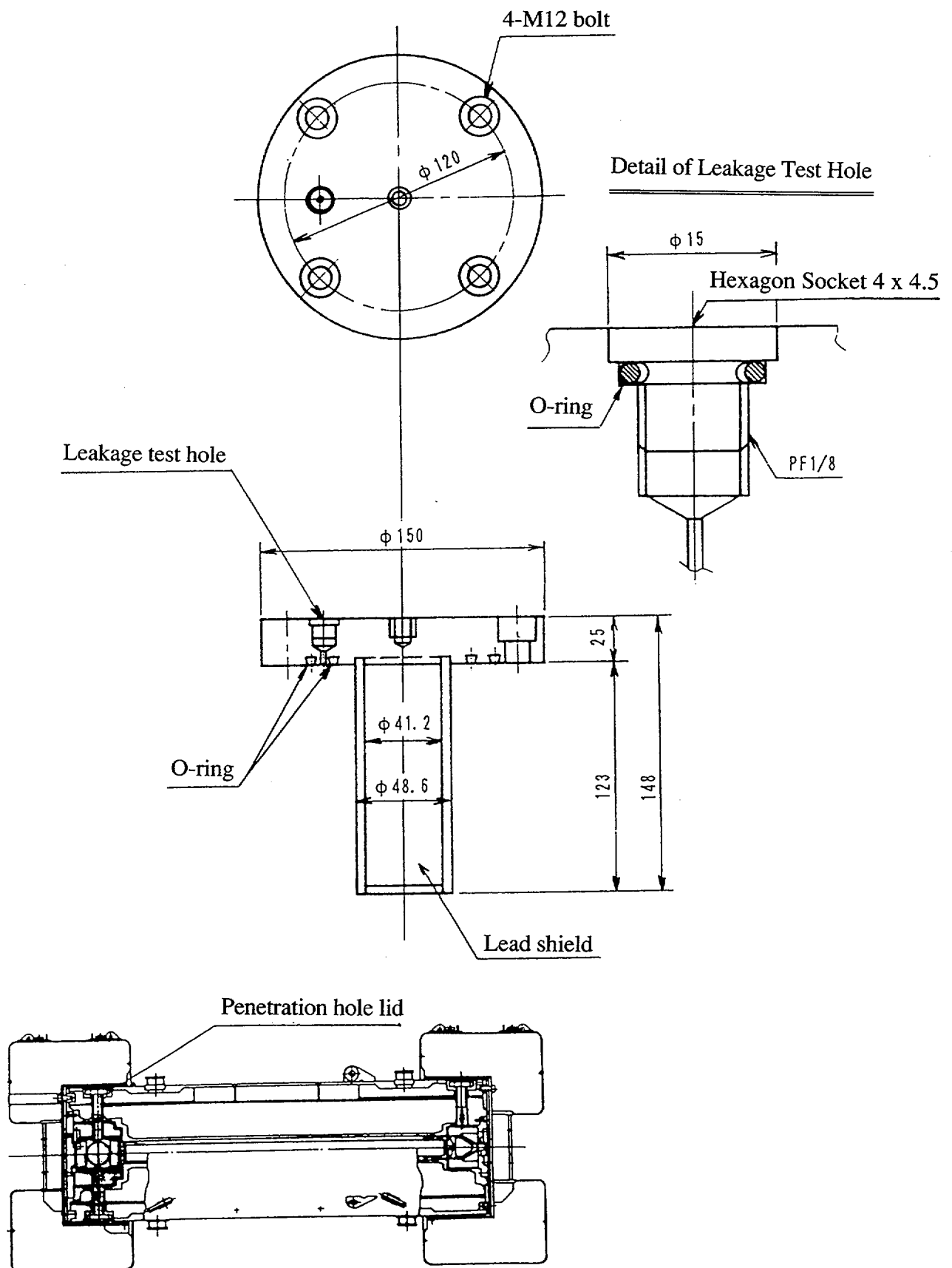


Fig. (I)-31 Penetration Hole Lid for Rotating Plug (in mm)

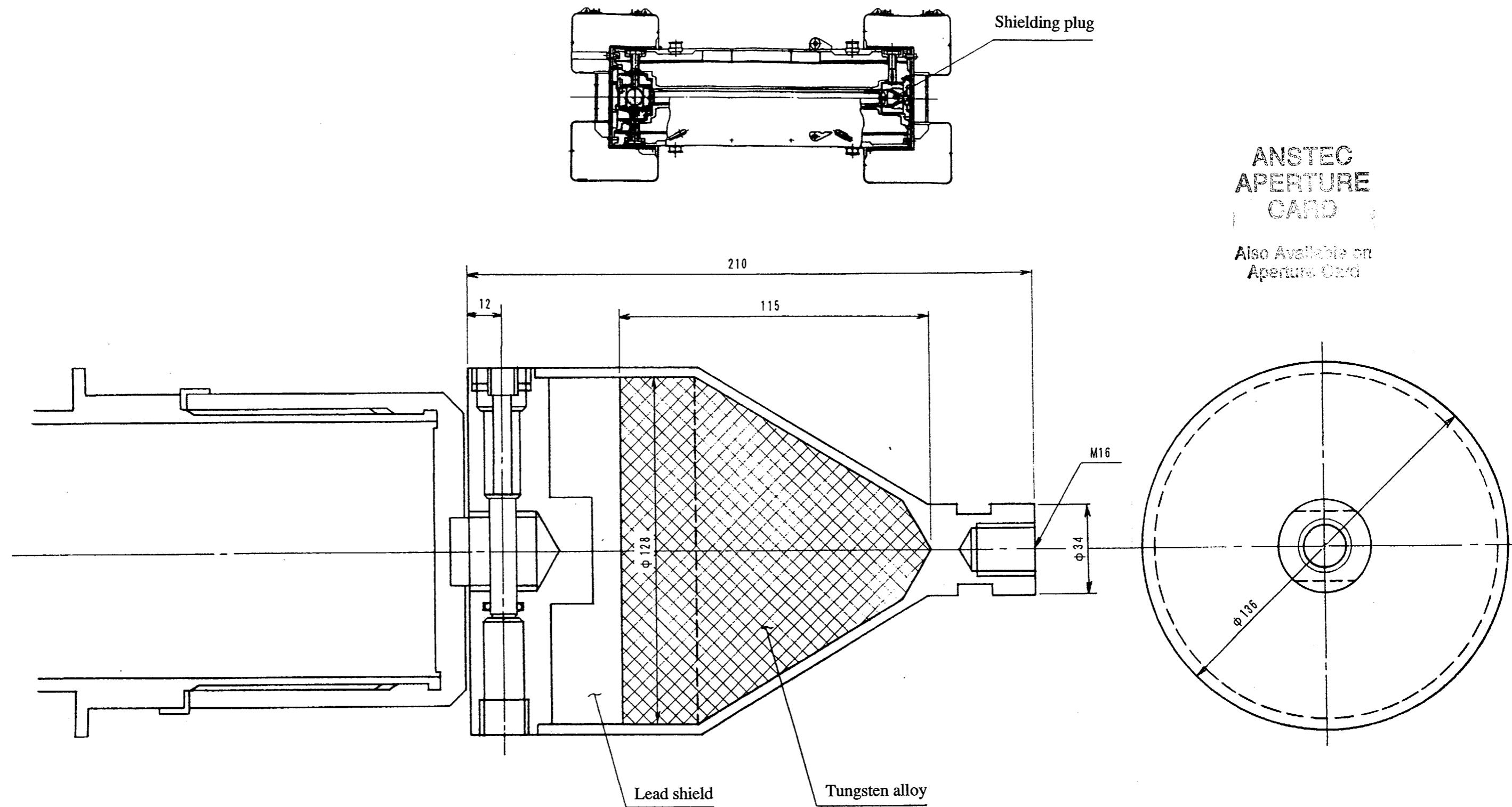
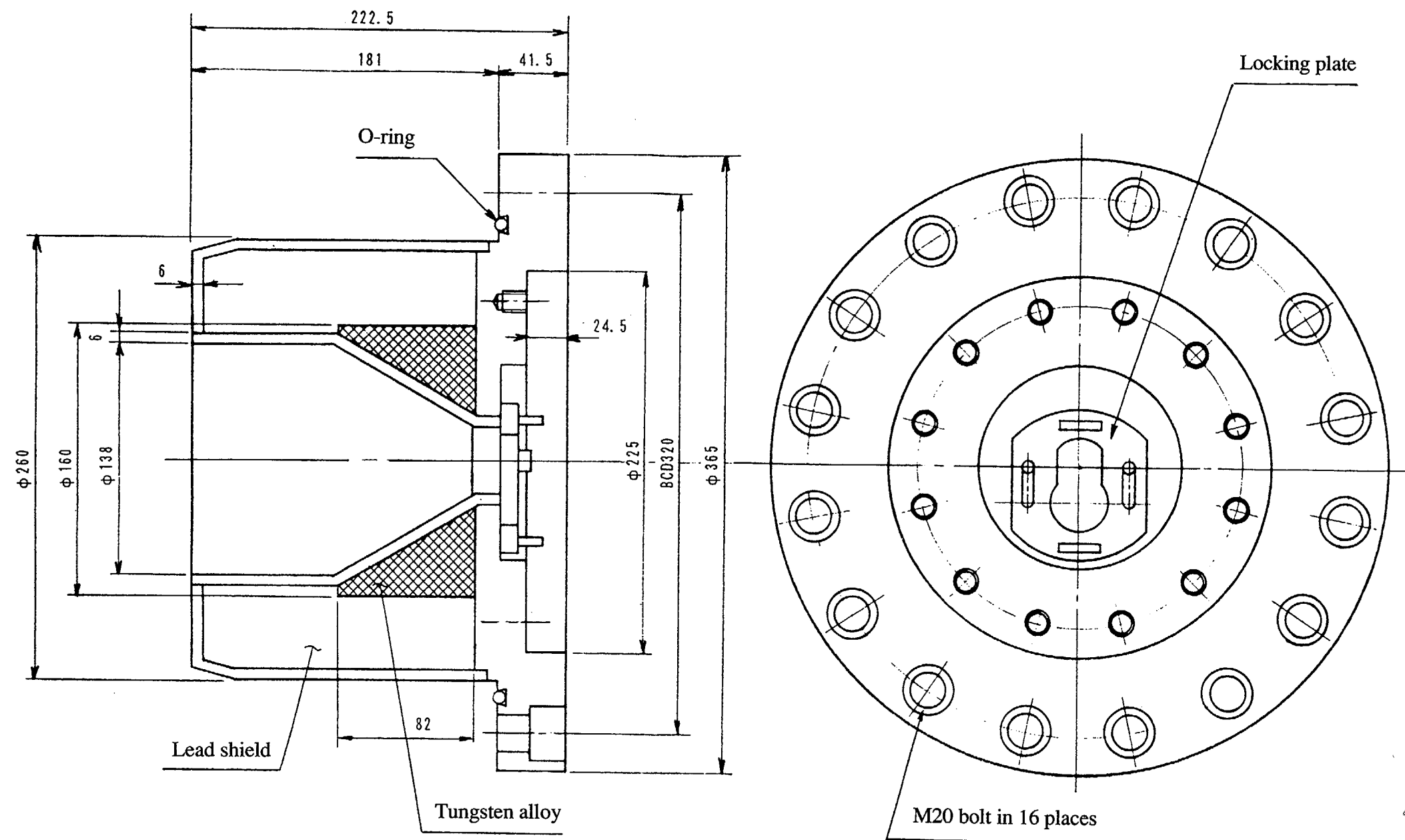


Fig. (I)-32 Shielding Plug (in mm)



**ANSTEC
APERTURE
CARD**

Also Available on
Aperture Card

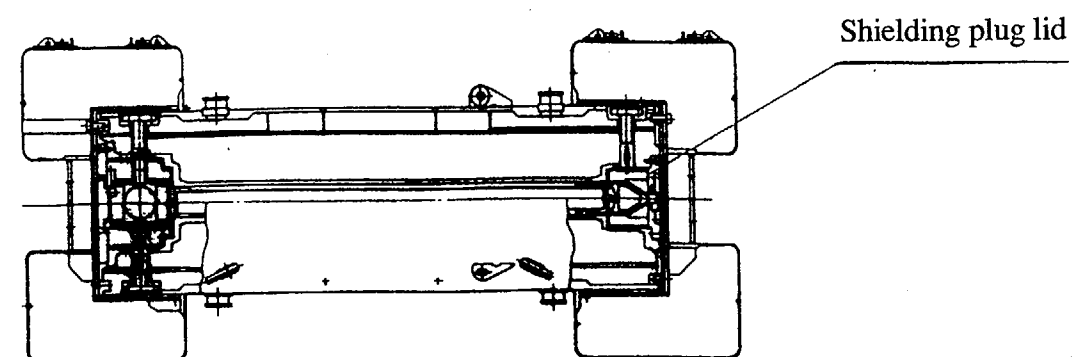


Fig. (I)-33 Shielding Plug Lid (in mm)

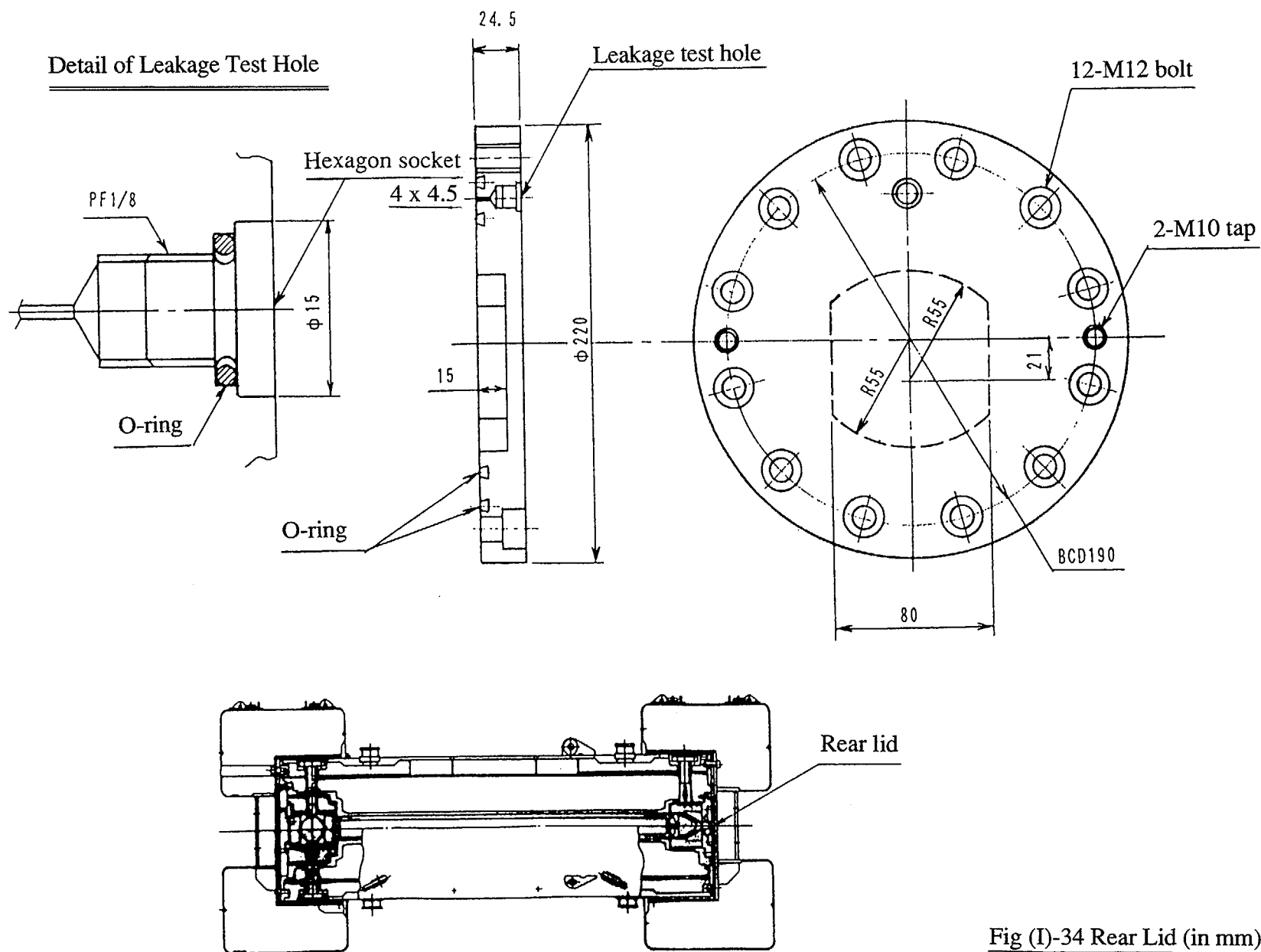


Fig (I)-34 Rear Lid (in mm)

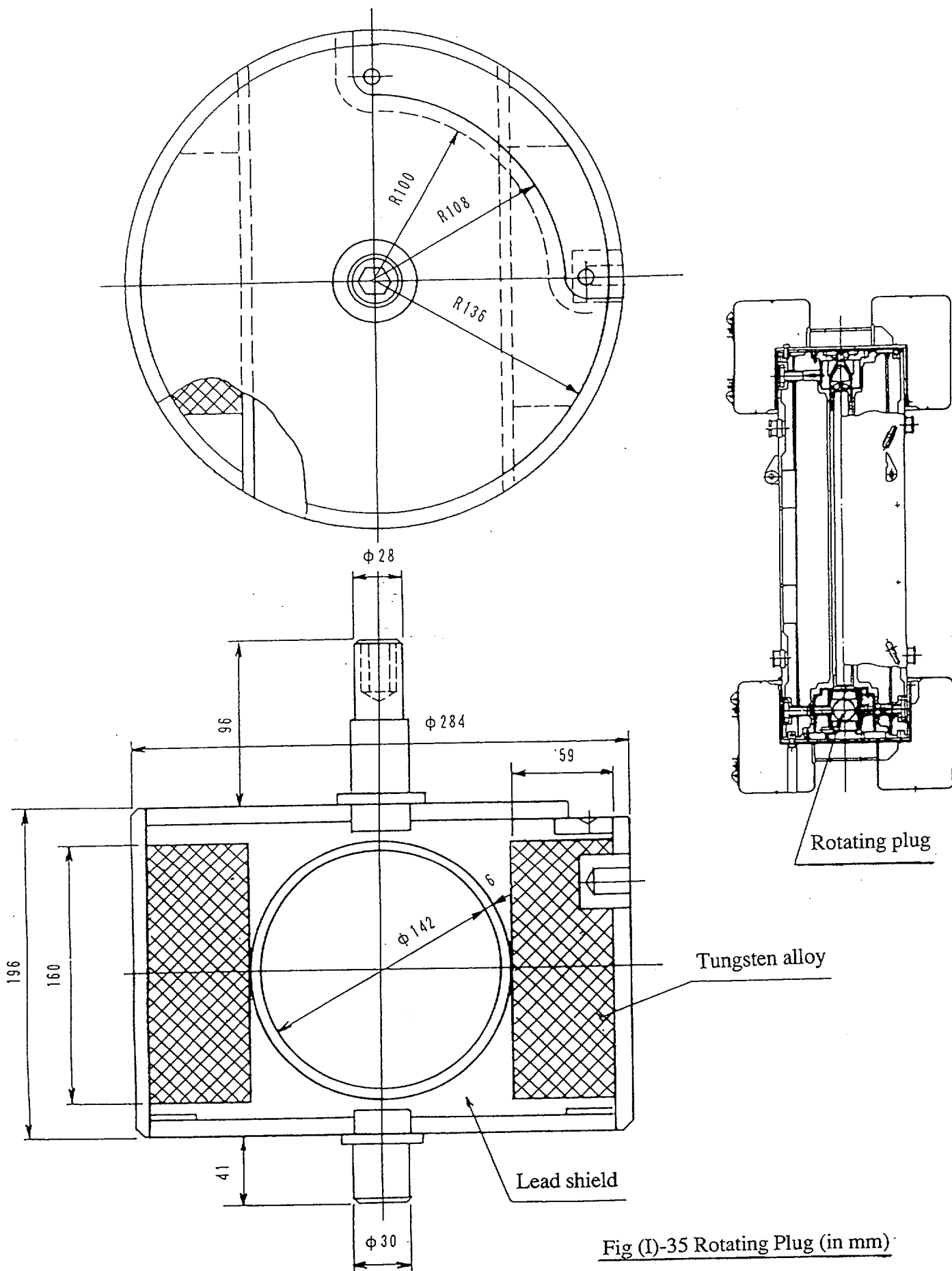
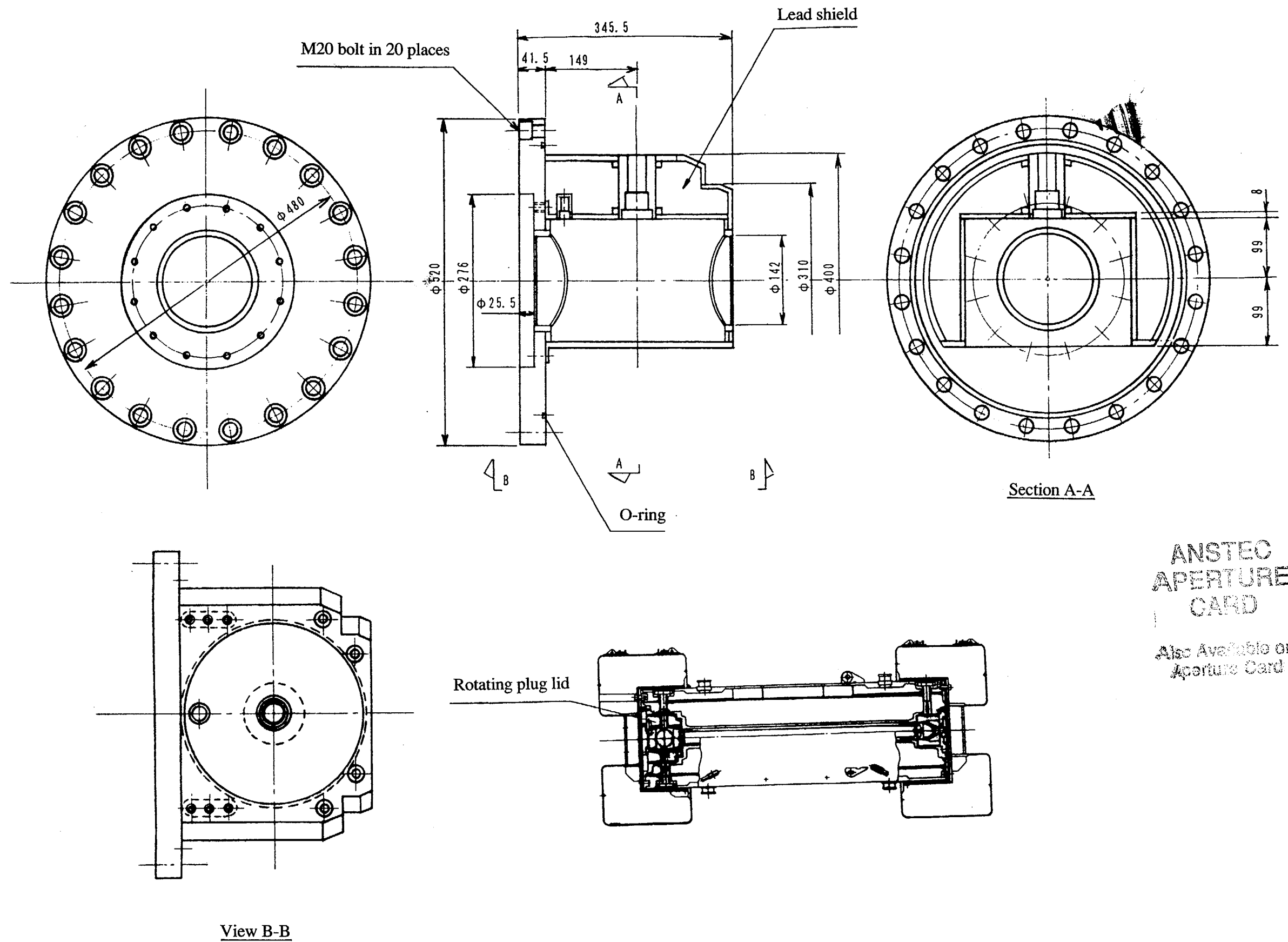


Fig (I)-35 Rotating Plug (in mm)

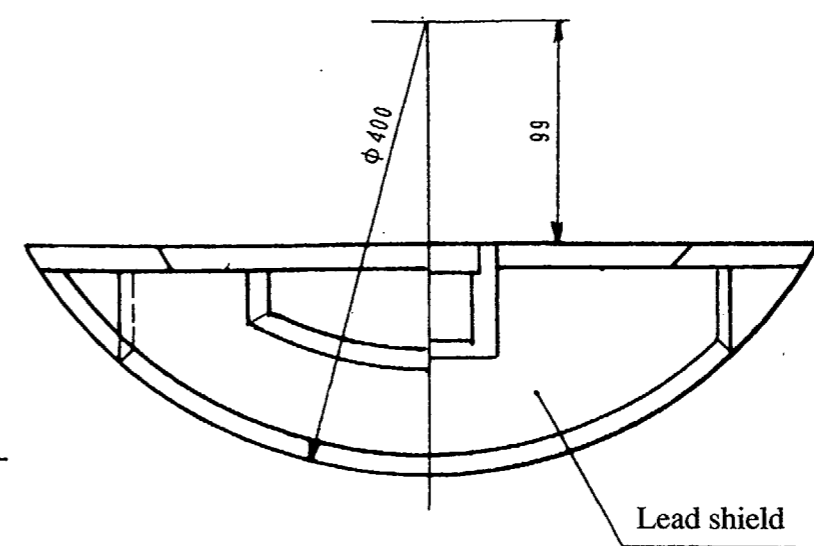
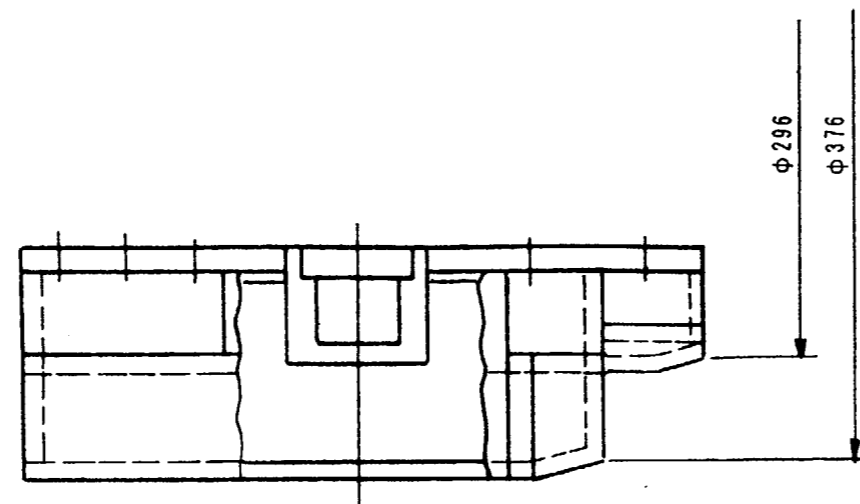


ANSTEC
APERTURE
CARD

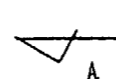
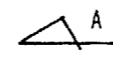
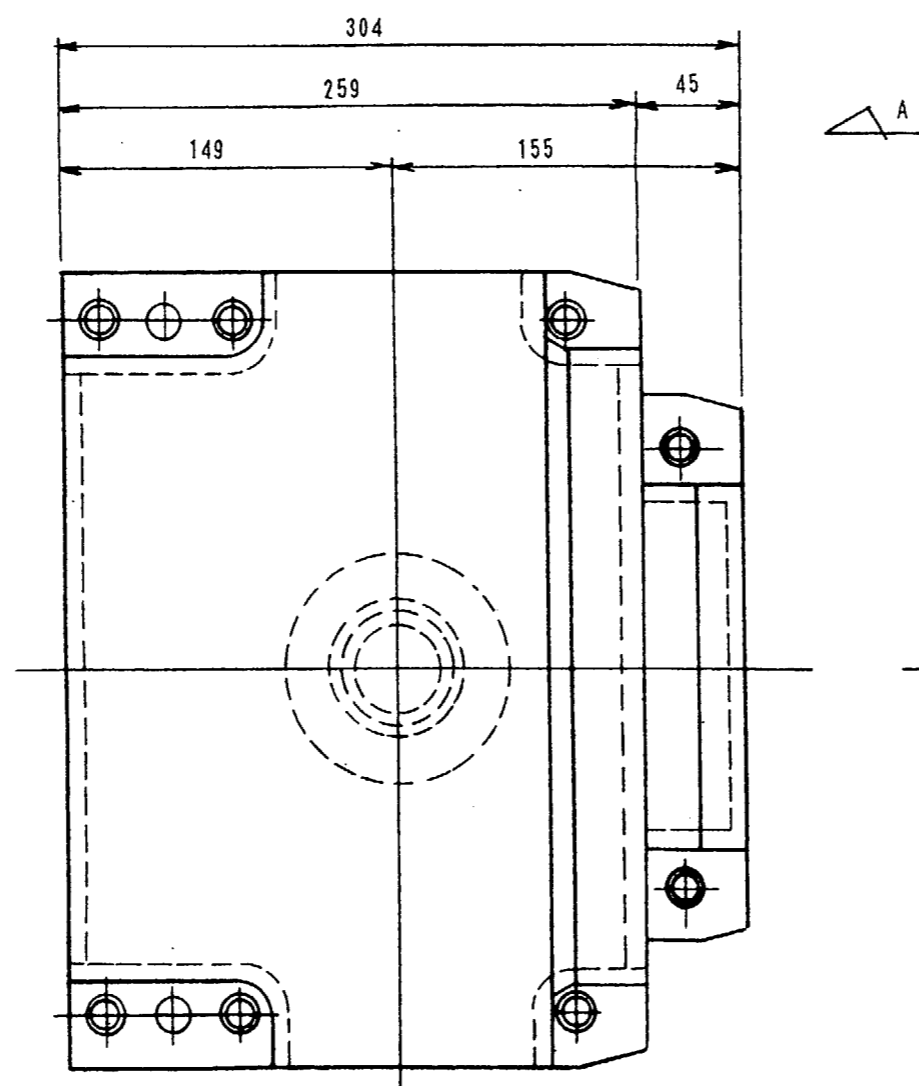
Also Available on
Aperture Card

Fig. (I)-36 Rotating Plug Lid (in mm)

9601260203 - 30

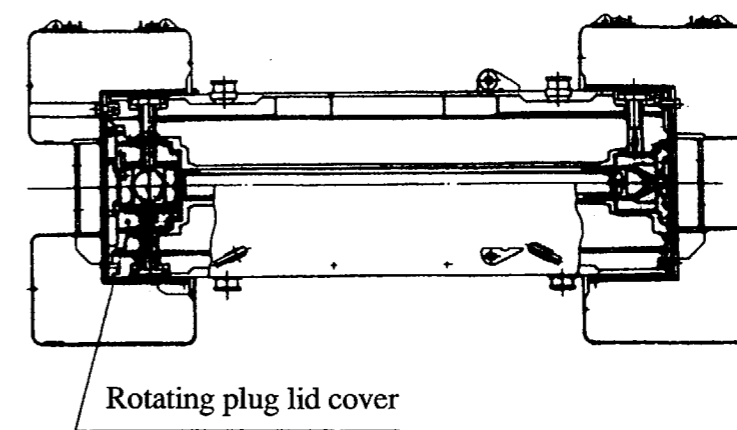


View A-A



ANSTEC
APERTURE
CARD

Also Available on
Aperture Card



Rotating plug lid cover

Fig. (I)-37 Rotating Plug Lid Cover (in mm)

9601260203 - 31

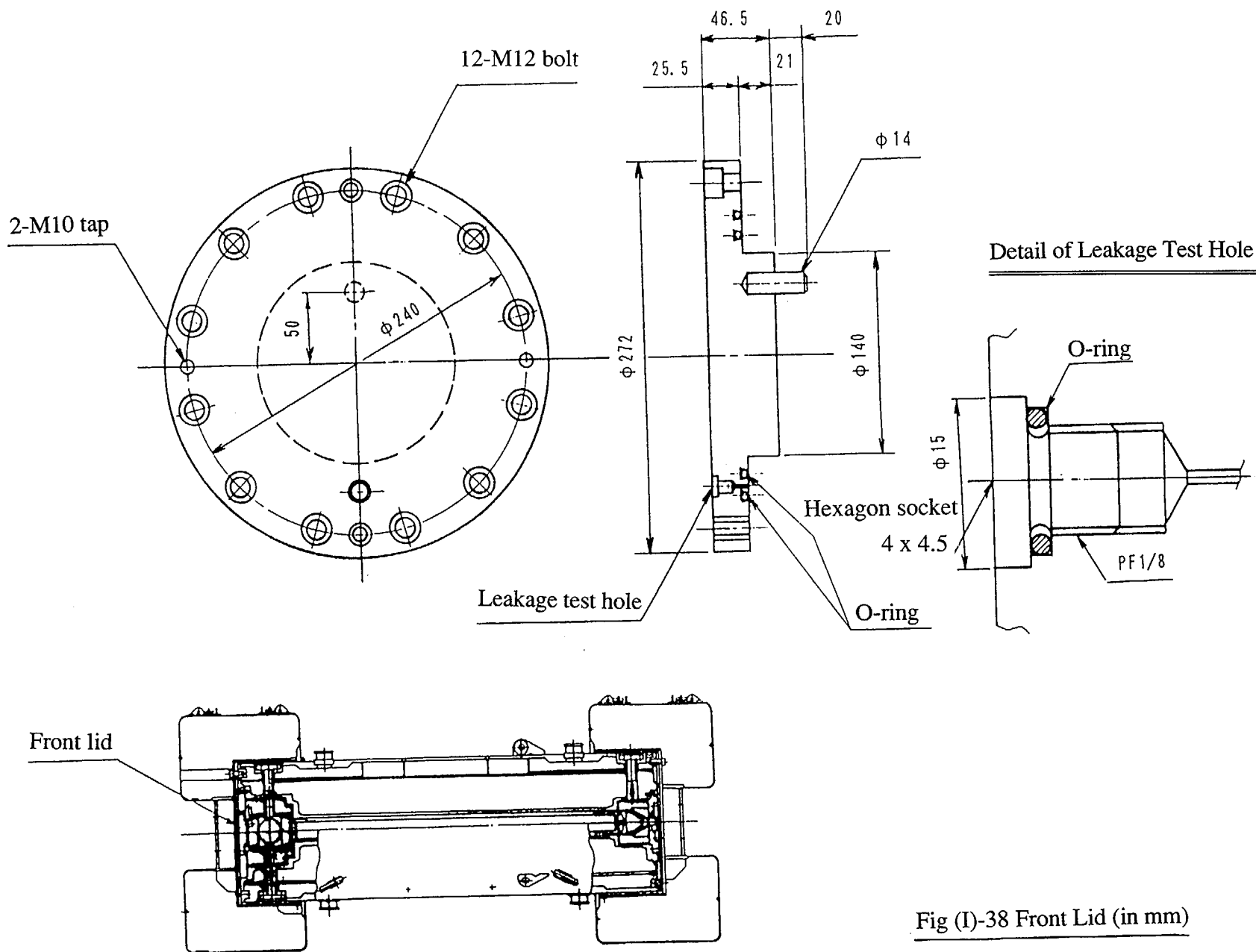


Fig (I)-38 Front Lid (in mm)

(I)-D Contents of the Packaging

D.1 Outline

Contents that are to be loaded inside the packaging include uranium-plutonium mixed oxide fuel that has been irradiated for testing and research purposes as well as radioactivated structural materials such as wrapper tubes. There are several different kinds of mixed oxide fuel classified according to differences in the size of their fissile region, as well as other specifications. For accommodation into the package, fuel can be broadly divided into two types on the basis of the burnup. Fuel with a burnup value of 110,000 MWD/MTM or less is referred to as Contents I, IV, V, VI and VII, or low-burnup pins, whereas fuel with a burnup of 200,000 MWD/MTM or less is referred to as Contents II and VIII, or higher-burnup pins. The test pieces of structural materials are referred to as Contents III.

- 1) Contents I : Low-burnup pins
- 2) Contents II : High-burnup pins
- 3) Contents III : Radioactive structural materials
- 4) Contents IV : Low-burnup pins (whose fertile region outweighs that of Contents I)
- 5) Contents V : Low-burnup pins (still lower than Contents I and IV in burnup)
- 6) Contents VI : Low-burnup pins (higher burnup than Contents I)
- 7) Contents VII : Low-burnup pins (whose fissile region outweighs that of Contents I)
- 8) Contents VIII : High-burnup pins (higher burnup than Contents II)

The package is capable of holding any one of the contents classified under the above eight categories.

D.2 Explanations of Contents

D.2.1 Contents I (Low-burnup pins)

Contents I are irradiated uranium-plutonium mixed oxide fuel elements whose burnup stands at 90,000 MWD/MTM or less. There are several different kinds of fuel elements that meet this burnup condition, and up to 15 fuel elements of these kinds can be combined and accommodated by the transportation packaging as Contents I. An example of fuel elements falling under the category of Contents I is shown in Fig. (I)-39. As can be seen from this figure, the central part of each fuel element consists of a fissile region of mixed oxide with enriched uranium of 90% or less and enhanced plutonium of 31% PuO_2 or less. This fissile region is sandwiched between the fertile regions which consist of natural uranium or depleted uranium. The composition of the fuel is shown in Table (I)-5. The fuel elements are cooled down for more than 180 days after irradiation. The maximum radioactivity and decay heat of Contents I are 2.03×10^{15} Bq and 260W or less, respectively. The specifications of Contents I are shown in Table (I)-5, and the prime nuclides contained in Contents I and their radioactivity are listed in Table (I)-7.

Concerning the accommodation of Contents I, fuel pins are placed into individual compartments of fuel supporting can I in groups of three (up to a total of 15 pins) as shown in Fig. (I)-15. The air inside fuel supporting can I is then replaced with helium, and the fuel supporting can is hermetically sealed by welding before it is placed inside the inner container.

D.2.2 Contents II (High-burnup pins)

Just like Contents I, Contents II are irradiated uranium-plutonium mixed oxide fuel elements. Their burnup values are much higher than those of Contents I and the maximum burnup value is 150,000 MWD/MTM. Several kinds of fuel elements fall under the category of Contents II. Up to six of these fuel elements can be combined for accommodation as Contents II. An example of such a combination is shown in Fig. (I)-40. Although Contents II are identical to Contents I in fuel composition, their irradiation periods are longer. Their cooling periods are in excess of 180 days, and they measure 4.96×10^{14} Bq in maximum radioactivity and 64W or less of decay heat. Contents II specifications are tabulated in Table (I)-5, while the prime nuclides contained in Contents II and their radioactivity are listed in Table (I)-7.

To put Contents II into the packaging, individual fuel elements are inserted into receiving tubes on a one-on-one basis. Then the individual receiving tubes are hermetically sealed by welding. These tubes are then placed on a rack to be placed inside the inner container.

D.2.3 Contents III

Contents III represent irradiated fuel cladding, wrapper tubes, or structural materials (stainless steel) such as test pieces to be subjected to materials testing. Although they may be contaminated by nuclear-fuel material or the like, they pose no problem with criticality. Furthermore, their contribution to the radioactivity of nuclear fuel material and the like is so small as to be negligible. Contents III specifications are shown in Table (I)-6, while the prime nuclides contained in Contents III and their radioactivity are listed in Table (I)-7.

Contents III may be placed directly into the inner container or inserted into fuel supporting cans before being placed into the inner container.

D.2.4 Contents IV

Contents IV represent irradiated uranium-plutonium mixed oxide fuel elements up to a burnup value of 90,000 MWD/MTM or less. There are several kinds of fuel elements that satisfy this burnup condition. Up to 14 of these fuel elements can be combined for accommodation as Contents IV. The central part of each fuel element consists of a fissile region of mixed oxide with enriched uranium of 90 w/o or less and enhanced plutonium of 31% PuO₂ or less. This fissile region is sandwiched between the fertile regions, which consist of natural uranium or depleted uranium.

The fertile region of Contents IV is longer than that of Contents I. The composition of the fuel is shown in Table (I)-5. The fuel elements are cooled down for more than 180 days after irradiation. The maximum radioactivity and decay heat of Contents IV are 1.99×10^{14} Bq and 250W or less, respectively. The specifications of Contents IV are shown in Table (I)-5, and the prime nuclides contained in Contents IV and their radioactivity are listed in Table (I)-7.

Concerning the accommodation of Contents IV into the transportation packaging, fuel pins are placed into the individual compartments of the fuel supporting can I in groups of three (up to a total of 14 pins) as shown in Fig. (I)-15. The air inside the fuel supporting can I is then replaced with helium, and the fuel supporting can is hermetically sealed by welding before it is placed inside the inner container.

D.2.5 Contents V

Contents V represent irradiated uranium-plutonium mixed oxide fuel elements up to a burnup value of 5,200 MWD/MTM or less. Up to 14 of these fuel elements can be combined for accommodation as Contents V. The central part of each fuel element consists of a fissile region of mixed oxide with enriched uranium of 23 w/o or less and enhanced plutonium of 18% PuO₂ or less. This fissile region is sandwiched between the fertile regions, which consist of natural uranium or depleted uranium.

The composition of the fuel is shown in Table (I)-5. The fuel elements are cooled down for more than 93 days after irradiation. The maximum radioactivity and decay heat of Contents V are 3.85×10^{15} Bq and 63W or less, respectively. The specifications of Contents V are shown in Table (I)-5, and the prime nuclides contained in Contents V and their radioactivity are listed in Table (I)-7.

Concerning the accommodation of Contents V into the package, fuel pins are placed into the individual compartments of fuel supporting can I in groups of three (up to a total of 14 pins) as shown in Fig. (I)-15. The air inside fuel supporting can I is then replaced with helium, and the fuel supporting can is hermetically sealed by welding before it is placed inside the inner container.

D.2.6 Contents VI

Contents VI represent irradiated uranium-plutonium mixed oxide fuel elements up to a burnup value of 110,000 MWD/MTM or less. Up to 9 of these fuel elements meeting this burnup condition can be combined for accommodation as Contents VI. The central part of each fuel element consists of a fissile region of mixed oxide with enriched uranium of 90 w/o or less and enhanced plutonium of 31% PuO₂ or less. This fissile region is sandwiched between the fertile regions, which consist of natural uranium or depleted uranium.

The composition of the fuel is shown in Table (I)-5. The fuel elements are cooled down for more than 300 days after irradiation. The maximum radioactivity and decay heat of Contents VI are 1.97×10^{15} Bq and 260W or less, respectively. The specifications of Contents VI are shown in Table (I)-5, and the prime nuclides contained in Contents VI and their radioactivity are listed in Table (I)-7.

To put Contents VI into the packaging, individual fuel elements are inserted into receiving tubes 6 on a one-on-one basis, and then these receiving tubes are hermetically sealed by welding. Up to nine of these hermetically sealed receiving tubes are then put into a supporting can to be placed inside the inner container.

D.2.7 Contents VII

Contents VII represent irradiated uranium-plutonium mixed oxide fuel elements up to a burnup value of 11,000 MWD/MTM or less. Up to six of these fuel elements can be combined for accommodation as Contents VII. The central part of each fuel element consists of a fissile region of mixed oxide with enriched uranium of 0.71 w/o or less and enhanced plutonium of 3.2% PuO₂ or less. This fissile region is sandwiched between the fertile regions, which consist of natural uranium or depleted uranium.

The composition of the fuel is shown in Table (I)-5. The fuel elements are cooled down for more than 3,600 days after irradiation. The maximum radioactivity and decay heat of Contents VII are 3.74×10^{13} Bq and 3W or less, respectively. The specifications of Contents VII are shown in Table (I)-5, and the prime nuclides contained in Contents VII and their radioactivity are listed in Table (I)-7.

Concerning the accommodation of Contents VII into the transportation packaging, fuel pins inserted into aluminum cans are put into the individual compartments of fuel supporting can II on a one-on-one basis (up to a total of six pieces) as shown in Fig. (I)-17. The air inside fuel supporting can II is then replaced with helium, and the fuel supporting can is hermetically sealed by welding before it is placed inside the inner container.

D.2.8 Contents VIII

Contents VIII represent irradiated uranium-plutonium mixed oxide fuel elements up to a burnup value of 200,000 MWD/MTM or less.

Up to nine of these fuel elements meeting this burnup condition can be combined for accommodation as Contents VIII. The central part of each fuel element consists of a fissile region of mixed oxide with enriched uranium of 97 w/o or less and enhanced plutonium of 31% PuO₂ or less. This fissile region is sandwiched between the fertile regions, which consist of natural uranium or depleted uranium.

The composition of the fuel is shown in Table (I)-5. The fuel elements are cooled down for more than 360 days after irradiation. The maximum radioactivity and decay heat of Contents VIII are 1.27×10^{15} Bq and 170W or less, respectively.

The specifications of Contents VIII are shown in Table (I)-5, and the radioactivity of Contents VIII are shown in Table (I)-7.

Concerning the accommodation of Contents VIII into the packaging, as shown in Fig. (I)-16, fuel elements are inserted into receiving tubes II on a one-on-one basis, then these receiving tubes are hermetically sealed by welding. Up to nine of these hermetically sealed receiving tubes are then placed into a supporting can to be placed inside the inner container.

Table (I)-5 Specifications of Nuclear-Fuel Contents (1/2)

Item	Contents I	Contents II	Contents IV	Contents V	Contents VI	Contents VII	Contents VIII
Designation	Irradiated test fuel elements	Same as left box	Same as left box	Same as left box	Same as left box	Same as left box	Same as left box
Dimensions							
Overall length (mm)	1,875 or less	1,000 or less	1,875 or less	Same as left box	1,793 or less	1,573 or less	1,800 or less
Length of fissile region (mm)	720 or less	360 or less	720 or less	Same as left box	1,400 or less	Same as left box	920 or less
Outer diameter of fuel cladding (mm)	5.5 ~ 6.5	Same as left box	Same as left box	Same as left box	13.5 or less	11.7 ~ 12.3	7.5 ~ 11.6
Thickness of fuel cladding (mm)	0.35 or more	Same as left box	Same as left box	Same as left box	Same as left box	0.7 or more	0.4 or more
Material							
Fuel	Uranium-plutonium mixed oxide (UO ₂ -PuO ₂)	Same as left box	Same as left box	Same as left box	Same as left box	Same as left box	Same as left box
Fuel cladding	Stainless steel (SUS316)	Same as left box	Same as left box	Same as left box	Same as left box	Zircaloy	Stainless steel (SUS316)
Quantity							
Number of fuel elements (pcs.)	15 or less	Equivalent to 6 pcs or less	14 or less	Same as left box	9 or less	6 or less	9 or less
Total weight of contents (g)	5,800 or less	1,350 or less	6,977 or less	Same as left box	3,800 or less	9,090 or less	4,950 or less
Weight of oxides (g)	3,150 or less	756 or less	4,592 or less	Same as left box	2,330 or less	7,290 or less	3,245 or less
Mixed oxide (Fissile region)	2,160 or less	432 or less	1,960 or less	Same as left box	1,590 or less	7,140 or less	1,710 or less
Uranium dioxide (Fertile region)	990 or less	324 or less	2,632 or less	Same as left box	740 or less	150 or less	1,535 or less
Fissile plutonium (g)	428 or less	57 or less	388 or less	233 or less	337 or less	171 or less	423 or less
Uranium (U) (g)	2,203 or less	589 or less	3,527 or less	3,736 or less	1,632 or less	6,530 or less	2,402 or less
Uranium-235 (U ²³⁵)	1,197 or less	273 or less	1,113 or less	327 or less	881 or less	47 or less	1,032 or less
Composition of fuel							
Fissile region							
Uranium enrichment (%)	90 or less	Same as left box	Same as left box	23 or less	90 or less	0.72 or less	97 or less
Plutonium enhancement (%PuO ₂)	31 or less	21 or less	31 or less	18 or less	31 or less	3.2 or less	31 or less

Table (I)-5 Specifications of Nuclear-Fuel Contents (2/2)

Item	Contents I	Contents II	Contents IV	Contents V	Contents VI	Contents VII	Contents VIII
Composition of plutonium isotopes (g)	1.18 or less	0.16 or less	0.73 or less	0.62 or less	0.43 or less	-	0.9 or less
Pu-238	472.47 or less	64.01 or less	290.42 or less	248.94 or less	348.00 or less	185.40 or less	450.0 or less
Pu-239	147.65 or less	20.00 or less	90.76 or less	77.79 or less	87.00 or less	18.14 or less	108.0 or less
Pu-240	59.06 or less	8.00 or less	36.30 or less	31.12 or less	21.70 or less	2.02 or less	18.0 or less
Pu-241	29.53 or less	4.00 or less	18.15 or less	15.56 or less	4.53 or less	0.20 or less	4.5 or less
Pu-242	8.86 or less	1.20 or less	5.45 or less	4.67 or less	2.17 or less	-	2.7 or less
Am-241	0.72 or less						
Fertile region	(Natural uranium or depleted uranium)	Same as left box	Same as left box	Same as left box	Same as left box	Same as left box	Same as left box
Uranium enrichment (%)							
Irradiation conditions							
Burnup (MWD/MTM)	90,000 or less	150,000 or less	90,000 or less	5,200 or less	110,000 or less	11,000 or less	200,000 or less
Specific output (MW/MTM)	300 or less	Same as left box	Same as left box	Same as left box	Same as left box	60 or less	166 or less
Irradiation time (days)	400 or less	700 or less	500 or less	50 or less	600 or less	500 or less	1,210 or less
Cooling time (days)	180 or more	Same as left box	Same as left box	93 or more	300 or more	3,600 or more	360 or more
Radioactivity (Bq)	2.03×10^{15} or less	4.96×10^{14} or less	1.99×10^{15} or less	3.85×10^{14} or less	1.97×10^{15} or less	3.74×10^{13} or less	1.27×10^{15} or less
Decay heat (W)	260 or less	64 or less	250 or less	63 or less	260 or less	3 or less	170 or less

Table (I)-6 Specifications of Contents III

Item	Specification
Material	Stainless steel
Irradiation conditions	
Fluence (nvt)	50×10^{22} or less
Flux (n/s/cm ²)	5.8×10^{15}
Weight (kg)	5 or less
Radioactivity (Bq)	1.63×10^{14} or less
Decay heat (W)	30 or less
Cooling time (days)	300 or more

Table (I)-7 Prime nuclides and their radioactivity (Bq)

Nuclide	Contents I	Contents II	Contents III	Contents IV	Contents V	Contents VI	Contents VII	Contents VIII
²³⁵ U	1.33×10^8	2.12×10^7	-	1.21×10^8	2.54×10^7	1.33×10^8	2.69×10^6	4.88×10^7
²³⁸ U	5.66×10^6	3.85×10^6		1.37×10^7	4.14×10^7	1.93×10^7	7.40×10^7	1.50×10^7
²³⁸ Pu	6.11×10^{11}	7.81×10^{10}		5.55×10^{11}	3.27×10^{11}	6.48×10^{11}	6.25×10^{10}	8.79×10^{11}
²³⁹ Pu	8.88×10^{11}	1.15×10^{11}		8.07×10^{11}	4.74×10^{11}	8.88×10^{11}	2.35×10^{11}	8.41×10^{11}
²⁴⁰ Pu	1.03×10^{12}	1.33×10^{11}		9.32×10^{11}	5.55×10^{11}	1.03×10^{12}	1.84×10^{11}	1.10×10^{12}
²⁴¹ Pu	1.98×10^{14}	2.55×10^{13}		1.79×10^{14}	1.06×10^{14}	1.98×10^{13}	1.85×10^{13}	5.78×10^{13}
²⁴² Pu	3.49×10^9	4.51×10^8		3.17×10^9	1.88×10^{10}	3.49×10^9	1.22×10^8	7.84×10^8
²⁴¹ Am	8.66×10^{11}	1.11×10^{11}		7.84×10^{11}	2.68×10^{10}	8.66×10^{11}	6.14×10^{11}	6.33×10^{11}
³ H	2.06×10^{11}	6.73×10^{10}	-	2.01×10^{11}	9.29×10^9	2.05×10^{11}	2.17×10^{10}	3.50×10^{11}
⁸⁵ Kr	1.68×10^{12}	5.44×10^{11}		1.67×10^{12}	1.05×10^{11}	2.79×10^{12}	1.97×10^{11}	6.34×10^{12}
⁹⁵ Zr	1.51×10^{14}	3.12×10^{13}		1.50×10^{14}	5.14×10^{13}	1.42×10^{14}	0	1.82×10^{13}
⁹⁵ Nb	2.91×10^{14}	6.07×10^{13}		2.67×10^{14}	7.07×10^{13}	2.73×10^{14}	0	3.86×10^{13}
¹⁰⁶ Ru	2.72×10^{14}	9.84×10^{13}		2.62×10^{14}	1.04×10^{14}	2.66×10^{14}	6.18×10^9	1.51×10^{14}
¹⁰⁶ Rh	2.72×10^{14}	9.84×10^{13}		2.62×10^{14}	1.04×10^{14}	2.66×10^{14}	6.18×10^9	1.51×10^{14}
¹⁴⁴ Ce	2.40×10^{14}	9.44×10^{13}		2.38×10^{14}	2.39×10^{13}	2.32×10^{14}	4.51×10^8	2.35×10^{14}
¹⁴⁴ Pr	2.40×10^{14}	9.44×10^{13}		2.38×10^{14}	2.39×10^{13}	2.32×10^{14}	4.51×10^8	2.35×10^{14}
²⁴² Cm	3.32×10^{13}	6.73×10^{12}		3.01×10^{13}	3.46×10^7	3.32×10^{13}	3.37×10^9	3.12×10^{12}
⁵⁴ Mn	2.67×10^{13}	5.99×10^{12}	6.62×10^{13}	2.40×10^{13}	1.37×10^{13}	2.67×10^{13}	0	2.75×10^{10}
⁵⁵ Fe	1.69×10^{13}	3.77×10^{12}	6.92×10^{13}	1.52×10^{13}	5.88×10^{11}	1.69×10^{13}	1.31×10^5	1.28×10^{11}
⁵⁸ Co	3.74×10^{12}	8.36×10^{12}	2.57×10^{13}	3.36×10^{12}	7.66×10^{12}	3.74×10^{12}	0	6.07×10^7
⁶⁰ Co	2.20×10^{12}	4.92×10^{11}	1.80×10^{12}	1.98×10^{12}	2.80×10^{10}	2.20×10^{12}	9.14×10^3	1.63×10^{11}
Total*	2.03×10^{15}	4.96×10^{14}	1.63×10^{14}	1.99×10^{15}	3.85×10^{14}	1.97×10^{15}	3.74×10^{13}	1.27×10^{15}

* The total figures include the radioactivity originating from other nuclides.

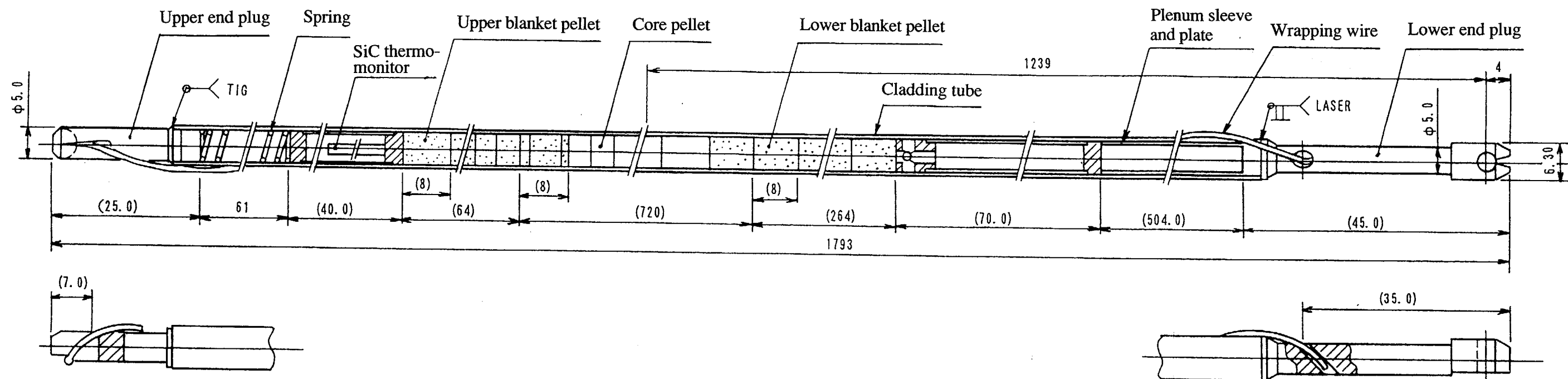


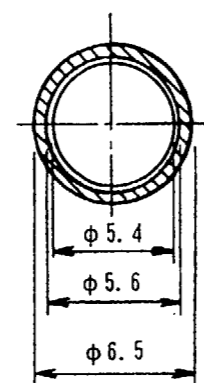
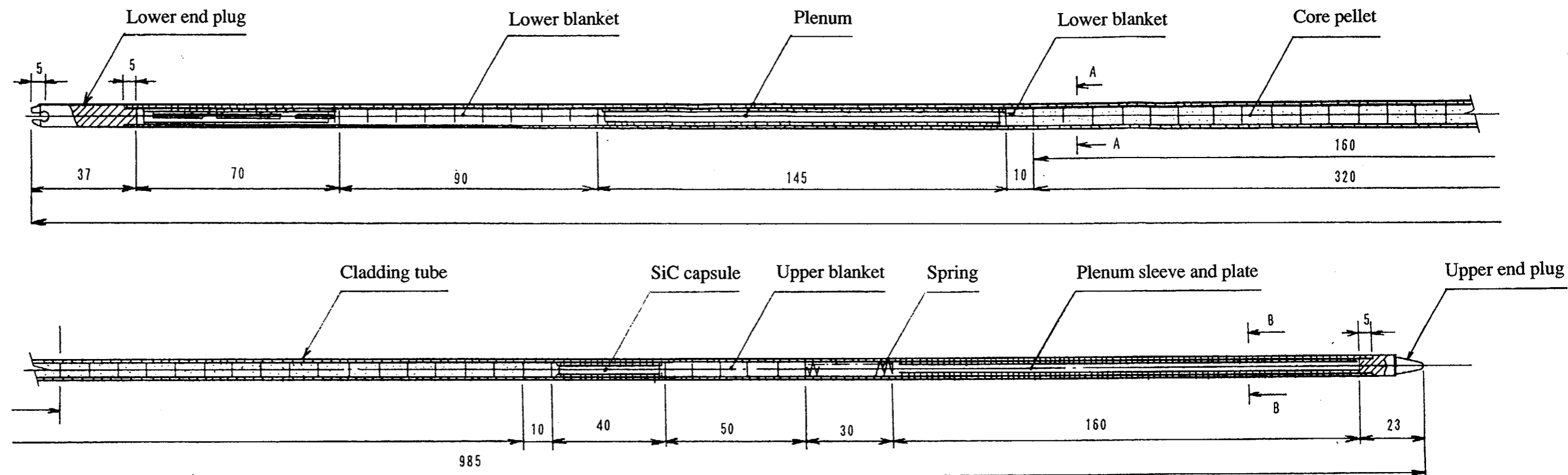
Fig. (I)-39 Contents I (an example of fuel elements) (in mm)

(PHENIX PNC-3)

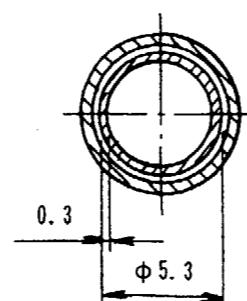
ANSTEC
APERTURE
CARD

Also Available on
Aperture Card

9601260203 -32



Section A-A



Section B-B

(RAPSODIE PNC-5)

ANSTEC
APERTURE
CARD

Also Available on
Aperture Card.

Fig. (I)-40 Contents II (an example of fuel elements) (in mm)

9601260203 - 33

CHAPTER II SAFETY ANALYSIS OF A PACKAGE FOR NUCLEAR MATERIAL

CHAPTER II SAFETY ANALYSIS OF A PACKAGE FOR NUCLEAR MATERIAL

This chapter outlines the safety analysis. A structural evaluation indicates that the packaging has sufficient structural strength, thermal and containment integrity under test conditions established by the relevant regulations. A mechanical test, drop test I, and drop test II (evaluating impact deceleration, shock absorber deformation, etc.) are conducted using a model of the packaging (1/2 scale model) to confirm the validity of an analysis method that includes the computer codes to be used.

Thermal analysis performed by calculations indicates that the packaging has sufficient thermal integrity under test conditions established by the relevant regulations. A thermal test is conducted using the models of a shock absorber to confirm the validity of an analysis method including the computer codes to be used and lumber's physical properties.

In a containment analysis gaseous contents are evaluated using Poiseuille - Knudsen's equation, while powder contents are evaluated using experimental results obtained to correlate the leakage rates of helium (He) gas and dioxide plutonium (Pu) powder obtained from the Battele Memorial Institute. The results show that the leak of a radioactive material from the package under test conditions established by the relevant regulations does not exceed the standard value.

To conduct a shield analysis, the radiation source intensity is analyzed using the depletion code ORIGEN, while the dose equivalent rate is analyzed using the transport calculation codes ANSIN and DOT3.5. The results show that the dose equivalent rate of the package under test conditions established by the relevant regulations does not exceed the standard value.

In a criticality analysis, evaluations are performed in accordance with the design conditions of a package for fissile material as prescribed by regulations. Two cases are considered; in the first, a single package of fissile materials is loaded, and in the second, any number of packages are loaded with no specified arrangement. In both cases, criticalities are analyzed by a method verified with the benchmark calculation using the multigroup Monte Carlo criticality program KENO-V. The results show that the nuclear fuel package maintains subcriticality.

(II)-A STRUCTURAL EVALUATION

A.1 Structural Design

A.1.1 Outline

This packaging consists of an outer container, inner container, and front and rear shock absorbers.

As shown in Fig. (I)-1, the outer container is a double-cylindrical structure consisting of an outer shell and an inner shell. In the double-cylindrical structure, a neutron shielding resin, adiabatic cement under accident test conditions, and gamma-ray shielding lead are filled sequentially from the outside. An intermediate shell exists between the resin and cement layers near both ends of the outer container. This section of the outer container is a triple-cylindrical structure. To allow the heat generated in the contents to escape during normal transport, several rows of heat dispersion fins welded longitudinally to the inside of an outer shell are inserted into the central resin layer. In order to allow gas generated in the cement layer to escape under accident test conditions, and to prevent the increase of pressure in the outer container, eight small holes are provided, each penetrating through the resin and fin layers to the outer shell. A fusible plug is installed at the mouth of the holes.

As shown in Fig. (I)-2, the outer shell is integrated into the inner shell through the end plate at both ends. A lifting trunnion, a pivoting trunnion, front and rear base plates, four lifting lugs for horizontal operation, and four fastening lugs in vertical position are provided on the outside of the outer shell. The lifting trunnion is used for vertical lifting, while the pivoting trunnion is used as a rotation axis when the position is changed from horizontal to vertical. The pivoting trunnion is also used to tie a package down to the transport skid together with the rear base plate. The front and rear base plates are used when placing the packaging horizontally on a floor rather than on a transport skid. The lifting lugs for horizontal operation are used for horizontal lifting, while the fastening lugs in the vertical position are used when fixing the package in the vertical position. Bolts are inserted into the holes of the fastening lugs in vertical position and sealed to prevent the lugs from accidentally being used for horizontal lifting purposes.

The outer container has penetration holes that enable access from the outside when operating the front and rear sampling valves shown in Fig. (I)-24, and a penetration hole through which a handle is inserted to operate the rotating plug that will be described later. These penetration holes are designed so that containment is assured by the front and rear sampling valve lids and the penetration hole lid, all of which are equipped with double O-rings. The sampling valves are used to sample the internal gas and investigate radioactivity contamination.

The outer container is designed so that it is covered with a shielding plug lid and a rear lid from the rear end, and a rotating plug lid and a front lid from the front end. As in the case of the sampling valve lids and the penetration hole lid, these lids have double O-rings constituting the boundary of the containment together with the outer container's inner shell (see Fig. (I)-22). The shielding plug lid (see Fig. (I)-33) holds the shielding plug (see Fig. (I)-32) installed at the rear end of an inner container that will be described later so that the axial shielding effect of a package is enhanced. The shielding plug lid also uses lead and a tungsten alloy, which improves the shielding effect as in a shielding plug. It is fixed to the end plate of the outer container with bolts. The rear lid is fixed to the shielding plug lid with bolts. The rotating plug lid (see Fig. (I)-36) is integrated into a rotating plug lid cover (see Fig. (I)-37) so that it can incorporate the

rotating plug (see Fig. (I)-35). The rotating plug lid is fixed with bolts to the end plate of the outer container.

The rotating plug is a thick disk-type plug that has a shaft as shown in Fig. (I)-8. It has a cylindrical penetration hole with the same inner diameter as that of the inner shell perpendicular to the axis. The rotating plug is incorporated into the rotating plug lid and rotating plug lid cover so that its axis coincides with the axis of the penetration hole of the outer container. The tip of the shaft appears at the bottom of a penetration hole of the outer container. A hexagonal socket is provided at the tip of the shaft. The rotating plug is operated by inserting a handle that coincides with this hexagonal hole from the outside of the outer container. The rotating plug is opened or closed 90 degrees by rotating the this handle.

As shown in Fig. (I)-23, a shock absorber is installed at each end of the outer container and functions as a buffer for the package when it is dropped. Balsa wood is covered with a stainless steel plate. Alumina cement is filled into the inside of the cover plate and acts as an insulating material. Ten fusible plugs are installed on the surface of the front shock absorber, and ten such plugs are installed on the rear shock absorber. These plugs allow gas generated in the cement layer and balsa wood to escape under accident test conditions, thereby preventing excessive pressure increase in the shock absorbers. A lifting lug is installed on the side of each shock absorber and sealed during transport to prevent the lugs from accidentally being used for horizontal lifting.

The inner container has a stainless cylindrical structure as shown in Fig. (I)-9. When the contents are accommodated in the packaging, the inner container is put into the outer container after the inner container has been loaded with the contents. During transport, the inner container is connected with a shielding plug that fixes the contents. Fuel supporting cans I and II, a supporting can, and receiving tube II are used for the low-burnup pins (Contents I, IV, V, VI, and VII) transport and they are also used for Contents VIII of high-burnup pins (see Figs. (I)-11, 12, and 13). These cans and tube, which hold the contents, are contained in the inner container. Receiving tube I and a rack are used for high-burnup pin (Contents II) transport. Each stainless receiving tube I, containing one fuel pin, is fixed in the position of the rack as shown in Fig. (I)-14 and then, the rack is placed in the inner container. These fuel supporting cans I and II, and receiving tubes I and II are welded and hermetically sealed after the fuel pins are put inside them. For more information, see Chapter I.

A.1.2 Design Criteria

This package shall be designed based on the design conditions outlined below and shall satisfy the design criteria described in subsection A.1.2.2.

A.1.2.1 Design Conditions

The following design conditions are considered.

1. General requirements (during normal transport)

- (1) No chemical nor galvanical reaction shall occur between materials of the packaging, and between the materials and radioactive contents.
- (2) The materials of the packaging shall be able to withstand changes in the ambient

temperature (-40 to 38°C), as such changes are expected during transport, and shall not become brittle at low temperatures (-40°C).

- (3) The lifting device of a package shall be able to withstand sudden lifting. The safety factor in this case is "3".
- (4) The soundness of the tie-down device and packaging shall be ensured for acceleration (10 G in the progressive direction, 5 G in the horizontal direction, and 2 G in the vertical direction) generated during transport.
- (5) The packaging shall not cause any resonance to vibration transmitted from the vehicle.
- (6) The containment system shall be designed so that it cannot be opened accidentally.
- (7) The containment system (all the lids of the outer container's inner shell and the outer container's penetration part) shall satisfy the conditions outlined below.
 - (a) The intensity and performance of the containment system shall be ensured for any rise in internal pressure and thermal expansion caused by an increase in temperature due to the decay heat of the contents.
 - (b) The intensity and performance of the containment system shall be ensured even if the ambient atmospheric pressure drops to 25 kPa.

2. Normal test conditions

- (1) During a water spray test, no water shall flow into the outer container.
- (2) In a free-drop test from a height of 0.6 m, the intensity and containment of a package shall be ensured, and the shape of its contents shall be maintained.
- (3) The package shall maintain its integrity without suffering any damage during the stacking test under a compression load of five times the mass of the actual package.
- (4) The outer container shall not be penetrated by a 6-kg mild steel bar dropped from a height of 1 m during a penetration test.
- (5) The integrity of this package shall be ensured even if it is left unattended for a period of one week at an ambient temperature of 38 to -40°C after conditions (1) through (4) above have been satisfied.

3. Accident test conditions

- (1) In a free-drop test from a height of 9 m, the intensity and containment of the package shall be ensured and the shape of its contents shall be maintained.
- (2) In a penetration test in which a 6 kg mild steel bar is dropped from the height of 1 m, the intensity and containment of the package shall be ensured and the shape of its contents shall be maintained.
- (3) In a thermal test (an exposure test in which the package is left in an environment of 800°C for 30 minutes), the intensity and containment of a package shall be ensured.
- (4) In a water immersion test at a depth of 15 m, the intensity and containment of this package's containment system shall be ensured.
- (5) The integrity of the package shall be ensured even if it is left for a period of one week in an environment with an ambient temperature ranging between -40°C and +38°C after conditions (1) through (4) above have been satisfied.
- (6) No changes shall occur in terms of its configuration relative to the criticality even if the package is subjected to tests (2) and (3) above one after the other.

A.1.2.2 Design Criteria

This subsection defines the design criteria used for a structural evaluation as follows:

- (1) Tensile stress and compression stress shall be evaluated based on the yield stress (σ_y) of the material in use. To evaluate shear stress, 60% of the yield stress shall be used as the design criteria.
- (2) In evaluating the stress generated on the welded section, the welding efficiency will be taken to be 60%.
- (3) The lifting device and tie-down device are evaluated based on the criteria defined in (1) and (2) above.
- (4) Deformation of the rear and front shock absorbers is only acceptable if it does not affect the outer container.
- (5) The yield stress shall be used to evaluate all the bolts used in the containment system (inner shell of the outer container, rear lid unit, front lid unit, penetration hole lid part, and sampling valve lid parts). Displacement of the parts that ensure the containment of the packaging and the O-rings shall be evaluated according to criteria that requires that displacement not exceed the squeezed distance of the O-ring.
- (6) To evaluate strength against impact (a short-term dynamic load) under accident test conditions, dynamic tensile strength (σ_{ud}) is used. This value is equal to the static tensile strength (σ_u) multiplied by 1.2.¹⁾
- (7) To evaluate thermal stress, the tensile strength (σ_u) shall be used as the design criteria if the stress generated is secondary stress.
- (8) If the allowable service temperatures are known, use them within the range, and mechanical properties obtained under such temperature conditions shall be used as the design criteria.
- (9) Design criteria for materials or devices with special specifications will be defined on a case-by-case basis.
Table (II)-A.1 through Table (II)-A.3 summarize the above design conditions and analysis methods for each item to be analyzed.
Analysis results quantitatively obtained using mathematical expressions are evaluated by using the following margin of safety (M.S.):

$$\text{Margin of safety} = \frac{\text{Design Criteria}}{\text{Evaluation Result}} - 1$$

The analyzed object maintains its integrity if the margin of safety is positive.

1) L. B. Shappert and J. H. Evans: Analysis of the SRP25-ton Target Tube Cask, p90 ORNL-TM-3531

Table (II)-A.1 Structural Design Conditions and Analysis Methods [Normal Transport Conditions]

(No. 1)

(II)-A-5

Analysis item	Design conditions						Analysis method		Remarks
	Reference	Material	Tem- pera- ture	Design load			Applicable mathematical expression or element	Design criteria	
				Type	Safety factor	Element			
Chemical and galvanic reactions									
Chemical reaction	Table II-A.9			Corrosion		Activation	Existence of activation	No	
Galvanic reaction	Table II-A.9			Corrosion		Potential differ- ence	Existence of water	No	
Low-temperature strength	Table II-A.10		-40°C	Brittle at low temperatures	1	Applicable strength	Allowable service temperature (minimum)	-40°C or less	
Containment system									
Lid				Opening due to unauthorized use		Possibility of unauthorized use	Possibility of opening the lids covered by shock absorbers	No	
Sampling valve				Same as above.		Same as above.	Same as above.	No	
Lifting device									
(1) Lifting lug for horizontal operation									
Lug ring part	Fig. II-A.5	SUS304	80°C	Package weight	3	Shear	$\tau = \frac{3 F}{2 A}$	0.6 σ_y	τ : Shear stress F: Wire tension A: Sectional area of lifting lug σ_y : Yield stress
Lug welded section	Fig. II-A.5	SUS304	80°C	Package weight	3	Tension	$\sigma = \frac{F \sin 30^\circ}{A}$ $\tau = \frac{F \cos 30^\circ}{A}$ $\sigma_p = \frac{\sigma}{2} + \sqrt{\left(\frac{\sigma}{2}\right)^2 + \tau^2}$	0.6 σ_y	σ : Tensile stress τ : Shear stress σ_p : Principal stress
Outer shell	Fig. II-A.6	SUS304	80°C	Package weight	3	Bending	$\sigma = \frac{M}{Z}$	σ_y	M: Bending moment Z: Section modulus of the outer shell

Table (II)-A.1 Structural Design Conditions and Analysis Methods [Normal Transport Conditions]

(No. 2)

(II)-A-6

Analysis item	Design conditions						Analysis method		Remarks
	Reference	Material	Tem- pera- ture	Design load			Applicable mathematical expression or element	Design criteria	
				Type	Safety factor	Element			
(2) Lifting trunnion Trunnion mounting part	Fig. II-A.7	SUS304	80°C	Package weight	3	Shear	$\tau = \frac{4}{3} \frac{W_L}{nA}$	0.6 σ_y	W_L : Design load n: Number of trunnions A: Sectional area of the mounting part
Outer shell (Trunnion mounting part)	Fig. II-A.8	SUS304	80°C	Package weight	3	Bending	$\sigma = \frac{M}{Z}$	σ_y	M: Mounting part moment Z: Section modulus
						Bending	$\sigma_b = \frac{M}{Z}$	σ_y	M: Bending moment of the ring Z: Section modulus of the ring
						Shear	$\tau_t = \frac{15a+9b}{5a^2b^2} T$		
							$\sigma = \frac{\sigma_b}{2} + \sqrt{\left(\frac{\sigma_b}{2}\right)^2 + \tau_t^2}$	σ_y	
Outer shell		SUS304	80°C	Package weight	3	Tension	$\sigma = \frac{W_v}{S}$	0.6 σ_y	W_v : Design load S: Sectional area of the outer shell
End plate	Fig. II-A.10	SUS304	80°C	Package weight	3	Tension	$\sigma_t = \frac{3W}{2\pi nt^2} \left(1 - \frac{2a^2}{a^2-b^2} \left(\log \frac{a}{b}\right)\right)$	σ_y	W: Design load t: End-plate thickness
							$\sigma_o = \frac{3W}{2\pi nt^2} \left(1 - \frac{2b^2}{a^2-b^2} \left(\log \frac{a}{b}\right)\right)$	0.6 σ_y	b: Radius of a rigid body n: Number of end plates

Table (II)-A.1 Structural Design Conditions and Analysis Methods [Normal Transport Conditions]

(No. 3)

Analysis item	Design conditions						Analysis method		Remarks
	Reference	Material	Tem- pera- ture	Design load			Applicable mathematical expression or element	Design criteria	
				Type	Safety factor	Element			
Tie-down device (1) Rear base plate (welded section)	Fig. II-A.13	SUS304	80°C	Longitudinal direction 10 G Transversal direction 5 G Vertical direction 2 G	1	Bending and tension Compression Shear	$\sigma = \frac{M_t}{Z_t} + \frac{M_t}{Z_t} + \frac{R_{Bv}}{A}$ $\tau = \sqrt{\left(\frac{R_{Bt}}{A}\right)^2 + \left(\frac{R_{Bv}}{A}\right)^2}$ $\sigma_p = \frac{\sigma}{2} + \sqrt{\left(\frac{\sigma}{2}\right)^2 + \tau^2}$	0.6 σ_y	M_t : Bending moment Z_t : Section modulus M_t : Bending moment Z_t : Section modulus R_{Bv} : Reaction force in the vertical direction A : Sectional area R_{Bt} : Reaction force in the axial direction R_{Bv} : Reaction force in the vertical direction A : Sectional area
(2) Pivoting trunnion	Fig. II-A.14	SUS304	80°C	Longitudinal direction 10 G Transversal direction 5 G Vertical direction 2 G	1	Bending and tension Shear	$\sigma = \frac{M_v}{Z_v} + \frac{R_{Tv}}{A}$ $\tau = \frac{4}{3} \times \frac{R_{Tv}}{A}$ $\sigma_p = \frac{\sigma}{2} + \sqrt{\left(\frac{\sigma}{2}\right)^2 + \tau^2}$	σ_y	M_v : Bending moment R_{Tv} : Reaction force in the horizontal direction Z_v : Section modulus A : Sectional area R_{Tv} : Reaction force in the vertical direction A : Sectional area

(II)-A-7

Table (II)-A.1 Structural Design Conditions and Aalysis Methods [Normal Transport Conditions]

(No. 4)

Analysis item	Design conditions						Analysis method		Remarks
	Reference	Material	Tem- pera- ture	Design load			Applicable mathematical expression or element	Design criteria	
				Type	Safety factor	Element			
(3) Outer shell	Fig. II-A.15	SUS304	80°C	Longitudinal direction 10 G Transversal direction 5 G	1	Bending	$\sigma = \frac{M}{Z}$	σ_y	M: Bending moment of the shell Z: Section modulus of the shell plate
Pressure			80°C	Influence of external pressure	1	Pressure resistance	Existence of the influence of external pressure	No	Evaluated under accident test conditions
Vibration		SUS304	80°C	Natural frequency	1	Resonance frequency	$f_n = C \sqrt{\frac{EI}{\gamma A \ell^4}}$	10 Hz or more	fn: Resonance frequency C: Coefficient E: Modulus of longitudinal elasticity I: Moment of inertia of area τ : Mass density A: Sectional area ℓ : Packaging length

(II)-A-8

Table (II)-A.2 Structural Design Conditions and Analysis Methods [Normal Test Conditions]

(No. 1)

Analysis item	Design conditions						Analysis method		Remarks
	Reference	Material	Tem- pera- ture	Design load			Applicable mathematical expression or element	Design criteria	
				Type	Safety factor	Element			
Normal test conditions Thermal test Thermal expansion Inner shell Outer shell	Fig. II-A.16 Fig. II-A.16	SUS304 SUS304	85°C 72°C	Thermal stress Thermal stress	1 1	Tension Tension	Finite element calculation code ANSYS	σ_y σ_y	
Water spray test			80°C	Water and drain resistance	1	Influence by water	Water and drain resistance	Influ- ence by water	
Free-drop test	Table II-A.18	SUS304 Balsa wood	80°C	Deformation	1	Absorption of energy	Numerical calculation by SHOCK-2	Thick- ness of the shock absorber	

Table (II)-A.2 Structural Design Conditions and Analysis Methods [Normal Test Conditions]

(No. 2)

Analysis item	Design conditions						Analysis method		Remarks
	Reference	Material	Tem- pera- ture	Design load			Applicable mathematical expression or element	Design criteria	
				Type	Safety factor	Element			
Stacking test Outer shell	Fig. II-A.20	SUS304	80°C	Package weight	1	Bending	$M_B = \left(\frac{5}{2}W + W_s\right)X + R_A(X - \ell_1) + R_B(X - \ell_1 - \ell_2) + \frac{1}{2}WX^2$ $\sigma = \frac{M_B}{Z}$		M _B : Bending moment W: Package weight W _s : Shock absorber weight R _A : Load supported with a pivoting trunnion R _B : Load supported with a rear base plate x: Length between a container's front end and the rear base plate ℓ ₁ : Length between the container's front end and the pivoting trunnion ℓ ₂ : Length between the pivoting trunnion and the rear base plate w: Uniform load along the package Z: Section modulus of the outer shell
				Uniform load multiplied by 5					
Penetration Outer shell	Fig. II-A.21	SUS304	80°C	Drop of a mild steel bar	1	Deformation	$\delta^3 - 3r\delta^2 + \frac{3U}{\pi \sigma_s} = 0$	Damage to the outer shell	δ: Deformation r: End radius of the mild steel bar U: Drop energy σ _s : Deformation stress
Free drop onto each corner or onto each of the quarters of each rim									

(II)-A-10

Table (II)-A.3 Structural Design Conditions and Analysis Methods [Accident Test Conditions]

(No. 1)

II-V-II

Analysis item	Design conditions						Analysis method		Remarks
	Reference	Material	Tem- pera- ture	Design load			Applicable mathematical expression or element	Design criteria	
				Type	Safety factor	Element			
Drop test I Shock absorber deformation	Table II-A.18	Balsa wood		Free drop from a 9 m height	1	Deformation	$WH = \int A(\delta)F(\delta)d\delta$		W: Package weight H: Drop height A(δ): Sectional area of the shock absorber balsa wood's deformation part F(δ): Deformation-to-str ess curve of the balsa wood
Impact deceleration		Balsa wood		Free drop from a 9 m height	1	Impact deceleration	$G = \frac{A(\delta)F(\delta)}{W}$ (Calculation code SHOCK-2)		G: Impact deceleration δ: Shock absorber deformation
Vertical drop (1) Vertical drop at an angle with the rear part striking first Outer shell	Fig. II-A.23	SUS304	80℃	Impact load	1	Compression	$\sigma = \frac{F}{S}$	σ_{UD}	σ: Compression stress
Inner shell	Fig. II-A.24	SUS304	90℃	Impact load	1	Compression	$\sigma = \frac{F}{S}$	σ_y	S: Sectional area of the shell
Shielding plug lid flange part	Fig. II-A.26	SUS304	80℃	Impact load	1	Bending	Finite element calculation code ANSYS	σ_{UD}	
Sampling valve lid fastening bolt	Fig. II-A.27	SUS304	80℃	Impact load	1	Shear	$\tau = \frac{WG}{nA}$	$0.6 \sigma_y$	W: Weight of a sampling valve lid G: Impact acceleration n: Number of bolts A: Sectional area of the bolt
Inner container		SUS304	80℃	Impact load	1	Buckling	P=WG	P_k	P_k : Buckling load
Fuel supporting can		SUS304	80℃	Impact load	1	Buckling	P=WG	P_k	

Table (II)-A.3 Structural Design Conditions and Analysis Methods [Accident Test Conditions]

(No. 2)

Analysis item	Design conditions						Analysis method		Remarks
	Reference	Material	Tem- pera- ture	Design load			Applicable mathematical expression or element	Design criteria	
				Type	Safety factor	Element			
Rack supporting part	Fig. II-A.28	SUS304	350°C	Impact load	1	Tension	$\sigma = \frac{3W}{4t^2} \left(\frac{4a^4(m+1)\log\frac{a}{b}}{a^2(m+1)} - \frac{a^4(m+3)+b^4(m-1)+4a^2b^2}{b^2(m-1)} \right)$	σ_{UD}	σ : Bending stress at the inner diameter of the rear lid w : Distributed load a : Outer radius of load surface b : Inner radius of load surface m : Reciprocal of Poisson's ratio t : Plate thickness of fuel supporting can
	Fig. II-A.29	SUS304	350°C	Impact load	1	Compression	$\sigma = \frac{WG}{A}$	σ_{UD}	σ : Compression stress W : Weight of rack and its contents G : Impact acceleration A : Sectional area of supporting rod
	Rack end plate	Fig. II-A.29	SUS304	350°C	Impact load	1	Bending	$\sigma = \frac{3W}{2\pi t^2} \left(\frac{2a^2(m+1)\log\frac{a}{b}}{a^2(m+1)} + \frac{a^2(m-1)-b^2(m-1)}{b^2(m-1)} \right)$	

(II)-A-12

Table (II)-A.3 Structural Design Conditions and Analysis Methods [Accident Test Conditions]

(No. 3)

(II)-A-13

Analysis item	Design conditions						Analysis method		Remarks
	Reference	Material	Tem- pera- ture	Design load			Applicable mathematical expression or element	Design criteria	
				Type	Safety factor	Element			
Receiving tube I	Fig. II-A.29	SUS304	350℃	Impact load	1	Buckling	P = WG	P _k	W: Receiving tube weight G: Impact acceleration P: Buckling load
(2) Vertical drop with the front part striking first Rotating plug lid	Fig. II-A.32	SUS304	80℃	Impact load	1	Bending	Finite element calculation code ANSYS	σ _{UD}	
Inner container	Fig. II-A.35	SUS304	350℃	Impact load	1	Buckling	P = WG	P _k	W: Weight of shielding plug and inner container G: Impact acceleration P: Buckling load
Horizontal drop Outer shell	Fig. II-A.37	SUS304	80℃	Impact load	1	Bending	$\sigma = \frac{WG\ell}{8I} \cdot e$	σ _{UD}	W: Package weight G: Acceleration ℓ: Supporting interval
Inner shell	Fig. II-A.37	SUS304	90℃	Impact load	1	Bending	$\sigma = \frac{WG\ell}{8I} \cdot e$	σ _y	I: Moment of inertia of an area e: Distance between main axis and sectional edge
Fuel supporting can	Fig. II-A.38	SUS304	350℃	Impact load	1	Bending	$\sigma = \frac{WG\ell}{Z}$	0.6 σ _{UD}	W: Weight of a fuel pin and a receiving tube II
Receiving tube	Fig. II-A.39	SUS304	350℃	Impact load	1	Bending	$\sigma = \frac{WG\ell}{12Z}$	σ _{UD}	ℓ: Length of spacer arm Z: Section modulus of spacer

Table (II)-A.3 Structural Design Conditions and Analysis Methods [Accident Test Conditions]

(No. 4)

(II)-A-14

Analysis item	Design conditions						Analysis method		Remarks
	Reference	Material	Tem- pera- ture	Design load			Applicable mathematical expression or element	Design criteria	
				Type	Safety factor	Element			
Sampling valve lid	Fig. II-A.40	SUS304	80°C	Impact load	1	Bending	$\sigma = \frac{3Pb^2}{8h^2} \left(4(1+\nu) \log \frac{a}{b} + 4 - (1-\nu) \frac{b^2}{a^2} \right)$	σ_y	P: Distributed load
Penetration hole lid									W: Flange weight G: Acceleration d: Diameter of plug b: Radius of the concentrated loading area h: Plate thickness of flange a: Radius of support ν : Poisson's ratio
Sampling valve lid fastening bolt and Penetration hole lid fastening bolt	Fig. II-A.41	SUS630	80°C	Impact load	1	Tension	$\sigma = \frac{WG}{nA}$	σ_y	W: Flange weight G: Acceleration n: Number of bolts A: Sectional area
Corner drop				9 m drop	1	Impact deceleration Deformation	$G = \frac{A(\delta)F(\delta)}{W}$ $WH = \int A(\delta)F(\delta)d\delta$		
Shielding plug lid fastening bolt	Fig. II-A.42	SUS630	80°C	Impact deceleration	1	Bending	$\sigma = \frac{MC}{I}$	σ_y	M: Bending moment C: Distance to bolt furthest from (A-A)
Rotating plug lid fastening bolt	Fig. II-A.43	SUS630	80°C	Impact deceleration	1	Bending	$\sigma = \frac{MC}{I}$	σ_y	I: Moment of inertia
Oblique drop	Fig. II-A.45	Balsa wood	80°C	9 m drop	1	Deformation	Calculation code SHOCK-2	Shock absorber thick- ness	

Table (II)-A.3 Structural Design Conditions and Analysis Methods [Accident Test Conditions]

(No. 5)

Analysis item	Design conditions						Analysis method		Remarks
	Reference	Material	Tem- pera- ture	Design load			Applicable mathematical expression or element	Design criteria	
				Type	Safety factor	Element			
Mechanical test Drop test II Center of outer shell	Fig. II-A.46	SUS304 Alloy	80°C	Penetration	1	Plate thickness not to be penetrated	$t = \left(\frac{W}{\sigma_u} \right)^{0.71}$	Thick- ness of plate used	W: Package weight σ_u : Tensile strength
				Impact load	1	Bending	$\sigma = \frac{M}{Z}$	σ_{UD}	
Horizontal drop on to the shock absorber	Fig. II-A.47	Balsa wood SUS304	80°C	1 m drop	1	Deformation	$U = \frac{\pi}{4} d^2 \sigma_B \delta + C_1 C_2 \pi d t \sigma h$	Shock absorber thick- ness	U: Absorption energy h: Deformation thickness σ : Tensile strength t: Plate thickness d: Diameter of the mild steel bar σ_B : Crushing stress of balsa wood δ : Deformation of shock absorber C_1, C_2 : Coefficients
Vertical drop on to the shock absorber	Fig. II-A.48	Fir- plywood SUS304	80°C	1 m drop	1	Deformation	$Wh = \frac{\pi \delta}{3} \sigma_f (R^2 + Rr + r^2)$	Shock absorber thick- ness	W: Package weight h: Drop height σ_f : Crushing stress of ply-wood R: Radius of deformed part r: Radius of deformed part δ : Deformation

(II)-A-15

Table (II)-A.3 Structural Design Conditions and Analysis Methods [Accident Test Conditions]

(No. 6)

(II)-A-16

Analysis item	Design conditions						Analysis method		Remarks
	Reference	Material	Tem- pera- ture	Design load			Applicable mathematical expression or element	Design criteria	
				Type	Safety factor	Element			
Vertical drop on the end part of the shock absorber	Fig. II-A.49	Balsa wood SUS304	80°C	1 m drop	1	Deformation	$Wh = \frac{\pi}{4}d^2\sigma_B\delta + C_1C_2\pi dt\sigma h$	Shock absorber thick- ness	σ_B : Crushing stress of balsa wood C_1 : Coefficient C_2 : Coefficient d : Diameter of the mild steel bar σ : Tensile strength h : Deformation depth
Thermal test									
Thermal expansion									
Inner shell	Fig. II-A.50	SUS304	112°C	Thermal stress	1	Tension	Finite element calculation code	σ_U	
Outer shell	Fig. II-A.50	SUS304	700°C	Thermal stress	1	Compression	ANSYS	σ_U	
Stress calculation									
Inner shell	Fig. II-A.54	SUS304	200°C	Internal pressure	1	Tension	$\sigma = p \frac{\frac{k^2}{R^2} + 1}{k^2 - 1}$	σ_y	p : Internal pressure k : Modulus = b/a a : Inner radius b : Outer radius
Shielding plug lid unit	Fig. II-A.55	SUS304	200°C	Internal pressure	1	Bending	Finite element calculation code ANSYS	σ_y	
Rotating plug lid unit	Fig. II-A.56	SUS304	200°C	Internal pressure	1	Bending	Finite element calculation code ANSYS	σ_y	
Penetration hole lid unit	Fig. II-A.57	SUS304	200°C	Internal pressure	1	Bending	Finite element calculation code ANSYS	σ_y	

Table (ID-A.3 Structural Design Conditions and Analysis Methods [Accident Test Conditions]

Analysis item	Design conditions						Analysis method		Remarks
	Reference	Material	Tem- pera- ture	Design load			Applicable mathematical expression or element	Design criteria	
				Type	Safety factor	Element			
Fuel supporting can	Fig. II-A.58	SUS304	400°C	Internal pressure	1	Bending	$\sigma = \frac{3W}{8\pi mt^2} (3m+1)$	σ_y	W: Load = πpa^2 p: Internal pressure a: Radius t: Plate thickness m: Reciprocal of Poisson's ratio
Receiving tube	Fig. II-A.59	SUS304	350°C	Internal pressure	1	Tension	$\sigma = \frac{PR}{t}$	σ_y	P: Internal pressure R: Radius t: Plate thickness
Water immersion									
Rotating plug box	Fig. II-A.60	SUS304	90°C	External pressure	1	Compression	$\sigma = \frac{k^2 + \frac{k^2}{R^2}}{k^2 - 1} p$	σ_y	k: Modulus = b/a a: Inner radius b: Outer radius R: Modulus = r/a r: Mean radius

(II)-A-17

A.2 Weight and Center of Gravity

Table (II)-A.4 shows the package weight list. The structure of the packaging is almost axially symmetrical. As shown in Fig. (II)-A.1, the center of gravity (C.G.) when its contents are loaded is located on the axial line approximately 1,610 mm from the rear end (shielding plug side) of a package. The values shown in Table (II)-A.5 which are settled on the basis of the values in Table (II)-A.4 shall be used for a structural evaluation of the design weight of the package to ensure that the analysis is on the safe side.

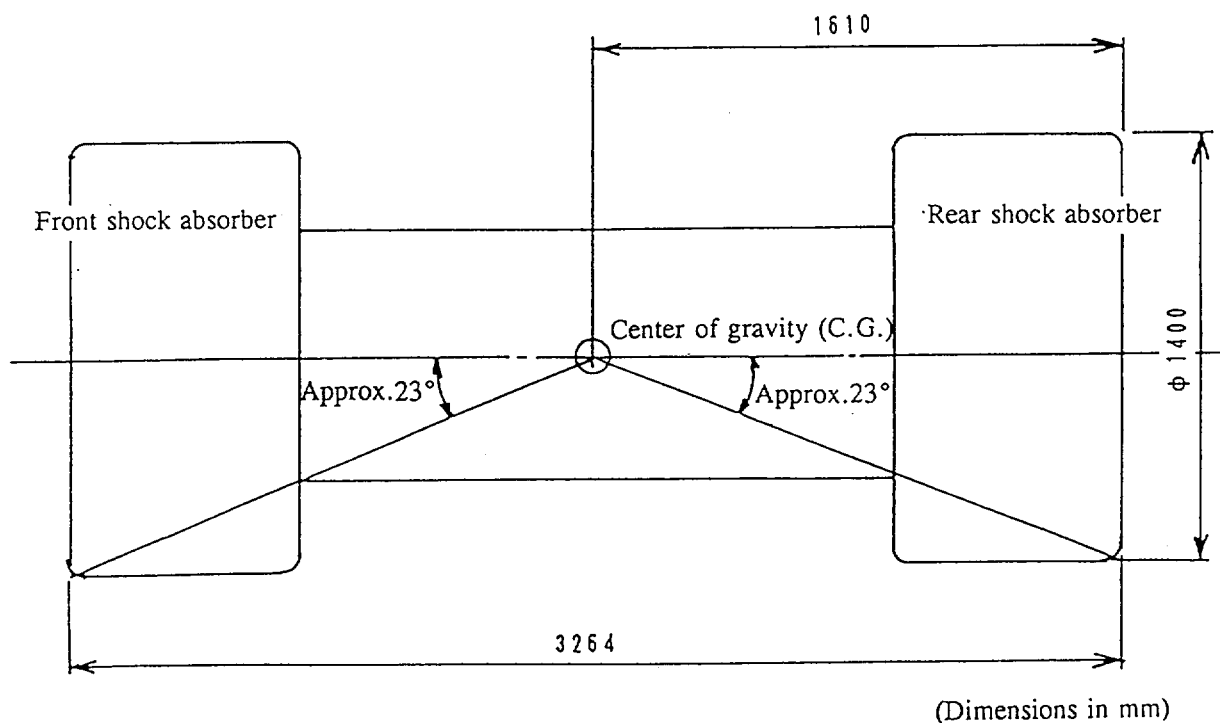


Fig. (II)-A.1 Position of the Center of Gravity of the Package

Table (II)-A.4 Package Weight List

(kg)

Item	Contents I (multi-pins)	Contents II (multi-pins)	Contents III (structural material)	Contents VI	Contents VII
Shell of outer container	8,750				
Shielding plug lid	120				
Shielding plug	30				
Rear lid	7				
Rotating plug	125				
Rotating plug lid	220				
Rotating plug lid cover	75	Same as left box.	Same as left box.	Same as left box.	Same as left box.
Front lid	15				
Rear sampling valve lid	6				
Front sampling valve lid	5				
Penetration hole lid	6				
Inner container	35				
Rear shock absorber	750				
Front shock absorber	750				
(Sub Total)	10,894	10,894	10,894	10,894	10,894
Fuel supporting can I	25	-	-	-	-
Contents I, IV, and V	10				
Rack		20			
Receiving tube I + Contents II	-	11	-	-	-
Contents III (structural material)	-	-	5	-	-
Supporting can				20	
Receiving tube II + Contents VI and VIII	-	-	-	15	-
Fuel supporting can II					20
Contents VII	-	-	-	-	12
Total package weight	10,929	10,925	10,899	10,929	10,926

Table (II)-A.5 Design Weight of a Package under Structural Evaluation

Item to be inspected	Break down (kg)		Design weight (kg)
Lifting strength - Horizontal lifting	Package* Shock absorber Transport skid	9,500 750x2 1,500**	12,500
Lifting strength - Vertical lifting	Package*	9,500	9,500
Tie-down strength	Package	11,000	11,000
Drop strength	Package	11,000	11,000

Notes: * Does not include the shock absorber weight because the package is lifted after the shock absorbers are removed.
** The transport skid weight shall be 1,500 kg to ensure safety.

A.3 Mechanical Properties of Materials

Table (II)-A.6 shows the mechanical properties of the principal materials used for a structural analysis under a normal temperature. Table (II)-A.7 and Fig. (II)-A.2 show the temperature dependence of the tensile strength and the yield strength of the stainless steel 304 (SUS304), 630 (SUS630) and 316 (SUS316). SUS304 is used for strength items such as the outer and inner shells of the outer container, the inner container, the lids and other parts. SUS630 is used for the bolts, and SUS316 is used for the fuel pin cladding tubes. Table (II)-A.8 shows the temperature dependence of the longitudinal elasticity modulus of stainless steel SUS304 and stainless steel SUS630. As shown in the figures and tables above, the strength of stainless steel is reduced as the temperature rises. Therefore, when the strength of the stainless steel parts is evaluated under normal transport conditions (general requirements, normal test conditions, and accident test conditions, an analysis, which adopts the mechanical strength of the material under the maximum temperature that can possibly be reached under each condition, gives results that are on the safe side. Structural evaluations will also be conducted in this manner.

The dynamic crushing stress when balsa wood is used as a shock absorber is obtained by a dynamic compression test¹⁾ using a test piece. Fig. (II)-A.3 shows the function of the deformation rate. The crushing stress of fir-plywood is also determined in the same manner as described above. (See Table (II)-A.6.)

The resin compression strength of neutron shielding material packed in an outer container can also be obtained through such testing. This test conforms to ASTM D695-61T. Table(II)-A.6 shows the resulting information.

-
- 1) The test piece is cylindrical and has a diameter of 76 mm. An impact load is applied in the axial direction. If the load is applied perpendicularly to a grain of wood, two test pieces, 120 mm and 160 mm high, are used. If it is applied parallel to the grain, two test pieces, 40 mm and 55 mm high, are used. The side of each test piece is restrained by a hoop made of the same material. The hoop is in turn restrained by a steel pipe. A weight, which is equipped with an acceleration converter, is placed on the test piece. The test piece is dropped from the height of 9 m together with the weight. The dynamic crushing stress is obtained by processing the signal from an accelerometer when the test piece hits the ground.

Table (II)-A.6 Mechanical Properties of the Packaging's Principal Materials (under a Normal Temperature)

Part name	Material	Symbol (JIS)	Yield stress (N/mm ²)	Tensile stress (N/mm ²)	Elongation (%)	Melting point (°C)	Coefficient of linear thermal expansion (1/°C)	Modulus of longitudinal elasticity (N/mm ²)	Density (g/cm ³)	Remarks
Body (shell and lid) trunnion	Stainless steel	SUS304	205 (21.0)	519 (53.0)	40		16.4x10 ⁻⁶	1.95x10 ⁵	7.93	(1)
Fastening bolt	Stainless steel	SUS630 (H1150)	725 (74.0)	931 (95.1)	16		9.4x10 ⁻⁶	2.01x10 ⁵	7.93	(1)
Lead shield	Lead	(Special)		49		327	29.3x10 ⁻⁶	1.66x10 ⁴	11.34	(2)
Cladding tube	Stainless steel	SUS316	205 (21.0)	519 (53.0)	40		16.4x10 ⁻⁶	1.95x10 ⁵	7.93	(1)
Bush	Bronze casting	BC2	127	245			21.2x10 ⁻⁶	9.61x10 ⁴	8.53	(2)
Heat dispersion fin	Non-oxygen copper plate	C1020P	138	196			16.5x10 ⁻⁶	1.10x10 ⁵	8.96	(2)
Insulating cement	Alumina cement		60 *1				7 ~ 11x10 ⁻⁶	2.94x10 ⁴	3.26	(3)
Resin	Polyester		47 *1	8.67			60.0x10 ⁻⁶ (20 ~ 80°C)	1.57x10 ³	1.1	(4)
Packing material of shock absorber	Fir-plywood		44 *2						0.54	(4)
Bismuth						271				

Notes: 1) *1: Compressive stress

*2: Collapsing stress

2) The figures in parentheses (appearing in the stress columns) are the values presented in units of kg/mm².

3) Reference

(1) ASME Sec III, Division I

(2) Kikai Sekkei Binran (Handbook of machine design)

(3) Data from Asahi Glass Co., Ltd.

(4) Test report in Kimura Chemical Plants Co., Ltd.

Table (II)-A.7 Tensile Stress and Yield Stress of Stainless Steel under Each Temperature

Tempera- ture (°C)	SUS304		SUS630		SUS316	
	Tensile stress (N/mm ²)	Yield stress (N/mm ²)	Tensile stress (N/mm ²)	Yield stress (N/mm ²)	Tensile stress (N/mm ²)	Yield stress (N/mm ²)
-40	*1068	*234	*1441	*1333	*716	*282
20	530	217	930	738	516	216
80	496	180	930	682	516	184
90	491	174	930	672	516	179
100	485	174	930	665	515	175
200	445	144	908	620	496	149
350	437	123	863	574	492	126
400	435	118	834	558	492	122
450	427	113	786	529	481	120
500	413	110	765	478	463	118
700	254**	102**	-	-	-	-

Note: Reference: ASME Sec III, Division 1
*: Sutenresu Koza (Lecture on stainless steel) (Nihon Kogyo Shuppan)
**: Kinzoku Zairyo Koon Data Shu (Collection of metallic material high-temperature data) (Yoken-Do)

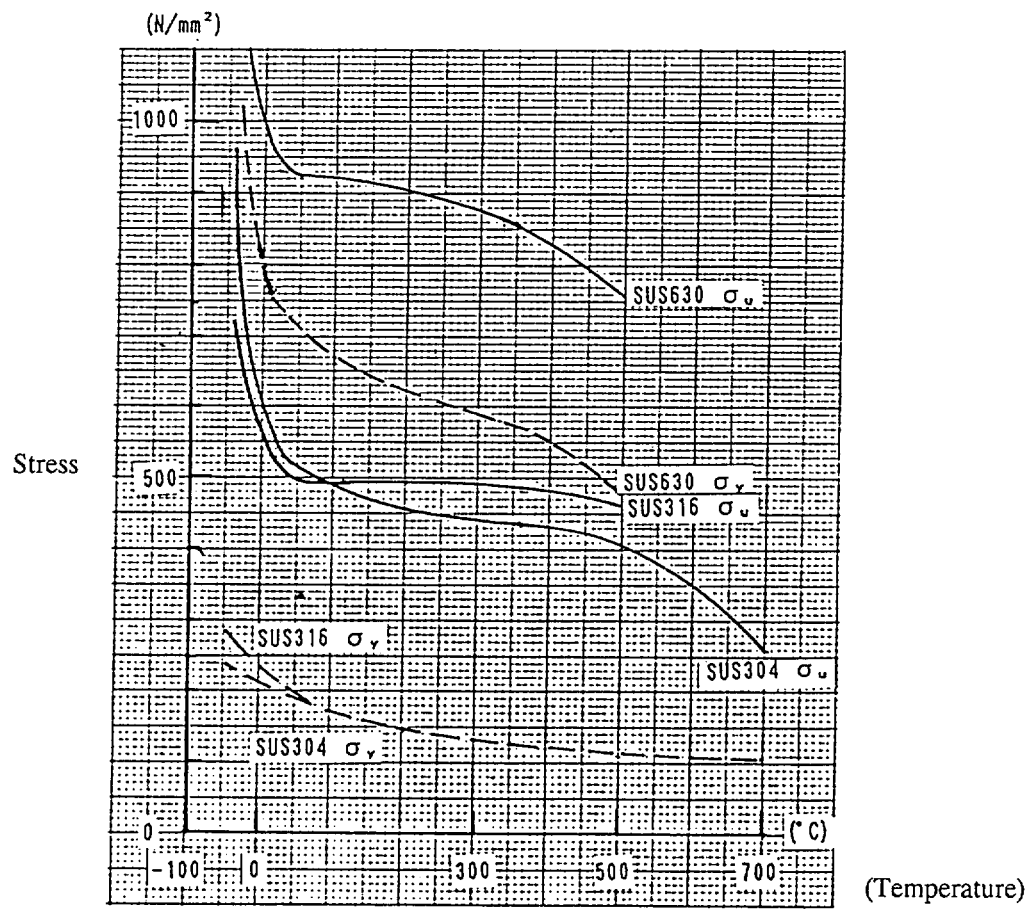


Fig. (II)-A.2 Tensile Stress and Yield Stress of Stainless Steel

Table (II)-A.8 Longitudinal Elasticity Modulus of Stainless Steel at High Temperatures

Material	SUS304	SUS630
Temperature (°C)		
-40	2.0x10 ⁵ N/mm ²	2.23x10 ⁵ N/mm ²
80	1.91x10 ⁵	2.13x10 ⁵
100	1.91x10 ⁵	2.12x10 ⁵
200	1.83x10 ⁵	2.06x10 ⁵
350	1.72x10 ⁵	1.99x10 ⁵
400	1.67x10 ⁵	1.94x10 ⁵
450	1.63x10 ⁵	-
500	1.58x10 ⁵	-

Note: ASME Sec III, Division 1

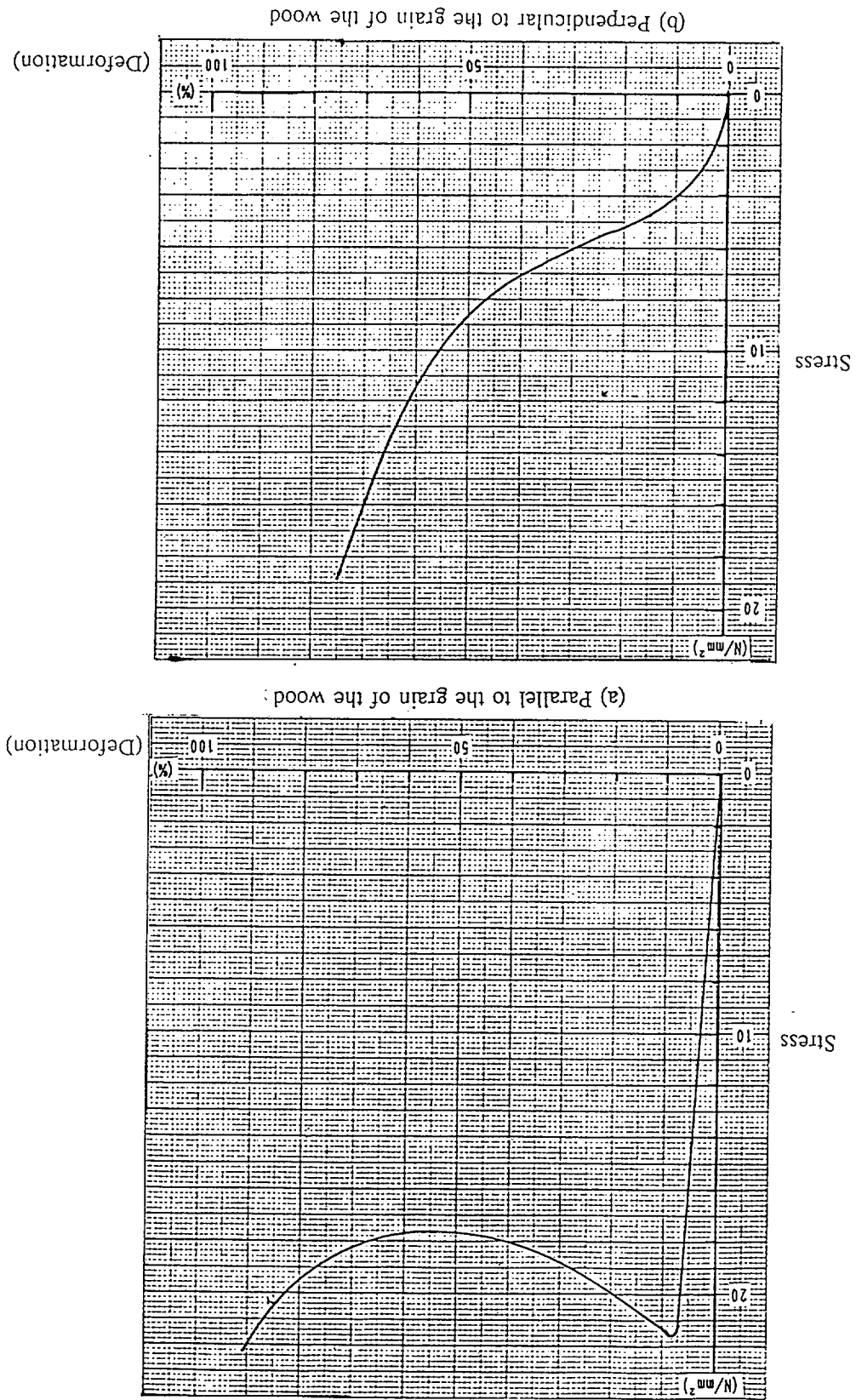


Fig. (III)-A.3 Crushing Curve of Balsa Wood

A.4 Package Requirements

A.4.1 Chemical and Galvanic Reactions

Table (II)-A.9 shows a list of different materials which will make contact with each other in the packaging.

Table (II)-A.9 Materials of a different kinds making contact with each other

Components in contact	Materials in contact
Inner shell Lead shield	Stainless steel Lead
Cement layer Lead shield	Alumina cement Lead
Cement layer Resin layer	Alumina cement Polyester resin
Resin layer Heat dispersion fin	Polyester resin Copper
Outer shell Heat dispersion fin	Stainless steel Copper
Intermediate shell Cement layer	Stainless steel Alumina cement
Intermediate shell Resin layer	Stainless steel Polyester resin
Outer shell Resin layer	Stainless steel Polyester resin
Lids O-ring	Stainless steel Fluoro rubber
Metal receptacle Bush	Stainless steel Bronze
Rotating plug Bush	Stainless steel Bronze
Boss Fusible plug	Stainless steel Bismuth
Cover plate of the shock absorber	Stainless steel Fir-plywood
. Shock absorber	Balsa wood
Lead shield Tungsten shield	Lead Tungsten

Stainless steel and lead, and copper or bronze and bismuth are in contact with each other in solid form. In this case, no chemical nor galvanic reactions occur. Balsa wood and fir-plywood are covered with stainless steel to control moisture. Therefore, no chemical or galvanic reactions occur due to the contact between the stainless steel and balsa wood or fir-plywood.

Fluoro rubber and resin (polyester resin) have no corrosive properties. Therefore, no chemical or galvanic reactions occur when the fluoro rubber and resin are in contact with stainless steel or copper. Stainless steel and resin are in contact with each other in a dry state; therefore, no chemical or galvanic reactions occur. Alumina cement is combined with water and filled; therefore, no excess water remains.

No chemical nor galvanic reactions take place in the contact part between the alumina layer and lead, or between the stainless steel and resin.

A.4.2 Low-Temperature Strength

This package preserves its integrity even if it is left unattended at a temperature of -40°C .

This packaging has a watertight structure. Under normal test conditions, no water enters the package during a water spray test. This package is a dry package. There is no liquid in the package. Consequently, the integrity of the package is never adversely affected by frozen liquid (e.g., water).

Table (II)-A.10 shows the allowable service temperature (minimum) for each of the materials used in this packaging.

The stainless steel (SUS304) used to enhance the strength of this container is fit for that purpose under temperatures lower than -190°C ,¹⁾ and no brittle fracture occurs at a temperature of -40°C . The stainless steel (SUS630 H1150) used for the fastening bolt maintains sufficient impact strength at a temperature of -40°C . The fluoro rubber packing used for the boundary of containment has a minimum service temperature of -50°C . The function of the packing is thus retained at a temperature of -40°C .

The minimum allowable service temperature of lead is -180°C . The performance of lead as a shield is retained at a temperature of -40°C . A sample test has confirmed that the shield performance of tungsten alloy is retained.

Since a sample test shows that the performance of resin used as a shield is also retained, the shielding integrity will not deteriorate.

A sample test³⁾ was also conducted on alumina cement at a temperature of -50°C . This test showed²⁾ that cubical expansion caused by freezing causes no problem. Therefore, performance will not deteriorate. Judging from the above, this package can retain its performance at a low temperature of -40°C .

1) JIS B8243, pressure vessels

2) Sample test of tungsten alloy and resin

Samples (tungsten alloy: $\phi 2 \times 5$ cm, resin: $\phi 5 \times 1$ cm) packed between two blocks of dry ice ($30 \times 30 \times 10$ cm, and sublimation temperature: -78.5°C), surrounded by an insulating material (asbestos that is 5-cm thick), and left unattended for five days. As a result, the state of each sample is exactly the same as it was before the test.

3) Kimura Chemical Plants Co., Ltd.: TN6-4 gata Yusobutsu Alumina Cement no Teion Jikken Hookoku 1980 (Report on low temperature experiments with alumina cement for the TN6-4 package)

Table (II)-A.10 Allowable Service Temperature (Minimum)

Material	Allowable service temperature (minimum)
Stainless steel (SUS304)	-190°C ¹⁾
Stainless steel (SUS630 H1150)	-40°C ²⁾
Lead	-180°C ³⁾
Tungsten alloy	-70°C *
Resin	-70°C *
Balsa wood	-60°C ⁴⁾
Alumina cement	-50°C ⁵⁾
Fluoro rubber	-50°C ⁶⁾

The service temperature marked with * have been obtained by sample tests.

1) JIS B8243, pressure vessels
2) Sutenresu kou no netsushori (Heat treatment of stainless steel), The Nikkan Kogyo Shimbun Ltd.
3) Namari Handbook (Lead handbook), page 60, Society for Nihon Lead Zinc Demand Research, 1975
4) A.C. Knoell: Environment and physical effects on the response of balsa wood as an energy dissipator, page 29, TEC No. 32-944, 1966
5) Kimura Chemical Plants Co., Ltd.: TN6-4 gata Yusobutsu Alumina Cement no Teion Jikken Hookoku (Report on low temperature experiments with alumina cement for the TN6-4 package)
6) Nippon Valqua Industries, Ltd.: Valqua review, page 11, Volume 21, No. 5

A.4.3 Containment System

Fig. (I)-22 shows the containment boundary of this packaging. The boundary of containment consists of the inner surface of the inner shell that constitutes the shell of the outer container, the front and rear sampling valve lids, the penetration hole lid for the rotating plug, the shielding plug lid and the rear lid of the rear lid unit, as well as the rotating plug lid and the front lid of the front lid unit.

The front and rear sampling valve lids and penetration hole lid for the rotating plug are designed so that containment is secured using double O-rings. A leakage test hole is provided between the double O-rings of these lids. The containment of these lids is confirmed by inspecting the leakage rate through a leakage test prior to shipment.

Sampling valves and an orifice plug that fixes the rotating plug to the inner shell are also provided to enhance the containment of the package.

The shielding plug lid and rotating plug lid are also designed so that the containment is ensured by an O-ring. Like the rear and front sampling valve lids, the front and rear lids have a double O-ring and leakage test hole. The containment of these lids is confirmed by inspecting the leakage rate through a leakage test prior to shipment. The front and rear lid units are covered with front and rear shock absorbers, and are designed so that they are not directly hit by a mild steel bar in drop test II under accident test conditions.

The front and rear shock absorbers are fixed to the end plates of the shell of the outer container, each with twelve hexagonal socket head bolts. As shown in Fig. (I)-23, each shock absorber has a single sealing lug. When the shock absorbers are fixed to the outer container, the hole of this lug coincides with that of the sealing lug installed on the external surface of the outer container. A wire is passed through the holes of the sealing lugs to seal the container so that no shock absorber is removed because of unauthorized use during transport. Therefore, the lids of the outer container that make up the containment system cannot be opened accidentally.

In addition to the containment boundary described above, this package also has fuel supporting cans and receiving tubes that act as a secondary containment system for the contents. The fuel supporting cans and receiving tubes are designed so that containment is ensured by welding.

A.4.4 Lifting Device

A.4.4.1 Outline

As shown in Fig. (I)-2, a lifting trunnion, a pivoting trunnion, four lifting lugs for horizontal operation, and four fastening lugs in vertical position are provided on the external surface of the outer container. The lifting trunnion is used for vertical lifting with the special lifting equipment as shown in Fig. (I)-4. The pivoting trunnion is used as a rotation axis when the position of the package is changed from horizontal to vertical or from vertical to horizontal on the transport skid. As shown in Fig. (I)-3, the pivoting trunnion is also used to fasten the package to the transport skid together with the rear base plate with bolts. The lifting lugs for horizontal operation are used for horizontal lifting that employs eyebolts and a four-point-hanging wire rope as shown in Fig. (I)-5. The fastening lugs in vertical position are used to tie down the outer container in a vertical position using a wire rope when its contents are loaded or unloaded. The fastening lugs in vertical position are sealed with bolts to avoid improper use for horizontal lifting. The front and rear base plates are used for horizontal placing on a floor other than the transport skid.

As shown in Fig. (I)-23, the shock-absorption equipment consists of front and rear shock absorbers. The front and rear shock absorbers are fixed to the end plates of the shell of the outer container, each with twelve hexagonal socket head bolts. A sealing lug is installed in each shock absorber. The shock-absorber sealing lugs are connected to the sealing lug of the outer container, and are sealed with a wire. Therefore, opening lids are provided for the outer container so that it cannot be opened inadvertently. The front and rear shock absorbers are equipped with two lifting lugs on each side. These lifting lugs are used to lift the container after the shock absorbers are removed. Wire ropes are connected to the lifting rings of the lifting lugs for two-point lifting. During transport, the lifting rings are folded on the lugs and sealed to prevent them from being used to horizontally lift the package. The lifting devices used for this package are as follows:

- (1) Lifting lug for horizontal operation (for horizontal lifting)
- (2) Lifting trunnion (for vertical lifting)

To demonstrate the integrity of the lifting device, stress values generated in the device when it is lifting the package are obtained through calculation taking into account every part related to its integrity and comparing the obtained results with the design criteria. For these calculations, a valve, which is three times the design weight is used as the design load to demonstrate that the device can sufficiently withstand sudden lifting of the package.

A.4.4.2 Load Conditions

As described above, the design load is represented by three times the design weight as shown in Table (II)-A.5.

In other words,

- (1) Three methods are used to lift the package horizontally:
 - The package is lifted together with its shock absorbers and the transport skid to which the package is attached.
 - The package is lifted together with the shock absorbers, but with the transport skid removed.
 - Only the package (the outer container and the inner container with the contents) is lifted.

However, for this analysis, an evaluation will be conducted while the shock absorbers and transport skid are still attached to the outer container. Therefore, the package will be at its maximum weight and the results will be on the safe side.

Consequently, the design load W_H is;

$$\begin{aligned} W_H &= 9.807 \times 12,500 \times 3 \\ &= 3.68 \times 10^5 \text{ N} \end{aligned}$$

- (2) In vertical lifting, the package is lifted with the shock absorbers, but without the transport skid, using the special lifting equipment as shown in Fig. (I)-4. The lifting weight is 9,500 kg. The design load W_v is;

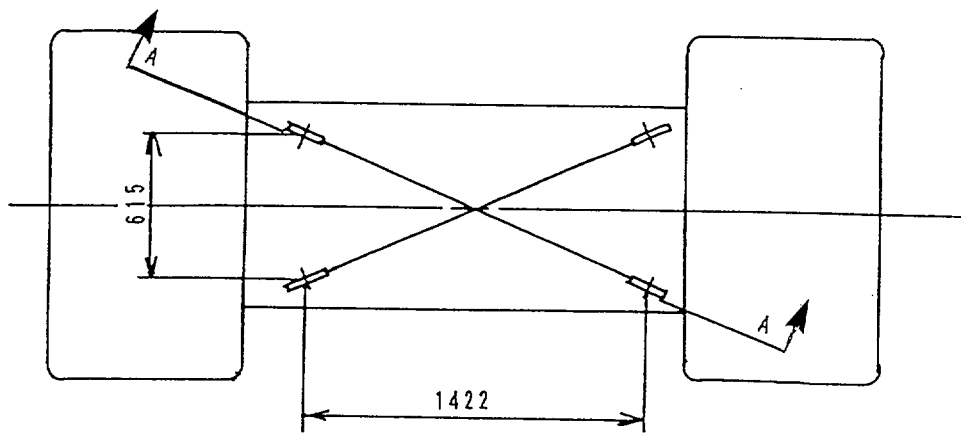
$$\begin{aligned} W_v &= 9.807 \times 9,500 \times 3 \\ &= 2.79 \times 10^5 \text{ N} \end{aligned}$$

The yield stress ($\sigma_y = 180 \text{ N/mm}^2 (\approx 18.4 \text{ kg/mm}^2)$) of the lifting device material (SUS304) is used as the design criterion for the bending stress and the tensile stress generated in the lifting device. The temperature of the lifting device is assumed to be 80°C to be on the safe side with respect to the maximum temperature (72°C) of the package's outer shell during transport, which is obtained as the result of thermal analysis. As described in A.3, "Mechanical Properties of Materials", the strength of stainless steel decreases as the temperature rises. If the strength at high temperatures is used as a criterion, the result of the evaluation will be on the safe side. For shear stress, 60% of the yield stress value ($0.6\sigma = 108 \text{ N/mm}^2 (\approx 11.0 \text{ kg/mm}^2)$) is used as a design criterion value. The stress at each welded part is analyzed assuming a welding efficiency of 60%.

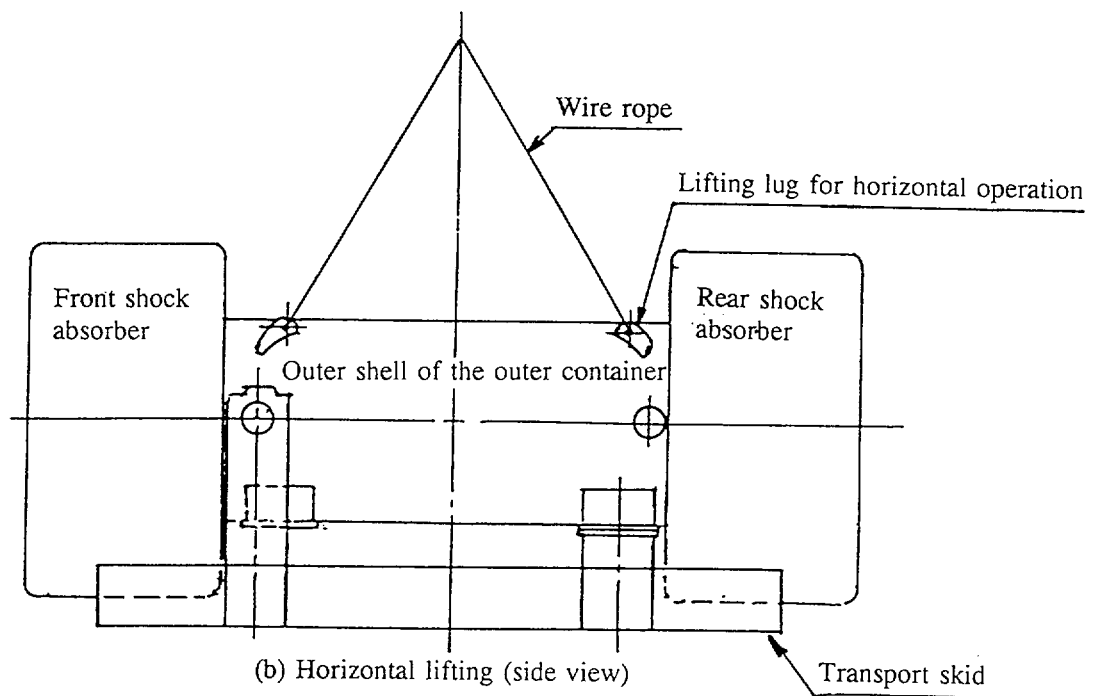
A.4.4.3 Stress Calculation

A.4.4.3.1 Horizontal Lifting

As shown in Fig. (II)-A.4, bending stress is generated in the outer shell of the outer container when the lifting lugs are used during horizontal lifting. This section is analyzed to demonstrate that the ring part of the lifting lug for horizontal operation and the lug part welded to the outer shell shown in Fig. (II)-A.5 do not rupture when the package is lifted at four points using a wire rope, and that the outer shell is not deformed by the stress generated at the outer shell during lifting.



(a) Horizontal lifting (plane view)



(b) Horizontal lifting (side view)

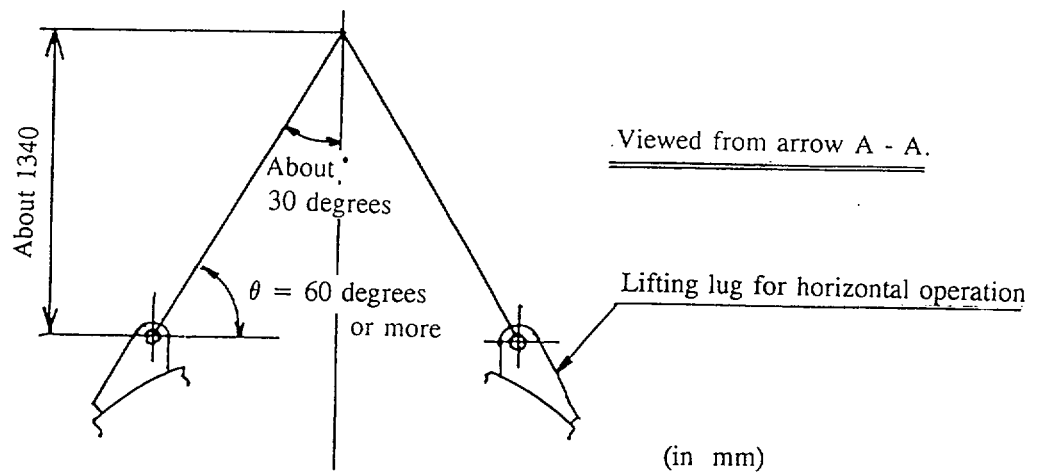


Fig. (II)-A.4 Horizontal Lifting

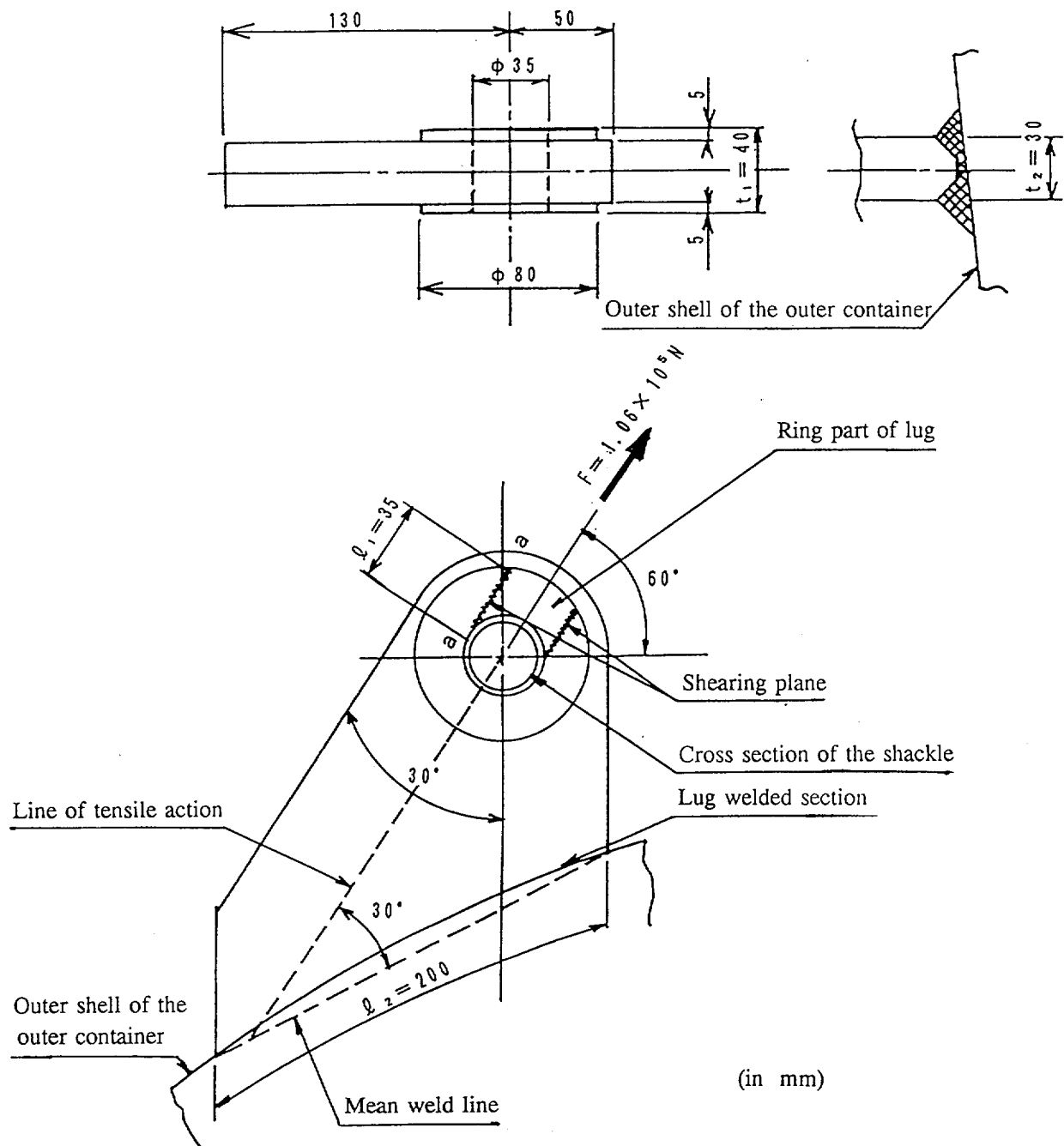


Fig. (II)-A.5 Lifting Lug for Horizontal Operation

(1) Lifting lug for horizontal operation

This section will demonstrate that the ring part of the lifting lug for horizontal operation and the welded section of the lifting lug for horizontal operation do not rupture during lifting.

(a) The ring part of the lifting lug for horizontal operation

Shear stress is generated in the ring part of the lifting lug for horizontal operation (hereafter called "the ring part") by the tension that is generated in a lifting wire rope. The tension (F) that is generated in the lifting wire rope is given by the expression below.

$$F = \frac{W_H}{n \sin \theta}$$

where

W_H :	Design load during horizontal lifting	$3.68 \times 10^5 \text{ N}$
n :	Number of lugs	4
θ :	Lifting angle of the wire rope	60 degrees or more

A specified rope is used so that the lifting angle (θ) of a wire rope shown in Fig. (II)-A.4 will be 60 degrees or more. When the lifting angle (θ) is 60 degrees, the tension (F) reaches a maximum.

$$\begin{aligned} F_{\max} &= \frac{3.68 \times 10^5}{4 \times \sin 60^\circ} \\ &= 1.06 \times 10^5 \text{ N} \end{aligned}$$

The stress on the ring part is calculated using this value, while the stress on the welded section of the lifting lug for horizontal operation will be determined in the next section. In Fig. (II)-A.5, the shear stress (τ) occurring in the a-a section is expressed by the equation;

$$\tau = \frac{3}{2} \cdot \frac{F_{\max}}{A} \quad 1)$$

where

F_{\max} :	Shear stress (= wire rope tension)	$1.06 \times 10^5 \text{ N}$
A:	Sectional area to which a shear load is applied	

$$A = 2t_1 \ell_1$$

t_1 :	Thickness of the plate to which a shear load is applied	40 mm
ℓ_1 :	Length of the section to which a shear load is applied	35 mm

$$\begin{aligned} A &= 2 \times 40 \times 35 \\ &= 2.8 \times 10^3 \text{ mm}^2 \end{aligned}$$

1) Nihon Kikai Gakkai: Kikai Kogaku Benran (Kaitei 6 pan) p. 4-59, 1979 (The Japan Society of Mechanical Engineers: Handbook of Mechanical Engineering (sixth edition), page 4-59, 1979)

Using the above-mentioned value, the result will be;

$$\begin{aligned}\tau &= \frac{3}{2} \times \frac{1.06 \times 10^5}{2.8 \times 10^3} \\ &= 56.8 \text{ N/mm}^2 \\ &\approx 5.8 \text{ kg/mm}^2\end{aligned}$$

The shearing stress generated at the ring part during horizontal lifting is 56.8 N/mm² ($\approx 5.8 \text{ kg/mm}^2$). The allowable stress at the lug ring part is $0.6 \sigma_y = 108 \text{ N/mm}^2$ ($\approx 11.0 \text{ kg/mm}^2$). Therefore, the margin of safety (M.S.) will be;

$$\begin{aligned}M.S. &= \frac{108}{56.8} - 1 \\ &= 0.9\end{aligned}$$

Since the margin of safety is positive, the lug ring part is not sheared during horizontal lifting.

(b) The welding section of the lifting lug for horizontal operation

Since the lifting lug for horizontal operation is pulled by a lifting wire as shown in Fig. (II)-A.5, the tensile stress and shear stress are generated in the welded section of the lifting lug for horizontal operation (hereafter called "the lug welded section").

The angle between a wire rope tensile action line and a lug weld line is 30 degrees on average. The tensile stress (σ) that occurs at the lug welded section is shown by the equation;

$$\sigma = \frac{F_{\max} \cdot \sin 30^\circ}{A}$$

where

F_{\max} : Tension of the lifting wire $1.06 \times 10^5 \text{ N}$

A: Sectional area of the lug welded section

$$A = t_2 \ell_2$$

t_2 : Plate thickness of the lug 30 mm

ℓ_2 : Length of the lug welded section 200 mm

$$\begin{aligned}A &= 30 \times 200 \\ &= 6.0 \times 10^3 \text{ mm}^2\end{aligned}$$

Using the above-mentioned value, the result obtained is;

$$\begin{aligned}\sigma &= \frac{1.06 \times 10^5 \times \sin 30^\circ}{6.0 \times 10^3} \\ &= 8.83 \text{ N/mm}^2\end{aligned}$$

The shear stress (τ) generated in the lug welded section during horizontal lifting is shown by the equation;

$$\begin{aligned}\tau &= \frac{F_{\max} \cdot \cos 30^\circ}{A} \\ &= \frac{1.06 \times 10^5 \times \cos 30^\circ}{6.0 \times 10^3} \\ &= 15.3 \text{ N/mm}^2\end{aligned}$$

When the tensile stress and shear stress act at the same time, the combined stress (σ_p) is expressed by

$$\sigma_p = \frac{\sigma}{2} + \sqrt{\left(\frac{\sigma}{2}\right)^2 + \tau^2} \quad 1)$$

Using the above-mentioned value, the result obtained is;

$$\begin{aligned}\sigma_p &= \frac{8.83}{2} + \sqrt{\left(\frac{8.83}{2}\right)^2 + 15.3^2} \\ &= 20.3 \text{ N/mm}^2 \\ &\approx 2.1 \text{ kg/mm}^2\end{aligned}$$

The combined stress of the tensile stress and shear stress generated in the lug welded section during horizontal lifting is 20.3 N/mm². The allowable stress for the lug welded section is the value obtained by multiplying $\sigma_y = 180 \text{ N/mm}^2$ ($\approx 18.4 \text{ kg/mm}^2$) by a welding efficiency of 60%. Therefore, the margin of safety (M.S.) is;

$$\begin{aligned}M.S. &= \frac{180 \times 0.6}{20.3} - 1 \\ &= 4.3\end{aligned}$$

1) Nihon Kikai Gakkai: Kikai Kogaku Benran (Kaitei 6 pan) p. 3-4, 1979
(Japanese Mechanical Society: Handbook of Mechanical Engineering, page 3-4, 1979)

Since the margin of safety is positive, the lug welded section will not be damaged, and the strength will be maintained during horizontal lifting.

(2) Outer shell

As shown in Fig. (II)-A.6, the bending moment caused by the weight of the package and transport skid acts on the packaging body during horizontal lifting. This bending moment is actually sustained by the inner and outer shells of the outer container as well as the lead shield. In this section, the bending moment is assumed to be sustained by only the outer shell to be on the safe side. On this assumption, the analysis in this section will demonstrate that the maximum bending stress obtained is less than the allowable stress, and that therefore, the outer shell is not damaged during horizontal lifting. It is also assumed that the weight of the package (not including the weight of its shock absorbers) will be distributed uniformly along the outer shell and that the weight of each shock absorber will act as a concentrated load on the end of the outer shell, while the weight of the transport skid will act as a concentrated load on the pivoting trunnions and on the rear base plate. The safety factor of each load is "3".

The reaction force generated at the lifting lug is first obtained. As shown in Fig. (II)-A.6, based on the equilibrium of forces and the equilibrium of moments around point A, the following equations can be derived.

$$W_s + W_{K1} + R_A + W_{K2} + R_B + W_s + W\ell = 0$$

$$W_s (\ell_1 + \ell_2) + W_{K1}\ell_2 + \frac{1}{2} w (\ell_1 + \ell_2)^2 = W_{K2}\ell_3 + R_B (\ell_3 + \ell_4) \\ + W_s (\ell_3 + \ell_4 + \ell_5) \\ + \frac{1}{2} w (\ell_3 + \ell_4 + \ell_5)^2$$

where

W_s :	Load by a shock absorber	$9.807 \times 750 \times 3 = 2.21 \times 10^4 \text{ N}$
W_{K1} :	Load from the pivoting trunnion on the transport skid	$9.807 \times 735 \times 3 = 2.16 \times 10^4 \text{ N}$
W_{K2} :	Load from the rear base plate on the transport skid	$9.807 \times 765 \times 3 = 2.25 \times 10^4 \text{ N}$
R_A :	Load generated in the lifting lug	
R_B :	Load generated in the lifting lug	
w :	Distributed load by package	

$$= \frac{3W}{\ell}$$

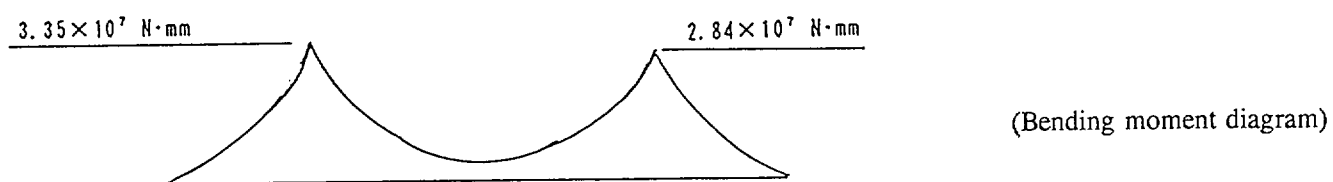
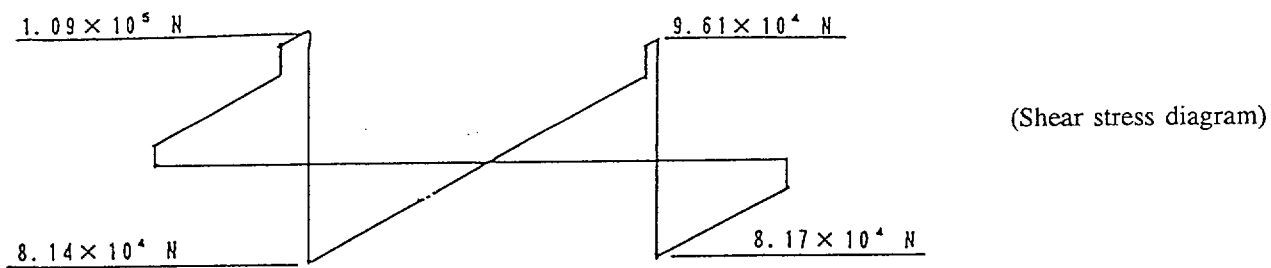
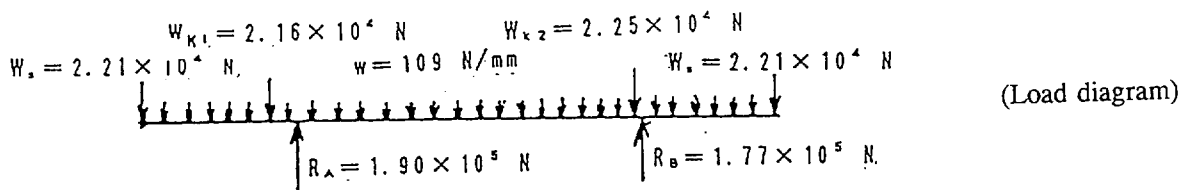
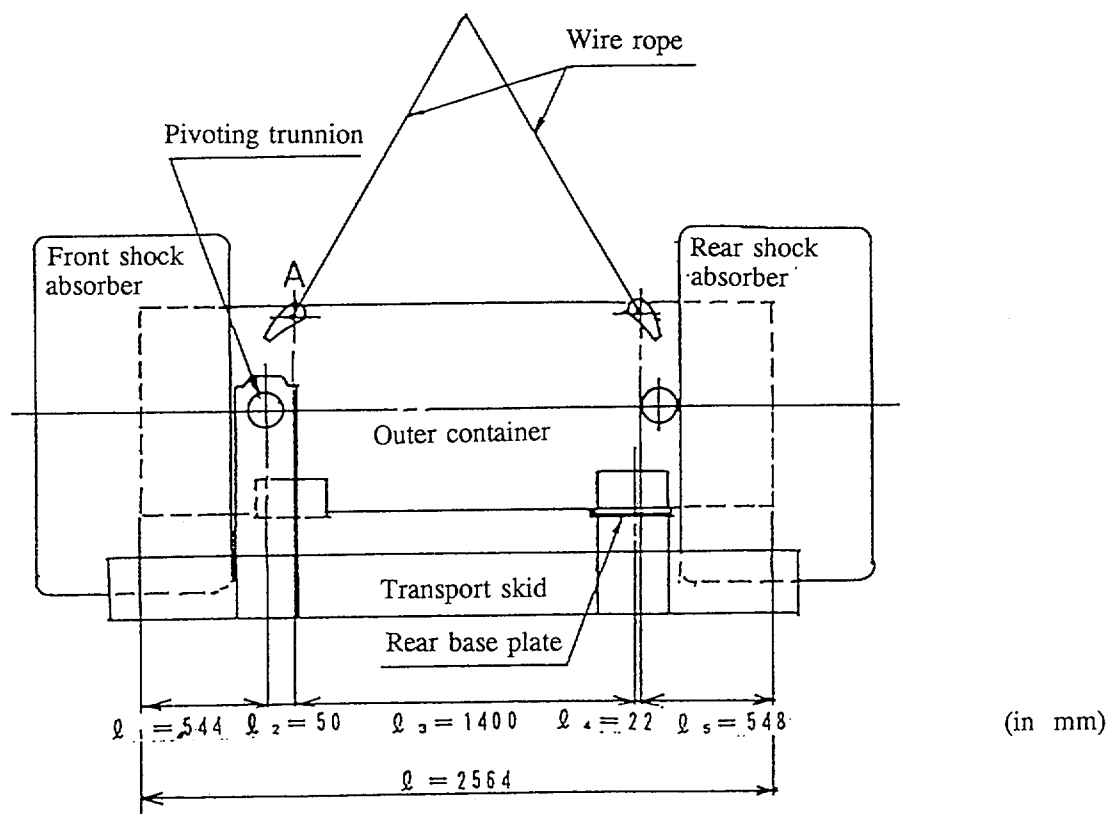


Fig. (II)-A.6 Analysis of the Outer Shell during Horizontal Lifting

W: Weight of the package
(not including the weight of the shock absorbers) 9500 kg
 ℓ : Length of the packaging 2564 mm

$$W = \frac{9.807 \times 3 \times 9500}{2564}$$

$$= 109 \text{ N/mm}$$

ℓ_1 : Moment arm (See Fig. (II)-A.6.) 544 mm
 ℓ_2 : Moment arm " 50 mm
 ℓ_3 : Moment arm " 1400 mm
 ℓ_4 : Moment arm " 22 mm
 ℓ_5 : Moment arm " 548 mm

The solutions to the above two equations are;

$$R_A = -1.90 \times 10^5 \text{ N}$$

$$R_B = -1.77 \times 10^5 \text{ N}$$

The load diagram in Fig. (II)-A.6 shows the distribution of these loads. Next, the load is integrated by distance to obtain the shear stress, and the shear stress is integrated by distance to obtain the bending moment. The shear stress $F(x)$ and bending moment $M(x)$ \times mm away from the front end of the packaging are shown by the equations below.

Position	Shear stress	Bending moment
$0 \leq x < 544$	$F(x) = W_s + wx$ $= 2.21 \times 10^4 + 109x$	$M(x) = W_s x + \frac{1}{2} wx^2$ $= 2.21 \times 10^4 x + \frac{1}{2} \times 109x^2$ $= 2.21 \times 10^4 x + 54.5x^2$
$544 \leq x < 594$	$F(x) = W_s + W_{K1} + wx$ $= 2.21 \times 10^4 + 2.16 \times 10^4 + 109x$ $= 4.37 \times 10^4 + 109x$	$M(x) = W_s x + W_{K1} (x - \ell_1) + \frac{1}{2} wx^2$ $= 2.21 \times 10^4 x + 2.16 \times 10^4 \times (x - 544) + 54.5x^2$ $= -1.18 \times 10^7 + 4.37 \times 10^4 x + 54.5x^2$
$594 \leq x < 1994$	$F(x) = W_s + W_{K1} + R_A + wx$ $= 2.21 \times 10^4 + 2.16 \times 10^4 - 1.90 \times 10^5 + 109x$ $= -1.46 \times 10^5 + 109x$	$M(x) = W_s x + W_{K1} (x - \ell_1) + R_A \times (x - \ell_1 - \ell_2) + \frac{1}{2} wx^2$ $= 2.21 \times 10^4 x + 2.16 \times 10^4 \times (x - 544) - 1.90 \times 10^5 \times (x - 544 - 50) + 54.5x^2$ $= 1.01 \times 10^8 - 1.46 \times 10^5 x + 54.5x^2$

Position	Shear stress	Bending moment
$1994 \leq x < 2016$	$F(x) = W_s + W_{K1} + R_A + W_{K2} + wx$ $= 2.21 \times 10^4 + 2.16 \times 10^4$ $-1.90 \times 10^5 + 2.25 \times 10^4 +$ 10^9x $= -1.24 \times 10^5 + 10^9x$	$M(x) = W_sx + W_{K1}(x - \ell_1) + R_A$ $\times (x - \ell_1 - \ell_2) + W_{K2}$ $\times (x - \ell_1 - \ell_2 - \ell_3) + \frac{1}{2} wx^2$ $= 2.21 \times 10^4x + 2.16 \times 10^4$ $\times (x - 544) - 1.90 \times 10^5$ $\times (x - 544 - 50) + 2.25 \times 10^4$ $\times (x - 544 - 50 - 1400) + 54.5x^2$ $= 5.63 \times 10^7 - 1.24 \times 10^5x + 54.5x^2$
$2016 \leq x < 2564$	$F(x) = W_s + W_{K1} + R_A + W_{K2} + R_B$ $+ wx$ $= 2.21 \times 10^4 + 2.16 \times 10^4$ $-1.9 \times 10^5 + 2.25 \times 10^4$ $-1.77 \times 10^5 + 10^9x$ $= -3.01 \times 10^5 + 10^9x$	$M(x) = W_sx + W_{K1}(x - \ell_1) + R_A$ $\times (x - \ell_1 - \ell_2) + W_{K2}$ $\times (x - \ell_1 - \ell_2 - \ell_3) + R_B$ $\times (x - \ell_1 - \ell_2 - \ell_3 - \ell_4) + \frac{1}{2} wx^2$ $= 2.21 \times 10^4x + 2.16 \times 10^4$ $\times (x - 544) - 1.9 \times 10^5$ $\times (x - 544 - 50) + 2.25 \times 10^4$ $\times (x - 544 - 50 - 1400)$ $- 1.77 \times 10^5 (x - 544 - 50$ $- 1400 - 22) + 54.5x^2$ $= 4.13 \times 10^8 - 3.01 \times 10^5x + 54.5x^2$

The shear stress and bending moment diagrams in Fig. (II)-A.6 show the results of the calculation above. The maximum bending moment (M) is generated at point A. The value of the moment is obtained as follows:

$$M = 3.35 \times 10^7 \text{ N}\cdot\text{mm}$$

The bending stress (σ) generated at the outer shell is given by the expression below.

$$\sigma = \frac{M}{Z}$$

Z: Section modulus of outer shell¹⁾

$$Z = \frac{\pi}{32} \times \frac{d_o^4 - d_i^4}{d_o}$$

d_o :	Outer diameter of outer shell	800 mm
d_i :	Inner diameter of outer shell	768 mm
	(Minimum value of thickness)	

1) Nihon Kikai Gakkai: Kikai Kogaku Benran, p. 4-51, 1979
(The Japan Society of Mechanical Engineers: Handbook of Mechanical Engineering, page 4-51, 1979)

$$Z = \frac{\pi}{32} \times \frac{800^4 - 768^4}{800}$$

$$= 7.57 \times 10^6 \text{ mm}^3$$

$$\sigma = \frac{3.35 \times 10^7}{7.57 \times 10^6}$$

$$= 4.43 \text{ N/mm}^2$$

$$= 0.45 \text{ kg/mm}^2$$

The allowable stress of the outer shell is $\sigma_y = 180 \text{ N/mm}^2$ ($\approx 18.4 \text{ kg/mm}^2$), and therefore the margin of safety (M.S.) is given by

$$M.S. = \frac{180}{4.43} - 1$$

$$= 39$$

The outer shell thus has sufficient strength and does not bend.

The analysis results above show that the lifting lug for horizontal operation and the package have sufficient strength when the package is lifted horizontally.

A.4.4.3.2 Vertical Lifting

The package is vertically lifted with the special lifting equipment without the shock absorbers and transport skid, as shown in Fig. (II)-A.7. As a result of this vertical lifting, shear stress is generated in the lifting trunnion, and bending stress is generated in the trunnion mounting part. Moreover, stress is generated in the shell part and in the end plates of the outer container because it is being lifted with the trunnions. Then, the strength at these four places is analyzed. The results show that the package is sound for vertical lifting.

(1) Trunnion

The shear stress (τ) generated in the lifting trunnion mounting part during vertical lifting is given by the expression below.

$$\tau = \frac{4}{3} \cdot \frac{W_v}{2A} \quad 1)$$

where

W_v : Design load during vertical lifting $2.79 \times 10^5 \text{ N}$

A : Sectional area of the lifting trunnion

$$A = \frac{\pi}{4} d^2$$

1) Nihon Kikai Gakkai: Kikai Kogaku Benran, p. 4-59, 1979

(The Japan Society of Mechanical Engineers: Handbook of Mechanical Engineering, page 4-59, 1979)

d: Diameter of lifting trunnion

100 mm

$$A = \frac{\pi}{4} \times 100^2 = 7.85 \times 10^3 \text{ mm}^2$$

and thus

$$\tau = \frac{4}{3} \times \frac{2.79 \times 10^5}{2 \times 7.85 \times 10^3}$$

$$= 23.7 \text{ N/mm}^2$$

$$\approx 2.42 \text{ kg/mm}^2$$

The allowable shear stress is $0.6\sigma_y = 108 \text{ N/mm}^2$ ($\approx 11.0 \text{ kg/mm}^2$), so the margin of safety (M.S.) is given by

$$M.S. = \frac{108}{23.7} - 1$$

$$= 3.5$$

Since the margin of safety is positive, the trunnion part is not sheared during vertical lifting.

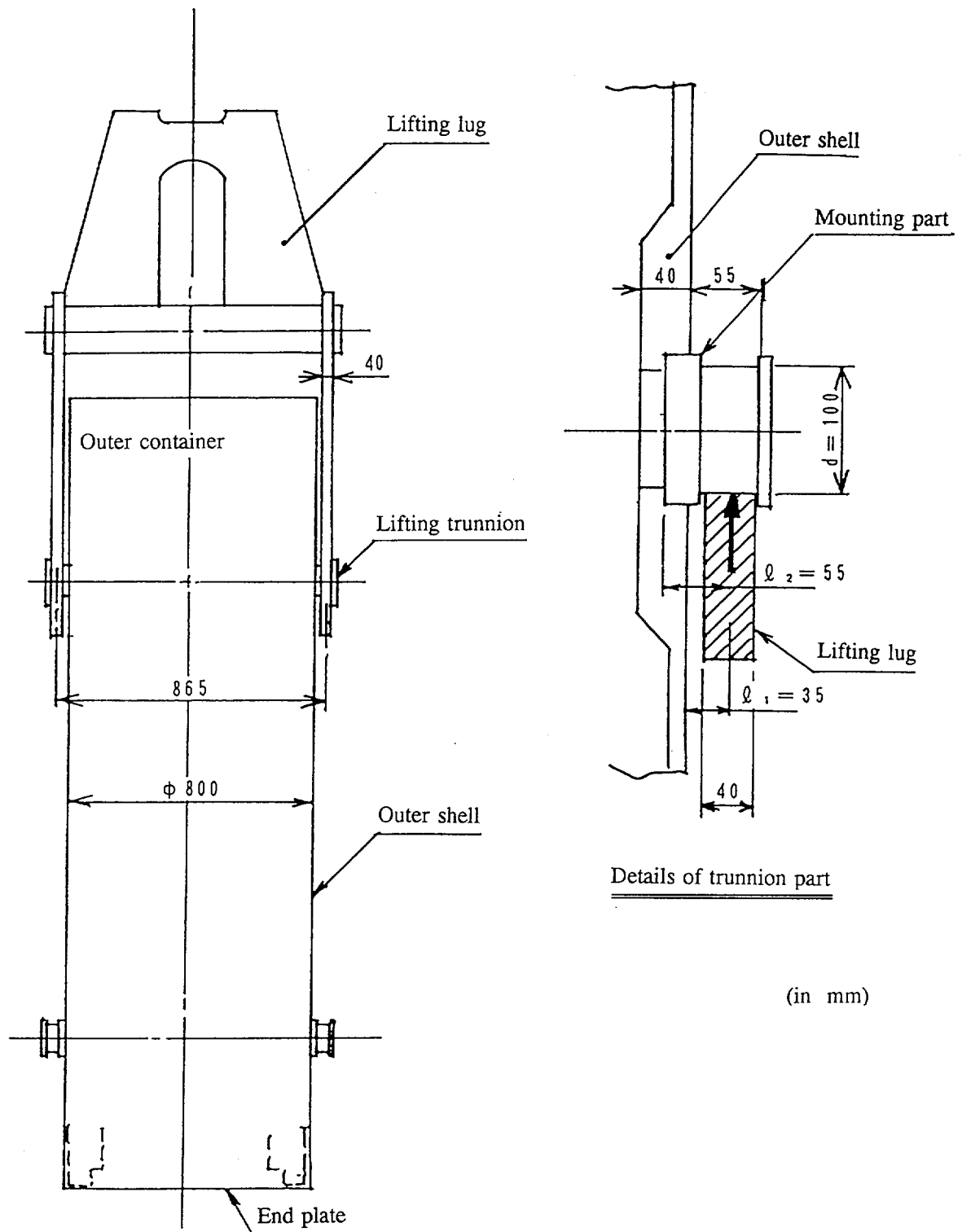


Fig. (II)-A.7 Analysis Model of the Lifting Trunnion

(2) Lifting trunnion mounting part

The bending moment operates in the mounting part (the root of the trunnion) of the lifting trunnion onto the outer shell during vertical lifting. The bending stress generated in this state is evaluated to indicate that the trunnion mounting part is sound. As shown in Fig. (II)-A.7, the moment arm becomes $\ell_1 = 35$ mm (maximum) according to the lifting position of the lifting lug. The moment arm ℓ_2 in Fig. II-A.7 is used when investigating the strength of the outer shell described later.

The bending stress (σ) generated in the lifting trunnion mounting part during vertical lifting is given by the expression below.

$$\sigma = \frac{M}{Z}$$

where

M: Bending moment generated in the mounting part

$$M = \frac{W_v}{2} \ell_1$$

W_v :	Design load during vertical lifting	2.79×10^5 N
ℓ_1 :	Moment arm	35 mm

$$\begin{aligned} M &= \frac{2.79 \times 10^5}{2} \times 35 \\ &= 4.88 \times 10^6 \text{ N}\cdot\text{mm} \end{aligned}$$

Z: Section modulus of the lifting trunnion

$$Z = \frac{\pi}{32} d^3$$

d:	Diameter of the lifting trunnion	100 mm
----	----------------------------------	--------

$$\begin{aligned} Z &= \frac{\pi}{32} \times 100^3 \\ &= 9.82 \times 10^4 \text{ mm}^3 \end{aligned}$$

Using the numeric values obtained above, the bending stress is;

$$\begin{aligned} \sigma &= \frac{4.88 \times 10^6}{9.82 \times 10^4} \\ &= 49.7 \text{ N/mm}^2 \\ &\approx 5.08 \text{ kg/mm}^2 \end{aligned}$$

The allowable stress is $\sigma_y = 180 \text{ N/mm}^2$ ($\approx 18.4 \text{ kg/mm}^2$), so the margin of safety (M.S.) is given by

$$\begin{aligned} M.S. &= \frac{180}{49.7} - 1 \\ &= 2.6 \end{aligned}$$

Since the margin of safety is positive, the trunnion mounting part stands against the bending stress caused by the special lifting equipment and is not damaged.

The above analysis results show that the lifting trunnion retains sufficient strength for vertical lifting and functions as a lifting lug. The pivoting trunnion also has the same shape as the lifting trunnion. Therefore, the pivoting trunnion has strength equivalent to that of the lifting trunnion even if it is vertically lifted using a vertical lifting lug because of unauthorized use.

(3) Outer container shell part

The stress generated in the outer container shell part during vertical lifting is assumed to be sustained by only the outer shell for analysis to be on the safe side. As shown in Fig. (II)-A.8, the outer container shell part consists of a section (300 mm wide) with a 40-mm plate thickness that supports the trunnion mounting part and another section with a 16-mm plate thickness. Therefore, the bending stress near the trunnion mounting part is assumed to be sustained by the thicker plate section, while the stress applied to the whole outer shell is evaluated in the thin plate section.

(a) Outer shell trunnion mounting part

Analysis in this subsection shows that the bending moment caused by the lifting trunnion during vertical lifting can be supported by the outer shell trunnion mounting part alone. The lifting trunnion is installed in the thicker plate section (40-mm thick and 300-mm wide) of the outer shell.

As shown in Fig. (II)-A.8, only this thicker plate section is modeled in the form of a ring to calculate the stress generated in this section. With only this ring, the outer shell satisfactorily withstand the bending stress.

The loading conditions during vertical lifting can be indicated by model "a" in Fig. (II)-A.8. These loads are separated into models "b" and "c" for investigation.

In model "b", a torsional moment (T_0) resulting from the reaction force acting on the lifting trunnion with a moment arm of (ℓ_2) is applied to the ring. A bending moment (M_1) and torsional moment (T_1) are generated in each radial direction of the ring by this moment.

In model "c", the weight of the package acts on the ring as a uniform load (q) and this load is supported by two trunnion mounting parts. As a result, a bending moment (M_2) and torsional moment (T_2) are generated. By the total ($M = M_1 + M_2$ and $T = T_1 + T_2$) of the moment in models "b" and "c", therefore the bending stress and shear stress are generated in the outer shell. This combined stress can then be used to check that the outer shell is sound.

The torsional moment (T_0) caused by the lifting trunnion is given by the expression below.

$$T_o = \frac{W_v}{2} \times \ell_2$$

where

$$W_v: \text{ Design load during vertical lifting } 2.79 \times 10^5 \text{ N}$$

$$\ell_2: \text{ Moment arm } 55 \text{ mm}$$

and thus

$$\begin{aligned} T_o &= \frac{2.79 \times 10^5}{2} \times 55 \\ &= 7.67 \times 10^6 \text{ N}\cdot\text{mm} \end{aligned}$$

As shown in Fig. (II)-A.8, the bending moment (M_1) and the torsional moment (T_1) that act on ring elements in the position at an angle of θ from the trunnion mounting position are obtained from the torsional moment (T_0). The bending moment (M_1) acts on the perpendicular section of the ring elements in the vertical direction to the section as shown in Fig. (II)-A.9. Meanwhile, the torsional moment (T_1) acts in a parallel direction to the section. Considering that the ring elements are located to the right and left with the trunnion in the center, each moment is given by

$$M_1 = \frac{T_o}{2} \sin\theta$$

$$T_1 = \frac{T_o}{2} \cos\theta$$

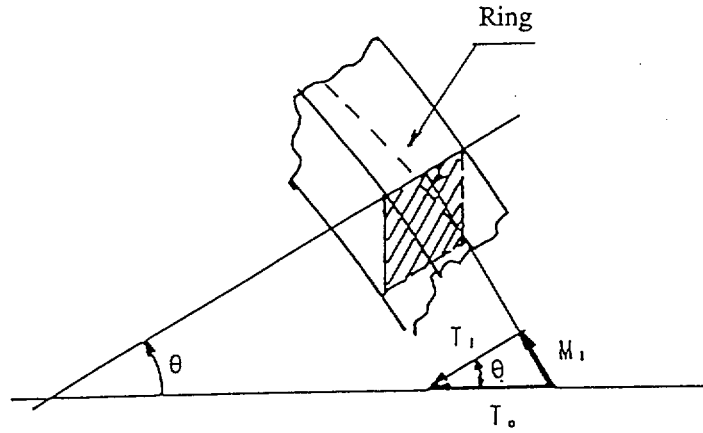


Fig. (II)-A.9 Relation of the Bending Moment and Torsional Moment

The uniform load (q) based on the weight of the package is given by the expression below.

$$q = \frac{W_v}{2\pi r}$$

where

W_v : Design load during vertical lifting $2.79 \times 10^5 \text{ N}$
 r : Mean radius of a ring 380 mm

$$q = \frac{2.79 \times 10^5}{2 \times \pi \times 380}$$

$$= 117 \text{ N/mm}$$

The bending moment (M_2) and torsional moment (T_2)¹⁾ generated in each part of the ring by the uniform load (q) are given by

$$M_2 = -qr^2 \left(1 - \frac{\pi}{2} \sin\theta\right)$$

$$T_2 = +qr^2 \left(\theta + \frac{\pi}{2} \cos\theta - \frac{\pi}{2}\right)$$

1) "How to Find Deflection and Moment of Ring and Accurate Beams" Product Engineering, pages 70 to 80, 1963

For vertical lifting, the bending moment (M) and torsional moment (T) occurring at the ring are indicated by combining each of the components described above.

$$M = M_1 + M_2$$

$$= \frac{T_o}{2} \sin\theta - qr^2 \left(1 - \frac{\pi}{2} \sin\theta\right)$$

$$T = T_1 + T_2$$

$$= \frac{T_o}{2} \cos\theta + qr^2 \left(\theta + \frac{\pi}{2} \cos\theta - \frac{\pi}{2}\right)$$

Using these moments, the stress acting on the ring is obtained. Bending stress (σ) is given as follows by the bending moment (M):

$$\sigma = \frac{M}{Z}$$

where

Z: Section modulus of the ring

$$Z = \frac{ba^2}{6}$$

a: Width of the ring 300 mm
b: Thickness of the ring 40 mm

$$Z = \frac{40 \times 300^2}{6} = 6.00 \times 10^5 \text{ mm}^3$$

Using the torsional moment (T), the shear stress (τ) is given by

$$\tau = \frac{15a + 9b}{5a^2b^2} T \quad 1)$$

$$= \frac{15 \times 300 + 9 \times 40}{5 \times 300^2 \times 40^2} T$$

$$= 6.75 \times 10^{-6} T$$

1) Atsumaro Shimizu: Zairyo Rikigaku (Strength of Materials), page 161, Kyoritsu Shuppan

The stress when angle θ is changed from 0 to 90 degrees every five degrees is calculated based on the expression above. Table (II)-A.11 shows the calculation result. In this table, $\sigma +$ and $\sigma -$ represent the combined stress of σ and τ . They are given by the expression below.

$$\sigma_{\pm} = \frac{\sigma}{2} \pm \sqrt{\left(\frac{\sigma}{2}\right)^2 + \tau^2}$$

The maximum combined stress is generated (60 N/mm²) when angle θ is 25 degrees. The allowable stress of the outer shell is $\sigma_y = 180$ N/mm² (≈ 18.4 kg/mm²), so the margin of safety (M.S.) is given by

$$\begin{aligned} M.S. &= \frac{180}{60} - 1 \\ &= 2.0 \end{aligned}$$

The outer shell thus has sufficient strength for the vertical lifting load. As a result, no deformation occurs in this case.

Table (II)-A.11 Stress Generated in the Outer Shell (during Vertical Lifting)

Angle	Bending moment	Torsional moment	Stress			
θ (°)	M (N • mm)	T (N • mm)	σ (N/mm ²)	τ (N/mm ²)	$\sigma+$ (N/mm ²)	$\sigma-$ (N/mm ²)
0	-1.69x10 ⁷	3.84x10 ⁶	28.1	25.9	15.3	43.6
5	-1.43x10 ⁷	5.20x10 ⁶	23.7	35.1	25.2	48.9
10	-1.16x10 ⁷	6.33x10 ⁶	19.4	42.7	34.1	53.5
15	-9.04x10 ⁶	7.23x10 ⁶	15.1	48.8	41.8	56.9
20	-6.51x10 ⁶	7.91x10 ⁶	10.8	53.4	48.2	59.1
25	-4.51x10 ⁶	8.37x10 ⁶	6.7	56.4	53.2	60.0
30	-1.71x10 ⁶	8.62x10 ⁶	2.8	58.1	56.7	59.6
35	5.31x10 ⁵	8.67x10 ⁶	0.08	58.5	58.9	58.0
40	2.64x10 ⁶	8.53x10 ⁶	4.4	57.5	59.8	55.4
45	4.59x10 ⁶	8.22x10 ⁶	7.6	55.5	59.4	51.7
50	6.38x10 ⁶	7.74x10 ⁶	10.5	52.2	57.8	47.1
55	8.00x10 ⁶	7.11x10 ⁶	13.3	47.9	55.1	41.7
60	9.42x10 ⁶	6.35x10 ⁶	15.6	42.8	51.3	35.6
65	1.06x10 ⁷	5.47x10 ⁶	17.7	36.9	46.8	29.1
70	1.17x10 ⁷	4.50x10 ⁶	19.4	30.3	41.5	22.1
75	1.18x10 ⁷	3.44x10 ⁶	20.7	23.2	35.7	15.1
80	1.30x10 ⁷	2.33x10 ⁶	21.6	15.6	30.0	8.20
85	1.34x10 ⁷	1.17x10 ⁶	22.2	7.90	24.8	2.50
90	1.35x10 ⁷	1.88x10 ⁶	22.4	0.00	22.4	0.00
			σ max		59.8	-60.0

(b) Outer shell

During vertical lifting, the lifting load acts on the shell part of the outer container. The lifting load is assumed to be sustained by only the thin plate section of an outer shell, to be on the safe side. Under these conditions, the tensile stress generated in the fusible plug section of the outer shell is obtained to indicate that the outer shell is not damaged.

The tensile stress generated in the outer shell is given by the expression below.

$$\sigma = \frac{W_v}{S}$$

where

W_v : Design load during vertical lifting 2.79×10^5 N

S : Sectional area of the outer shell

$$S = \frac{\pi}{4} (d_1^2 - d_2^2) - ntd$$

d_1 : Outer diameter of the outer shell	800 mm
d_2 : Inner diameter of the outer shell	768 mm
n : Number of fusible plugs on the same circumference	4
t : Plate thickness of the outer shell	16 mm
d : Mean diameter of a fusible plug's penetration hole	15 mm

$$\begin{aligned} S &= \frac{\pi}{4} (800^2 - 768^2) - 4 \times 16 \times 15 \\ &= 3.84 \times 10^4 \text{ mm}^2 \end{aligned}$$

$$\begin{aligned} \sigma &= \frac{2.79 \times 10^5}{3.84 \times 10^4} \\ &= 7.26 \text{ N/mm}^2 \\ &\approx 0.74 \text{ kg/mm}^2 \end{aligned}$$

Considering the welding efficiency of the outer shell, if the design criterion value $0.6\sigma_y = 108 \text{ N/mm}^2$ ($\approx 11.0 \text{ kg/mm}^2$) is used, the margin of safety (M.S.) is given by

$$\begin{aligned} M.S. &= \frac{108}{7.26} - 1 \\ &= 14 \end{aligned}$$

Therefore, the outer shell has sufficient strength for the lifting load.

(4) End plate of the outer container

The weight of the inner shell, lead shield, and resin layer is mostly supported by the outer shell due to friction resulting from their contact with each other in the direction of a diameter. The weight of the lead shield is supported by front and rear end plates via the inner shell. In this section, all the loads are assumed to be sustained by the front and rear end plates. The stress generated under these conditions is calculated and indicates that no deformation occurs in the end plates.

As shown in Fig. (II)-A.10, the center portion of the front end plate is strongly constructed with a front lid (the center portion of the rear end plate is constructed with the rear lid). Consequently, the following analysis model is used:

As shown in Fig. (II)-A.10, the center portion is assumed to consist of a flat rigid plate, and the outer radius of the rigid body is assumed to be the same as the inner radius of the lead shield. The radius of the outer fixed edge of the end plate is assumed to be the same as the inner radius of the outer shell.

The stress to be generated is sustained by the front and rear end plates via the inner shell, and is therefore divided equally. The stress (σ_i) and (σ_o) generated in the inner and outer ends are given by the expression¹⁾ below.

$$\sigma_i = \frac{3W_v}{2\pi nt^2} \left\{ 1 - \frac{2a^2}{a^2 - b^2} \left(\log_e \frac{a}{b} \right) \right\}$$

$$\sigma_o = \frac{3W_v}{2\pi nt^2} \left\{ 1 - \frac{2b^2}{a^2 - b^2} \left(\log_e \frac{a}{b} \right) \right\}$$

W_v :	Design load during vertical lifting	2.79×10^5 N
t:	Thickness of the end plate	16 mm
n:	Number of end plates	2
a:	Radius of the fixed end	384 mm
b:	Radius of the rigid body	290 mm

$$\sigma_i = \frac{3 \times 2.79 \times 10^5}{2 \times \pi \times 2 \times 16^2} \left\{ 1 - \frac{2 \times 384^2}{384^2 - 290^2} \left(\log_e \frac{384}{290} \right) \right\}$$

$$= -79.8 \text{ N/mm}^2$$

$$\approx -8.2 \text{ kg/mm}^2$$

$$\sigma_o = \frac{3 \times 2.79 \times 10^5}{2 \times \pi \times 2 \times 16^2} \left\{ 1 - \frac{2 \times 290^2}{384^2 - 290^2} \left(\log_e \frac{384}{290} \right) \right\}$$

$$= 66.2 \text{ N/mm}^2$$

$$\approx 6.8 \text{ kg/mm}^2$$

1) R. J. Roark; Formulas for Stress and Strain, page 222, Mcgraw Hill Book, 1965

For the stress in the inner circumference, the margin of safety (M.S.) is given as follows by the analysis criterion value $\sigma_y = 180 \text{ N/mm}^2 (\approx 18.4 \text{ kg/mm}^2)$.

For the stress in the outer circumference, the analysis criterion value $0.6\sigma_y = 108 \text{ N/mm}^2 (\approx 11.0 \text{ kg/mm}^2)$ is used, as it is a welding part. The respective margin of safety is given by

$$\begin{aligned} M.S. &= \frac{180}{79.8} - 1 \\ &= 1.2 \end{aligned}$$

and,

$$\begin{aligned} M.S. &= \frac{108}{66.2} - 1 \\ &= 0.6 \end{aligned}$$

Therefore, no deformation occurs in the end plates during lifting.

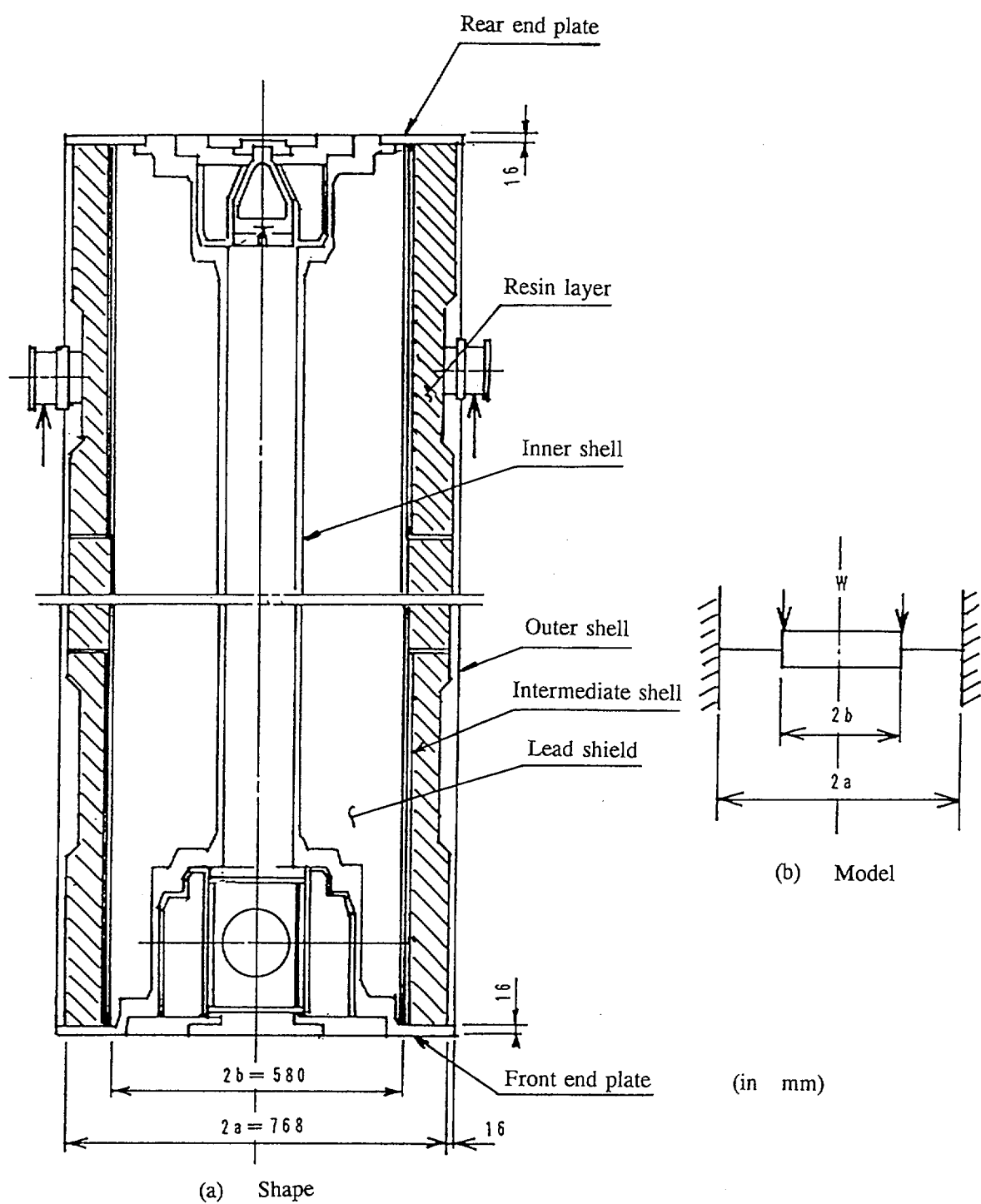


Fig. (II)-A.10 End Plate Analysis Model

A.4.5 Tie-down Device

A.4.5.1 Outline

As shown in Fig. (II)-A.11, this package is designed so that it is fixed to the special transport skid using the rear base plate and the pivoting trunnion. The tie-down devices used in this package are a rear base plate and pivoting trunnion.

The rear base plate is fixed to the transport skid with bolts, and the pivoting trunnion is supported by the bearing supports of the transport skid and fixed by bolting the retaining piece.

To absorb the thermal expansion of the packaging, a pivoting trunnion receptacle has a longitudinal hole in the axial direction, and the axial force of the package is not applied to the pivoting trunnion.

The acceleration that acts on the package during transport is set to calculate the stress generated at each part of the tie-down devices. The resulting stress does not exceed the design criterion value. This indicates that the tie-down devices maintain its performance during transport.

A.4.5.2 Analysis Conditions

The acceleration that acts during transport on the package mounted on the transport skid is set as follows:

(II)-A-56

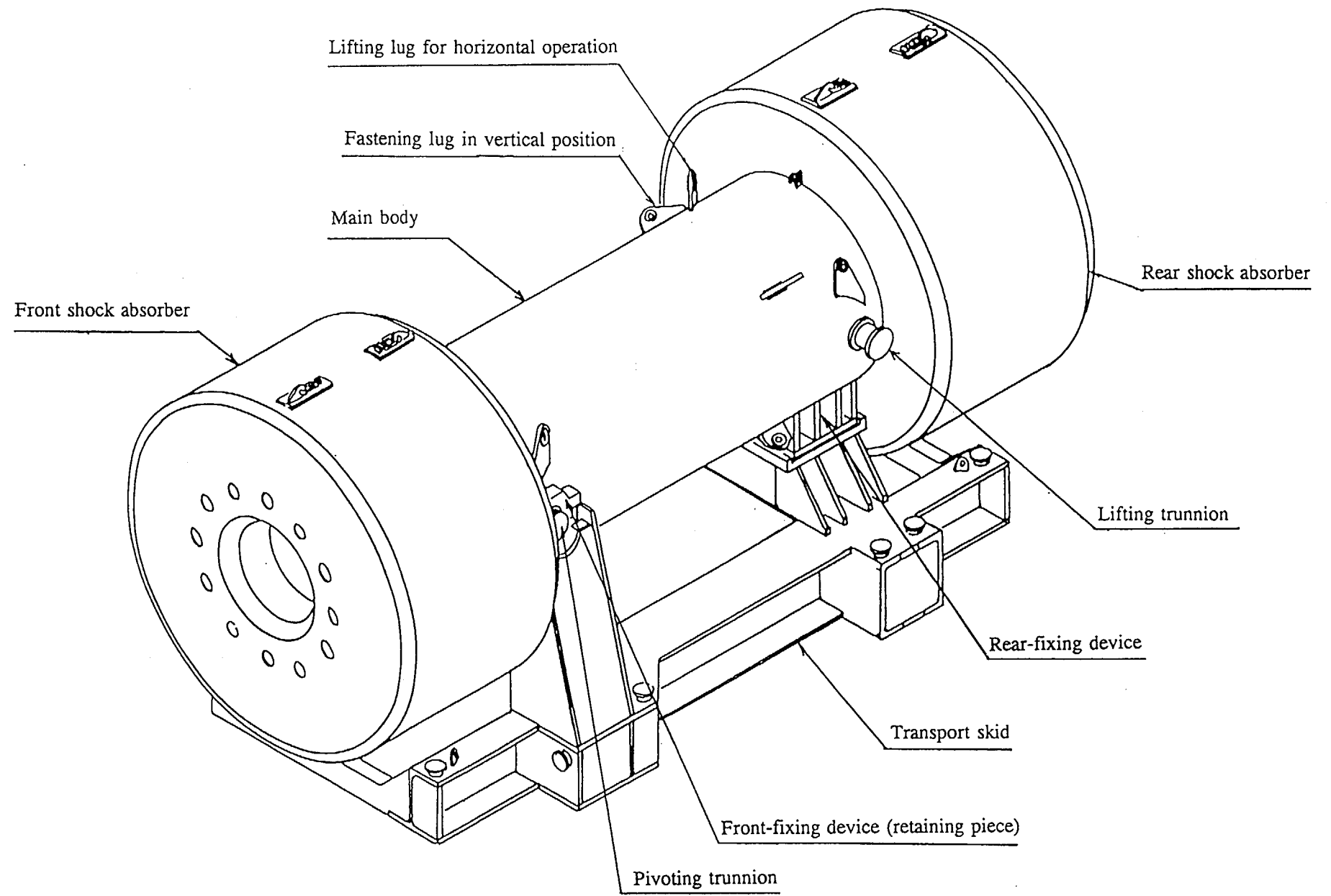


Fig. (II)-A.11 Package Equipped with the skid in Transport

- | | |
|--|-----|
| (a) Horizontal acceleration in the direction in which the vehicle travels ¹⁾
(Longitudinal acceleration) | 10G |
| (b) Horizontal acceleration in the transverse direction
(Transversal acceleration) | 5G |
| (c) Vertical acceleration | 2G |

The stress generated at each part of the tie-down devices is calculated on the assumption that these loads simultaneously act on the center of a package's gravity. The yield stress of the tie-down devices (SUS304) at 80°C is used as the design criterion (a welding efficiency of 60% is assumed for the welded sections). Since thermal analysis shows that the temperature of the outer shell during transport is 72°C, the yield stress at 80°C is used as the reference value, to be on the safe side.

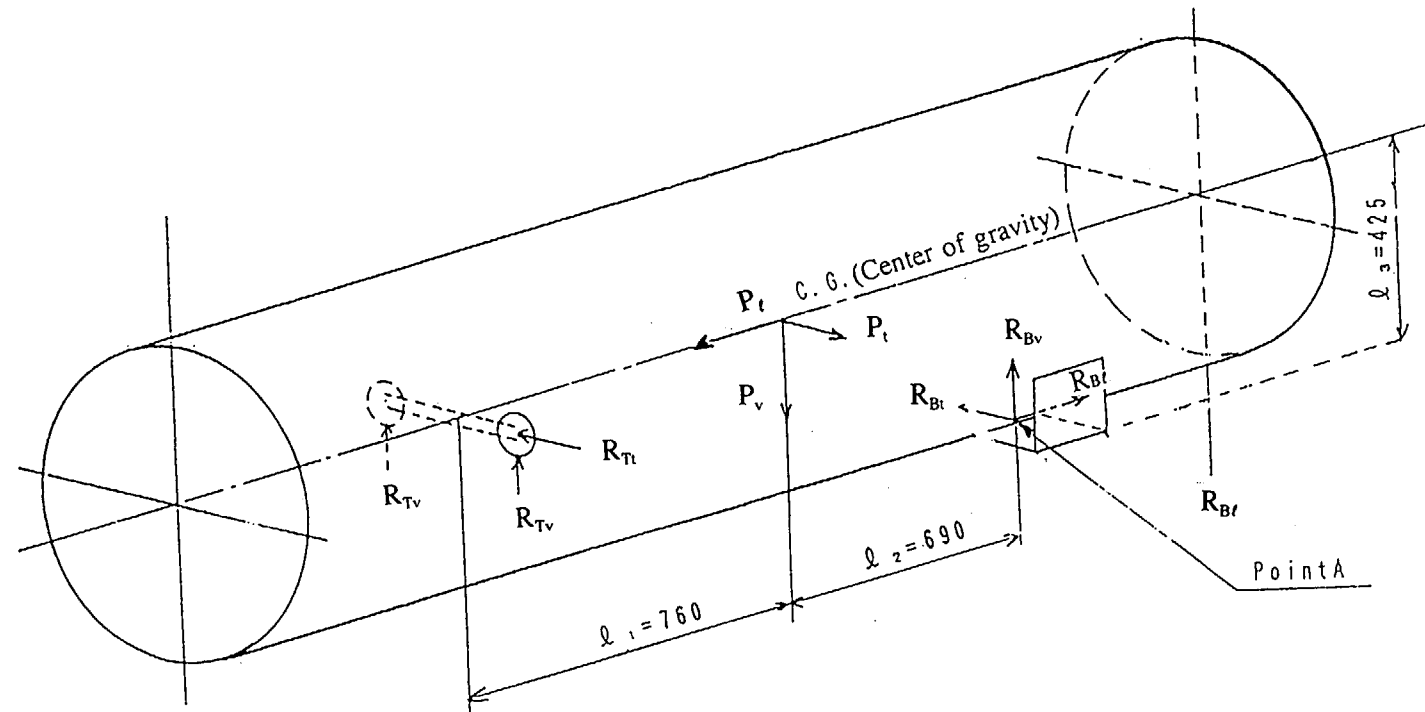
The longitudinal load P_l is supported by the reaction force R_{Bl} generated at the base plate receptacle of the rear base plate transport skid together with the reaction force $2R_{Tv}$ generated at the pivoting trunnions' bearing supports due to the moment, which is a product of the longitudinal load and the distance between the center of gravity of the package and constraint point A at the lowest point of the rear base plate. On one side, the transversal load P_t is supported by the reaction forces, R_{Bl} and R_{Tl} , generated at the rear base plate receptacle and at the bearing support for the pivoting trunnion, respectively. Moreover, the vertical load P_v is supported on both sides by the reaction forces, R_{Bv} and $2R_{Tv}$, generated at the rear base plate receptacle and at the pivoting trunnions' bearing supports respectively.

As shown in Fig. (II)-A.12, the rear base plate receives reaction force R_{Bl} , R_{Bt} , and R_{Bv} , while the pivoting trunnion receives reaction force $2R_{Tv}$ and R_{Tl} .

1) U. S. NRC: 10-CFR 71, p364

Loads are defined as follows:

Load that acts on the center of gravity		Reaction force that acts on the rear base plate		Reaction force that acts on the pivoting trunnion	
In the longitudinal direction of the packaging:	P_t	In the longitudinal direction of the packaging:	R_{Bt}		
In the transversal direction of the packaging:	P_t	In the transversal direction of the packaging:	R_{Bt}	In the transversal direction of the packaging:	R_{Tt}
In the vertical direction of the packaging:	P_v	In the vertical direction of the packaging:	R_{Bv}	In the vertical direction of the packaging:	R_{Tv}



(in mm)

Fig. (II)-A.12 Analysis Model of the Tie-down Device

Considering all possible loading conditions which depend on the load of the package (11,000 kg) and the direction of the acting forces (acceleration), these reaction forces are determined by the equilibrium of the forces in three directions (longitudinal, transversal, and vertical directions) and the equilibrium of the moments at the lowest point of the rear base plate.

If the symbols for load, reaction force, and moment arm length are determined as shown in Fig. (II)-A.12, the equilibrium-conditional equations are as follows:

$$\Sigma F = 0$$

$$P_t = R_{Bt} \quad (\text{Equilibrium condition for longitudinal load})$$

$$P_t = R_{Bt} \quad (\text{Equilibrium condition for transversal load})$$

$$P_v = R_{Bv} + 2R_{Tv} \quad (\text{Equilibrium condition for vertical load})$$

$$\Sigma M_B = 0$$

$$P_v \cdot \ell_2 + P_t \cdot \ell_3 = 2R_{Tv} \cdot (\ell_1 + \ell_2)$$

$$P_t \cdot \ell_2 = R_{Tt} \cdot (\ell_1 + \ell_2)$$

The above equations (substituting $\ell_1 = 760$ mm, $\ell_2 = 690$ mm and $\ell_3 = 425$ mm) give the following results;

$$R_{Bt} = P_t$$

$$R_{Bt} = \frac{P_t \cdot \ell_1}{\ell_1 + \ell_2} = 0.52P_t$$

$$R_{Bv} = \frac{P_v \cdot \ell_1 - P_t \cdot \ell_3}{\ell_1 + \ell_2} = 0.52P_v - 0.29P_t$$

$$R_{Tt} = \frac{P_t \cdot \ell_2}{\ell_1 + \ell_2} = 0.48P_t$$

$$R_{Tv} = \frac{1}{2} \cdot \frac{P_v \cdot \ell_2 - P_t \cdot \ell_3}{\ell_1 + \ell_2} = \frac{1}{2} (0.48P_v + 0.29P_t)$$

The loading conditions are the following four conditions;

Load condition 1

$$\begin{aligned} P_{\ell} &= 10 \times 9.807 \times 11,000 = 1.079 \times 10^6 \text{N} \\ P_t &= 5 \times 9.807 \times 11,000 = 5.394 \times 10^6 \text{ N} \\ P_v &= 2 \times 9.807 \times 11,000 = 2.158 \times 10^6 \text{ N} \end{aligned}$$

Load condition 2

$$\begin{aligned} P_{\ell} &= -10 \times 9.807 \times 11,000 = -1.079 \times 10^6 \text{N} \\ P_t &= 5 \times 9.807 \times 11,000 = 5.394 \times 10^6 \text{ N} \\ P_v &= 2 \times 9.807 \times 11,000 = 2.158 \times 10^6 \text{ N} \end{aligned}$$

Load condition 3

$$\begin{aligned} P_{\ell} &= 10 \times 9.807 \times 11,000 = 1.079 \times 10^6 \text{N} \\ P_t &= 5 \times 9.807 \times 11,000 = 5.394 \times 10^6 \text{ N} \\ P_v &= -2 \times 9.807 \times 11,000 = -2.158 \times 10^6 \text{ N} \end{aligned}$$

Load condition 4

$$\begin{aligned} P_{\ell} &= -10 \times 9.807 \times 11,000 = -1.079 \times 10^6 \text{N} \\ P_t &= 5 \times 9.807 \times 11,000 = 5.394 \times 10^6 \text{ N} \\ P_v &= -2 \times 9.807 \times 11,000 = -2.158 \times 10^6 \text{ N} \end{aligned}$$

Table (II)-A.12 shows the reaction forces calculated under these load conditions.

Table (II)-A.12 Reaction Force List (Unit: N)

Load conditions	1	2	3	4
$R_{B\ell}$	1.079×10^6	-1.079×10^6	1.079×10^6	-1.079×10^6
R_{Bt}	2.805×10^5	2.805×10^5	2.805×10^5	2.805×10^5
R_{Bv}	-2.010×10^5	4.246×10^5	-4.246×10^5	2.010×10^5
R_{Tt}	2.589×10^5	2.589×10^5	2.589×10^5	2.589×10^5
R_{Tv}	2.089×10^5	-1.049×10^5	1.049×10^5	-2.089×10^5

A.4.5.3 Stress Calculation

When the reaction forces described in the preceding section act on each part of the tie-down devices, stress is generated as below. All the stress is calculated to indicate that the tie-down devices are sound.

- (1) Welded section of the rear base plate . . . Vertical stress (bending, tensile, and compression), shear stress, and principal stress
 - (2) Pivoting trunnion Vertical stress (bending and compression), shear stress, and principal stress
- The pivoting trunnion mounting part of the outer shell . . . Bending stress

A.4.5.3.1 Welded Section of the Rear Base Plate

As shown in Fig. (II)-A.13, the rear base plate is welded to the outer shell of the outer container. The reaction forces, R_{Bt} , R_{Bt} , and R_{Bv} act on the rear base plate (hereafter called "the base") as described in subsection A.4.5.2. The numerical values under the four loading conditions (Table (II)-A.12) are substituted into the equation for these reaction forces to calculate the maximum stress generated in the outer shell and the welded part, in order to evaluate their integrity. The rear base plate is welded to the circular arc of the outer container's outer shell as shown in Fig. (II)-A.13. Under this analysis, the sectional area of the welding section is assumed to be the same as the projected area on the base, to be on the safe side.

- a) Vertical stress (bending, tensile, and compression)
The vertical stress generated in the base is the bending stress generated by reaction forces, R_{Bt} and R_{Bv} , and the compression or tensile stress generated by the reaction force R_{Bv} . The vertical stress is given by the expression below.

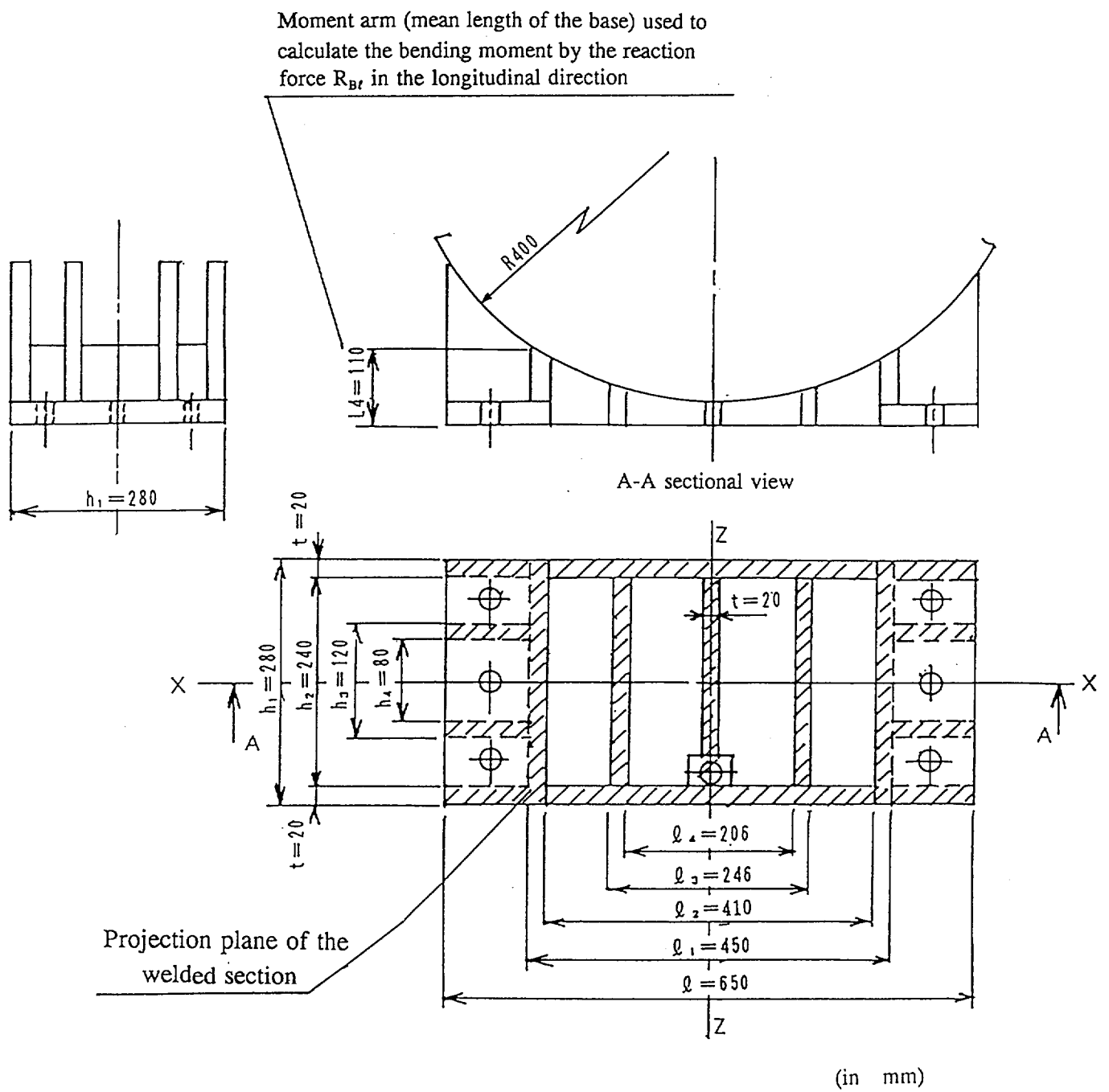


Fig. (II)-A.13 Welded Section of the Rear Base Plate

$$\sigma = \sigma_{Bl} + \sigma_{Bt} + \sigma_{Bv}$$

$$= \frac{M_l}{Z_t} + \frac{M_t}{Z_t} + \frac{R_{Bv}}{A}$$

where

σ : Vertical stress

σ_{Bl} : Bending stress generated by the reaction force R_{Bl} in the longitudinal direction

σ_{Bt} : Bending stress generated by the reaction force R_{Bt} in the transversal direction

σ_{Bv} : Compression or tensile stress generated by the reaction force R_{Bv} in the vertical direction

M_l : Bending moment generated by the reaction force R_{Bl} in the longitudinal direction

$$M_l = R_{Bl} \times L_4$$

R_{Bl} : Reaction force in the longitudinal direction = 1.08×10^6 N

L_4 : Moment arm (mean length of the base) = 110 mm

$$M_l = 1.08 \times 10^6 \times 110$$

$$= \pm 1.19 \times 10^8 \text{ N}\cdot\text{mm}$$

M_t : Bending moment generated by the reaction force R_{Bt} in the transversal direction

$$M_t = R_{Bt} \times L_4$$

R_{Bt} : Reaction force in the transversal direction = 2.81×10^5 N

L_4 : Moment arm (mean length of the base) = 110 mm

$$M_t = 2.81 \times 10^5 \times 110$$

$$= 3.09 \times 10^7 \text{ N}\cdot\text{mm}$$

R_{Bv} : Reaction force in the vertical direction = $\pm 4.25 \times 10^5$ N

Z_t : Section modulus around the X-X axis (transversal direction) of the base

$$Z_t = \frac{I_t}{\frac{h}{2}}$$

I_t : Moment of inertia of the area around the X-X axis (transversal direction) of the base

$$I_t = \frac{\ell}{12} (h_1^3 - h_2^3) + \frac{1}{12} n t h_2^3 + \frac{(\ell - \ell_1)}{12} (h_3^3 - h_4^3)$$

ℓ : Projection length of the welded section (Fig. (II)-A.13) = 650 mm

ℓ_1 : Projection length of the welded section (Fig. (II)-A.13) = 450 mm

h_1 : Projection length of the welded section (Fig. (II)-A.13) = 280 mm

h_2 : Projection length of the welded section (Fig. (II)-A.13) = 240 mm

h_3 : Projection length of the welded section (Fig. (II)-A.13) = 120 mm

h_4 : Projection length of the welded section (Fig. (II)-A.13) = 80 mm

t : Projection length of the welded section (Fig. (II)-A.13) = 20 mm

n : Number of stiffening plates = 5

$$I_t = \frac{650}{12} (280^3 - 240^3) + \frac{1}{12} \times 5 \times 20 \times 240^3 + \frac{1}{12} \times (650 - 450) \times (120^3 - 80^3)$$
$$= 5.76 \times 10^8 \text{ mm}^4$$

and thus

$$Z_t = \frac{5.76 \times 10^8}{\frac{280}{2}}$$
$$= 4.11 \times 10^6 \text{ mm}^3$$

Z_t : Section modulus around the Z-Z axis (longitudinal direction) of the base

$$Z_t = \frac{I_x}{\frac{\ell}{2}}$$

I_x : Moment of inertia of the area around the Z-Z axis (longitudinal direction) of the base

$$I_x = \frac{1}{12} (h_1 - h_2) \ell^3 + \frac{1}{12} h_2 (\ell_1^3 - \ell_2^3) + \frac{1}{12} h_2 (\ell_3^3 - \ell_4^3) + \frac{1}{12} h_2 t^3 + \frac{1}{12} (h_3 - h_4) (\ell^3 - \ell_1^3)$$

ℓ : Projection length of the welded section (Fig. (II)-A.13) = 650 mm

ℓ_1 : Projection length of the welded section (Fig. (II)-A.13) = 450 mm

ℓ_2 : Projection length of the welded section (Fig. (II)-A.13) = 410 mm

ℓ_3 : Projection length of the welded section (Fig. (II)-A.13) = 246 mm

ℓ_4 : Projection length of the welded section (Fig. (II)-A.13) = 206 mm

h_1 : Projection length of the welded section (Fig. (II)-A.13) = 280 mm

h_2 : Projection length of the welded section (Fig. (II)-A.13) = 240 mm

h_3 : Projection length of the welded section (Fig. (II)-A.13) = 120 mm

h_4 : Projection length of the welded section (Fig. (II)-A.13) = 80 mm

t : Projection length of the welded section (Fig. (II)-A.13) = 20 mm

$$\begin{aligned} I_x &= \frac{1}{12} \times (280 - 240) \times 650^3 + \frac{1}{12} \times 240 (450^3 - 410^3) + \frac{1}{12} \times 240 \times (246^3 - 206^3) \\ &\quad + \frac{1}{12} \times 240 \times 20^3 + \frac{1}{12} \times (120 - 80) \times (650^3 - 450^3) \\ &= 2.09 \times 10^9 \text{ mm}^4 \end{aligned}$$

and therefore

$$\begin{aligned} Z_t &= \frac{2.09 \times 10^9}{\frac{650}{2}} \\ &= 6.43 \times 10^6 \text{ mm}^3 \end{aligned}$$

A: Sectional area of the base

$$A = \ell (h_1 - h_2) + n t h_2 + (\ell - \ell_1) (h_3 - h_4)$$

ℓ : Projection length of the welded section (Fig. (II)-A.13) = 650 mm

ℓ_1 : Projection length of the welded section (Fig. (II)-A.13) = 450 mm

h_1 : Projection length of the welded section (Fig. (II)-A.13) = 280 mm

h_2 : Projection length of the welded section (Fig. (II)-A.13) = 240 mm

h_3 : Projection length of the welded section (Fig. (II)-A.13) = 120 mm

h_4 : Projection length of the welded section (Fig. (II)-A.13) = 80 mm

t : Projection length of the welded section (Fig. (II)-A.13) = 20 mm

n : Number of stiffening plates = 5

$$\begin{aligned} A &= 650 \times (280 - 240) + 5 \times 20 \times 240 + (650 - 450) (120 - 80) \\ &= 5.80 \times 10^4 \text{ mm}^2 \end{aligned}$$

If the plus (+) and minus (-) signs are freely set using the numeric values above, the maximum value is given by

$$\sigma = \frac{M_t}{Z_t} + \frac{M_t}{Z_t} + \frac{R_{Bv}}{A}$$

$$= \frac{1.19 \times 10^8}{4.11 \times 10^6} + \frac{3.09 \times 10^7}{6.43 \times 10^6} + \frac{4.25 \times 10^5}{5.80 \times 10^4}$$

$$= 41.1 \text{ N/mm}^2$$

(b) Shear stress

The shear stress generated in the rear base plate is produced by the reaction forces R_{Bt} and R_{Bt} shown in Fig. (II)-A.12. This shear stress is given by the expression below.

$$\tau = \sqrt{\tau_l^2 + \tau_t^2}$$

$$= \sqrt{\left(\frac{R_{Bt}}{A}\right)^2 + \left(\frac{R_{Bt}}{A}\right)^2}$$

where

R_{Bt} : Reaction force in the longitudinal direction = $\pm 1.08 \times 10^6 \text{ N}$

R_{Bt} : Reaction force in the transversal direction = $\pm 2.81 \times 10^5 \text{ N}$

A: Sectional area of the base (from (1)-(a)) $5.80 \times 10^4 \text{ mm}^2$

$$\tau = \sqrt{\left(\frac{\pm 1.08 \times 10^6}{5.80 \times 10^4}\right)^2 + \left(\frac{\pm 2.81 \times 10^5}{5.80 \times 10^4}\right)^2}$$

The maximum value is

$$\tau = 19.2 \text{ N/mm}^2$$

(c) Principal stress

From the vertical stress (σ) and shear stress (τ) determined by (a) and (b) above, the principal stress (σ_p) is given by the expression below.

$$\sigma_p = \frac{\sigma}{2} \pm \sqrt{\left(\frac{\sigma}{2}\right)^2 + \tau^2}$$

where

σ : Vertical stress = 41.1 N/mm^2

τ : Shear stress = 19.2 N/mm^2

and thus

$$\begin{aligned}\sigma_p &= \frac{41.1}{2} \pm \sqrt{\left(\frac{41.1}{2}\right)^2 + 19.2^2} \\ &= 48.7 - 7.57 \text{ N/mm}^2 \\ &\approx 4.94 - 0.76 \text{ kg/mm}^2\end{aligned}$$

Therefore, the maximum value of the principal stress in the welded section of the rear base plate is 48.5 N/mm², and the analysis criterion value of the welded section uses $0.6\sigma_y = 108 \text{ N/mm}^2$ ($\approx 11.0 \text{ kg/mm}^2$) (material: SUS304, temperature: 80°C).

The margin of safety (M.S.) is thus given by

$$\begin{aligned}M.S. &= \frac{108}{48.7} - 1 \\ &= 1.2\end{aligned}$$

The welded section of the rear base plate ensures strength and soundness during transport.

A.4.5.3.2 Pivoting Trunnion and the Mounting Part of its Outer Shell

(1) Pivoting trunnion

As described in subsection A.4.5.2, the reaction force R_{Tt} in the transversal direction and the reaction force R_{Tv} in the vertical direction act on the pivoting trunnion. The numeric values under loading conditions (Table (II)-12) are substituted for to these reaction forces so that the vertical stress and shear stress can be determined. Using the determined stress values, the maximum stress to be generated is determined, and indicates that the pivoting trunnion has sufficient strength.

Fig. (II)-A.14 shows the analysis model.

(a) Vertical stress (bending and compression)

The vertical stress occurring in the pivoting trunnion is generated by the bending stress produced by the reaction force R_{Tv} in the vertical direction, and the stress produced by the reaction force R_{Tt} in the transversal direction. The trunnion is supported on both sides by the bearing supports for the pivoting trunnions. As shown in Fig. (II)-A.14, the transversal reaction R_{Tt} is completely supported on only one of the faces of the bottom of the trunnions. The reaction force R_{Tt} thus functions as a compressive force as shown in the figure.

The stress above is given by

$$\begin{aligned}\sigma &= \sigma_{Tv} + \sigma_{Tt} \\ &= \frac{M_v}{Z_v} + \frac{R_{Tt}}{A}\end{aligned}$$

where

σ : Vertical stress

σ_{Tv} : Bending stress generated by the reaction force R_{Tv} in the vertical direction

σ_{Tt} : Bending stress generated by the reaction force R_{Tt} in the transversal direction

M_v : Bending moment generated by the reaction force T_{Tv} in the vertical direction

$$M_v = R_{Tv} \times \ell$$

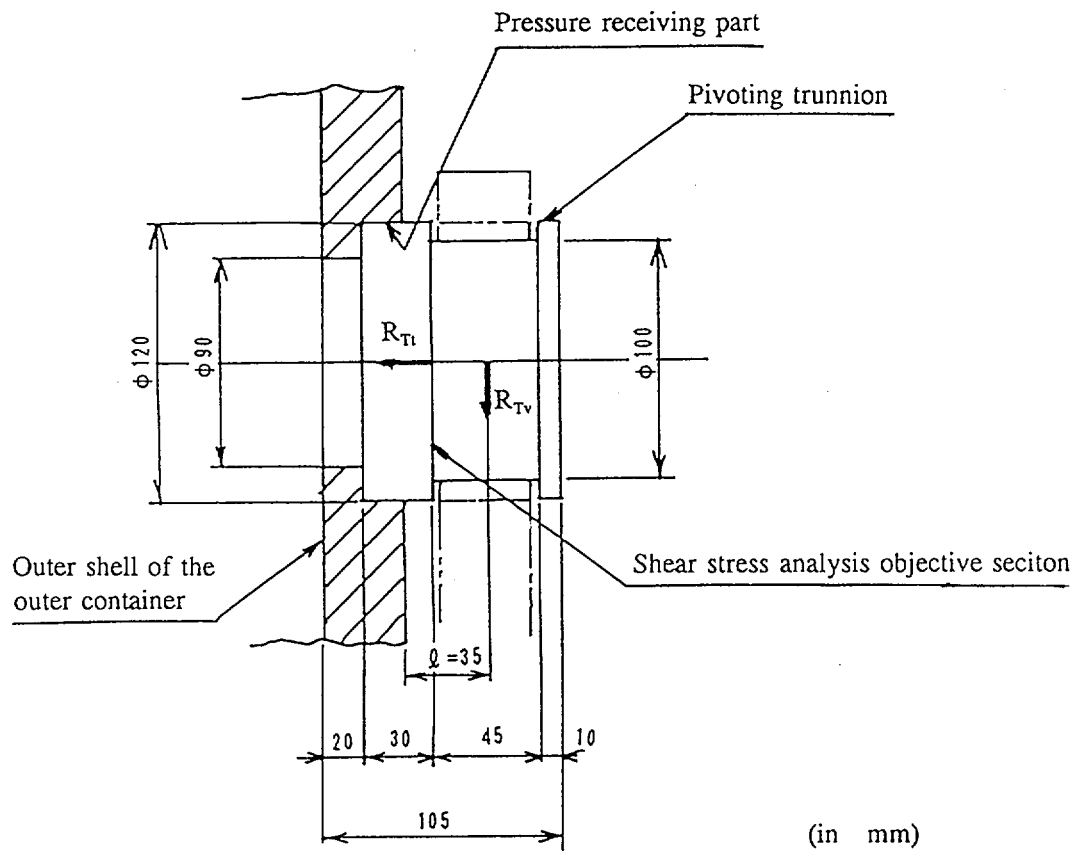


Fig. (II)-A.14 Analysis Model of the Pivoting Trunnion

R_{Tv} : Reaction force in the vertical direction = $\pm 2.09 \times 10^5$ N

ℓ : Moment arm = 35 mm

$$M_v = \pm 2.09 \times 10^5 \times 35 \\ = \pm 7.32 \times 10^6 \text{ N} \cdot \text{mm}$$

R_{Tl} : Reaction force in the transversal direction = 2.59×10^5 N

Z_v : Section modulus of the minimum trunnion diameter

$$Z_v = \frac{\pi}{32} d_1^3$$

d_1 : Minimum diameter of the trunnion = 100 mm

$$Z_v = \frac{\pi}{32} \times 100^3$$

$$= 9.82 \times 10^4 \text{ mm}^3$$

A: Area of trunnion's pressure receiving part

$$A = \frac{\pi}{4} (d_2^2 - d_1^2)$$

d_1 : Inner diameter of the pressure receiving part = 90 mm

d_2 : Outer diameter of the pressure receiving part = 120 mm

$$A = \frac{\pi}{4}(120^2 - 90^2) \\ = 4.95 \times 10^3 \text{ mm}^2$$

If the plus (+) and minus (-) signs are freely set using the numeric values indicated above, the maximum value is given by

$$\sigma = \frac{M_v}{Z_v} + \frac{R_T}{A} \\ = \frac{7.32 \times 10^6}{9.82 \times 10^4} + \frac{2.59 \times 10^5}{4.95 \times 10^3} \\ = 127 \text{ N/mm}^2$$

(b) Shear stress

The shear stress in the pivoting trunnion will now be evaluated. As shown in Fig. (II)-A.14, the shear stress is generated by the reaction force R_{Tv} in the transversal direction.

This shear stress (τ) is given by the expression below.

$$\tau = \frac{4}{3} \times \frac{R_{Tv}}{A}$$

where

τ : Shear stress

R_{Tv} : Reaction force in the vertical direction = $\pm 2.09 \times 10^5 \text{ N}$

A : Cross sectional area of the pivoting trunnion

$$A = \frac{\pi}{4} d_1^2$$

d_1 : Minimum diameter of the pivoting trunnion = 100 mm

$$A = \frac{\pi}{4} \times 100^2 \\ = 7.85 \times 10^3 \text{ mm}^2 \\ \tau = \frac{4}{3} \times \frac{\pm 2.09 \times 10^5}{7.85 \times 10^3} \\ = \pm 35.5 \text{ N/mm}^2$$

The maximum value of the shear stress τ is 35.5 N/mm².

(c) Principal stress

Using the vertical stress (σ) and shear stress (τ) obtained from (a) and (b) above, the principal stress generated in the trunnion is given by the expression below.

$$\sigma_p = \frac{\sigma}{2} \pm \sqrt{\left(\frac{\sigma}{2}\right)^2 + \tau^2}$$

where

σ_p : Principal stress

σ : Vertical stress = 127 N/mm²

τ : Shear stress = 35.5 N/mm²

$$\begin{aligned}\sigma_p &= \frac{127}{2} \pm \sqrt{\left(\frac{127}{2}\right)^2 + 35.5^2} \\ &= 136 - 9.25 \text{ N/mm}^2 \\ &\approx 13.9 - 0.95 \text{ kg/mm}^2\end{aligned}$$

The maximum value of the principal stress in the pivoting trunnion is 136 N/mm², and the design criterion value of the pivoting trunnion uses $\sigma_y = 180 \text{ N/mm}^2$ ($\approx 18.4 \text{ kg/mm}^2$) (material: SUS304, temperature: 80°C).

The margin of safety (M.S.) is thus given by

$$\begin{aligned}M.S. &= \frac{180}{136} - 1 \\ &= 0.32\end{aligned}$$

Consequently, the pivoting trunnion maintains its strength and soundness during transport.

(2) The pivoting trunnion mounting part of the outer shell

The pivoting trunnion mounting part of the outer shell receives reaction force R_{Tv} in the vertical direction, as described in subsection A.4.5.2, from the pivoting trunnion and bending stress is generated. This bending stress is obtained using the analysis model shown in Fig. (II)-A.15. As indicated by this analysis model, the section in which the pivoting trunnion is installed is examined using the analysis model of a ring (40-mm thick and 350-mm wide). The result shows that this section of the outer shell alone can sufficiently withstand the stress.

As shown in model "a", the inertia force (assumed to be distributed in a cosine) of the package is balanced with the force ($2 R_{Tv}$) that acts on the pivoting trunnion. The load conditions in models "b" and "c" are evaluated separately.

- (i) In model "b", the bending moment M_1 is generated at point B by reaction force R_{Tv} in the vertical direction that acts on the pivoting trunnion. The bending moment M_1 is given by the expression below.

$$M_1' = R_{Tv} \times \ell$$

where

M_1' : Bending moment occurring at point B

R_{Tv} : Reaction force in the vertical direction = $\pm 2.09 \times 10^5 \text{N}$

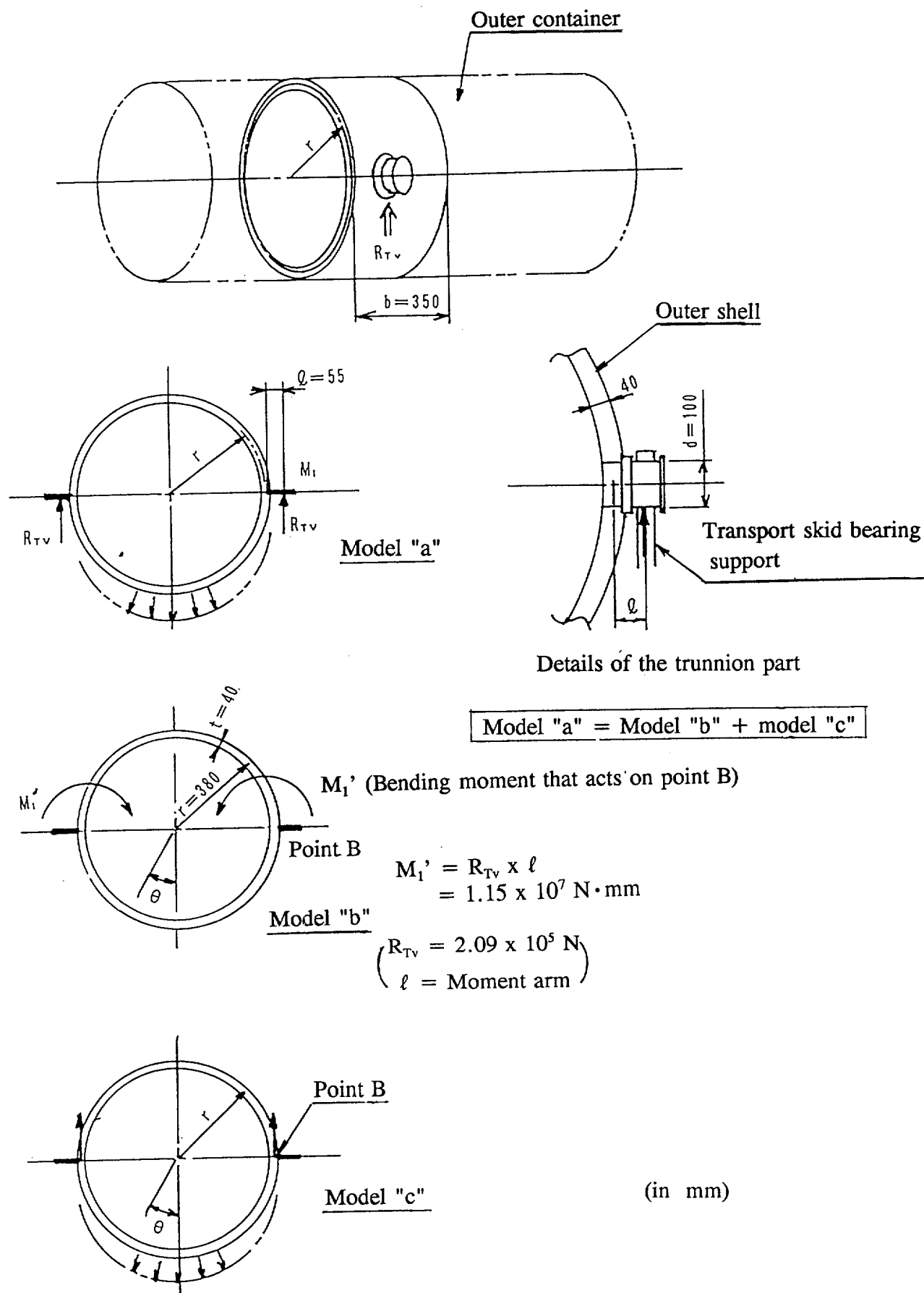


Fig. (II)-A.15 Outer Shell (Trunnion Mounting Part)

ℓ : Moment arm = 55 mm
(See Fig. (II)-A.15.)

$$M_1 = 2.09 \times 10^5 \times 55 \\ = 1.15 \times 10^7 \text{ N}\cdot\text{mm}$$

The bending moment M_1 generated in each part of the outer shell (ring) by the bending moment M_1' that acts on point B becomes a function of angle θ . Therefore, the bending moment M_1 is given by the following two expressions:¹⁾

$$\text{For } 0 \leq \theta \leq \frac{\pi}{2}$$

$$M_1 = -M_1' (0.5 - 0.6366 \cos\theta)$$

$$\text{For } \frac{\pi}{2} \leq \theta \leq \pi$$

$$M_1 = M_1' (0.5 + 0.6366 \cos\theta)$$

where

M_1 : Bending moment occurring in each part of outer shell

M_1' : Bending moment that acts on point B

θ : Angle indicating each part of the outer shell.
See Fig. (II)-15.

- (ii) In model "c", the bending moment M_2 generated by the distributed load in the outer shell (ring) is given by the following two expressions:

$$\text{For } 0 \leq \theta \leq \frac{\pi}{2}$$

$$M_2 = R_{Tv} \cdot r (0.6366\theta \cdot \sin\theta + 0.7958 \cos \theta - 0.9053)$$

$$\text{For } \frac{\pi}{2} \leq \theta \leq \pi$$

$$M_2 = R_{Tv} \cdot r \cdot (0.1592 \cos\theta + 0.0947)$$

where

M_2 : Bending moment generated in the outer shell (ring) by the distributed load

R_{Tv} : Reaction force in the vertical direction = $\pm 2.09 \times 10^5 \times \text{N}$

r : Mean radius of the outer shell (ring) = 380 mm

θ : Angle indicating each part of the outer shell.
See Fig. (II)-13.

- (iii) The composite bending moment M is obtained from (i) and (ii) above.

1) "How to Find Deflection and Moment of Ring and Arcuate Beams"
Product Engineering p70-80, 1968

The composite bending moment M is the sum of M_1 and M_2 , and is given by the expression below.

$$\text{For } 0 \leq \theta \leq \frac{\pi}{2}$$

$$M = -M_1 \cdot (0.5 - 0.6366 \cos\theta) + R_{Tv} \cdot r (0.6366 \sin\theta + 0.7958 \cos\theta - 0.9053)$$

$$\text{For } \frac{\pi}{2} \leq \theta \leq \pi$$

$$M = M_1 \cdot (0.5 + 0.6366 \cos\theta) + R_{Tv} \cdot r (0.1592 \cos\theta + 0.0947)$$

Using the composite bending moment M , the bending stress (σ) is given by

$$\sigma = \frac{M}{Z}$$

where

- σ : Bending stress
- M : Composite bending moment
- z : Modulus of reaction

$$z = \frac{1}{6} b t^2$$

- b : Width of the outer shell (ring) = 350 mm
- t : Thickness of the outer shell (ring) = 40 mm

$$\begin{aligned} z &= \frac{1}{6} \times 350 \times 40^2 \\ &= 9.33 \times 10^4 \text{ mm}^3 \end{aligned}$$

The composite bending moment is a function of angle θ . Table (II)-A.13 shows the M_1 , M_2 , and M values, and the (σ) values obtained when angle θ is changed every $1/36 \pi$ (= 5 degrees).

As shown in Table (II)-A.13, the maximum bending stress is generated when angle θ is 90 degrees and its value is 142 N/mm^2 ($\approx 14.5 \text{ kg/mm}^2$). The design criterion value of the outer shell uses $\sigma_y = 180 \text{ N/mm}^2$ ($\approx 18.4 \text{ kg/mm}^2$) (material: SUS304, temperature: 80°C).

Consequently, the margin of safety (M.S.) is given by the expression below.

$$\begin{aligned} M.S. &= \frac{180}{142} - 1 \\ &= 0.27 \end{aligned}$$

The outer shell thus has sufficient strength. In this case, no deformation occurs due to bending stress.

Table (II)-A.13 Stress Generated in the Outer Shell (Horizontal Lifting)

Angle	Bending moment			Stress
θ (°)	M_1 (N·mm)	M_2 (N·mm)	M (N·mm)	σ (N/mm ²)
0	1.57×10^6	-8.69×10^6	-7.12×10^6	-76.2
5	1.54×10^6	-8.55×10^6	-7.01×10^6	-75.0
10	1.46×10^6	-8.12×10^6	-6.66×10^6	-71.3
15	1.32×10^6	-7.42×10^6	-6.10×10^6	-65.3
20	1.13×10^6	-6.47×10^6	-5.30×10^6	-57.1
25	8.84×10^5	-5.29×10^6	-4.41×10^6	-47.2
30	5.90×10^5	-3.93×10^6	-3.34×10^6	-35.6
35	2.47×10^5	-2.41×10^6	-2.16×10^6	-23.1
40	-1.42×10^5	-7.94×10^5	-9.36×10^5	-10.0
45	-5.73×10^5	8.70×10^5	2.97×10^5	3.1
50	-9.87×10^6	2.52×10^6	1.48×10^6	15.8
55	-1.54×10^6	4.10×10^6	2.56×10^6	27.3
60	-2.09×10^6	5.55×10^6	3.46×10^6	37.0
65	-2.65×10^6	6.79×10^6	4.14×10^6	44.3
70	-3.24×10^6	7.76×10^6	4.51×10^6	48.3
75	-3.85×10^6	8.38×10^6	4.53×10^6	48.5
80	-4.47×10^6	8.59×10^6	4.12×10^6	44.1
85	-5.11×10^6	8.33×10^6	3.22×10^6	34.5
90	5.74×10^6	7.51×10^6	1.26×10^6	142
95	5.11×10^6	6.42×10^6	1.15×10^6	123
100	4.47×10^6	5.32×10^6	9.80×10^5	104
105	3.85×10^6	4.25×10^6	8.10×10^5	86.7
110	3.24×10^6	3.19×10^6	6.44×10^5	68.9
115	2.65×10^6	2.18×10^6	4.83×10^5	51.7
120	2.09×10^6	1.20×10^6	3.29×10^5	35.2
125	1.55×10^6	2.69×10^5	1.82×10^5	19.5
130	1.04×10^6	-6.06×10^5	4.37×10^5	4.7
135	5.73×10^5	-1.42×10^6	-8.46×10^5	-9.0
140	1.42×10^5	-2.16×10^6	-2.02×10^6	-21.6
145	-2.47×10^5	-2.83×10^6	-3.08×10^6	-33.0
150	-5.90×10^5	-3.43×10^6	-4.02×10^6	-43.0
155	-8.84×10^5	-3.93×10^6	-4.82×10^6	-51.6
160	-1.13×10^6	-4.36×10^6	-5.49×10^6	-58.7
165	-1.32×10^6	-4.69×10^6	-6.01×10^6	-64.4
170	-1.46×10^6	-4.93×10^6	-6.39×10^6	-68.4
175	-1.54×10^6	-5.07×10^6	-6.61×10^6	-70.9
180	-1.57×10^6	-5.12×10^6	-6.69×10^6	-71.6
Maximum value				142

A.4.6 Pressure

This subsection examines the case in which the ambient pressure of the package decreases to 25 kPa. As shown in Table (II)-A.14, the pressure of the inner shell under normal test conditions is 60 kPa. Therefore, considering the negative pressure when the ambient pressure decreases from 101 kPa to 25 kPa, the inner shell have an internal pressure of;

$$60 + (101 - 25) = 136 \text{ kPa(G)}$$

The analysis in subsection A.6.3.2 under accident test conditions indicates that this package maintains its containment integrity at an internal pressure of 192 kPa(G), which is obtained by the analysis.

Therefore, this package ensures containment even if the external pressure decreases to 25 kPa.